Fall 12-1-2018

A New Generation of Functional Polyisobutylenes for Advanced Applications

Corey M. Parada
University of Southern Mississippi

A NEW GENERATION OF FUNCTIONAL POLYISOBUTYLENES FOR ADVANCED APPLICATIONS

by

Corey Michael Parada

A Dissertation
Submitted to the Graduate School,
the College of Arts and Sciences
and the School of Polymer Science and Engineering
at The University of Southern Mississippi
in Partial Fulfillment of the Requirements
for the Degree of Doctor of Philosophy

Approved by:

Dr. Robson F. Storey, Committee Chair
Dr. Jeffrey S. Wiggins
Dr. Derek L. Patton
Dr. William L. Jarrett
Dr. Xiaodan Gu

Dr. Robson F. Storey Committee Chair	Dr. Jeffrey S. Wiggins Director of School	Dr. Karen S. Coats Dean of the Graduate School

December 2018

ABSTRACT

Polyisobutylene (PIB) is a fully saturated, aliphatic polymer of high commercial importance due to its superior gas barrier properties and high chemical/oxidative stability. One commercial end-use for PIB is in insulated glass windows (IGU), where it acts as a gas/moisture barrier and sealant. Under certain adverse conditions, catastrophic failure of the PIB sealant may result in aesthetic and functional failure of the IGU, which necessitates replacement of the unit. Thus, there exists a need to improve current generations of thermoplastic PIB sealants to be able to withstand the harsh environments found in current real-world applications.

In the first project, we synthesized a library of PIB macromers bearing (meth)acrylate moieties via the acid catalyzed cleavage/alkylation of poly(isobutylene-co-isoprene) (butyl rubber) or via living polymerization and subsequent reactive end-quenching with phenoxyalkyl acrylates. The macromers were then crosslinked in the presence of a photoinitiator using UV light, and the curing kinetics were measured. The viscoelastic and tensile properties of the resulting networks were then tested and compared.

In the second project, nitrile containing small molecules were added in the presence of cationized PIB chain ends to study their quenching efficiency. This technique, known as the Ritter reaction, represents a hitherto unreported route towards acrylamide functionalized telechelic PIBs. Under a variety of conditions, we demonstrated that PIB substrates were prone to carbocationic rearrangement rather than amide formation, but we successfully synthesized a new family of oligo-isbutenyl acrylamides via this route.

In the third project, we demonstrated that quenchers derived from resorcinol, a commodity chemical derived from certain wood species, displayed superior quenching efficiency compared to known alkoxybenzenes. These quenchers were synthesized to possess a variety of functional groups, and the highly active phenyl ring allowed for quantitative quenching at significantly reduced time frames while simultaneously requiring lower Lewis acid demand compared to previously studied alkoxybenzenes.

In the fourth project, we investigated the efficacy of 2,6-di-*tert*-butylphenol, a common antioxidant, as a quenching agent in the aforementioned cleavage/functionalization reaction. The resulting PIBs contained a mixture of mono- and di-tert-butylphenol moieties covalently bound to the PIB backbone and chain ends, which displayed superior resistance towards thermal and thermo-oxidative degradation compared to commercially available PIBs and PIBs synthesized via living polymerization.

ACKNOWLEDGMENTS

Firstly, I'd like to acknowledge and thank my advisor Dr. Robson F. Storey. You challenged me to think critically, but you allowed me the freedom to exercise my creative spirit in the pursuit of unexplored areas of research. As an advisor, you fostered a research environment focused on professional and personal improvement. As a friend, you offered your support and advice when life threw curve balls. I will be forever grateful for your endless guidance and patience. Additionally, I would like to thank my committee: Dr. Jarrett, Dr. Wiggins, Dr. Patton, Dr. Lott, and Dr. Gu for their support during my tenure. Also, I would like to acknowledge Dr. Daniel Savin for his friendship and guidance during the early years of my graduate career.

I would like to acknowledge the undergraduate students that I have had the pleasure of working with: Harrison Livingston, Grace Parker, Nathaniel Prine, Kyle Guess, and Samuel Hanson. Your contributions to this work are greatly appreciated. I wish the best for each of you.

Finally, I would like to acknowledge the graduate students and post-docs of the Storey Research Group who I worked most closely with during my time at USM: Mark Brei, Bin Yang, Morgan Heskett, Garrett Campbell, Logan Dugas, Richard Cooke, Travis Holbrook, Jie "Tom" Wu, and Adekunle "Paul" Olubummo. I couldn't ask for a more supportive group of individuals, and our daily conversations has given me a lifetime of memories.

DEDICATION

I would like to dedicate this work to my family.

To Ralph, Ann, Megan, and Jessica Parada:

Your support and unselfish love throughout my life has been immeasurable. This work is a reflection of your endless encouragement. Although I may adventure to uncharted waters, a sailor always knows the way to home port.

To Daniel Cisneros

My brother, you have inspired me to achieve things I never thought possible.

To my Aunts, Uncles and Cousins:

Ya'll are the foundation that has supported me during my time at USM. I couldn't ask for a more supportive family.

To my Grandparents:

Ya'll always believed in me. I miss each and every one of you so much.

And finally, to Samantha:

You fill my heart with joy every day. You have been an ocean of comfort and love; without you, none of this would have been possible. Your encouragement is the wind in my sails. Our next chapter awaits.

TABLE OF CONTENTS

LIST OF TABLES

LIST OF ILLUSTRATIONS

LIST OF SCHEMES

CHAPTER I – Introduction to Butyl Rubber and Isobutylene

The synthetic chemist, when tasked with designing or synthesizing a new compound, generally starts with a literature search. Oftentimes, a productive literature search not only reveals the desired technique or synthetic route, but also shows how developments in the specific area evolved throughout history. From this, the chemist can gain an appreciation for the evolution of knowledge about the specific topic. Thus, to fully appreciate the motivation for this work, the author feels that a short, concise history of the evolution of rubber chemistry is necessary. Detailed histories can be found elsewhere[1,2,3,4]

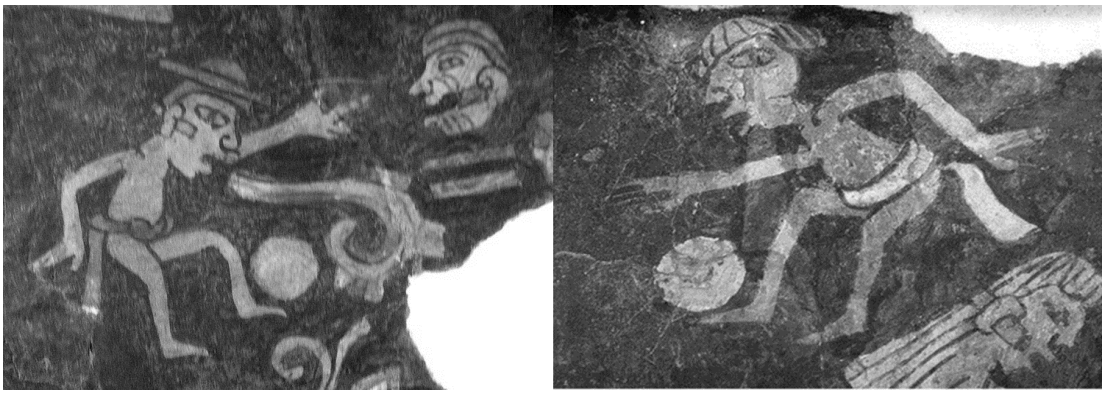

Figure 1.1 Close-up of the Tepantitla mural in Teotihuacan, Central Mexico, depicting two ballplayers participating in the Mesoamerican Ballgame. Archeological evidence indicates that the balls were formed using natural rubber and other materials. Wikimedia Commons. Photo credit to Daniel Lobo.

1.2 The Early Years

The history of the evolution of natural and synthetic rubber is an intricate and fascinating one. Natural rubber (*cis*-1,4-polyisoprene) is almost exclusively sourced from *hevea brasiliensis*, which is found naturally in Central and South America. Although archeological evidence suggests that Ancient Mesoamerican cultures used rubber goods as far back as 1600 BCE (Figure 1.1), the first reported use of natural rubber was by

Christopher Columbus in 1496, who described the material as being used by indigenous Mesoamericans for textiles, containers, sporting equipment, and as a waterproofing sealant.[2,5,6] By the late 1700's, rubber samples were routinely being exported to Europe for further study. During the early 1800's, the first patents for rubber-based consumer products were issued in the United States and Europe; however the materials were found to melt in hot weather and/or become brittle in cold weather.[5] The first chemical reaction of natural rubber in the presence of sulphur (i.e. the vulcanization process) was reported by Faraday in 1827.[7] Notably, it was not until 1839 that the commercial importance of the vulcanization process (i.e. crosslinking reaction in the presence of sulfur) was realized, when Charles Goodyear recognized that vulcanized materials were immune to melting or breaking in temperature extremes.[2,6]

As the end of the 19th century approached, the cultivation and production of natural rubber became as lucrative as the commercial consumption of rubber products. In 1876, rubber seeds were smuggled from South America and planted throughout Indonesia, which soon began to outproduce South American sourced natural rubber.[2,5] Geopolitical instability within several rubber producing South American countries led to a widening of the production gap between Indonesian and South American rubber sources. At the turn of the 20th century, mass production of industrial and consumer goods such as textiles, hosing, and automobiles drove demand for natural rubber products. Although natural rubber was still recognized as the gold standard for elastomer applications, economic instability within South America and the fluctuating supply of natural rubber from Indonesia catalyzed the chemical industry to search for appropriate synthetic substitutes.[5] The search for synthetic alternatives was accelerated during World

War 1, when British naval blockades forced German chemical manufacturers to replace natural rubber with synthetic rubbers for the German war effort.[2,8]

During the interwar period, changes in Germany's economic policies resulted in increased investments in German chemical and rubber manufacturing capabilities, and Germany began to lead the world in synthetic rubber research. Simultaneously, Japanese militaristic expansion of Indonesia resulted in a global shortage of natural rubber, which required Allied countries to invest heavily in their own rubber manufacturing.[2,5] Following the outbreak of war, the United States brought its full manufacturing weight to bear on the war effort, famously and seamlessly transitioning assembly lines from manufacturing consumer goods to production of war matériel. Less famously, but just as important to the war effort, was the US's militarization of the rubber industry to find suitable synthetic elastomers for use in warfare.[3]

Following World War II, the Cold War and subsequent Arms Race and Space Race drove a renaissance within the fields of polymer chemistry, polymer physics, and polymer science.[33,9] Technological developments gained from defense applications often spilled over into the consumer markets. This was conspicuously noticeable in the field of rubber technology, where synthetic rubbers gradually began to find use in applications ranging from sports equipment to textiles to automobiles to aerospace.[10] This was due in large part to the low cost of oil-based monomers and the ease of manufacturing, but arguably the most significant factor was the realization that synthetic rubbers could be molecularly engineered to possess considerably different chemical and physical properties by controlling the (co)monomer composition.[7]

1.3 Ionic Polymerizations: Theory and the Road to the Understanding

Early synthetic rubbers developed by Germany primarily included butadienes as the elastomeric component and styrene or acrylonitrile as the hard component. These copolymers, named Buna S (butadiene-styrene) and Buna N (butadiene-acrylonitrile), were traditionally synthesized via an anionic polymerization mechanism, which along with cationic polymerizations make up the two types of ionic polymerizations.[11] Ionic polymerizations, like free-radical polymerizations, proceed via a chain-growth polymerization mechanism.[12,13] Unlike free-radical polymerizations, however, ionic polymerizations are extremely sensitive to reaction conditions,[6,14] monomer purity,[15] the presence of additives/contaminants,[6,16] and monomer reactivities.[8] The development and understanding of ion-induced chain polymerizations took place over the course of hundreds of years, spanning from the Late Renaissance world of alchemy, to the World War years, to the Space Age and beyond.

Although the theory of ion induced chain polymerizations was first proposed by Staudinger in 1920,[17] it is generally accepted that the first reported ionic polymerization predated Staudinger by 131 years when, in 1787, Bishop Richard Watson described the formation of a viscous oil upon addition of turpentine to boiling sulfuric acid.[18] Soon after Staudinger proposed his theory, Ziegler reported the first anionic polymerization of butadiene in 1928, in which he reported that sequential additions of butadiene to an *in situ* polymerization resulted in a proportional increase of the polymer molecular weight.[19]

The first theoretical treatise including discussion of a cationic polymerization mechanism was attributed to Whitmore in 1934 (incidentally with isobutylene as the monomer).[20] The first actual cationic polymerization was apparently performed by

Williams in 1940,[21] who showed that the polymerization of styrene could occur by addition of $SnCl_4$. Williams demonstrated that the resulting polymer backbone was identical in structure to the material formed from the decomposition of benzoyl peroxide in the presence of styrene. This gave irrefutable evidence of a cation-induced polymerization mechanism and led to new families of ionically polymerizable monomers.

One of these new polymerizable monomers was isobutylene, which can be isolated from natural gas refinery processes. Concurrent to the studies of Whitmore and Williams, the cationic polymerization of isobutylene to form high polymers was first reported by Otto and Muller-Conradi in 1937, who were jointly issued German Patent 641-281.[22] At temperatures ranging between -40 and -80 °C, using BF_3 as a catalyst, low molecular weight PIBs (< 5,000 g/mol) were obtained. Otto and Muller-Conradi had improved upon a process demonstrated by Butlerov, who showed that isobutylene oligomers could be formed in the presence of BF_3 or Bronsted Acids;[23] however the formation of high molecular weight polymers was still elusive. A general mechanism of the process advanced by Otto and Muller-Conradi is shown in Scheme 1.1. Within 3 years of Otto and Muller-Conradi's findings, Thomas and coworkers reported PIBs possessing molecular weights of 3×10^6 g/mol.[24] At the time, these materials were viewed mainly as a curiosity due to their totally saturated aliphatic backbone, which precluded their use in applications that required vulcanization. Thus, PIB homopolymers were not seen as a commercially viable alternative to natural rubber and were relegated to specialty applications.[6]

Thomas and Sparks improved upon their original patent in 1944 when they reported the formation of high molecular weight PIB copolymers, which consisted of

either poly(isobutylene-*co*-butadiene) or poly(isobutylene-*co*-isoprene).[25] Both copolymers contained a backbone unsaturation due to the diene incorporation, which allowed these materials to participate under vulcanization reactions to form crosslinked rubbers.[26] As this process matured, the isoprene formulation became the preferred formulation (Figure 1.2), and the butyl rubber industry was born.

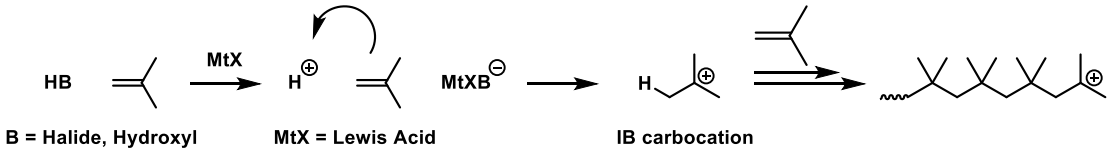

Scheme 1.1 General initiation and propagation mechanism of isobutylene in the presence of a cation and a Lewis acid cocatalyst.

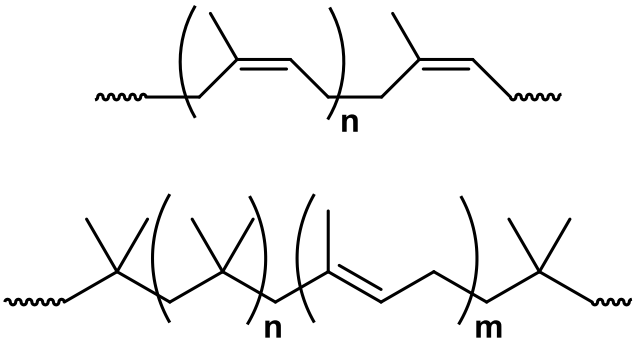

Figure 1.2 Chemical structure of natural rubber (cis-1,4-polyisoprene, top) and butyl rubber (poly(isobutylene-*co*-isoprene), bottom).

As the commercial developments of ionic polymerizations focused on synthesizing new elastomers, academicians turned their attention towards imparting greater control over the polymerization mechanism. The first breakthrough occurred in the area of anionic polymerizations, when in 1956, Szwarc and coworkers reported the living anionic polymerization of styrene.[27,28] Due to the absence of termination events, unique polymer architectures (Figure 1.3) are possible, and narrow molecular weight

distributions (MWD, often interchangeably referred to as polydispersity index (PDI)) along with targeted molecular weights can be realized.[29] Another result of living polymerizations is the preservation of the polymer chain end functionality, which allows for the synthesis of telechelic polymers and block copolymers. This topic will be discussed in greater detail later.

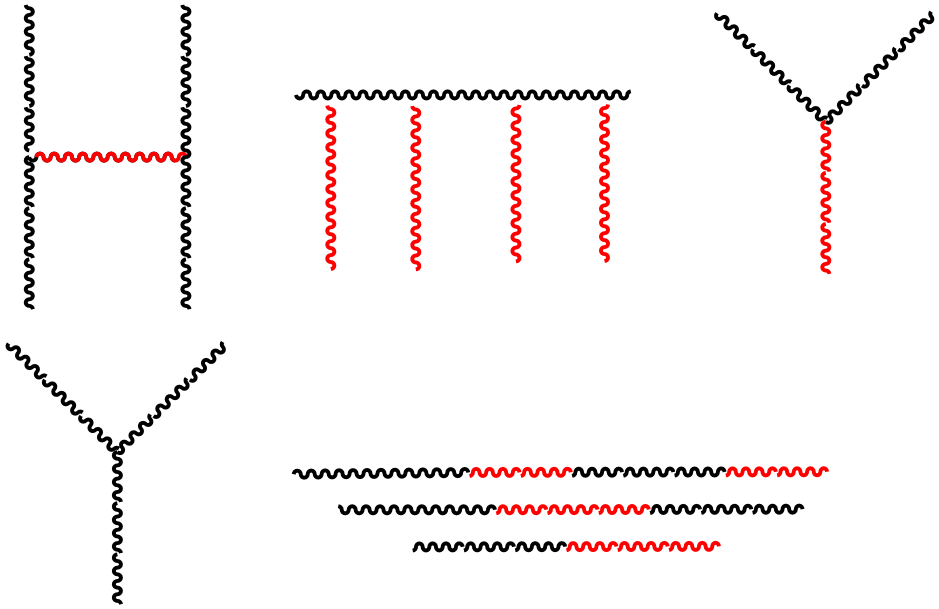

Figure 1.3 Various morphologies achievable via living polymerizations including polymeric combs, homostars, hetero-stars, and block copolymers

1.4 Mechanistic Considerations

Although living anionic polymerizations were realized in the 1950's, the search for living cationic polymerization conditions lagged considerably. Mechanistically, ionic polymerizations can suffer from the same termination events that plague radical polymerizations: namely premature termination via chain transfer reactions.[30] However, cationic chain ends differ significantly in their structure compared to carbanions and free radicals. Carbanions maintain a full octet of valence electrons, meaning they are

relatively stable and less susceptible to side reactions. Comparatively, radical chain ends contain one unpaired electron and are inherently neutral, yet highly reactive species. By comparison, carbenium ions contain 6 electrons, leaving an empty orbital and an overall deficient octet. Thus, carbenium ions are extremely reactive; the lifetime of these species rarely exceeds a few seconds.[30] As a result, polymers synthesized through carbocationic mechanisms have historically possessed broad MWDs and poorly defined structures due to their susceptibility towards to a variety of side reactions, including carbocation rearrangement, hydrogen abstraction, and chain transfer.

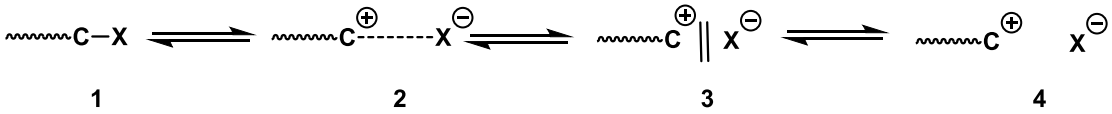

Figure 1.4 The Winstein ionicity spectrum of cationic polymers, which represents covalently bound chain ends (1), contact-ion pairs (2), solvent separated species (3), and free ions (4).

As recently as the mid-1970's, critics within the academic community doubted that living cationic polymerizations could ever be fully realized.[31] Reaction conditions such as solvent media, reaction temperature, monomer nucleophilicity, and nucleophilicity and size of the counterion were thought to contribute, either synergistically or individually, to the high reactivity of carbenium ions by affecting the ionicity of the propagating chain end. This is a highly unusual and unique phenomenon inherent to all ionic polymerizations. Unlike the active chain ends in radical polymerizations, which all consist of an identical radical species, ionic chain ends can exist as any number of active or inactive species, shown in Figure 1.4.[31] This concept is known as the Weinstein ionicity spectrum, which describes the inactive/dormant chain ends as covalently bound species (Species 1), a complex-ion pair (one that is ionized, yet

under the influence of the counterion species, Species 2), a solvent-separated pair (one that is ionized, yet under the influence of the solvent medium, Species 3) and dissociated free ions (Species 4). Uncontrolled carbocationic polymerizations often consist of a high concentration of free ions, leading to chain transfer reactions (Figure 1.5).[32] Free ions also result in rapid propagation, which often cause temperature exotherms, which synergistically increase the likelihood of side reactions.

The effect of solvent polarity on the chain end ionicity is relatively straightforward. As solvent polarity is increased, the equilibrium of the propagating chain end shifts to the right, promoting the formation of solvent separated ions and free ions. Cationic polymerizations also display unique characteristics with regard to reaction temperature. Interestingly, decreasing the reaction temperature generally shifts the chain end equilibrium to the right; this results in an increase in the monomer run number (that is, the number of monomer units added to a propagating chain before collapse of the chain end). Notably, however, the prevalence of side reactions decreases as reaction temperature is lowered. This is due to the observation that, for cationic systems, the activation energies of initiation and propagation are lower than the activation energies of chain transfer and termination.[33,34] Thus, side reactions and premature termination events can effectively be "frozen out" in cationic polymerizations.

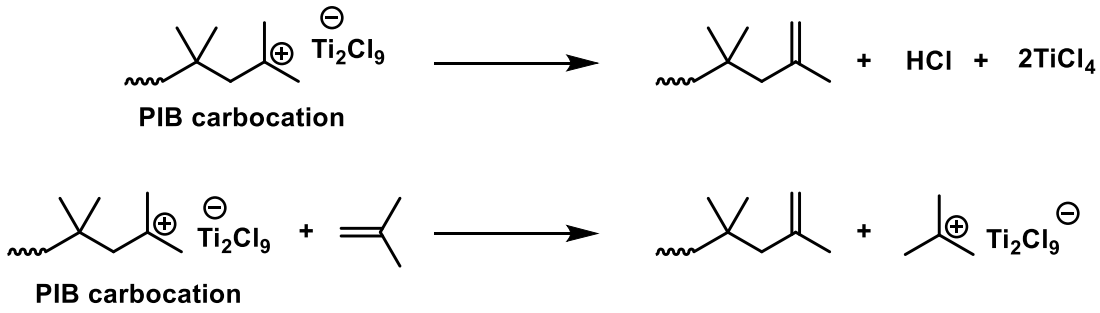

Figure 1.5 Two types of chain transfer reactions due to β-hydrogen abstraction. In the top reaction, the β-abstraction is unimolecular, due to increased acidity of the proton adjacent to the carbocation. The top reaction, which is bimolecular, occurs via a chain transfer to initiator.

Two factors that have an obvious effect on chain end ionicity are the strength of the Lewis acid and the size of the Lewis acid/counterion complex. Generally, anionic polymerizations have counterions that approximate point charges (e.g. Li^+ or Na^+) and the effect of the counterion on the propagating chain end is significant. On the other hand, cationic polymerizations have bulky counterions (e.g. $Ti_2Cl_9^-$), and thus they tend to interact less strongly with the carbenium ion and are less susceptible to solvent effects. The relative nucleophilicity of the counterion, however, plays a significant role in cationic polymerizations; strong Lewis acids such as $AlCl_3$ result in less nucleophilic counterions and extremely fast, uncontrollable polymerizations; while BCl_3, a much weaker Lewis acid, results in very slow and highly controlled polymerizations. Thus, judicious choice of the Lewis acid can reduce the prevalence of side reactions.

Another, less obvious factor that can lead to uncontrolled carbocationic polymerizations is the initiating species. Uncontrolled carbocationic polymerizations are often carried out in commercial processes using protic species such as HCl or adventitious H_2O in the presence of an alkyl-aluminum Lewis acid catalyst. Other Lewis acids (e.g. $TiCl_4$, $AlCl_3$, $SnCl_4$, or BCl_3) can also be used, depending on the desired

polymerization rate. Under normal conditions, Bronsted acids by themselves are not effective initiators in carbocationic polymerizations due to the nucleophilicity/basicity of the counterion (i.e. conjugate base). Use of these initiators often results in a variety of side reactions. For highly nucleophilic counterions, such as F^-, Cl^- or Br^-, a kinetic competition between the counterion and the monomer often results in addition of the counterion to the carbocation, rather than addition of monomer. Thus, a simple addition product, rather than polymerization and the formation of high polymers, is isolated.[35] Even in the presence of Lewis acid catalysts, a strongly basic counterion can lead to chain transfer via abstraction of a β-hydrogen, either during the initiation or propagation steps.[30,36] Steric interactions, carbocation stability, and monomer nucleophilicity can also lead to β-hydrogen abstraction, which are described in detail elsewhere.[8,30,37,38]

Ideally, a "truly living" polymerization is one in which chain-breaking or chain-terminating events are suppressed in their entirety. However, all "real" polymerizations undergo chain-transfer/termination events to some extent. Thus, for a "real" polymerization to be deemed sufficiently living, chain-transfer/termination events must occur at such a slow rate relative to propagation that they cannot be detected.[30] These types of systems allow for a number of interesting synthetic and kinetic phenomena. For systems with fast initiation, the total number of polymer chains is equivalent to the molar amount of the initiator, and precise control of number-average molecular weights (Mn) can be achieved. Various classes of compounds have been studied as carbocationic initiators, and these classes can influence many aspects of the polymerization (e.g. molecular weight dispersity, polymerization kinetics, and initiation efficiency).[14,39]

As discussed previously, the active chain end in radical polymerizations exists as a neutral radical species, and all active chain ends are comparable. Ionic chain ends can exist as any number of combinations along the Weinstein spectrum, and are therefore easily susceptible to reaction conditions to which radical polymers are immune. Thus, to reduce the likelihood of side reactions and/or termination events, careful control of the ionicity of the propagating cationic chain end should be undertaken. If the equilibria lie too far to the left (i.e. covalent chain ends) the polymerization rate proceeds too slowly to be useful; if too far to the right, an uncontrollable polymerization results. Thus, a controllable polymerization should ideally consist of chain ends with an equilibrium between a covalently bound species and a contact-ion pair.

Secondly, careful solvent and Lewis acid selection can provide a homogenous system in which the Lewis acid is capable of re-ionizing a dormant chain end. This equilibrium between active and dormant species is illustrated in Scheme 1.2. The re-activation of dormant chains permits the continued consumption of monomer, after the initial termination event has occurred. Additionally, a reversible-termination equilibrium has proven to be the cornerstone for the development of controlled isobutylene polymerizations, and other newer types of controlled/living polymerization such as group transfer and "living" free radical polymerizations.

1.5 Towards Living Polymerization

Taking these factors into account, it can easily be understood why the discovery of living cationic polymerizations followed the discovery of living anionic polymerizations by almost 30 years. Winstein's work on the characterization of ionic species,[32,40,41] however, resulted in a new paradigm of understanding in the field of ionic

polymerizations, which set the foundation for the techniques that would evolve into living cationic polymerization conditions.

The development of these conditions, and direct evidence to support Winstein's theory, took decades of research and a trial and error approach by multiple research groups. In 1975, Higashimura *et al.* demonstrated that styrene polymerizations initiated with acetyl perchlorate resulted in a bimodal distribution of molecular weight.[42] As the polymerization reaction proceeded to longer time frames, the lower molecular weight polymers steadily increased in molecular weight while the higher molecular weight species remained unaffected. Higashimura attributed this to the existence of two types of chain end ionicities: a highly reactive free ion (which resulted in the high molecular weight) and a combination of contact/solvent-separated ion pairs, which resulted in a steadily growing polymer.[42] Higashimura hypothesized that the relatively moderate solvent polarity of dichloromethane promoted the formation of free ions. Subsequent studies by the Higashimura group demonstrated that unimodal molecular weight distributions could be obtained using styrenic or vinylic monomers in less polar (co)solvents.[43,,45] During the same time period, Higashimura also demonstrated that similar unimodal distributions could be obtained using an iodine (I_2) initiating system.[46]

A key stepping stone towards achieving living carbocationic polymerizations was the development of quasiliving polymerizations.[47] Whereas non-living polymerizations often contain a large population of active free ions, leading to irreversible termination reactions, the development of quasiliving polymerizations utilized reversible termination reactions, which drove the propagating chain end ionicity to the left (i.e. contact-ion pairs and dormant species). These experimental conditions allowed for the instantaneous

population of active chain ends to be kept sufficiently low, such that the propensity for side reactions and chain transfer events was significantly low (Scheme 1.2). These experimental conditions included monomer starvation techniques (i.e. a slow, albeit continuous, addition of monomer to an active polymerization),[48,49,50] the incorporation of a common-ion salt,[51,52] or judicious choice of solvent/Lewis acid.[48,53,54] Another development in quasiliving polymerizations was Kennedy's development of "inifers" (initiator-transfer agents), which have been extensively studied.[55,56,57,58] In all cases, however, the resulting Mn values were less than theoretical, and broad molecular weight distributions were indicative of low initiation efficiency or the presence of side reactions. Thus, these systems were considered "not truly living" by many critics.[31]

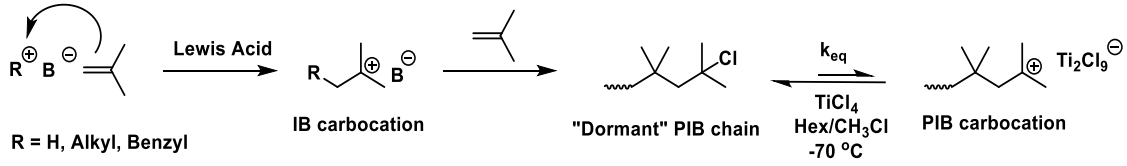

Scheme 1.2 Mechanism of isobutylene initiation and propagation under quasi-living polymerization conditions.

The breakthrough occurred in 1984, when Higashimura *et al.* reported the living polymerization of isobutyl vinyl ethers initiated by an HI/I_2 binary mixture.[59] Further studies using varying alkyl vinyl ethers[60] confirmed that under moderately cold temperatures (e.g. -5 to -35 °C), these systems displayed characteristics of living polymerizations, namely a direct proportion of polymer Mn to monomer conversion, and a linear increase in polymer Mn with additional charges of monomer to an *in situ* polymerization. The polymers also possessed nearly monodisperse MWDs with Mn values that were close to the calculated theoretical value. Following Higashimura's

seminal report, living polymerizations were reported for isobutylene,[61] propenyl ethers,[60] phthalimide functionalized vinyl ethers,[62] styrene,[63] and *p*-alkoxystyrenes.[64,65]

The development of polyisobutylene materials deserves special consideration. Isobutylene is a commercially important monomer that finds use in the adhesives, sealants, rubber, and synthetic oil industries. Notably, it has been widely established that isobutylene only forms high polymers via a cationic polymerization mechanism. Of these applications, the rubber and synthetic oil industries account for a significant portion of yearly isobutylene consumption. Additionally, academic interest in the design of advanced polyisobutylene based materials has risen steadily since the 1970's.[55,66-67,68,69]

1.6 Chemistry of Polyisobutylene

Polyisobutylene (PIB) is a fully saturated, aliphatic polymer derived from the cationic polymerization of isobutylene. For many applications, chemical functionality must be introduced into PIB for its practical utilization. Commercially available high molecular weight PIBs are often copolymers of isobutylene and isoprene (e.g. 98:2 isobutylene:isoprene),[70] which is commonly referred to as butyl rubber and/or isobutylene isoprene rubber (IIR). Low to moderate molecular weight PIBs are often homopolymers that find use in a variety of specialty applications, such as oil dispersants and lubricants, adhesives and tackifiers, and thermoplastic sealants. These homopolymers are produced industrially by a temperature controlled, chain-transfer-dominated process. This process is carried out between -10 to -30 °C and results in olefinic unsaturations of the PIB chain-end, which can either be *endo* olefin (15-25%) or *exo* olefin (75-85%) as shown in Figure 1.6. PIBs bearing primarily exo-olefin termini

(methyl vinylidene), termed highly reactive (HR) PIB, are desired due to their higher reactivity in downstream functionalization reactions.

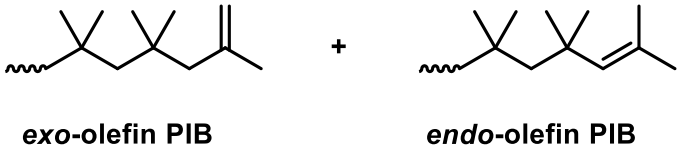

Figure 1.6 Chemical structures of *endo*-olefin and *exo*-olefin PIB.

New catalysts and improved processes toward HR PIB, which employ different polymerization techniques than those performed in industry, have been the subject of active investigations by several academic groups since the late 1970's. Early techniques included the "inifer method"[55,71] and later, the living techniques described above.[36] A benefit to using these routes is the opportunity of synthesizing telechelic PIB's bearing functionalities greater than 1. For PIBs synthesized via these techniques, tertiary-chloride end-groups can be obtained by quenching an *in-situ* polymerization with methanol, which effectively kills the Lewis Acid catalyst (BF_3, BCl_3, or $TiCl_4$). Traditionally, *tert*-chloride functionalized PIB was then transformed into the *exo* olefin (methyl vinylidene) by reaction with *t*BuOK in refluxing THF[55] or EtOK in refluxing THF/EtOH.[72] This approach is inherently inconvenient, as it requires long reaction times (~20 h), multiple purification steps, and results in the inevitable formation of a small amount (3-10%) of the *endo*-olefin.[73]

More recently, nearly quantitative *exo*-olefin-terminated PIBs have been synthesized via addition of a small molecule to a living carbocationic polymerization, usually after complete monomer consumption. This process, which can occur via two mechanisms, have collectively been referred to as the "direct quench" method. Nielsen *et*

al. reported the synthesis of methallyl terminated PIBs via the addition reaction of methallyl trimethylsilane to a PIB carbocation.[74] Methallyl terminated PIBs are structurally identical to *exo* olefin, and the synthetic route was nearly identical to a method developed by Wilczek and Kennedy a decade before.[75] A popular route using the direct quench method is via the controlled elimination reaction of a β-hydrogen. The Storey group has had great success using this technique, showing that hindered bases,[76] alkoxysilanes,[77] alkyl ethers,[78] or alkyl sulfides[79] can form the *exo* olefin with minimal side reactions. Whether via the addition reaction of organosilanes or the elimination reaction in the presence of the aforementioned species, the direct quenching process has been shown to form nearly quantitative *exo*-olefinic PIBs while simultaneously reducing the need for long reaction times and multiple purification steps.

The olefinic termini, whether obtained from the direct quenching method, post-polymerization modification of *tert*-chloride functional PIB, or the chain transfer dominated process favored by industry, is a valuable intermediate towards other functional groups. This is due to their higher reactivity in downstream functionalization reactions. Commercial polymers synthesized via this route include derivatives of PIB-succinic anhydride (PIBSA), which is a key intermediate in the lubricating oils and fuel industry.[80,81] Commercially, PIBSA is produced via an Alder-*ene* reaction between *exo*-olefin-terminated PIB and maleic anhydride, usually under high temperature and pressure. This reaction is shown in Scheme 1.3.

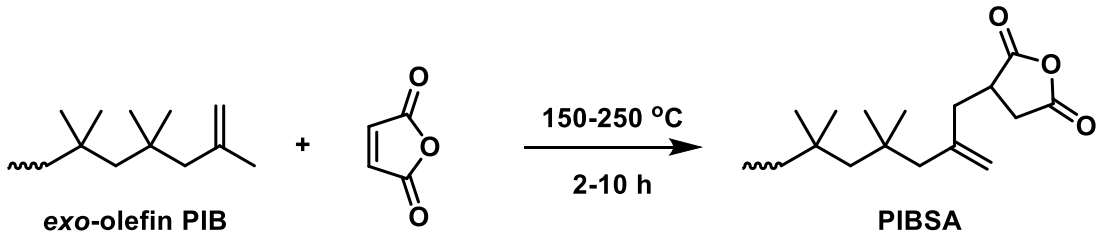

Scheme 1.3 Industrial synthesis of PIBSA

A number of academic research groups have also demonstrated the utility of *exo*-olefin-terminated PIBs, as well. The Kennedy group, among others, has worked extensively towards the functionalization of *exo*-olefin PIBs with a variety of chemistries.[82,83,84] Chang and coworkers reported the synthesis of epoxide-terminated PIBs via the classic epoxidation reaction of olefins using *m*-chloroperoxybenzoic acid, which were then isomerized in the presence of $ZnBr_2$ to give aldehyde terminated PIBs.[57] Kemp *et al.* have reported that ozonolysis of the *exo*-olefin end groups forms ozonide chain ends, which can be reduced in the presence of trimethylphosphite to give methyl ketones.[68] These ketones could then be oxidized to yield carboxylic acid terminated PIBs. *Exo*-olefin PIBs have also been utilized as substrates for thiol-ene[85] and Friedel-Crafts alkylation reactions.[86]

Similar to the wide utility of *exo*-olefin-terminated PIBs, hydroxyl-terminated PIBs have also allowed for the synthesis of advanced materials. One of the earliest routes towards achieving hydroxyl-functional PIBs was reported by Iván and Kennedy, who utilized the hydroboration-oxidation reaction to form primary hydroxyl terminated PIBs.[15,87] These materials can be further reacted with chlorotrimethylsilane to yield trimethylsilane-terminated PIBs or with an isocyanate to give a urethane.[15] Kennedy *et al.* have also reported the formation of hydroxyl-terminated PIBs via the reduction of the

aldehyde functionalized PIBs described above. The ketone-terminated PIBs described by Kemp *et al.* can be converted to secondary hydroxyls via reduction in the presence of lithium aluminum-hydride.[68] Guhaniyogi and coworkers reported the synthesis of phenol-terminated PIBs via the Friedel-Crafts alkylation reaction using phenol and BF_3-etherate.[86] Epoxidation of these materials was subsequently reported,[88] to form glycidyl-ether-terminated PIBs, which were then utilized to form PIB based epoxy networks.

Although *exo*-olefin and hydroxyl-functionalized PIBs are highly modular synthetic intermediates, their use requires multiple synthetic procedures that include purification, washing, and drying steps between each synthetic transformation. Additionally, the use of cleaning solvents and high concentrations of toxic/explosive reactants creates a high volume of chemical waste. These factors reduce the commercial viability of obtaining advanced PIB materials, which has limited the commercial application of end functional polyisobutylenes to the lubrication and oil additives market.

One attractive method towards PIB functionalization is the use of small molecule reactants that cap the growing polymer chain end, a process which is known as "end quenching." Similar to the direct-quenching method used to synthesize *exo*-olefin PIB, these small molecule reactants can be added *in-situ* to a polymerization after complete monomer consumption to functionalize the PIB chain-end. These "quenching agents" often possess a chemical functionality that is different from *exo*-olefin, and in some cases may contain multiple functionalities. End-quenching is elegant in its utility and simplicity, as it overcomes many of the drawbacks that are inherently present in the previously described routes. Notably, it has proven to be a direct and quantitative route towards functionalized PIBs, which reduces the time and multiple purification procedures

required for systems functionalized via post-polymerization modification. Also, telechelic PIBs synthesized via reactive end-quenching have allowed for new generations of thermoplastic elastomeric materials[89] and other advanced applications.[70,90] One significant drawback of the end-quenching route, however, is the strict criteria for small molecules that can be used as end-quenching agents. A quencher molecule must preferentially react with the carbocationic chain end, rather than the more abundant Lewis acid, and the quenching reaction must compete kinetically with decomposition pathways of the carbocation, particularly carbocation rearrangement. Furthermore, reaction conditions that promote end-quenching (namely, the requirement for dilute conditions and low reaction temperatures) have proven to be commercially unviable.

The direct functionalization of living PIB via the end-quenching approach has been reported using quenching agents of several characteristic types, many of which contain functional groups other than *exo*- lefin. One early type of quenching agent consisted of olefins that add only once to the living PIB chain, either due to steric hindrance or low nucleophilicity/reactivity of the quenched species, hindering further reaction. Feldthusen and coworkers reported the use of diphenyl ethylene, which results in a highly stable and sterically hindered end-group which prevents further addition reactions from taking place.[91] More recently, De and coworkers reported the use of C_4 olefins (primarily butadiene) that result in allyl-chloride-functionalized PIBs.[92] As mentioned earlier, the addition reaction of organosilanes containing allyl or methallyl functional groups have been reported, which are also examples of end-quenching.

The Storey group has had particular success demonstrating the utility of aromatic substrates as quenching agents (Scheme 1.4). Heterocyclic aromatic substrates, such as

n-alkyl pyrroles, have been reported to effectively cap living PIB chain ends,[93,94] but significant work has been dedicated towards the utilization of alkoxybenzenes.[95,96] Alkoxybenzenes bearing various chemical functionalities are commercially available, and primary bromide functionalized PIBs have proven to be highly modular substrates that allow for further modification.[90,96,97] Additionally, synthetic modification of an alkoxybenzene prior to its use as a quenching agent has allowed for the synthesis of various PIB derivatives for advanced applications.[70,98] Finally, phenolic PIBs can be quantitatively synthesized in a one pot process using isopropyl functionalized alkoxybenzenes.[96]

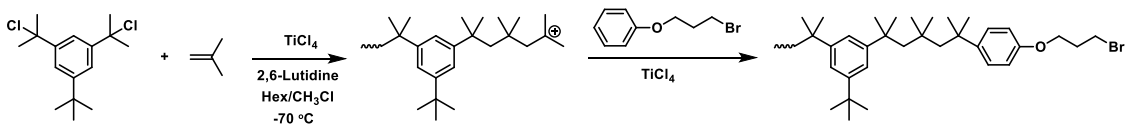

Scheme 1.4 End-quenching of a living polyisobutylene chain end with (3-bromopropoxy)benzene.

Recently, there has been interest in PIB macromonomers possessing more highly reactive terminal unsaturations, especially (meth)acrylate[70,98,99,100] and vinyl ether.[90] These systems may be cured by thermal or photo-initiated radical chain polymerization, or in the case of vinyl ether, by photo-initiated cationic polymerization. Among a number of potential biomedical and industrial applications for these materials, an application of particular interest is their use in the formation of PIB-based thermosets for sealant and gas barrier applications. For example, traditional PIB sealants used in insulating glass units (IGU) consist of high molecular weight PIB thermoplastics that are

applied at elevated temperature as a melt; however, these materials tend to creep under certain adverse circumstances, resulting in eventual aesthetic and/or mechanical failure. PIB thermosets represent an attractive replacement, as they can be applied at room temperature and upon curing, exhibit superior rheo-mechanical properties and are creep resistant.

1.7 Functional Polyisobutylenes via Unconventional Methods

The synthesis of multifunctional PIBs via living carbocationic polymerizations are synthetically complex and require expensive initiators, specialized equipment, and highly trained operators. Until 2017, some unconventional methods describing the synthesis of multifunctional PIBs had been reported, to varying degrees of success. In 1969, a patent application detailing the synthesis of difunctional PIBs using molecular sieves was filed, but the initiation and functionalization mechanisms were poorly understood.[101] Furthermore, the average functionality claimed using this process was approximately 1.8, meaning these systems were not truly difunctional.

Another method of synthesizing multifunctional PIBs is via a degradative process using butyl rubber substrates. As mentioned previously, butyl rubbers consist of long segments of polyisobutylene with a small fraction of isoprene units randomly dispersed throughout the polymer. The resulting backbone unsaturation (from the isoprene residue) is often used as a crosslinking junction in butyl rubber vulcanization reactions, but it can also be used as a reactive site for epoxidation[102] and ozonation[103] reactions. When butyl rubbers are subjected to ozonolysis, significant molecular weight degradation has been reported and the resulting materials were observed to possess ketone, aldehyde, and carboxylic acid moieties.[104] The molecular weight degradation was hypothesized to

occur via formation of an ozonide intermediate, which then cleaves to form the aforementioned carbonyl containing compounds. Ozonolysis reactions have also been reported on acrylate-butadiene copolymers,[105] in a process that was described by the authors as the "constructive degradation;" this term was coined to describe the degradation of a high molecular weight polymer, resulting in lower molecular weight, multifunctional polymers. Similarly, Chasmawala *et al*. utilized poly(isobutylene-*co*-butadiene) substrates in the presence of trialkyl-borane catalysts via a cross-metathesis reaction, although this approach required expensive catalysts and reagents.[106]

Using a similar approach, Kennedy *et al.* reported that Lewis and Bronsted acids could degrade butyl and halo butyl rubbers via a protonation/cleavage reaction.[107] The proposed mechanism involves protonation of the main-chain unsaturation followed by a cleavage event that yields two new chain ends. Of these two chains, one possesses an olefin functionality while the other contains a tertiary chloride moiety. Although this approach was proposed to have some synthetic utility, the absence of a nucleophile or chain capping agent would allow for significant rearrangement of the carbocationic chain end and loss of functionality.

Forty seven years later, Campbell and coworkers corrected this deficiency and were the first to report the synthesis of multifunctional telechelic PIBs via a constructive-degradation approach, a process which they termed "cleavage/alkylation".[108] An overview of this process is shown in Scheme 1.5. Using (3-bromopropoxy)benzene as a quenching agent and a variety of reaction temperatures, reaction times, and catalysts, Campbell *et al.* demonstrated that multifunctional PIBs bearing an easily displaceable

primary bromide moiety could be synthesized without the need for specialized equipment, exhaustively purified starting materials, or rigorously dried conditions.

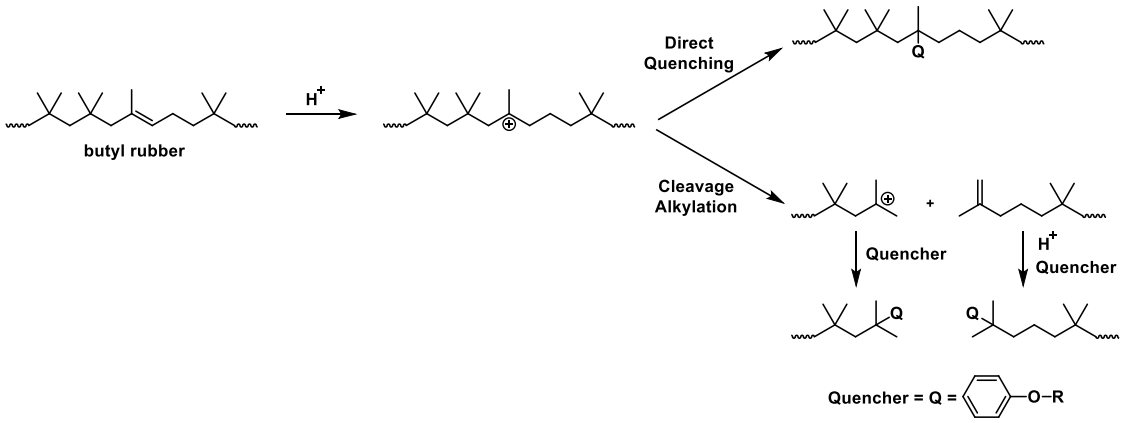

Scheme 1.5 Mechanistic representation of the cleavage/alkylation reaction of butyl rubber in the presence of a quenching agent.

From the humble beginnings of boiling mixtures of turpentine and sulfuric acid, through the militarization of the rubber industry for Allied War effort and the development of living polymerization conditions that allowed for precise control over polymer morphology and functionality, the areas of polymer science and rubber technology have continuously evolved. Within these areas, the discovery of the cleavage/alkylation process represents a burgeoning approach towards the development of advanced materials. The following chapters show our small contribution towards furthering the understanding and utility of the cleavage/alkylation process, and the field of cationic polymerizations and rubber technology as a whole.

CHAPTER II – SYNTHESIS, CHARACTERIZATION, AND PHOTOPOLYMERIZATION OF (METH)ACRYLATE FUNCTIONAL POLYISOBUTYLENE MACROMERS PRODUCT BY CLEAVAGE/ALKYLATION OF BUTYL RUBBER

This chapter was co-authored by C. Garrett Campbell, Bin Yang, and Robson Storey.

2.1 Abstract

Telechelic linear polyisobutylene (PIB) prepolymers bearing bromide moieties were prepared via acid catalyzed cleavage/alkylation reactions of butyl rubber in the presence of (3-bromopropoxy)benzene. The primary bromide moiety was then reacted with potassium (meth)acrylate, resulting in a library of (meth)acrylate functionalized linearPIB prepolymers. The number average functionalities (F_n) of these PIB prepolymers ranged from 2.8–7.9 and the functional equivalent weights ranged from 2,300-4,700 g/mol according to ^{1}H NMR and GPC-MALLS. For comparative purposes, a trifunctional PIB telechelic homostar prepolymer was synthesized via living polymerization and end quenched with 4-phenoxy-1-butyl acrylate, and the f_{avg} and equivalent weight was found to be 3.0 and 3,034 g/mol, respectively. Additionally, GPC-MALLS analysis indicated that targeted molecular weights of each macromer were achieved with the absence of coupling, chain end degradation, or premature polymerization of the (meth)acrylate moieties. Each prepolymer was photocured into a film using Darocur 1173 photoinitiator, and the curing kinetics were monitored by real time Fourier-transform infrared spectroscopy. Generally, all systems reached ~100% conversion by 1800 s, but the linear PIB prepolymers displayed slower curing rates

compared to the homostar PIB macromer, which reached 100% conversion after only 212 s. Moreover, the curing rate of the linear PIBs was apparently dictated by the molecular weight of the prepolymer; lower molecular weight linear PIBs were found to have faster curing rates than their higher molecular weight counterparts, despite having fewer acrylate groups to participate in the photocuring reaction. The thermo-mechanical transitions and crosslink density of each film were determined by dynamic mechanical analysis, and the mechanical behavior was measured via tensile testing. Results from tensile testing indicated that the molecular weight, functional equivalent weight, and morphology of the PIB prepolymers all had a significant effect on the Young's modulus of the resulting networks. The percent strain at break for most networks ranged from 34-54%, but the network derived from the lowest molecular weight PIB reached 113% strain before failure. Finally, the percent extractables from each film were measured using sol fraction experiments.

2.2 Introduction

Polyisobutylene (PIB) and PIB-based copolymers have been used in a wide variety of applications including adhesives, sealants, tackifers, and strength modifiers, fuel and lubricating oil additives, barrier elastomers and other rubber applications, and biomedical devices.[70,109] PIB-based polymers are often chosen for these applications due to their low gas permeability, excellent damping characteristics, general inertness, especially toward oxygen and ozone, and resistance to harsh solvents and stress cracking.[6] However, PIB homopolymers are unsuitable for conventional vulcanized rubber applications due to their totally saturated backbone, and must be copolymerized with a suitable diene to provide main chain unsaturations for sulfur vulcanization.[110]

Butyl rubber, a copolymer consisting of isobutylene and isoprene (95-98% isobutylene) is one such copolymer, and is widely regarded as the industry standard for synthetic rubber based sealants due to its low air permeability and superior resistance to heat and ozone degradation.[6]

Crosslinked polyisobutylene polymers can also be created by performing end-linking reactions on end-functional or telechelic polyisobutylenes, prepared either through the inifer method or by living carbocationic polymerization.[58] A prime example of this approach is the crosslinking of hydroxyl-telechelic PIBs with polyisocyanates and optional chain extenders to create PIB-based polyurethanes.[111] Although telechelic PIBs have been around since the late 1970's, only recently have PIB homopolymers been terminally functionalized with photoreactive functional groups, to create photopolymerizable telechelic PIB macromers.[85],[112-] Considering the abundance of literature on photoinitiated radical crosslinking reactions and the commercial importance of thermosetting acrylate and methacrylate resins in the coatings, adhesive, and construction industries, it is interesting that only until recently has this chemistry been explored as a means of creating PIB based networks.

Previous work in our laboratory has focused on the *in situ* functionalization of PIB via alkoxybenzene quenching of living polymerizations. [95,96] Of specific relevance to this work was the application of alkoxybenzene quenching towards synthesis of photopolymerizable (meth)acrylate-terminated PIBs. Quenching of living PIB with a phenoxyalkyl (meth)acrylate compound yielded a (meth)acryloxyalkyl-terminated PIB macromer directly.[98] Alternately, living PIB was quenched with isopropoxybenzene, followed by cleavage of the isopropoxy group and subsequent reaction with

(meth)acryloyl chloride, to yield an aromatic (meth)acryloxyphenyl-terminated PIB macromer.[69] Both routes were used to produce three-arm star PIB (meth)acrylates, which were photocured into networks.

Campbell and Storey recently reported a method for producing multifunctional PIBs via acid-catalyzed cleavage/alkylation reactions (constructive degradation) of PIB-based copolymers such as butyl rubber in the presence of an alkoxybenzene.**Error! Bookmark not defined.** Herein, we describe the synthesis of a library of constructively degraded PIB macromers bearing phenoxypropyl (meth)acrylate moieties and their use as photopolymerizable macromers to form UV cured networks. The resulting films were characterized, and the results are compared to a PIB network formed from telechelic macromers made via traditional living polymerizations.

2.3 Experimental

2.3.1 Materials

Hexane (anhydrous, 95%), methanol (anhydrous, 99.8%), methylene chloride (anhydrous, 99.8%), heptane (anhydrous, 98%), dimethylformamide (anhydrous, 95%), titanium tetrachloride ($TiCl_4$) (99.9%), 2,6-lutidine (99.5%), (3-bromopropoxy)benzene (anhydrous, 98%), tetrahydrofuran (THF) (anhydrous, 99.9%), tetrabutylammonium bromide (99%), dichloromethane-d_2 (DCM-d_2,f CD_2Cl_2), 4-methoxyphenol (MEHQ) (99%), acrylic acid (anhydrous, 98%), methacrylic acid (anhydrous, 98%), phenoxybutyric acid (98%), borane−tetrahydrofuran complex (BH_3·THF, 1 M), and potassium carbonate (K_2CO_3), were purchased from Sigma-Aldrich and used as received. Magnesium sulfate ($MgSO_4$) (anhydrous), sulfuric acid (98%), chloroform-d ($CDCl_3$), and diethyl ether (anhydrous, 95%) were purchased and used as received from Fisher

Scientific. The photoinitiator Darocur 1173 (2-hydroxy-2-methyl-1-phenylpropan-1-one) was purchased from Ciba and used as received. Isobutylene (IB, BOC Gases) and methyl chloride (Gas and Supply) were dried by passing the gaseous reagent through a column of $CaSO_4$/molecular sieves/$CaCl_2$ and condensing within a N_2-atmosphere glovebox immediately prior to use. The acrylate quencher, 4-phenoxy-1-butyl acrylate,[98] and potassium (meth)acrylate were synthesized as previously reported and stored at 0 °C. The trifunctional initiator, 1,3,5-tris-(1-chloro-methyl-ethyl)-benzene (TCC), was prepared by first synthesizing 1,3,5-tri(1-hydroxyl-1-methylethyl)benzene (TCOH) according to a literature procedure,**Error! Bookmark not defined.** followed by reaction of the latter with dry HCl at 0 °C.[116] Butyl rubber samples (EXXON™ Butyl 365 and Butyl 068) were obtained from ExxonMobil Corporation. Characterization via GPC/MALLS and ^{1}H NMR indicated that Butyl 365 had a number average molecular weight (M_n) of 1.91 x 10^5 g/mol with a molecular weight distribution (MWD) of 1.66, and the mole fraction of isoprene (IP) comonomer units in the copolymer, F_{IP}, was determined to be 0.0230 (IB units/IP units = 42.5).[108] For Butyl 068, the M_n and MWD were measured to be 3.37 x 10^5 g/mol and 1.29, and the F_{IP} was determined to be 0.0108 (IB units/IP units = 91.6).

2.3.2 Instrumentation

Nuclear magnetic resonance (NMR) spectra were obtained using a 300 MHz Bruker AVANCE III NMR (TopSpin 3.1) spectrometer. All ^{1}H chemical shifts were referenced to TMS (0 ppm). Samples were prepared by dissolving the polymer in either $CDCl_3$ or CD_2Cl_2 (5%, w/v) and charging this solution to a 5 mm NMR tube. For quantitative integration, 32 transients were acquired using a pulse delay of 27.3 s. For the

PIB prepolymers prepared via living polymerization, the signal due to the phenyl protons of the initiator (7.17 ppm, 3H, singlet) was chosen as an internal reference for functionality analysis.

Real time (RT)-FTIR monitoring of isobutylene polymerizations was performed using a ReactIR 45m (Mettler-Toledo) integrated with a N_2-atmosphere glovebox (MBraun Labmaster 130).[117,118] Isobutylene conversion during polymerization was determined by monitoring the area above a two-point baseline of the absorbance at 887 cm^{-1}, associated with the = CH_2 wag of isobutylene.

Number-average molecular weights (M_n) and molecular weight distributions (MWD) were determined using a gel-permeation chromatography (GPC) system consisting of a Waters Alliance 2695 separations module, an online multi-angle laser light scattering (MALLS) detector fitted with a gallium arsenide laser (power: 20 mW) operating at 658 nm (miniDAWN TREOS, Wyatt Technology Inc.), an interferometric refractometer (Optilab T-rEX, Wyatt Technology Inc.) operating at 35 °C and 685 nm, and either two PLgel (Polymer Laboratories Inc.) mixed E columns (pore size range 50-10^3 Å, 3 μm bead size) or two mixed D columns (pore size range 50-10^3 Å, 5 μm bead size). Freshly distilled THF served as the mobile phase and was delivered at a flow rate of 1.0 mL/min. Sample concentrations were ca. 5-8 mg of polymer/mL of THF, and the injection volume was 100μL. The detector signals were simultaneously recorded using ASTRA software (Wyatt Technology Inc.), and absolute molecular weights were determined by MALLS using a *dn*/*dc* calculated from the refractive index detector response and assuming 100% mass recovery from the columns.

Photopolymerization kinetic data were obtained using transmission RT-FTIR spectroscopy by monitoring the disappearance of the (meth)acrylate absorbances at 1638 and 1615 cm^{-1}. The RT-FTIR studies were conducted using a Nicolet 8700 spectrometer with a KBr beam splitter and a DTSG detector with a 320-500 nm filtered UV light source with an intensity of 18.5 $mW \cdot cm^{-2}$. Each sample was degassed under vacuum for 12 h, sandwiched between two NaCl plates, and exposed to a UV light. For all samples, the UV source was turned on after a 10 s delay to provide an adequate baseline. A series of scans were recorded, where spectra were taken approximately 1 scan/3.3 s with a resolution of 6 cm^{-1} for 1800 s.

Dynamic mechanical analysis (DMA) was conducted using a Q800 (TA Instruments) instrument in air using tensile mode. The frequency was set at 1 Hz, the pre-load static force at 0.005 N, the oscillatory amplitude at 15 μm, and the track setting at 125%. Sample dimensions were approximately 12×6.6×0.80 mm. Experiments were performed at a heating rate of 3 °C/min and a temperature range of -100 to 50 °C and analyzed with TA Universal Analysis software. T_g was recorded as the onset temperature of the drop of the storage modulus and as the temperature corresponding to the peak of the tan δ curve, and the two were compared. Peak deconvolutions were carried out using Origin 9.1 software.

The fraction of unreacted macromers in cured samples (sol fraction) was determined by solvent extraction experiments, performed in triplicate. Samples (5.0×5.0×0.80 mm) were cut from UV cured networks and immersed in 10 mL dry THF at room temperature. The sample was removed from THF after 60 h and placed in a tared

scintillation vial. After drying in a vacuum oven overnight at room temperature, the sample weight was recorded.

Tensile testing of PIB networks was conducted using a MTS Alliance RT/10 system and MTS Testworks 4 software. Specimens were cut into bars with dimensions of 60 × 6.6 × 0.75 mm, clamped using a 500 N load cell, and tested at a crosshead speed of 5 mm/min at room temperature, following ASTM D 638.45. Young's modulus was determined from the initial slope of the stress vs. strain curves. The reported values were the average of at least three different specimens.

2.3.3 Synthesis of Trifunctional PIB Acrylate.

Trifunctional living PIB was synthesized and quenched with 4-phenoxy-1-butyl acrylate via previously reported methods.[98] Polymerization and quenching reactions were performed within an N_2-atmosphere glovebox equipped with a cryostated heptane bath. To a dry 1 L 4 neck round-bottom flask, equipped with an overhead stirrer, thermocouple, and ReactIR probe, and immersed in the heptane bath, were charged 165 mL chilled hexane, 248 mL chilled methyl chloride, 0.182 mL (1.60 mmol) 2,6-lutidine, 2.46 g (8.00 mmol) TCC, and 105 mL (1.30 mol) chilled IB. The mixture was equilibrated to -70 °C with stirring, and polymerization was initiated by addition of 0.47 mL (neat and at room temperature, 4.3 mmol) $TiCl_4$, followed by an additional 0.47 mL of $TiCl_4$ after 10 min. Monomer conversion was monitored using RT-FTIR data, and upon full conversion (75 min), 4-phenoxy-1-butyl acrylate (10.1 mL, 48.0 mmol) and $TiCl_4$ (9.59 mL, 87.5 mmol) were sequentially added to quench the reaction. Conversion of the quenching reaction was monitored via ^1H NMR by comparing the ratio of the aromatic initiator protons to the phenoxy methylene tether protons, and upon full

conversion the balance of the reaction was terminated with chilled methanol. The reactor was then transferred to a fume hood and slowly warmed to room temperature to allow evaporation of methyl chloride, after which the PIB was concentrated under an N_2 stream. The resulting mixture was precipitated into methanol under vigorous stirring, after which the methanol layer was decanted. The precipitate was collected by re-dissolution in fresh *n*-hexane, and the resulting solution was re-precipitated into excess methanol. The precipitate was collected by re-dissolution in fresh hexane, and the resulting solution was washed twice with deionized water, dried over Na_2SO_4, and then vacuum stripped to yield the isolated polymer. The product was then characterized via GPC-MALLS and ^{1}H NMR.

2.3.4 Acid-Catalyzed Cleavage/Alkylation of Butyl Rubber.

The following is a representative procedure adapted from Campbell *et al.*[Error! Bookmark not defined.] A 2 L round bottom flask equipped with a magnetic stir-bar was charged with Butyl 365 (50.58 g, 20.6 mmol isoprene units) and dissolved in 750 mL of n-hexane and 500 mL dichloromethane. The reaction mixture was chilled to -70 °C, and (3-bromopropoxy)benzene (50.5 g, 0.235 mol), conc. H_2SO_4 (1.25 mL), and $TiCl_4$ (25.0 mL , 0.228 mol) were added in quick succession under stirring. The reaction was stirred at -70 °C for 20 h, after which it was quenched with chilled methanol. The resulting solution was warmed to room temperature and concentrated under an N_2 stream, after which it was purified using the procedure described above. After vacuum stripping, the product was characterized via GPC-MALLS and ^{1}H NMR.

2.3.5 (Meth)acrylate-Modification of Product of Cleavage/Alkylation of Butyl Rubber.

The following is a representative procedure. A 1L round-bottom flask was charged with the product obtained from the cleavage/alkylation of butyl rubber (12.174 g, 4.97 mmol alkyl bromide equivalents) dissolved in 700 mL of a 50:50 (v:v) mixture of heptane:DMF, MEHQ (0.5321 g, 4.286 mmol), tetrabutylammonium bromide (0.2874 g, 0.8915 mmol), and potassium acrylate (1.521 g, 13.81 mmol). The flask was fitted with a reflux condenser equipped with a dry N_2 inlet/outlet, and the system was purged for 15 minutes prior to heating. The N_2 purge was maintained over the course of the reaction. The mixture became monophasic upon heating to 90 °C, and the resulting solution was refluxed at 90 °C overnight. Reaction conversion can be monitored via ^{1}H NMR by tracking the shift of the terminal methylene peak of the quencher from 3.62 ppm to 4.34 ppm, which corresponds to the disappearance of the primary bromide and appearance of the acrylate. Upon full conversion, the reaction mixture was cooled. The resulting biphasic mixture was transferred to separatory funnel, and the DMF layer was removed. The heptane layer was then washed with deionized (DI) water three times and concentrated under an N_2 stream. The concentrated mixture was then precipitated into methanol and purified following the procedure mentioned above. The dried polymer was then characterized via ^{1}H NMR and GPC-MALLS to ensure the absence of premature crosslinking. The methacrylate functionalized derivative was synthesized using the same method.

2.3.6 Preparation of Films.

Various formulations of PIB and photoinitiator were prepared and cured using the following representative procedure. To a small scintillation vial were charged 1.0 g of trifunctional PIB acrylate and Darocur 1173 photoinitiator (20 mg, 2 wt %), and the two

were mixed thoroughly with a spatula by hand. For higher molecular weight PIBs, 2.00 mL of pentane was added to reduce the viscosity and ensure homogenous mixing. The mixture was cast upon a glass slide that was pre-treated with Rain X and degassed in a vacuum oven overnight. After degassing, a 0.75 mm Teflon spacer was added, and the sample was immediately sandwiched between a second pre-treated glass slide and subsequently cured for 30 min under a medium pressure mercury UV lamp at an intensity of 18.5 mW cm^{-2}. For the curing kinetics studies, each formulation was cast upon a salt plate, rather than the treated glass slides described above, and degassed in a vacuum overnight. After curing, each film was extracted with excess THF for 60 h followed by drying under high vacuum for 24 h. The pre- and post-extraction film weights were compared, and the percent extractable material in the network was calculated.

2.4 Results and Discussion

2.4.1 Synthesis of Trifunctional acrylate-terminated PIB

The ^{1}H NMR spectrum of trifunctional PIB quenched with 4-phenoxy-1-butyl acrylate is shown in Figure 2.1. Alkylation exclusively *para* to the alkoxy moiety was observed as evidenced by the clean doublets of the aromatic quencher protons (6.80 ppm, 7.23 ppm). The intensity of the olefinic protons (5.70-6.50 ppm) relative to the methylene tether protons (triplets at 3.98 and 4.22 ppm) indicated no decomposition of the acrylate. Quantitative comparison of the methylene tether protons or the acrylate olefinic protons relative to the aromatic initiator protons also indicated complete functionalization of all PIB chain ends. The GPC chromatogram of the purified trifunctional PIB acrylate, shown in Figure 2.2, indicated that no coupling, degradation, or polymerization of the acrylate moiety occurred during purification. Measurement via

GPC-MALLS showed that the M_n and MWD of the polymer were 10,000 g/mol and 1.05, respectively.

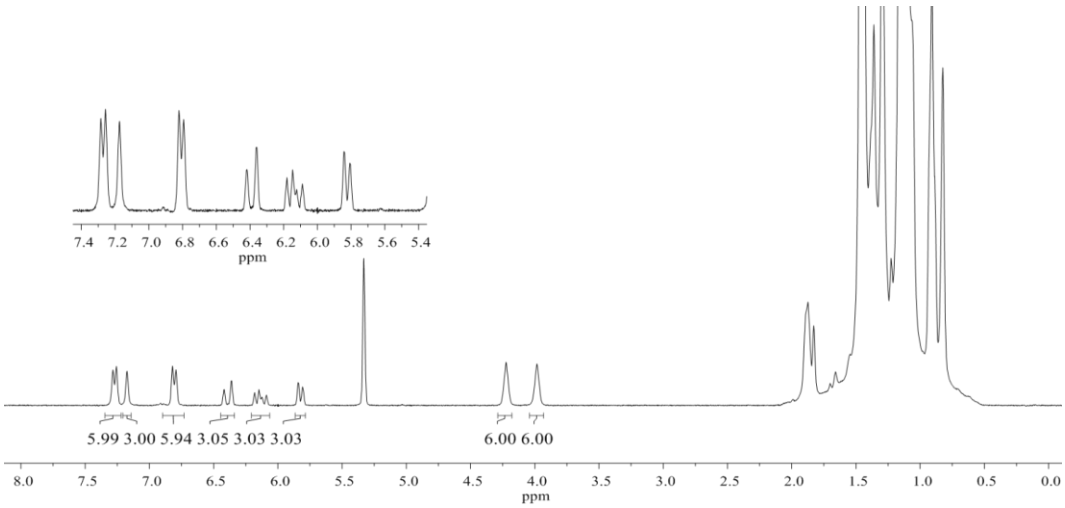

Figure 2.1 ^{1}H NMR (300 MHz, DCM-d_2, 25 °C) spectrum of trifunctional PIB acrylate, synthesized via living polymerization of isobutylene at -70 °C and end-quenched with 4-phenoxy-1-butyl acrylate. Integrations are referenced to the initiator residue at 7.18 ppm.

2.4.2 Synthesis of Multifunctional PIBs by Cleavage/Alkylation of Butyl Rubber.

Cleavage/alkylation reactions on butyl rubber substrates represent a cost effective, facile method of producing multifunctional PIBs possessing a linear morphology with functional groups both pendant to the PIB backbone and covalently attached to the polymer chain ends.**Error! Bookmark not defined.** The cleavage/alkylation process is highly modular, and a range of molecular weights and functionalities can be easily obtained by modifying temperature, reaction time, choice of Lewis acid catalyst and its concentration, quencher concentration, and/or isoprene content of the starting butyl rubber. Typically, the end product contains no residual backbone unsaturation, i.e., all isoprene repeat units either undergo cleavage or addition reaction with the quencher. The functional equivalent weight (EW_Q) of the product, defined as the mass of polymer per equivalent of covalently attached quencher moieties, can be calculated as previously reported,**Error!**

Bookmark not defined. from the ratio of isobutylene repeat units per quencher units, IB/Q, determined using ^{1}H NMR. The number average functionality of the product, F_n, is then calculated as M_n/EW_Q.

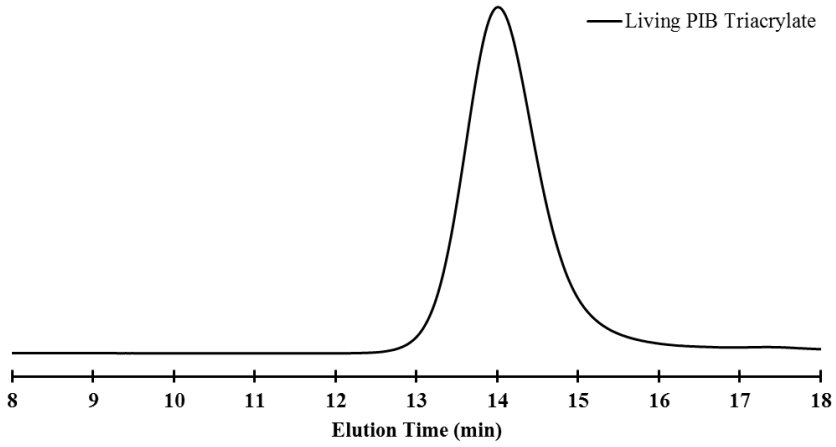

Figure 2.2 GPC chromatogram of trifunctional PIB acrylate, synthesized via living polymerization of isobutylene at -70 °C, followed by end-quenching with 4-phenoxy-1-butyl acrylate. Characterization via GPC confirmed the absence of radical crosslinking after sample workup.

Two butyl rubber substrates were used to demonstrate the modularity of the cleavage/alkylation process and the range of molecular weights and functionalities that can be isolated: ExxonMobil Butyl 365 (F_{IP} = 0.0230 (IB units/IP units = 42.5)) and Butyl 068 (F_{IP} = 0.0108 (IB units/IP units = 91.5). (3-Bromopropoxy)benzene was used as the quenching agent to allow for easy post-polymerization modification via nucleophilic substitution of the primary bromide. The reaction conditions and resulting M_n, MWD, IB/Q, EW_Q, and F_n values are listed in Table 2.1.

Figure 2.3 compares the GPC chromatograms for the Butyl 068 reactant and various products obtained therefrom by cleavage/alkylation in the presence of (3-bromopropoxy)benzene quencher (Table 2.1, Trials 2-4). These three trials show that increasing the quencher concentration relative to the concentration of IP units promotes

backbone quenching at the expense of cleavage and systematically raises the M_n and F_n of the product at a relatively constant EW_Q.

Table 2.1 Reaction Conditions for Cleavage/Alkylation Reactions on Various Butyl Rubbers[a]

Trial	Butyl Rubber[b]	Time (h)	[IP][c] (mM)	[Q][d] (M)	[$TiCl_4$] (M)	[H_2O] (mM)	[H_2SO_4] (mM)	M_n[e] (g/mol)	PDI	$\frac{IB}{Q}$	EW_Q[f] (g/eq)	F_n[g]
1	365	20	17	0.19	0.19		19	17,300	1.58	35.5	2,260	7.6
2	068	21	12	0.056	0.37	56		12,700	1.42	78.4	4,670	2.7
3	068	40	12	0.12	0.11		21	27,500	1.48	76.5	4,560	6.0
4	068	20	8.7	0.12	0.11		21	38,700	1.53	72.9	4,360	8.9

[a]All experiments were carried out using a 60/40 (v/v) hexane/methylene chloride cosolvent system at –70 °C. Molar concentration values at the reaction temperature were calculated using solvent volumes that were corrected for thermal expansion, as detailed in ref. 108, Supporting Information.

[b]EXXON™ Butyl 365 had Mn = 1.91 x105 g/mol and PDI = 1.61 (GPC), and 2.30 mol% isoprene units (NMR). EXXON™ Butyl 068 had Mn = 3.37 x105 g/mol and PDI = 1.29 (GPC), and 1.08 mol% isoprene units (NMR).

[c]IP = concentration of isoprene units from Butyl Rubber.

[d]Q = quencher = 3-(bromopropoxy)benzene.

[e]Number average molecular weight (GPC) of cleaved/alkylated product.

[f]Functional equivalent weight

g Number average functionality of cleaved/alkylated product with respect to attached quencher units.

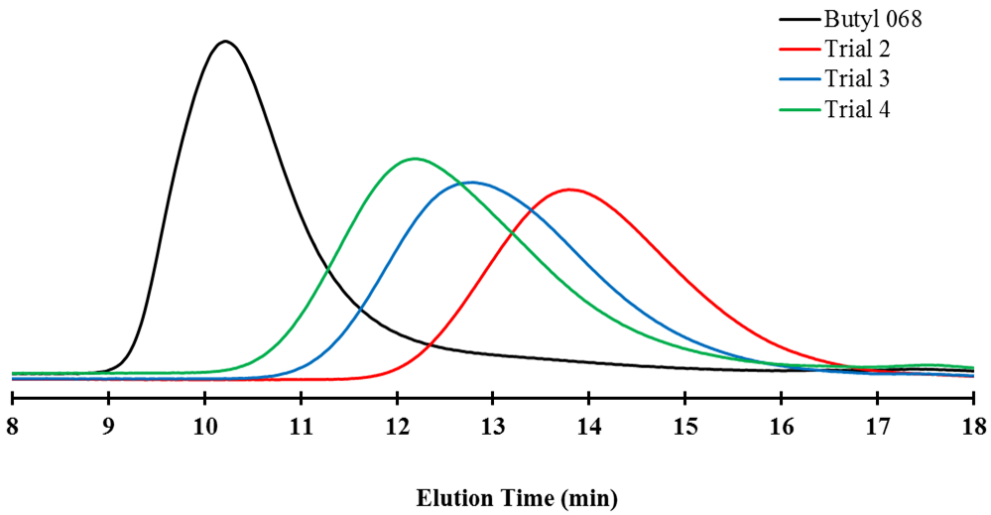

Figure 2.3 GPC chromatograms of Butyl 068 and the (3-bromopropoxy)benzene functionalized PIB macromer obtained therefrom by cleavage/alkylation (Trials 2-4).

Separate portions of the bromide-functionalized PIB resulting from cleavage/alkylation of Butyl 365 (Trial 1) were converted into acrylate- and methacrylate-functionalized macromers by reaction with potassium acrylate and potassium methacrylate, respectively. The ^{1}H NMR spectra of the bromide-functionalized product of the cleavage/alkylation reaction on Butyl 365 (Trial 1), along with the acrylate and methacrylate derivatives, are shown in Figure 2.4. Higher resolution spectra for the bromide precursor, acrylate macromer, and methacrylate macromer derived from Butyl 365 are included in the Appendix, Figures A.1-A.3; these spectra also contain integrations and the acrylate spectra (Figure A.2) includes a high-expansion of the olefinic region. Quantitative transformation from the bromide terminus to the acrylate terminus was confirmed by ^{1}H NMR, as shown in the middle spectrum in Figure 2.4.

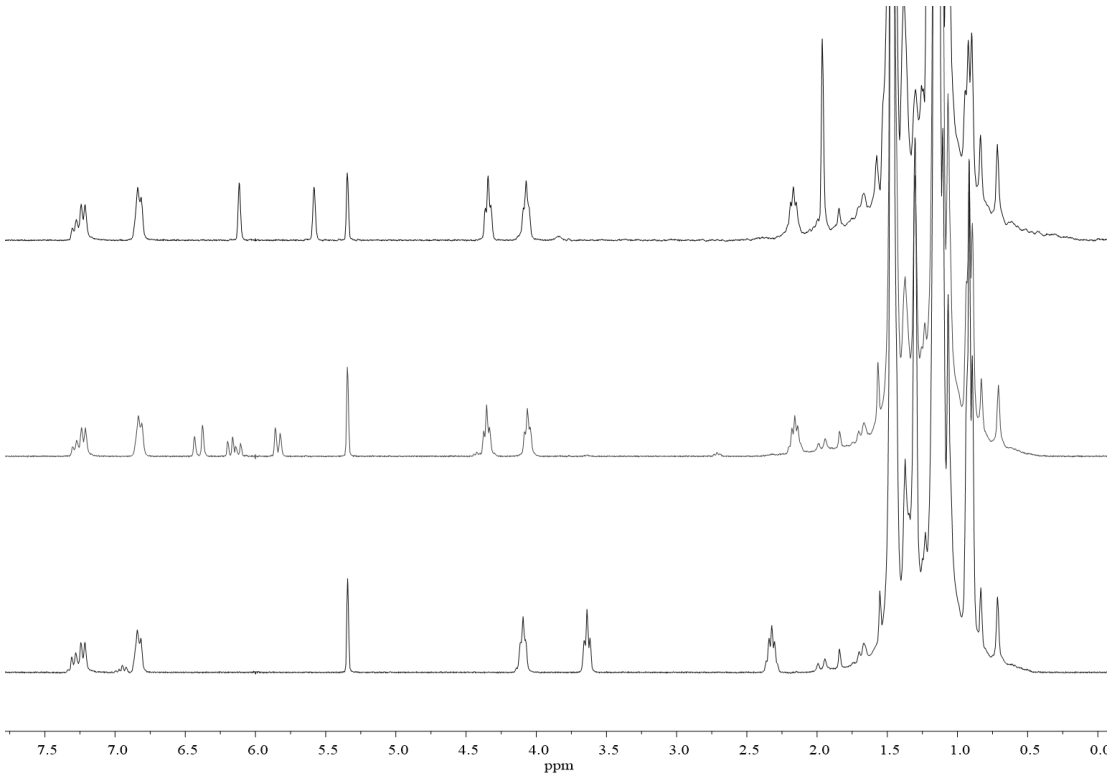

Figure 2.4 ^{1}H NMR (300 MHz, DCM-d_2, 25 °C) spectra of the (3-bromopropoxy)benzene functionalized PIB macromer (bottom) obtained from the cleavage/alkylation reaction of ExxonMobil Butyl 365. The acrylate (middle) and methacrylate (top) derivatives were synthesized via nucleophilic substitution with potassium acrylate or potassium methacrylate, respectively.

Evidence of formation of PIB acrylate was given by the appearance of resonances at 5.84 (doublet), 6.14 (quartet), and 6.40 ppm (doublet) as well as the downfield shift of the resonance associated with the terminal quencher methylene from 3.61 to 4.35 (triplet). The olefinic resonances observed in Figure 2.4 also mirror the resonances shown in Figure 2.1, providing further evidence of acrylate substitution.

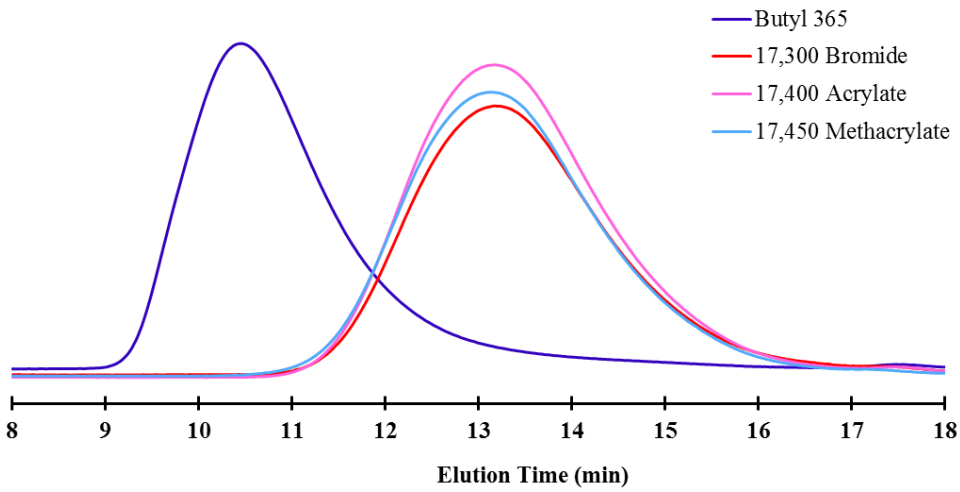

Figure 2.5 GPC chromatograms of Butyl 365 and the (3-bromopropoxy)benzene functionalized PIB macromer obtained therefrom by cleavage/alkylation. Also shown are the acrylate and methacrylate functionalized PIBs obtained from the substitution reaction of sodium (meth)acrylate with the bromine functionalized macromer.

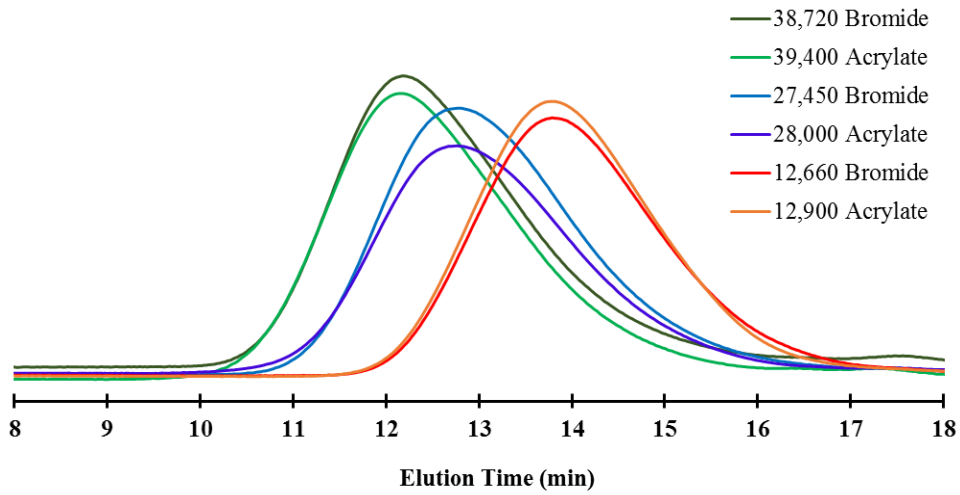

Figure 2.6 GPC chromatograms of the acrylate-functionalized PIBs compared to their primary bromide-functionalized precursors obtained from Butyl 068 (Trials 2-4). The acrylate functionalized products were synthesized via nucleophilic substitution using sodium acrylate.

Evidence of formation of PIB methacrylate (Figure 2.4, top) was given by the appearance of resonances at 5.58 (singlet) and 6.12 (singlet) as well as the downfield shift of the terminal methylene from 3.61 to 4.36 (triplet).

GPC chromatograms for Butyl 365 and its bromide, acrylate, and methacrylate-functionalized derivatives are shown in Figure 2.5; the chromatograms show that premature crosslinking or polymer backbone degradation during the course of nucleophilic substitution were not observed.

From the primary bromide PIBs obtained from Butyl 068 (Trials 2-4), photopolymerizable macromers were prepared via nucleophilic substitution with sodium acrylate. High-resolution NMR spectra, with peak integrations, for the bromide precursors and corresponding acrylate macromers from Butyl 068 (Trials 2-4) are included in the Appendix, Figures A4-A9. GPC chromatograms of the acrylate macromers and their primary bromide precursors are compared in Figure 2.6. Again, the chromatograms show that the acrylate-functionalized products did not undergo premature crosslinking, polymer degradation, or coupling reactions.

2.4.3 Photopolymerization and kinetics of PIB (M)A networks.

The curing kinetics of free-radical photopolymerizations involving (meth)acrylate-functional monomers and macromonomers have been exhaustively studied for a wide variety of systems.[119-128] For PIB-based (meth)acrylate systems, Tripathy *et al.* reported the curing kinetics of low molecular weight PIB (meth)acrylates and vinyl ether-functionalized PIBs[99] using an optical pyrometry technique developed by Crivello *et al*.[129] Real-time FTIR (RT-FTIR) is a more commonly used technique to monitor the kinetics of photopolymerization and was used by Yang *et al.* to monitor the photopolymerization curing kinetics of PIB-phenol (meth)acrylate macromers by tracking the disappearance of the (meth)acrylate olefin.[69]

Both Tripathy and Yang tested a wide variety of photoinitiators, curing conditions, and a range of PIB molecular weights. Although the results between Tripathy and Yang were generally in good agreement, Tripathy reported that the curing kinetics for their PIB (meth)acrylates were fastest for Irgacure 651, intermediate for Darocur 1173, and slowest for Irgacure 784. Yang, however, reported that Darocur 1173 gave the fastest curing kinetics and reached quantitative conversion while Irgacure 651 and Irgacure 784 were slower and in some cases failed to reach full conversion. Yang attributed this difference in curing kinetics to two factors. First, both Irgacure photoinitiators are solids at room temperature, while the Darocur 1173 photoinitiator is a liquid. Thus, the liquid Darocur could be more homogenously mixed throughout the PIB macromers via liquid-liquid diffusion. Secondly, solubility/miscibility of the photoinitiators may depend on the molecular weight of the polymer matrix. Tripathy's PIBs were very low molecular weight (~1,200 g/mol), while Yang's PIBs ranged from 3,000 g/mol to 10,000 g/mol. This suggests that lower molecular weight PIBs may solubilize solid photoinitiators better than higher Mn PIBs. For these reasons, Darocur 1173 was chosen to be the photoinitiator for this study.

Yang also studied the effect of photoinitiator concentration on the curing rate of trifunctional PIB (meth)acrylates with low M_ns (4,000 g/mol) produced by living polymerization from TCC trifunctional initiator. For those systems, Yang reported that curing rates increased with increasing photoinitiator concentration up to 2% (w/w) but that further increases in photoinitiator concentration produced negligible increases in curing rates. To determine whether a similar saturation phenomenon would occur in higher M_n systems, we replicated that study using a PIB triacrylate prepared similarly

from TCC but with M_n = 10,000 g/mol. Figure 2.7 shows kinetic data obtained at three different concentrations of Darocur 1173; acrylate conversion was measured by monitoring the disappearance of the acrylate peak from 1615-1638 cm^{-1}.

As shown in Figure 2.7, the formulations containing 2 and 5 wt % Darocur 1173 produced nearly identical conversion vs. time curves and both reached full conversion after 210 s, while the sample containing 1 wt% Darocur 1173 reached full conversion only after 240 s. These results are in agreement with Yang *et al.*[69]**Error! Bookmark not defined.** and show that photoinitiator saturation also occurs at higher M_n. As expected, the curing rates for the systems of Figure 2.7 are nearly identical to the curing rates for the high M_n systems (~10,000 g/mol) studied by Yang *et al.*[69]

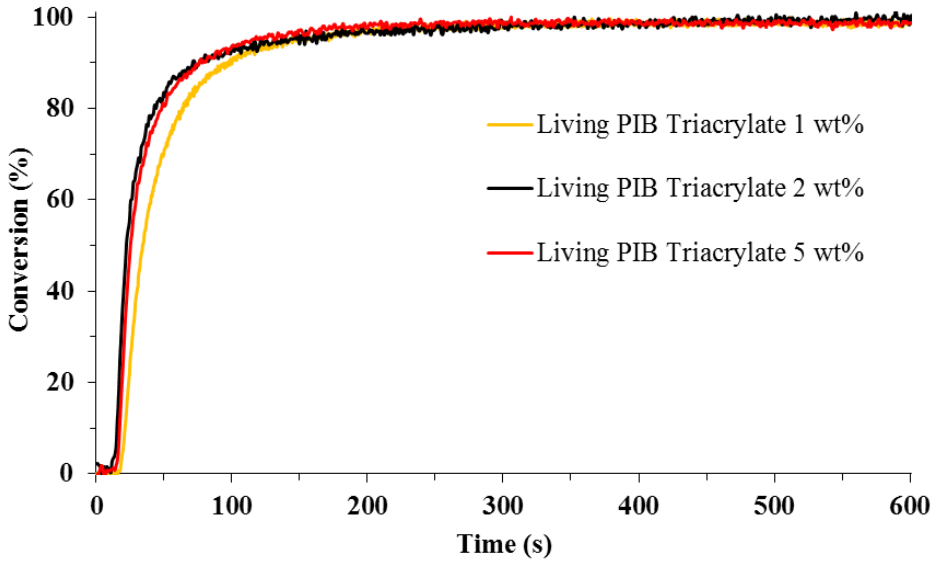

Figure 2.7 Conversion versus time for bulk photopolymerization of PIB triacrylate synthesized via living polymerization (M_n = 10,000 g/mol), formulated with different Darocur 1173 concentrations.

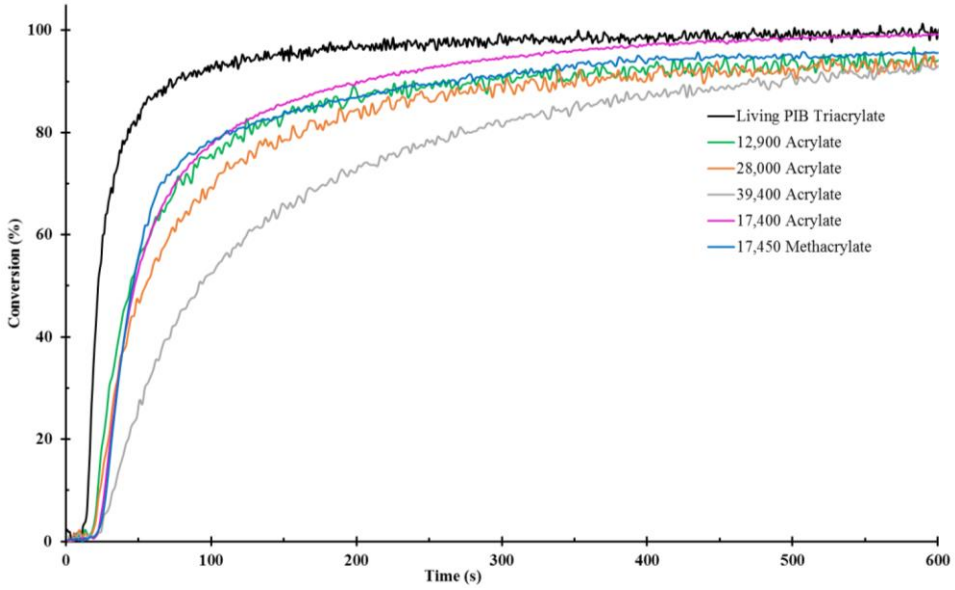

Figure 2.8 Conversion versus time for the various PIB (meth)acrylate prepolymers used in this study, expanded to show the first 600 s of curing. Each formulation was photopolymerized using Darocur 1173 at 2 wt%.

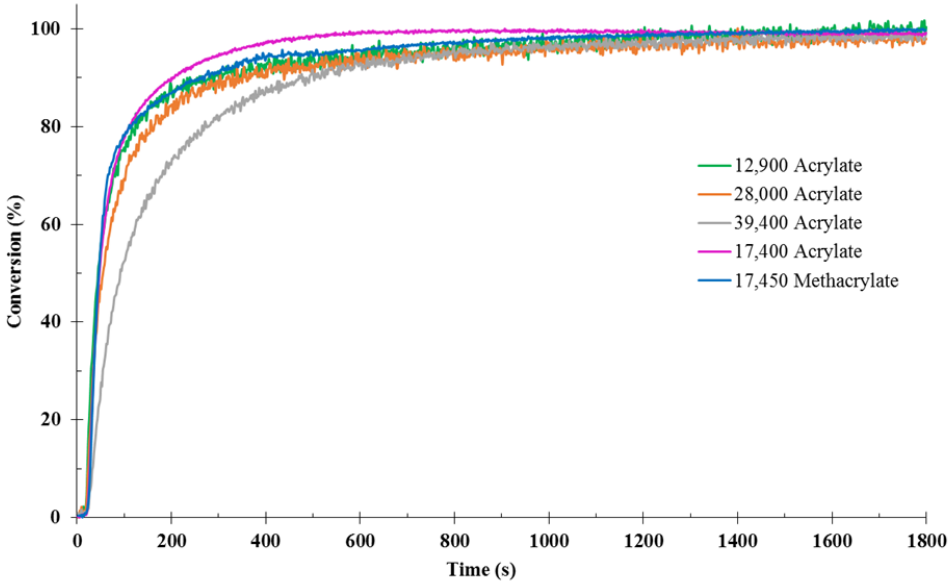

Figure 2.9 Conversion versus time for the linear PIB (meth)acrylate prepolymers to 1800 s. Each formulation was photopolymerized using Darocur 1173 at 2 wt%.

Figure 2.8 compares curing kinetics of the living PIB triacrylate control and the various linear macromers prepared via the cleavage/alkylation process and functionalized

via nucleophilic substitution of the bromide with potassium (meth)acrylate. Generally, the linear prepolymers had slower curing rates compared to the living PIB triacrylate. While the living PIB triacrylate reached 80% extent of cure in ~50 s, the linear PIB prepolymers achieved extents of cure of only ~35 – 65% in the same time frame. This trend was more pronounced at higher conversions, where the curing rates for all systems had slowed considerably. The living PIB triacrylate reached 90% conversion after 75 s and > 98% conversion at 212 s, while some linear systems reached > 98% only after 1200 s (Figure 2.9).

Of the linear macromers, those with the lowest functional equivalent weight, i.e., those derived from Butyl 365 (17,400 acrylate and 17,400 methacrylate) displayed the fastest curing kinetics, reaching > 98% conversion after 410 s and 834 s, respectively. The linear macromers derived from Butyl 068, which possessed higher functional equivalent weights, generally took longer to reach >98% conversion, and among this group, the curing rates slowed considerably as molecular weight increased. The linear macromers with the highest molecular weights (28,000 and 39,400 g/mol) reached >98% conversion after about 1200 s, even though they had F_n values similar to those of the ~17,400 systems. This is presumably due to immobilization and isolation of unreacted acrylate groups. The curing rate of the 12,900 Acrylate system, which had the lowest F_n of all the linear macromers tested, generally was faster than the systems with similar functional equivalent weights (i.e. the 28,000 and 39,400 Acrylate systems). This is presumably due to chain entanglement effects. The chain entanglement molecular weight is defined as the molecular weight at which a polymer system transitions from Newtonian to non-Newtonian flow. For PIB, this is around 17,000 g/mol.[130] For systems below this

molecular weight threshold, the shear viscosity/molecular weight correlation approaches unity as temperature increases. For systems at or above this molecular weight, the shear viscosity increases by a power factor of 3.4 with respect to molecular weight and is largely independent of temperature.

Thus, the existence of a highly viscous, highly entangled PIB macromer mixture gives rise to a variety of conditions that could potentially affect the curing kinetics. One limitation is the effect of molecular weight on the solubility/miscibility of the photoinitiator, which was discussed earlier. Also, as viscosity of the PIB increases, achieving a well dispersed mixture of photoinitiator/PIB becomes problematic. A solvent can be used to aid in mixing/casting (in cases of very high molecular weight PIBs, i.e., M_n > 30,000 g/mol, it becomes a requirement), but the excellent gas/solvent impermeability characteristics of PIB complicates the removal of solvent prior to monitoring the curing kinetics.

Other complicating factors with respect to the PIB molecular weight are the change in diffusional mobility of the acrylate moieties and possible autoacceleration via the Trommsdorff effect. Yang reported that higher M_n PIBs, which possess a lower concentration of acrylates and a higher viscosity than do their lower M_n counterparts, displayed faster curing rates during photopolymerization. Additionally, Yang reported that the electronic and steric effects of the PIB chain end (i.e. phenol (meth)acrylate vs. phenoxybutyl acrylate) were largely negligible during the curing process. Yang attributed both phenomena to the decreased diffusional mobility of the higher Mn PIB prepolymers, which resulted in lower rates of radical termination, eventually leading to auto-acceleration due to the Trommsdorff effect.

Interestingly, our linear systems synthesized via the cleavage/alkylation of butyl rubber exhibited the opposite behavior in terms of curing rate. For systems with similar functional equivalent weights (i.e. all systems derived from Butyl 068), an increase in molecular weight generally resulted in a decrease in curing rate. For systems with similar F_n (i.e. 17,400 Acrylate, 28,000 Acrylate, and 39,400 Acrylate), curing rates varied significantly, presumably due to viscosity arguments mentioned previously. These observations suggest that PIB morphology, in addition to PIB molecular weight, plays a significant role in the curing rates of PIB based (meth)acrylates.

2.4.4 Extent of Cure Analysis via Sol Fraction Experiments.

Percent conversion during photopolymerization of the (meth)acrylate crosslinking moiety can also be indirectly measured using sol fraction experiments. The percent extractables of each cured network should show an inverse correlation to the percent conversion of the (meth)acrylate olefin measured via RT FTIR. Thus, each film was immersed in THF for 60 h followed by rigorous vacuum drying, and sol fractions were calculated using the pre- and post-extraction weights. The percent extractables for each photocured formulation, taken as the average of three sol fraction experiments, are listed in Table 2.2.

These measurements show a few general trends. First, the sol fractions were uniformly low. This agrees qualitatively with the RT-FTR data, which showed that all formulations reached > 98% (meth)acrylate conversion. Also, a stark contrast was observed between the relatively high sol fractions of the living PIB triacrylate networks versus the relatively low sol fractions of the linear PIB macromer samples, presumably due to the difference in network morphology. For crosslinking reactions in general,

polymer chain mobility decreases as curing conversion increases, leading eventually to isolation of unreacted functional groups. The living PIB acrylate prepolymers possess a three-arm star morphology with relatively uniform arm lengths, with the reactive acrylate moiety on the chain ends. It is therefore a relatively compact coil with less tendency to overlap with neighboring coils. This may promote separation of unreacted (meth)acrylate groups from the propagating radicals, leading not only to lower (meth)acrylate double bond conversion but also to higher extractable matter due to increased radical termination events involving primary radicals from the photoinitiator. The linear PIB macromers, in contrast, are multifunctional linear molecules with greater opportunity for coil-coil overlap. This apparently causes less isolation of unreacted (meth)acrylate groups, leading to less extractables from the photoinitiator residue.

Table 2.2 Network Formulations and Percent Extractables for Various PIB Networks[a]

Entry	Macromer	Avg Extractable (%)
1	Living PIB Acrylate	3.59
2	12,900 Acrylate	1.67
3	28,000 Acrylate	2.09
4	39,400 Acrylate	1.96
5	17,400 Acrylate	1.42
6	17,450 Methacrylate	1.44

[a]Photoinitiator (Darocur 1173) concentration = 2 wt%

Other factors may account for the average extractable values recorded in Table 2.2. As reported by Tripathy[99] and Yang[69]**Error! Bookmark not defined.**, films derived from the photopolymerization of (meth)acrylate functionalized PIB macromers are inherently brittle and prone to fracture. Multiple transfers of the sample films (weighing, placement and removal of the sample into the scintillation vial, etc.) may result in sample fracture or sample loss, yielding a lower sample weight and thus a higher calculated percent

extractable. The extractable matter may also be small molecule products resulting from photoinitiator decomposition or residual solvent that was left over from the casting process.

2.4.5 Glass Transition Temperature and Crosslink Density of UV-cured PIB Networks.

Glass transition temperature (T_g) and crosslink density of the cured PIB networks were investigated using DMA analysis. Storage modulus and tan δ curves thereby obtained are shown in Figures 2.10 and 2.11, respectively, and data extracted from these curves are summarized in Table 2.3.

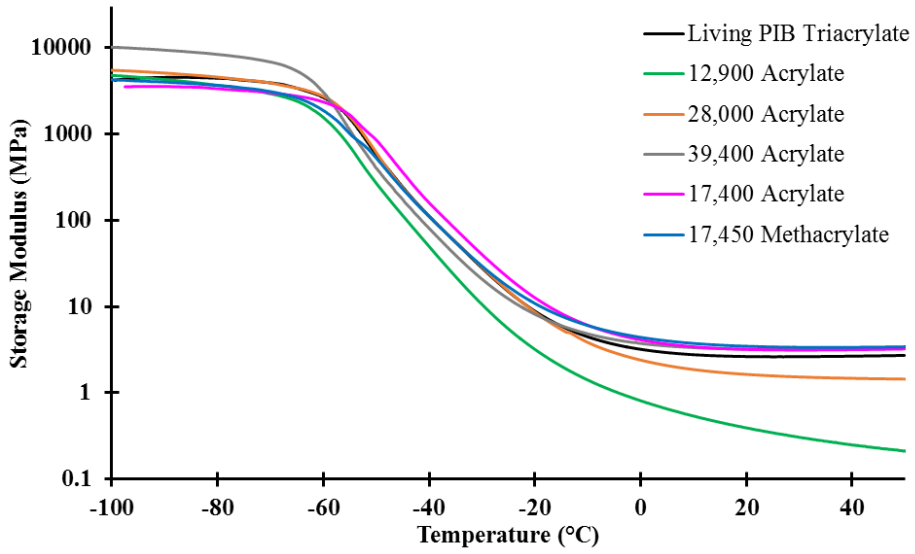

Figure 2.10 Storage modulus versus temperature for photocured PIB networks. Photopolymerizations were carried out using 2.0 wt% Darocur 1173.

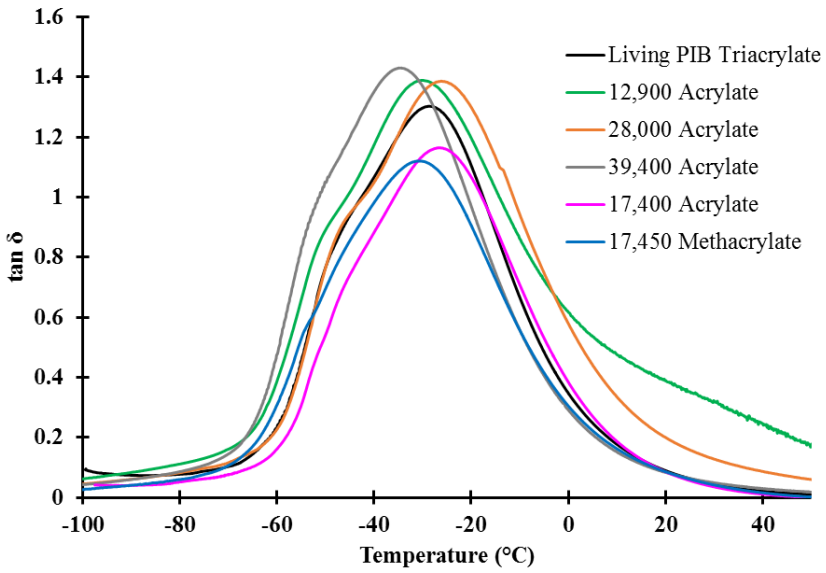

Figure 2.11 Tan δ versus temperature for photocured PIB. Photopolymerizations were carried out using 2.0 wt% Darocur 1173.

With respect to DMA data, T_g is usually reported as the temperature at the maximum of the tan delta (δ) peak, due to ease of reproducibility.[131] Alternatively, the T_g may be taken as the onset of the drop in storage modulus, but this onset may be ill defined in some systems. Unlike crystalline systems, amorphous systems often show poorly defined, broad drops in storage modulus and broad tan δ peaks, resulting in difficult T_g detection.[132,133] Notably, PIB-based networks possess two convoluted transitions in the tan δ curve, which further complicates an accurate specification of the T_g. The weaker of the two transitions, which appears to be a shoulder on the low temperature side of the more intense transition, is the actual T_g. The stronger, dominant transition is a sub-Rouse relaxation characteristic of the PIB backbone.[134] Thus, for PIB based networks, the onset of the drop in storage modulus may give a more accurate T_g.

In this work, T_gs were measured by both methods and reported in Table 2.3. The drop in storage moduli for all systems occurred between -66 °C and -68 °C, which agrees

well with the literature values for PIB (Tg ~ -66 °C).[135] Comparatively, the tan δ peaks were found to give noticeably higher T_g's than those measured by the previous method, a difference that is often more pronounced in non-crystalline materials.[136] Using peak deconvolution software, the T_g's were found to be between -52 °C to -47 °C.

Some general comments may be made regarding the overall shape and trends of the storage moduli and tan δ curves. First, the networks formed from living PIB triacrylate and from the linear macromers derived from Butyl 365 (17,400 Acrylate and 17,450 Methacrylate) possessed similar storage moduli and tan δ curves, and the T_gs for all three systems were relatively uniform. The uniformity of these systems probably results from the similar functional equivalent weights of these systems, which ranged from 2,300-3,000 g/mol. The networks formed from the macromers derived from Butyl 068, however, displayed significantly different behaviors in regard to storage modulus. The 12,900 Acrylate network possessed a glassy storage modulus very similar in value to the Butyl 365 and living PIB triacrylate systems, but after the drop in modulus associated with the T_g, the modulus continued to decrease at higher temperatures and never displayed a persistent rubbery plateau. The 28,000 Acrylate system also displayed a glassy storage modulus similar in value to the Butyl 365 and living PIB triacrylate systems, and it also displayed a slightly lower modulus in the rubbery regime. The 39,400 Acrylate system displayed a glassy modulus that was higher than any other system, but in the rubbery regime it behaved very similarly to the Butyl 365 and living PIB systems.

Regarding the tan δ curves, all networks displayed the intense, sub-Rouse relaxation characteristic of PIB, and on its low temperature side, a less-intense "shoulder"

peak. The low temperature shoulder, which represents the true PIB T_g, is listed in Table 2.3 for each system. Generally, all tan δ curves displayed the same shape, with two notable exceptions. The 12,900 Acrylate system displayed significant tailing on the high temperature side of the tan δ curve, and the 28,000 Acrylate system displayed a less significant but still noticeable shift towards higher temperatures before returning to baseline. These features are related to the lower rubbery moduli measured for these two systems (as shown in Figure 2.10) and can be attributed to the stiffness of the networks. Generally, an increase in network stiffness causes the drop in the tan δ at higher temperatures to become more severe.[132,137] In PIB networks crosslinked via (meth)acrylate functionalities, the incorporation of higher polyacrylate content or higher crosslink density causes a steeper decline in tan δ curve at high temperatures. Inversely, loosely crosslinked networks (i.e. lower acrylate content) display a less steep decline in tan δ and possibly significant tailing at higher temperatures.

For homogenously crosslinked systems, the value of the storage modulus at the rubbery plateau can be used to approximate crosslink density. Crosslink density, typically defined as the inverse of the average molecular weight between crosslinks (M_c), can influence many physical and structural properties of thermosets, including stiffness, elongation at break, strength, and brittleness.[138] The crosslink densities of the various cured network were determined from the value of the rubbery plateau modulus, using a literature method,[139] and are summarized in Table 2.3. An accurate crosslink density for the 12,900 Acrylate system could not be calculated due to the lack of a rubbery plateau, which was attributed to a loosely crosslinked (i.e. inhomogenously crosslinked) network.

Table 2.3 Dynamic Viscoelastic Properties and Crosslink Densities of UV-Cured PIB Networks

	Living	**12,900 Acrylate**	**28,000 Acrylate**	**39,400 Acrylate**	**17,400 Acrylate**	**17,450 Methacrylate**
M_n of PIB (g/mol)	10,070	12,900	28,000	39,400	17,400	17,450
T_g (E' drop) (°C)	-67.0	-67.9	-68.1	-68.84	-66.6	-67.9
T_g (tan δ peak) (°C)	-48.7	-52.0	-48.3	-53.4	-47.4	-51.9
Tan δ peak value	0.929	0.821	0.857	0.915	0.676	0.626
E' at T_g+60°C (tan δ peak) (MPa)	2.63	1.18	2.18	3.23	3.14	3.38
EW_Q (g/eq)	3,030	4,360	4,560	4,670	2,300	2,440
M_c (g/mol)	2,910	-	3,490	2,316	2,460	2,380

The calculated crosslink densities and M_c values, in conjunction with the tan δ and storage modulus plots, provide further insight into the physical properties of these networks. Previously Yang *et al.* reported[69] the effect of crosslink density on the viscoelastic and tensile properties of various PIB networks formed from trifunctional prepolymers. Generally, they observed that networks formed from low molecular weight PIB-phenol (meth)acrylate prepolymers (~3,000-4,000 g/mol) had higher crosslink densities than networks formed from moderate molecular weight PIB-phenol (meth)acrylate macromers (10,000 g/mol). This resulted in higher T_g's, higher storage moduli, and higher strain at break.

In this study, we sought to investigate the effect of crosslink density and prepolymer morphology on the tensile and viscoelastic properties of PIB networks. Notably, we observed that PIB networks obtained from linear PIB-(meth)acrylates possessed similar T_g's despite significantly different crosslink densities and functional equivalent weights. Also, the T_g's measured via storage modulus and tan δ were in good agreement with the T_g's reported previously.

2.4.6 Tensile Properties

Tensile testing was performed on all of the photocured PIB networks; stress-strain curves are shown in Figure 2.12, and data extracted from the curves are summarized in Table 2.4. Similarly to our previous report, all PIB networks displayed characteristic weak elastomeric behavior;[69] however, the morphology, molecular weight, and crosslink density of each macromer played a significant role in the tensile properties observed. The network formed from living PIB triacrylate displayed a comparatively moderate Young's modulus but had the lowest strain at break compared to all the other networks.

Considering the relative uniformity of the length of the polymer chains (as evidenced by its relatively narrow polydispersity of 1.05 from GPC/MALLS), it is logical to expect that cleavage of the crosslink junctions occurs within a very narrow range, resulting in sudden catastrophic failure rather than strain yielding.

PIB networks derived from the linear PIB macromers all displayed a higher strain at break compared to the living PIB system, but the functional equivalent weight and the molecular weight of each system had a significant effect on the Young's modulus. The systems with the highest Young's moduli were the two systems derived from Butyl 365, which had the higher isoprene content of the two butyl rubber starting materials. Thus, the resulting PIB macromers had a moderately high molecular weight (~17,400 g/mol) and high F_n (~7.08), and a much lower functional equivalent weight than the prepolymers derived from Butyl 068. With regard to the latter prepolymers, all displayed a lower Young's modulus than the living PIB system, but molecular weight had a significant effect on the Young's modulus of each system. The two higher molecular weight PIB macromers (28,000 and 39,400 g/mol) each displayed a higher Young's modulus than the lowest molecular weight PIB macromers (12,900 g/mol), which displayed the lowest Young's modulus and the most elasticity of all the samples tested. This is presumably due to the two higher molecular weight systems being above the chain entanglement weight of PIB, which increases the stiffness of the networks. Additionally, the highly elastic nature of the 12,900 Acrylate system as shown by tensile testing agrees well with the DMA results discussed in the previous section; namely, this system was shown to have the lowest stiffness of all of the networks tested in this study.

Table 2.4 Tensile Properties of the Various PIB Networks

	Living	**12,900 Acrylate**	**28,000 Acrylate**	**39,400 Acrylate**	**17,400 Acrylate**	**17,450 Methacrylate**
M_n of PIB (g/mol)	10,070	12,900	28,000	39,400	17,400	17,450
Youngs Modulus	1.19	0.134	0.444	0.538	1.78	1.33
Strain at break (%)	34.45	112.85	45.45	39.37	45.11	53.6
Strength at break	0.4105	0.1511	0.2019	0.212	0.8028	0.7104

58

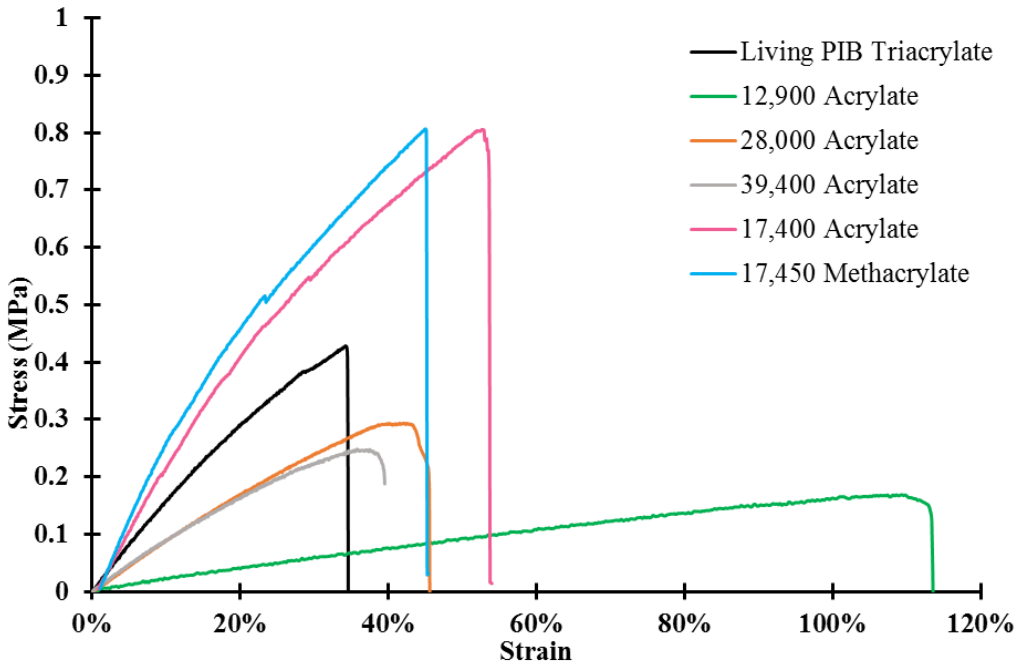

Figure 2.12 Typical stress-strain curves from each photocured PIB network.

Comparatively, the living PIB acrylate systems studied by Yang *et. al.* gave nominally lower strains at break compared to the linear PIB macromers reported herein, but the Young's moduli for Yang's systems were noticeably higher.[69] This is most likely due to the higher elasticity inherent in the linear macromers, in addition to molecular weight and crosslink density considerations.

2.5 Conclusion

A three-arm star PIB triacrylate prepolymer was prepared via end-quenching of living PIB with 4-phenoxy-1-butyl acrylate. Linear PIB macromers bearing (meth)acrylate moieties were prepared by the acid catalyzed cleavage/alkylation process on various grades of butyl rubber in the presence of 4-phenoxypropyl bromide, followed by the nucleophilic substitution of a (meth)acrylate. All prepolymers were found to be stable towards premature polymerization during workup and characterization.

PIB-(meth)acrylate prepolymers were photopolymerized using Darocur 1173 as a photoinitiator, and the curing kinetics were monitored via RT-FTIR. Lower concentrations of photoinitiators led to slower rates of photopolymerization, but beyond 2 wt% photoinitator saturation effects were observed in the living PIB triacrylate. As observed in previous studies, the rates of polymerization of PIB-acrylate prepolymers were found to be moderately faster than those of PIB-methacrylate prepolymers. Sol fraction experiments of the resulting films suggested that a high degree of double bond conversion for all formulations were achieved, but the brittleness of the films complicated the accuracy of the results.

Morphological differences in the PIB-(meth)acrylate prepolymers appeared to drastically affect the curing rates and mechanical properties of the resulting networks. Despite possessing significant differences in molecular weight and crosslink density, all of the networks were measured to have similar T_g's as calculated from storage modulus and tan δ curves.

Until recently, multifunctional PIB could only be synthesized using expensive and synthetically complex initiators, making industrial applications of PIB based networks impractical. Now, multifunctional PIB macromers and PIB based networks can be synthesized using widely available materials, allowing for novel industrial applications and widespread use. Future studies will focus on the inclusion of solid additives in the formulations, and the effect on tensile and gas barrier properties.

CHAPTER III FUNCTIONALIZATION OF POLYISOBUTYLENE AND POLYISOBUTYLENE OLIGOMERS VIA THE RITTER REACTION

Co-authored by Robson Storey

3.1 Abstract

The Ritter reaction, i.e. reaction of a carbocation with a nitrile, was carried out on polyisobutylene (PIB) using a variety of reaction conditions. End quenching of PIB carbocations with acrylonitrile under living polymerization conditions (methyl chloride (MeCl)/hexane 60/40 (v/v) solvent mixtures at -70 °C) resulted in either *tert*-chloride end groups or loss of chain end fidelity via carbocation rearrangement, as evidenced by NMR spectroscopy. *Exo*-olefin functionalized PIB substrates were also reacted with nitriles under a variety of reaction conditions including various acid and solvent medium combinations. In all cases, the result was either no reaction or PIB that had undergone severe backbone degradation, as determined via NMR spectroscopy and gel permeation chromatography. Finally, the Ritter reaction was performed on a series of *exo*-olefin functionalized oligoisobutylenes using acrylonitrile as the nitrile and either 60/40 dichloromethane/hexane or excess acrylonitrile as the solvent. In 60/40 dichloromethane/hexane, significant carbocation rearrangement and/or degradation resulted in a variety of isomeric, acrylamide-functionalized oligomers. In excess acrylonitrile, the desired Ritter reaction was the only reaction observed, resulting in the smooth formation of the terminal acrylamide. The various *N*-oligoisobutylacrylamides thus obtained represent new hydrophobic monomers useful for the introduction of hydrophobic moieties into acrylamide-based water-soluble polymers.

3.2 Introduction

Polyisobutylene (PIB) is a fully saturated hydrocarbon polymer that exhibits excellent gas barrier properties, high chemical resistivity, and excellent oxygen and ozone resistance.[135] For many applications, chemical functionality, typically olefinic unsaturation, must be introduced into PIB for its practical utilization. For example, the vast majority of high molecular weight PIBs sold commercially are actually copolymers of isobutylene and isoprene (e.g. 98:2 isobutylene:isoprene), known in the industry as butyl rubber, in which the isoprene-derived unsaturations enable sulfur vulcanization for elastomer applications such as tires, inner tubes, ball bladders, etc.[70,140,] and as sealants and adhesives.,[141] PIB homopolymers of low to moderate molecular weight are produced industrially by chain-transfer-dominated cationic homopolymerization, yielding mono-functional polymers with unsaturated termini. Polymers containing a high fraction of *exo*-olefin (methyl vinylidene) termini, known as high reactivity (HR) PIB, are desired because of their higher reactivity in downstream functionalization reactions, especially with maleic anhydride to produce PIB-succinic anhydride (PIBSA), a key intermediate in the lubricating oils and fuel industry.[80],[142,143,] New catalysts and improved processes toward HR PIB are the subject of active investigations by several groups.[144,145,146]

In addition to monofunctional PIBs produced industrially via chain transfer-dominated processes, difunctional (telechelic) and higher-functionality PIBs have been produced by laboratory researchers since the late 1970's, first via the "inifer method"[55] and later by living carbocationic polymerization.[147] For these materials as well, the *exo*-olefin terminus has been an important synthetic objective, due to its value as an intermediate toward other functional groups. The original approach towards *exo*-olefin

PIB involved reaction of *tert*-chloride-terminated PIB with *t*BuOK in refluxing THF[55] or EtOK in refluxing THF/EtOH;[72] however this approach is inconvenient due to long reaction times and the inevitable formation of a small amount of the *endo*-olefin.[148] More recently, quantitative *exo*-olefin-terminated PIB has been synthesized by direct "end-quenching" of living carbocationic PIB chain ends *via* addition reaction with methallyltrimethylsilane[74] or elimination reactions induced by hindered bases,[149] alkoxysilanes,[150] alkyl ethers,[151] or alkyl sulfides.[152] End-quenching has also allowed for the direct functionalization of living PIB with functional groups other than *exo*-olefin, using quencher molecules of several characteristic types including olefins that add only once to the chain,[153,154,155,] alkoxybenzenes,[95,96 ,98] and heterocyclic aromatics.[156,157] To effectively functionalize PIB, a quencher molecule must preferentially react with the carbocationic chain end, rather than the more abundant Lewis acid, and the quenching reaction must compete kinetically with decomposition pathways of the carbocation, particularly carbocation rearrangement.[118,158]

Recently, there has been interest in PIB macromonomers possessing more highly reactive terminal unsaturation, especially (meth)acrylate[69,99,,159,160,161,162] and vinyl ether.[99] These systems may be cured by thermal or photo-initiated radical chain polymerization, or in the case of vinyl ether, by photo-initiated cationic polymerization. Among a number of potential biomedical and industrial applications for these materials, an application of particular interest is their use in the formation of PIB-based thermosets for sealant and gas barrier applications. For example, traditional PIB sealants used in insulating glass units (IGU) consist of high molecular weight PIB thermoplastics that are applied at elevated temperature as a melt; however, these materials tend to creep under

certain adverse circumstances, resulting in eventual aesthetic and/or mechanical failure. PIB thermosets represent an attractive replacement, as they can be applied at room temperature and upon curing, exhibit superior rheo-mechanical properties and are creep resistant.

A potential, unexplored method for creating telechelic PIBs with highly reactive, polymerizable functionality, namely acrylamide, is the chain end functionalization of PIB via the Ritter reaction. This reaction, first reported in 1948 and depicted in Scheme 1, is an acid catalyzed addition reaction between a carbocation forming species and a nitrile, which results in the formation of a nitrilium ion that is further converted to an amide during workup.[163,164] Since its discovery, the Ritter reaction has been widely utilized to synthesize amides on both small molecules and polymers, and has been the subject of several comprehensive reviews, the most recent of which was published in 2014.[165,166,167] Even after decades of study, the Ritter reaction continues to be an attractive tool for synthetic chemists due to its high yield, tolerance towards a variety of catalysts and reaction conditions, and its remarkable utility and atom efficiency in forming amides from bulky substrates.[168,169,170]

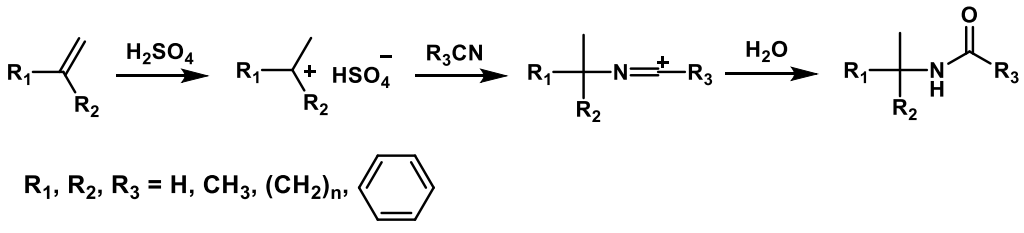

Scheme 3.1 Mechanism of amide formation via the Ritter reaction

Since the Ritter reaction has been shown to form amides in high yields using either Lewis and/or Bronsted acid catalysts, it potentially represents a highly modular

approach towards PIB chain-end functionalization, to enable the synthesis of terminal amide moieties via reactive end-quenching or modification of commercially available *exo*-olefin PIB substrates. Herein we describe application of the Ritter reaction to a variety of PIB substrates and small-molecule analogs in an effort to create new acrylamide-functionalized monomers and telechelic PIB macromers.

3.3 Experimental

3.3.1 Materials

Hexane (anhydrous, 95%), methanol (anhydrous, 99.8%), dichloromethane (anhydrous, 99.8%, DCM), dimethylformamide (anhydrous, 99%, DMF), dimethyl sulfoxide (anhydrous, ≥99.9%, DMSO), titanium tetrachloride (99.9%, $TiCl_4$), 2,6-lutidine (99.5%), tetrahydrofuran (anhydrous, 99.9%, THF), , triethylamine (anhydrous, ≥99.5%, TEA), phosphoric acid (aqueous, 85 wt%, H_3PO_4), 11-bromoundecane-1-ol (98%), sodium cyanide (97%), acryloyl chloride (97%), acrylonitrile (anhydrous, 98%, AN), dichloroacetic acid (≥99%, DCAc), hydroiodic acid (aqueous, 57 wt%, HI), and potassium carbonate (anhydrous, ≥99%, K_2CO_3) were purchased from Sigma-Aldrich and used as received. Magnesium sulfate (anhydrous, ≥99.5%, $MgSO_4$), sodium sulfate (anhydrous, ≥99%, Na_2SO_4), sulfuric acid (98%, H_2SO_4), chloroform (anhydrous, $CHCl_3$), chloroform-d ($CDCl_3$), hydrochloric acid (aqueous, 37 wt%, HCl), diethyl ether (anhydrous, 95%), acetonitrile (AceN, HPLC) sodium chloride (crystalline, ≥99.5%), sodium iodide (crystalline, ≥99.5%) and acetic acid (glacial, AcOH) were purchased and used as received from Fisher Scientific. Isobutylene (BOC Gases, IB) and methyl chloride (Gas and Supply, MeCl) were dried by passing the gases through columns of $CaSO_4$/molecular sieves/$CaCl_2$ and condensing within a N_2-atmosphere glovebox

immediately prior to use. The difunctional initiator, 5-*tert*-butyl-1,3-di(1-chloro-1-methylethyl)benzene (bDCC), was synthesized as previously reported, stored at 0°C, and freshly recrystallized before use.[96] Small-molecule oligoisobutylenes possessing *exo*-olefin termini (C_{12}, C_{16}, C_{20}) were graciously donated by Chevron Oronite Corporation, and used without further purification. Purities estimated by GC-MS were C_{12}, 91.2%, C_{16}, 78.0%, and C_{20}, 93.5%. Synthesis of the monofunctional *exo*-olefin PIB was previously reported (see Table 6, Entry 7 of reference 79). ^{1}H NMR showed this material to possess 83% *exo*-olefin and 17% *tert*-chloride end groups (Appendix, Figure A.10), and its number average molecular weight ($\overline{M}_n$) and polydispersity index (PDI = $\overline{M}_w/\overline{M}_n$) were 2,800 g/mol and 1.07, respectively, according to GPC. Although the chain ends of this material were not exclusively *exo* olefin, 83% *exo*-olefin functionality was deemed sufficient for proof of concept studies of the Ritter reaction on PIB substrates.

3.3.2 Instrumentation

Nuclear magnetic resonance (NMR) spectra were obtained using a 300 MHz Bruker AVANCE III NMR (TopSpin 3.1) spectrometer. All ^{1}H chemical shifts were referenced to TMS (0 ppm). Samples were prepared by dissolving the material in chloroform-d (5%, w/v) and charging this solution to a 5 mm NMR tube. For quantitative integration, 32 transients were acquired using a pulse delay of 27.3 s. For the PIB polymers prepared via living polymerization, the signal due to the phenyl protons of the initiator (7.17 ppm, 3H, singlet) was chosen as an internal reference for functionality analysis. For the oligoisobutylenes, the terminal methylene (~1.80 ppm, 2H, singlet) was used.

Real-time (RT)-ATR-FTIR monitoring of isobutylene polymerizations was performed using a ReactIR 45m reaction analysis system (Mettler-Toledo AutoChem, Inc.) integrated with a N_2-atmosphere glovebox (MBraun Labmaster 130). Isobutylene conversion during polymerization was determined by monitoring the area above a two-point baseline of the absorbance at 887 cm^{-1}, associated with the $=CH_2$ wag of isobutylene.

Number-average molecular weights ($\overline{M}_n$) and polydispersities (PDI = $\overline{M}_w/\overline{M}_n$) were determined using a gel-permeation chromatography (GPC) system consisting of a Waters Alliance 2695 separations module, a UV-Vis spectrophotometer (996 PDA, Waters Inc.) operating between 210-400 nm with a sampling rate of 1 scan/s, an online multi-angle laser light scattering (MALLS) detector fitted with a gallium arsenide laser (power: 20 mW) operating at 658 nm (miniDAWN TREOS, Wyatt Technology Inc.), an interferometric refractometer (Optilab t-rEX, Wyatt Technology Inc.) operating at 35°C and 685 nm, and either two PLgel (Polymer Laboratories Inc.) mixed E columns (pore size range 50-10^3 Å, 3 μm bead size) or two mixed D columns (pore size range 50-10^3 Å, 5 μm bead size). Freshly distilled THF served as the mobile phase and was delivered at a flow rate of 1.0 mL/min. Sample concentrations were ca. 5-7 mg of polymer/mL of THF, and the injection volume was 100μL. The detector signals were simultaneously recorded using ASTRA software (Wyatt Technology Inc.), and absolute molecular weights were determined by MALLS using a *dn*/*dc* calculated from the refractive index detector response and assuming 100% mass recovery from the columns.

The percent purity for each oligoisobutylene was measured via gas chromatography-mass spectrometry (GC-MS) using a Hewlett Packard 6890 gas

chromatograph with a 5970 series mass selective detector. Samples were injected (2.99 µL, 25:1 split ratio) into a 30 m Restek RTX-1 capillary column (0.32 mm i.d., 5.00 µm film thickness), and helium was used as the carrier gas at a constant flow of 1.3 mL/min. The column temperature was maintained at 50°C for 5.20 min, then heated to 180°C at 50°C/min and held for 2 min, and finally heated to 250°C at 10°C/min and held for 8 min, with a total run time of 24.80 min. The MS was operated in full-scan mode with an electron ionization energy of 35.3 eV, trap current of 250 µA, and source temperature of 162°C. HPLC-grade DCM was used in all experiments without further purification (DCM (HPLC), Fisher Chemicals). The purity of each oligoisobutylene was characterized by signal intensity of the main peak relative to total signal intensity of all peaks, expressed as a percent. The chromatograms and mass spectra are included in Supporting Information, Figures A.11-A.16.

3.3.3 End quenching of living carbocationic PIB with acrylonitrile.

The following procedure is representative and was performed within a N_2-atmosphere glovebox (MBraun Labmaster 130) equipped with a cryostated (FTS Kinetics) heptane bath. To a dry 250 mL 3 neck round-bottom flask, equipped with an overhead stirrer, thermocouple, and ReactIR probe, and immersed in a -70°C heptane bath, were charged 70.2 mL chilled hexane, 105 mL chilled methyl chloride, 2,6-lutidine (0.070 mL, 0.60 mmol, neat and at room temperature), bDCC (1.20 g, 4.20 mmol), and chilled IB (33.9 mL, 0.422 mol). The mixture was equilibrated to -70 ºC with stirring, and polymerization was initiated by sequential additions of $TiCl_4$ spaced 15 min apart (2 x 0.23 mL, total 4.2 mmol, neat and at room temperature). Monomer conversion was monitored using RT-ATR-FTIR data, and upon full conversion, an aliquot (2.00 mL) was

removed and precipitated into prechilled methanol. To the balance of the reaction was added AN (1.10 mL, 16.8 mmol, room temperature) immediately followed by a quenching increment of $TiCl_4$ (3.19 mL, 0.0291 mol). Aliquots were taken at 1 h increments to monitor conversion, and after 4 h the mixture was removed from the glove box and transferred to a fume hood. An ice/water slurry (30 mL) was slowly added to the mixture under vigorous stirring. The mixture was then slowly warmed to room temperature and concentrated under an N_2 stream to allow for the evaporation of volatiles. The resulting mixture was then precipitated into methanol under vigorous stirring, after which the methanol layer was decanted. The precipitate was collected by re-dissolution in a minimal volume of fresh *n*-hexane, and the resulting solution was re-precipitated into excess methanol. After decanting the methanol, the precipitate was collected by re-dissolution in fresh hexane, and the resulting solution was washed twice with deionized water, dried over Na_2SO_4, and then vacuum stripped to yield the isolated polymer. The pre-quench and post-quench products were then characterized via ^1H NMR and compared. Chain end composition was estimated by comparing the appropriate resonance signals to the resonance signal of the initiator residue (7.18 ppm).

3.3.4 Ritter reaction on *exo*-olefin-terminated PIB.

Two series of experiments were conducted using *exo*-olefin terminated PIB as the electrophilic reagent. In the first series, the Ritter reaction was performed using a variety of different solvent media and either AN (Trials 1.1-1.8) or AceN (Trial 1.9) as the nitrile substrate; the reaction conditions are listed in Table 3.1. A general procedure was as follows: To a scintillation vial equipped with a magnetic stirrer was charged *exo*-olefin PIB (1.00 g, 0.355 mmol) dissolved in 10 mL of solvent and AN (0.50 mL, 7.63 mmol).

At room temperature and under vigorous stirring, 0.50 mL of concentrated H_2SO_4 was added, and the scintillation vial was sealed. The mixture was stirred for 12 h, then quenched by pouring the reaction mixture into 50.0 mL of an ice/water slurry, and stirred for an additional hour. After concentrating the mixture under an N_2 stream, the PIB was precipitated into methanol, and worked up as described above. The resulting polymer was then characterized via ^{1}H NMR and GPC.

In the second series of experiments using *exo*-olefin PIB as the electrophilic reagent (Trials 2.1-2.12), different combinations of mineral/organic acids and solvents were used and 11-cyanoundecyl acrylate (CUA) was used as the nitrile substrate; reaction conditions are listed in Table 3.2. A general procedure was as follows: To a scintillation vial equipped with a magnetic stirrer was charged *exo*-olefin PIB (1.00 g, 0.355 mmol) dissolved in 10 mL of solvent and 11-cyanoundecyl acrylate (0.50 mL, 1.70 mmol, CUA). At room temperature and under vigorous stirring, a 0.50 mL aliquot of acid was added, and the scintillation vial was sealed. The mixture was stirred for 12 h, then quenched by pouring the reaction mixture into 50 mL of an ice/water slurry and stirred for an additional hour. After concentrating the mixture under an N_2 stream, the PIB was precipitated into methanol, and worked up as described above. The resulting polymer was characterized via ^{1}H NMR.

3.3.5 Synthesis of 11-cyanoundecan-1-ol.

11-Cyanoundecyl acrylate was synthesized in two steps from 11-bromoundecan-1-ol. In the first step, 11-bromoundecan-1-ol was converted to 11-cyanoundecan-1-ol, as follows: To a 250 mL round bottom flask equipped with a magnetic stirrer and condenser were charged 11-bromoundecan-1-ol (10.12 g, 0.0403 mol), sodium cyanide

(5.06 g, 0.103 mol), and 150 mL of DMSO. To aid in dissolution of the cyanide salt, 3 mL of DI water was added to the mixture. The mixture was purged continuously with N_2 and stirred at 60 ºC overnight. Upon reaching quantitative conversion as indicated by ^1H NMR, the reactor was removed from heat. After cooling to room temperature, the mixture was quantitatively transferred to a separatory funnel, and DCM was added until a 5/1 (v/v) DCM/DMSO ratio was achieved. A solution of 30% brine (w/w) was then added, and the mixture was vigorously shaken and allowed to stand until separation of the aqueous and organic layers. The organic layer was isolated, washed with brine (x2) and then DI H_2O (x3), dried with $MgSO_4$, filtered, and concentrated via vacuum stripping. The product, 11-cyanoundecan-1-ol, was an off-white crystalline solid (m.p. 40 ºC) soluble in all common organic solvents excluding alkanes. Yield: 7.82 g (> 98%).

3.3.6 Synthesis of 11-cyanoundecane acrylate (CUA).

Into a 250 mL, 3-necked round bottom flask equipped with a magnetic stirrer, a condenser with nitrogen inlet/outlets, and an addition funnel, were charged 11-cyanoundecan-1-ol (7.80 g, 0.0395 mol), TEA (7.26 g, 0.0717 mol), and 125 mL of DCM. The resulting solution was stirred and cooled to 0 °C by immersion of the flask into an ice bath. A solution of 6.00 mL (0.0738 mol) of acryloyl chloride in 25 mL DCM was charged to the addition funnel and then added dropwise to the reactor over a period of approximately 60 min. The mixture was allowed to gradually warm to room temperature and to react overnight. Upon completion of the reaction (monitored by ^1H NMR), the TEA hydrochloride precipitate was separated by vacuum filtration and extracted with fresh DCM. The combined filtrate and extract were transferred into a separatory funnel and washed with 20% HCl solution, 30 wt% brine, and then DI H_2O, to

remove residual reagents. To prevent polymerization, 5 mg of MEHQ was added to the organic layer, which was then separated, dried over Na_2SO_4 and concentrated by rotary evaporation to yield CUA as an amber liquid (9.21 g, 87% yield).

3.3.7 Ritter reaction on *exo*-olefin-terminated oligoisobutylenes (C_{12}, C_{16}, and C_{20}).

Two series of Ritter reactions were performed on small molecule PIB analogs to investigate the prevalence of carbocationic rearrangement on the PIB chain end. In the first series, the Ritter reaction was performed using AN as the solvent/nitrile substrate using the following procedure, which is representative. To a scintillation vial equipped with a magnetic stirrer were charged 10.0 mL (8.10 g, 0.153 mol) of AN and 2.00 g of either 2,4,4,6,6-pentamethyl-1-heptene (C_{12}), 2,4,4,6,6,8,8-heptamethyl-1-nonene (C_{16}), or 2,4,4,6,6,8,8,10,10-nonamethyl-1-undec-ene (C_{20}). The mixture was vigorously stirred for 10 min, and then 1.00 mL of concentrated H_2SO_4 was slowly added to the mixture. The mixture was stirred for 8 h, after which it was poured onto 15 g ice. The resulting mixture was stirred for 1 h, and then transferred into a separatory funnel and twice extracted with 25 mL diethyl ether. The ethereal layers were combined, and washed with three 100 mL portions of a 0.1 M solution of HCl. The ethereal layer was then washed with a sodium bicarbonate solution until neutral to pH paper, and then triple rinsed with a 30% (w/w) brine solution. The ethereal layer was finally dried over sodium sulfate and filtered, and the solvent was removed via vacuum stripping. In the case of C_{12}, a white crystalline solid (m.p. 58-59 ºC) was isolated, which was washed with pentane and dried under vacuum to yield 2.00 g (70% yield). Elemental composition calculated for $C_{15}H_{29}NO$ (%): C, 75.25; H, 12.21; N, 5.85; O, 6.68. Found: C, 75.89; H, 12.35; N, 5.68; O, 6.08. This material was found to be insoluble in water and aliphatic/aromatic solvents,

but soluble in ethers, halogenated solvents, ketones, amides and alcohols. For C_{16} and C_{20}, removal of the ethereal solvent resulted in light pink oils: for C_{16}, 1.73 g (66% yield) was collected, for C_{20}, 1.53 g (61% yield) was collected. In all cases, the resulting product was characterized via ^{1}H NMR.

In the second series, the Ritter reaction was performed in a 60:40 DCM:hexane cosolvent mixture using a procedure similar to the one outlined above. In each case the reaction mixture consisted of 1.00 mL (0.0153 mol) AN, 2.00 g of either C_{12}, C_{16}, or C_{20} oligoisobutylene, and 10.0 mL of DCM:hexane. In all cases, removal of the ethereal layer resulted in a viscous oil from which a white crystalline precipitate formed upon standing. Pentane was added to the mixture, and the crystalline precipitate was separated via vacuum filtration through a fritted glass (10-15 μm pore size) filter. The eluent was collected and pentane was removed via vacuum stripping to yield a colored, viscous oil (C_{12}: 1.77 g (62%); C_{16}: 1.70 (65%); C_{20}: 1.46 g (58%)). The white solid was washed with three 15 mL portions of pentane and dried to constant weight under vacuum. Both products were then characterized via ^{1}H NMR.

3.4 Results and Discussion

3.4.1 End quenching of living carbocationic PIB with acrylonitrile.

Our initial goal was reactive end quenching of living PIB via the Ritter reaction. Acrylonitrile was chosen as the nitrile substrate due to its commercial availability, low cost, and its potential to form telechelic PIB macromers. To investigate the efficacy of the Ritter reaction under living carbocationic polymerization conditions, first IB was polymerized under the following conditions: [bDCC] = 0.020 M, [IB] = 2.0 M, [2,6 lutidine] = 0.003 M, and [$TiCl_4$] = 0.020 mol L^{-1} using the 60/40 methyl chloride/hexane

solvent system at -70 ºC. Upon full monomer conversion (as measured by RT-ATR-FTIR, ~75 min), an aliquot was removed and precipitated into chilled methanol, to serve as a pre-quench comparison. The living carbocationic chain ends (CE) were then quenched by addition of 1.10 mL (0.0167 mol) of AN and 3.19 mL (0.0291 mol) $TiCl_4$ to the reactor. These conditions provided a molar ratio of quencher to chain end, [AN]/[CE], equal to 2.0 and an effective catalyst concentration $[TiCl_4]_{eff}$ = 0.07 M. $[TiCl_4]_{eff}$ was calculated as the available $[TiCl_4]$ remaining after formation of 1:1 complexes with 2,6 lutidine and acrylonitrile, and after scavenging of protic impurities (HA). Concentration of the latter was estimated to be about 2 mM within the glove box. Aliquots were taken at 1 h increments during the quenching process, and the reaction was terminated after 4 h with pre-chilled methanol.

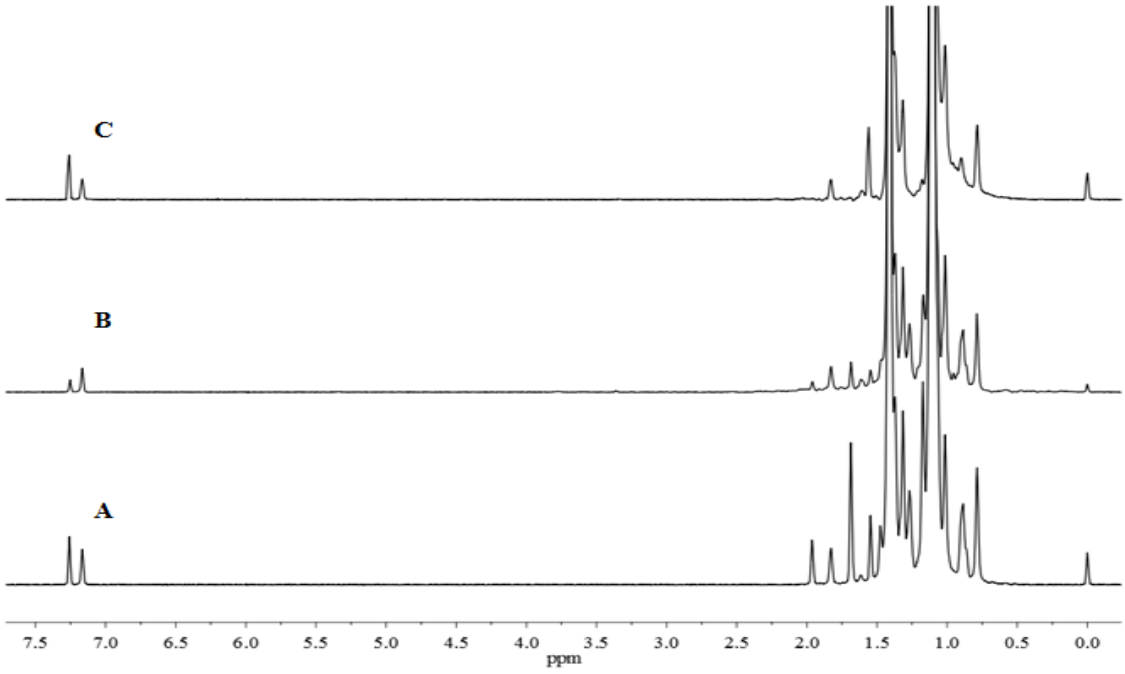

Figure 3.1 ^{1}H NMR (300 MHz, $CDCl_3$, 25 °C) spectra of (A) *tert*-chloride PIB, (B) PIB quenched with AN using $[TiCl_4]$ = 4[CE], and (C) PIB quenched with AN using $[TiCl_4]$ = 4.5[CE]. -70 °C; 60/40 methyl chloride/hexane; [AN]/[CE] = 2.0; quenching time = 4 h.

Figure 3.1 shows ^{1}H NMR spectra of the pre-quench aliquot (spectrum A) and the final end product after 4 h (spectrum B) of the quenching experiment described above. The former (spectrum A) displays resonance signals at 1.69 and 1.96 ppm, which correspond to the terminal methyl and methylene groups of the *tert*-chloride PIB chain. Integration of either of these resonances relative to the initiator resonance at 7.17 ppm indicated essentially quantitative *tert*-chloride chain end functionality for the pre-quench aliquot. These resonance signals were also observed in spectrum B, and integration indicated that about 40 mol% of the end groups of the final product remained as unreacted *tert*-chloride. However, spectrum B did not reveal any olefinic resonance signals typically associated with acrylate moieties (5.0-6.5 ppm), which demonstrated that the living PIB chain ends did not undergo a Ritter-type addition to form the desired acrylamide. Moreover, spectrum B revealed no other typical end group structures such as *exo*/*endo* olefin, coupled PIB, etc., suggesting that the remaining 60% of the end groups were lost to carbocation rearrangement of the active chain ends, as depicted in Scheme 3.2.

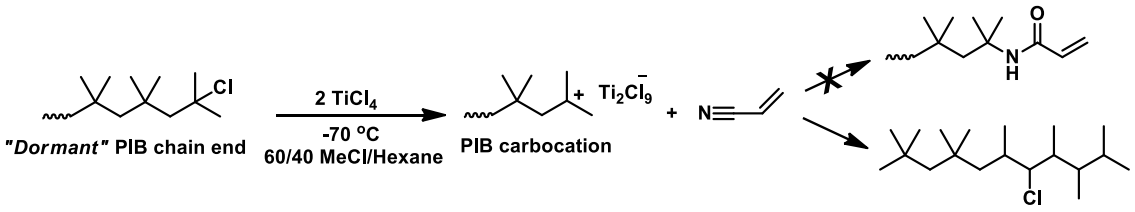

Scheme 3.2 The Ritter reaction of PIB with AN under living carbocationic polymerization conditions and competing carbocation rearrangement.

Support for this interpretation was provided by a second quenching experiment carried out at higher $[TiCl_4]_{eff}$. Living PIB chains were created under conditions identical to those described above. After removal of a pre-quench aliquot, the living chain ends

were quenched by addition of 1.10 mL (0.0167 mol) of AN and 3.64 mL (0.0291 mol) $TiCl_4$. These conditions provided the same [AN]/[CE] molar ratio as before (2.0), but in this case the $[TiCl_4]_{eff}$ was increased to 0.09 M. The ^1H NMR spectrum of the final product is shown as spectrum C in Figure 3.1. By increasing the effective catalyst concentration, all *tert*-chloride chain ends were converted within the 4 h reaction period, and like before, no trace of the intended acrylamide product or other typical PIB end groups was observed. A multitude of small peaks in the 1.70-2.25 ppm region of spectrum C signify the presence of a family of rearranged products, similar to the representative structure in Scheme 3.2, but possessing the *tert*-chloride function displaced at various lengths toward the initiator end of the chain. Expansions of spectra A-C of Figure 3.1 are provided in the Appendix (Figures A.17-A.19, respectively).

Similar carbocation rearrangements have been observed in other quenching situations, typically whenever the rate of quenching is slow and therefore cannot compete kinetically. For example, in quenching reactions involving phenoxyalkyl (meth)acrylates, complexation of the acrylate carbonyl oxygen with $TiCl_4$ causes retardation of the rate of quenching for alkylene tether lengths shorter than normal C_4.[98]

3.4.2 *exo*-Olefin PIB substrates.

Unsuccessful attempts in performing the Ritter reaction under living polymerization conditions led us to design two series of experiments using conditions that more accurately resembled the classical Ritter reaction, in which an olefin is protonated by a strong Bronsted acid in the presence of a nitrile, as shown in Scheme 3.3. Using this approach, we first set out to investigate the effect of solvent polarity on the

efficacy of the Ritter reaction on exo-olefin terminated PIB; the reaction conditions and products are summarized in Table 3.1.

Table 3.1 Experimental Conditions and Results for the Ritter Reaction of *exo*-Olefin PIB with AN in the Presence of H_2SO_4 at 25 °C.

Entry	Solvent	Solvent Polarity[51]	Product
1.1	Hexane	0.009	Chain end rearrangement
1.2	Toluene	0.099	Chain end rearrangement
1.3	Chloroform	0.259	Chain end rearrangement
1.4	DCM	0.309	Chain end rearrangement
1.5	THF	0.207	*exo*-olefin
1.6	Glyme	0.231	*exo*-olefin
1.7	MIBK	0.269	*exo*-olefin
1.8	Cyclohexanone	0.281	*exo*-olefin
1.9[b]	DCM	0.309	Chain end rearrangement

[a] [CE] = 0.0322 M; [AN] = 0.694 M; [HA] = 0.836 M; under stirring for 12 h.
[b] Acetonitrile was the nitrile substrate; [CE] = 0.0325M; [AceN] = 0.703 M; [HA] = 0.844 M.

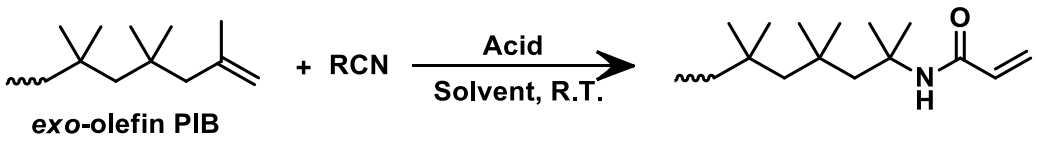

Scheme 3.3 Ritter reaction of PIB with RCN under "classical" Ritter reaction conditions

In the second series, the polarity of the nitrile substrate was modified by increasing the aliphatic content, and a variety of different organic acids were used. Two halogenated solvents ($CHCl_3$ and DCM) were used, due to their moderate polarity and their ability to dissolve PIB.

3.4.2.2 Effect of solvent polarity on the Ritter reaction of *exo*-olefin PIB.

PIB exhibits excellent solubility in (cyclo)aliphatic, aromatic, and halogenated hydrocarbon solvents, moderate solubility in some ketones and ethers, and poor solubility in alcohols, amides, and carboxylic acids. Accordingly, solvent polarity represents an inherent limitation when designing the reaction medium for PIB substrates. To test the efficacy of the Ritter reaction on *exo*-olefin PIB, several screening trials of the Ritter reaction were performed in a variety of solvent media, using *exo*-olefin PIB ([CE] = 0.0322 M) and H_2SO_4 ([HA] = 0.836 M) as an acid catalyst, with acrylonitrile ([AN] = 0.694 M) serving as the nitrile substrate. These experiments are designated Entries 1.1-1.8 in Table 3.1. Entry 1.9 was carried out under identical reaction conditions using acetonitrile (AceN) as the nitrile substrate ([CE] = 0.0325 M, [HA] = 0.844 M, [AceN] = 0.703 M), and is also included in Table 3.1. A description of the isolated products, along with solvent identities and their associated normalized polarities[171] are also included. The product obtained from each trial was characterized by ^{1}H NMR (Figures A.20-A.28) and GPC (Figure 3.3).

The desired amide product was not isolated for any of the reaction conditions described in Table 3.1 (as determined by ^{1}H NMR); however, some important observations and general trends were made from the data. In all trials, addition of the H_2SO_4 aliquot caused a slight discoloration of the initially clear solution, eventually forming a hazy, yellow mixture over the course of the reaction. In the presence of aliphatic, ethereal, or ketone solvents (Trials 1.1, 1.5-1.8), addition of the H_2SO_4 aliquot caused eventual precipitation of the PIB. In the remaining trials, the reaction mixture

formed an increasingly hazy suspension which would separate into two distinct layers in the absence of stirring.

In all trials, stirring was discontinued after 12 h. In Trials 1.2-1.4 and 1.9, the bottom layer was isolated as a water soluble, yellow liquid that was acidic to pH paper, and the top layer was a clear liquid that yielded a white precipitate when added into water. In Trials 1.1 and 1.5-1.8, the solution was decanted and concentrated under an N_2 stream, which did not yield any precipitate when added to water. In those trials, the precipitated PIB was collected from the reaction vial by dissolution into a minimum volume *n*-hexane and precipitated into water.

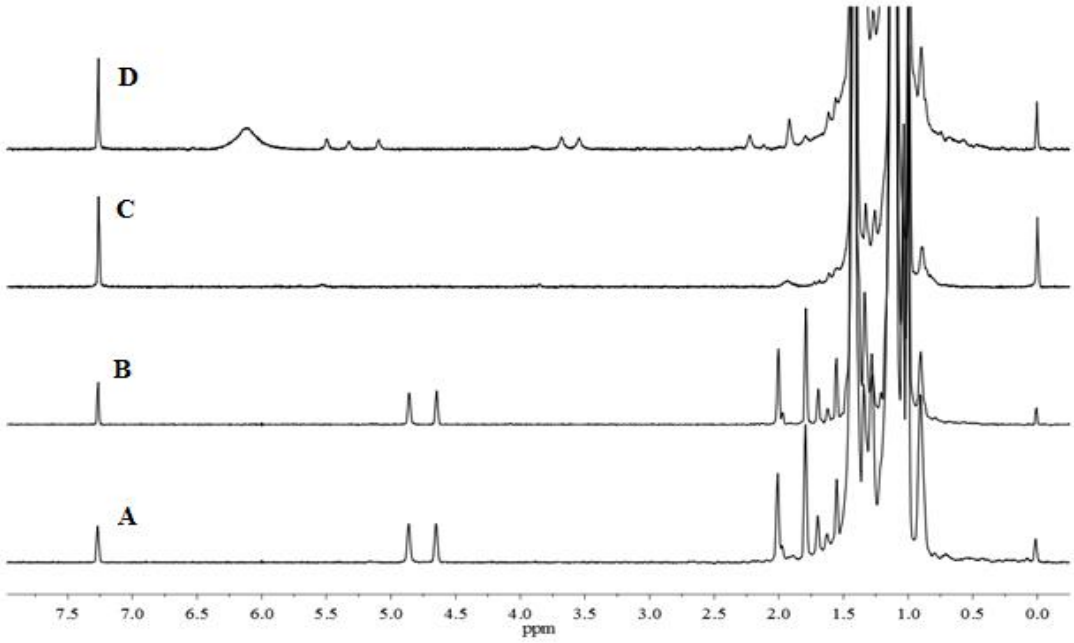

Figure 3.2 ^{1}H NMR (300 MHz, $CDCl_3$, 25 °C) spectra of (A) *exo*-olefin PIB, and the isolated product from the Ritter reaction of *exo*-olefin PIB with AN in (B) THF, (C) hexane, and (D) chloroform.

Comprehensive analysis of the ^{1}H NMR spectra and GPC chromatograms of Trials 1.1-1.9 provided insight into the various failure pathways of the Ritter reaction on

exo-olefin PIB. Figure 3.2 shows a comparison among the starting *exo*-olefin PIB (A) and the products isolated from THF (B), hexane (C), and chloroform (D).

Figure 3.2D is the spectrum of the product obtained in chloroform, which is representative of products obtained in aromatic and halogenated hydrocarbon solvents (Trials 1.2-1.4 and 1.9); the spectrum does not show the peaks characteristic of *exo*-olefin chain ends (4.64 and 4.85 ppm), but it does show a series of peaks ranging from 1.6-2.4 ppm, which is characteristic of the loss of chain end fidelity through carbocation rearrangement. These series of peaks can be observed in high expansions of this region, which are included in the Supporting Information (Figures A.21, A.23, and A.28, respectively). This series of peaks is also observed in Figure 3.2C, which is the spectrum of the product obtained in hexane (Trial 1.1); however, Figure 3.2D also displays a series of resonance signals ranging from 3.5 to 6.5 ppm that are absent in Figure 3.2C. Figure 3.2B (product obtained in THF, Trial 1.5) is presentative of aliphatic, ethereal, and ketone solvents (Trials 1.5-1.8); in these solvents the reaction essentially returned unreacted *exo*-olefin PIB.

The starting material and the products obtained from Trials 1.1-1.9 were also characterized via GPC, and the refractive index (RI) traces are shown in Figure 3.3. The RI traces from the products from Trials 1.1 and 1.5-1.8 show nearly uniform overlap with the starting material, indicating that polymer backbone degradation did not occur. These contrast significantly with the RI traces from the products from Trials 1.2-1.4 and 1.9, which show a series of peaks eluting after 17 min, suggesting extensive degradation of the polymer backbone.

From the ^{1}H NMR spectra and GPC chromatograms, two main failure mechanisms of the Ritter reaction on *exo*-olefin PIB can be suggested. In the presence of oxygen-containing solvents (Trials 1.5-1.8), the *exo*-olefin moiety remained intact after 12 h, and degradation of the polymer backbone was not observed. Additionally, PIB precipitation was observed during the course of the reaction, which suggests the sequestration of the acid by the oxygen moiety, resulting in a more polar reaction medium, causing eventual PIB precipitatation. Additionally, oxygen containing solvents may complex to the carbocationic chain end, hindering nucleophilic attack of the nitrile while simultaneously preventing carbocation rearrangement.

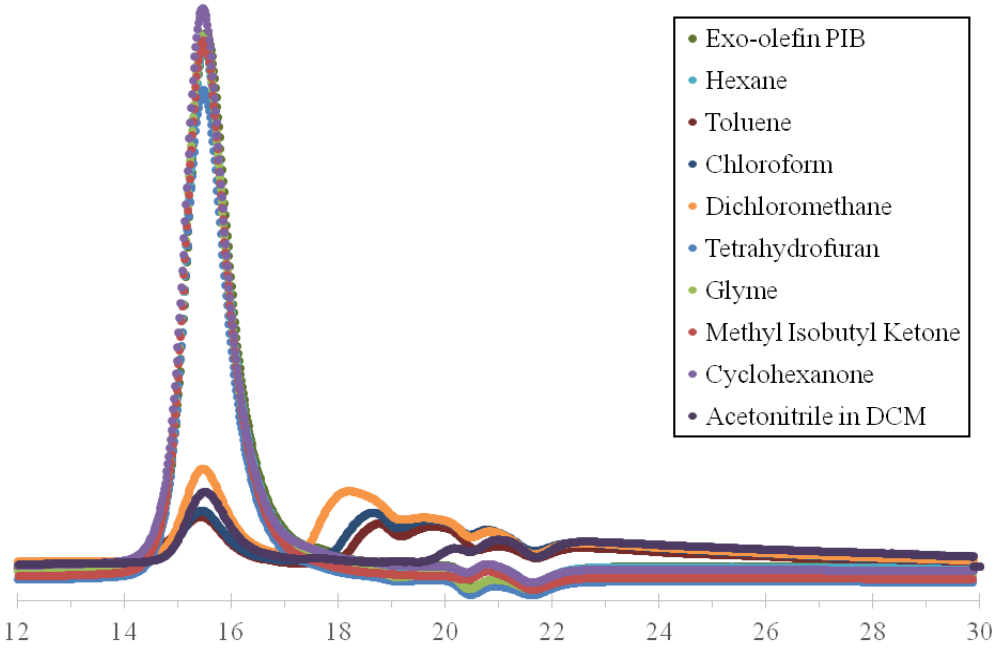

Figure 3.3 GPC chromatograms of *exo*-olefin PIB and the products from Trials 1.1-1.9, Table 3.1.

In non-oxygen containing solvents (Trials 1.1-1.4 and 1.9) loss of chain end fidelity was observed in all trials, and the extent of polymer backbone degradation

correlated to the polarity of the reaction medium. Generally, carbocation formation was retarded in aliphatic solvents due to low polarity; this has been shown in carbocationic polymerizations, where extremely slow polymerization rates are obtained without the use of more polar co-solvents. In Trial 1.1, where the solvent medium was hexane, we observed carbocation rearrangement of the PIB chain end, as evidenced by the disappearance of the olefinic peaks at 4.64 and 4.86 ppm via ^{1}H NMR, but significant backbone degradation of the polymer was not observed in GPC analysis. In the presence of aromatic and halogenated solvents (Trials 1.2–1.4 and 1.9), the increased polarity of the reaction medium promoted formation of the carbocation. Under conditions of slow nucleophilic attack by the nitrile, this apparently resulted in rearrangement and fragmentation, resulting in extensive degradation of the PIB backbone and a mixture of low molecular weight products.

3.4.2.3 Acid and Nitrile Screening.

From the observations made in Trials 1.1-1.9, a second series of screening trials was performed on *exo*-olefin PIB, in which the acid catalyst and nitrile substrate were varied. Due to the harsh nature of H_2SO_4, we elected to additionally use alternative acids with moderately lower acidities, which were also soluble in organic solvents. Additionally, we hypothesized that the inherent difference in polarity between AN and PIB may have inhibited interaction between the carbocation chain end and the nitrile, retarding the rate of the desired reaction and eventually leading to chain end rearrangement and degradation of the polymer backbone. This theory was supported by observations made in preliminary studies; when a high concentration of the AN was introduced into the reaction medium, immediate PIB precipitation occurred before

addition of the acid catalyst. This suggested that a more non-polar nitrile, ideally one that is PIB miscible, might be fitted with an acrylate function to produce a viable Ritter-type quencher molecule. Enhanced miscibility might allow for higher concentration of the nitrile and acceleration of the Ritter reaction rate relative to carbocation rearrangement. Thus, a new nitrile substrate was synthesized, 11-cyanoundecane acrylate (CUA), which contained a longer aliphatic tether to promote miscibility with PIB. ^{1}H NMR spectra of CUA and its precursors are included in the Appendix (Figures A.29-A.31).

Table 3.2 Experimental Conditions and Results for the Ritter Reaction of *exo*-Olefin PIB with 11-Cyanoundecane Acrylate (CUA) in the Presence of Various Acids at 25 ºC[a]

Entry	Solvent	Acid	Co-acid (v/v)	[HA] (M)	Result
2.1	DCM	H_2SO_4	-	0.836	carbocation rearrangement
2.2	DCM	AcOH	-	0.791	*exo*-olefin PIB
2.3[b]	DCM	AcOH,	25% H_2SO_4	0.594 + 0.209	carbocation rearrangement
2.4[b]	DCM	AcOH,	10% H_2SO_4	0.712 + 0.0836	carbocation rearrangement
2.5[b,c]	DCM	AcOH	10% H_2SO_4	0.712 + 0.0836	*exo*-olefin PIB
2.6[b]	$CHCl_3$	AcOH	10% H_3PO_4	0.712 + 0.0673	*exo*-olefin PIB
2.7	$CHCl_3$	H_3PO_4	-	0.673	*exo*-olefin PIB
2.8	$CHCl_3$	HCl (aq)	-	0.530	*exo*-olefin PIB
2.9	$CHCl_3$	HI (aq)	-	0.345	*exo*-olefin PIB
2.10	$CHCl_3$	DCAc	-	0.551	*exo*-olefin PIB
2.11	$CHCl_3$	HCl	-	-	tert-chloride PIB
2.12	$CHCl_3$	HI	-	-	*exo*-olefin PIB

[a] [CE] = 0.0322 M; [CUA] = 0.154 M
[b] Acid concentration reported as $[HA]_{acid}$ + $[HA]_{co\text{-}acid}$
[c] Acrylonitrile was the nitrile substrate; [CE] = 0.0322 M; [AN] = 0.694 M

Table 3.2 shows the results of reaction trials using CUA; the conditions of the Ritter reaction were varied using halogenated acids, organic acids, and strong acids with lower acidities than H_2SO_4. Surprisingly, the desired acrylamide product was not formed under any of the conditions of Table 3.2. The ^1H NMR spectrum for each isolated product is included in the Appendix (Figures A.32-A.43). In Trial 2.1, using H_2SO_4 as the acid catalyst resulted in a product that exhibited loss of the *exo*-olefin chain end and resonance signals typical of chain end rearrangement. In Trial 2.2, AcOH was used, but was shown to be unreactive towards the *exo*-olefin chain end. Two different co-acid systems were then attempted, which were pre-mixed in a separate scintillation vial before addition to the reaction mixture. Interestingly, Trial 2.4 showed loss of chain end fidelity when using the 10% H_2SO_4 co-acid mixture in the presence of CUA; however, the *exo*-olefin moiety remained intact in the presence of AN. The *exo*-olefin moiety was unreactive towards weaker acids, such as acetic acid, phosphoric acid, and dichloroacetic acid. The *exo*-olefin moiety was also unreactive towards aqueous mineral acids; however, in the presence of HCl gas, the isolated product was *tert*-chloride PIB. In the presence of HI gas, the *exo*-olefin moiety remained intact.

3.4.3 Ritter reaction on exo-olefin terminated oligoisobuytylene (C_{12},C_{16},C_{20}) distillates.

Convinced that the uniform failure of the Ritter reaction with PIB was due to slow kinetics resulting from incompatibility of polar nitrile compounds with PIB, two series of reactions were performed on C_{12}, C_{16}, and C_{20} oligoisobutylene distillates, which represent the trimer, tetramer, and pentamer of *exo*-olefin PIB. Reaction conditions and products are listed in Table 3.3. In the first series of reactions (Trials 3.1-3.3), AN was

used as both solvent and nitrile substrate, while in the second series (Trials 3.4-3.6), a 10.0 mL solution consisting of DCM:hexane (60:40) was used, which mimics the solvent conditions often used in living PIB polymerizations. ^{1}H NMR spectra of the starting oligoisobutylenes and products isolated from Trials 3.1-3.6 are included in the Appendix (Figures A.44-A.53).

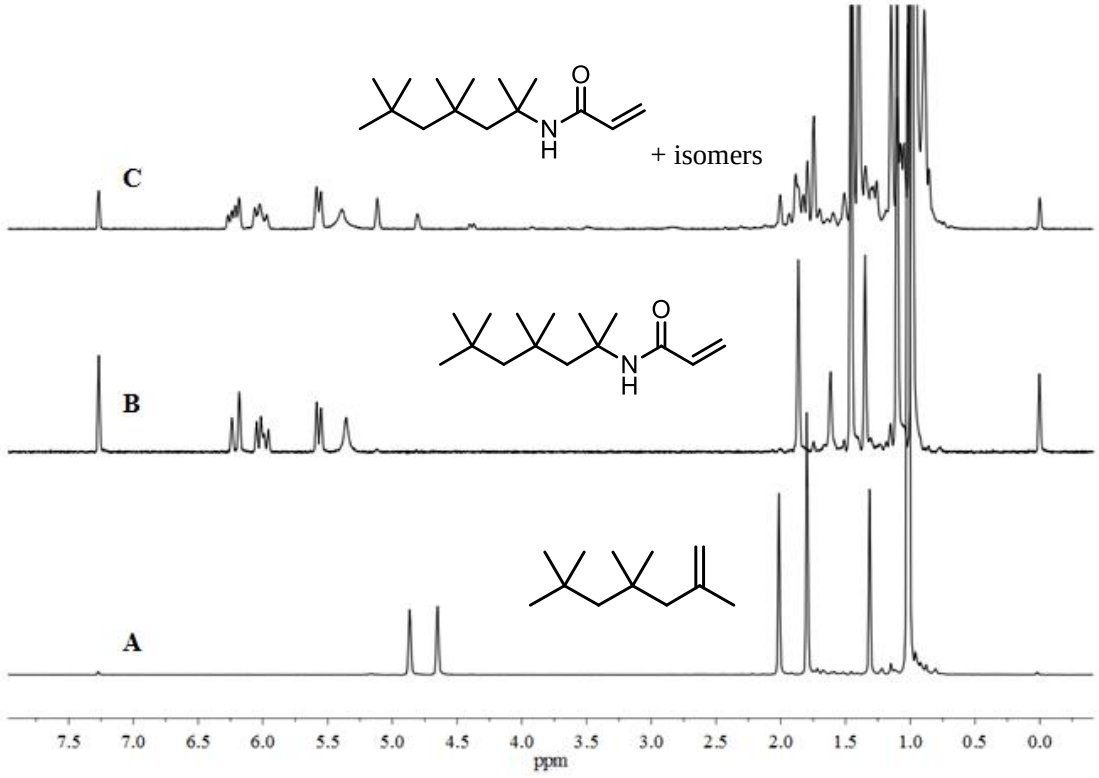

Figure 3.4 ^{1}H NMR spectra (300 MHz, $CDCl_3$, 25 °C) of the Ritter reaction of C_{12} and acrylonitrile (AN): (A) C_{12} reactant, (B) product obtained using AN as both solvent and nitrile reactant, and (C) products using DCM/hexane as the solvent.

The starting oligoisobutylenes were produced from fractional distillation of mixed oligoisobutylenes obtained as a by-product of the commercial HR PIB process. For each *exo*-olefin oligoisobutylene (C_{12}, C_{16}, and C_{20}), the principle impurity was the *endo*-olefin isomer (peak at 5.15 ppm in Figures 3.4-3.6, spectrum A, and in Figures A.35-A.37). This was predicted to have no effect upon the Ritter reaction, since upon protonation,

both isomers yield the identical carbocation. Additionally, GC-MS analysis (Figures A.11-A.16) indicated that the C_{16} sample contained a small amount of C_{12}, and the C_{20} sample contained small amounts of C_{12} and C_{16}.

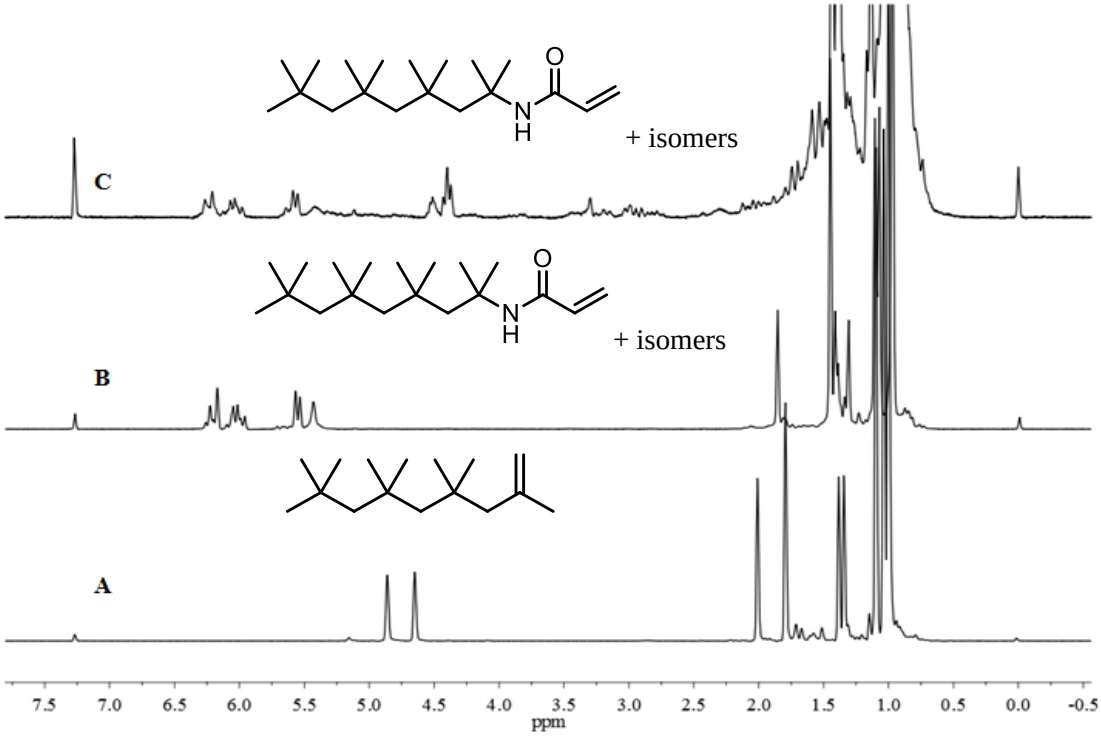

Figure 3.5 ^{1}H NMR spectra (300 MHz, $CDCl_3$, 25 °C) of the Ritter reaction of C_{16} and acrylonitrile (AN): (A) C_{16} reactant, (B) product obtained using AN as both solvent and nitrile reactant, and (C) products obtained using DCM/hexane as the solvent.

Figures 3.4-3.6 include comparative ^{1}H NMR spectra of (A) the *exo*-olefin-terminated oligoisobutylene reactant, (B) the products formed using AN as both solvent and nitrile reactant, and (C) the products formed under dilute conditions, for C_{12}, C_{16}, and C_{20}, respectively. Although acrylamide functionalized oligomers were isolated in all trials, the products isolated using AN as both solvent and reactant differed significantly from those isolated using DCM/hexane as solvent. For the C_{12} oligomer, comparison of Figure 3.4A to Figure 3.4B shows the quantitative disappearance of olefinic protons at

4.65 ppm and 4.86 ppm, and the appearance of crisp doublets at 5.55 ppm and 6.18 ppm and a multiplet at 6.00 ppm, which are characteristic of acrylate protons. Additionally, the aliphatic region (0.50-2.25 ppm) displays similar signals in both spectra. This indicates that the acrylamide product formed under concentrated conditions (i.e. using AN as solvent) with no detectable isomerization via carbocation rearrangement. This trend continued in Figure 3.5 and Figure 3.6, but new peaks in the aliphatic region in Figures 3.5B and 3.6B indicate the formation of isomeric oligomers, which suggests a direct correlation between carbocation rearrangement and higher aliphatic content in the oligomer backbone.

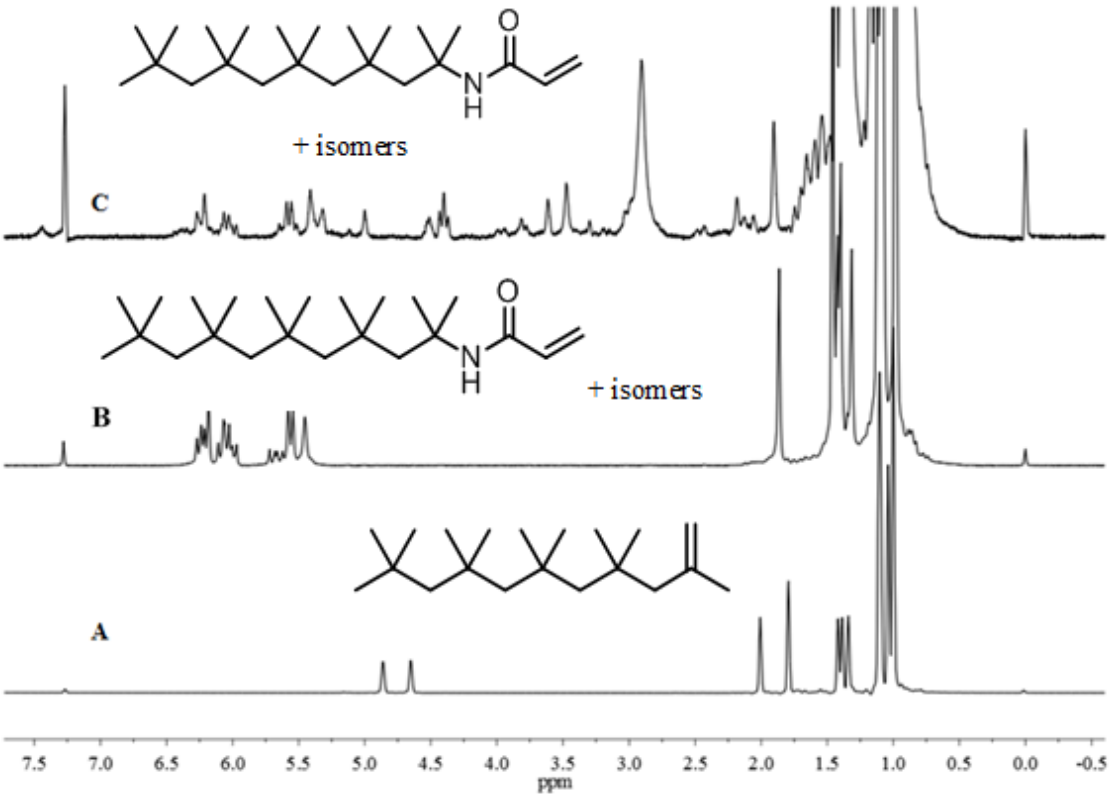

Figure 3.6 ^{1}H NMR spectra (300 MHz, $CDCl_3$, 25 °C) of the Ritter reaction of C_{20} and acrylonitrile (AN): (A) C_{20} reactant, (B) product obtained using AN as both solvent and nitrile reactant, and (C) products obtained using DCM/hexane as the solvent.

Also included in Figures 3.4, 3.5, and 3.6 are ^{1}H NMR spectra of the products obtained when the Ritter reaction was carried out on C_{12}, C_{16}, and C_{20} in the presence of a DCM/hexane co-solvent system. Comparison of the ^{1}H NMR spectrum of the products (spectrum C in each figure) with that of the respective starting material (spectrum A) suggests significant isomerization, as indicated by the variety of new peaks in the aliphatic region and the region spanning 3–5 ppm. Also, the loss of signal resolution and change in splitting patterns of the acrylate protons differ significantly between spectra B and C; this difference is noticeable in Figure 3.4 and becomes even more pronounced in Figures 3.5 and 3.6.

During sample workup of the reactions conducted using DCM/hexane, a white crystalline precipitate was isolated from the product mixture, which was found to be insoluble in hexane and other nonpolar solvents. Characterization via ^{1}H NMR confirmed this material to be *tert*-butyl acrylamide (Figure A.53), which indicates the onset of backbone degradation of the oligomer. As shown in Table 3.3, there is a direct correlation between the amount of isolated *tert*-butyl acrylamide and the number of isobutyl units in the oligomer backbone.

Table 3.3 Experimental Conditions and Results for the Ritter Reaction on PIB Oligomers with AN in the Presence of H_2SO_4 at 25 °C.

Trial	Substrate	Solvent	[CE] (M)	[AN] (M)	[H_2SO_4] (M)	Product	*tert*-butyl acrylamide (g)
3.1	C_{12}	AN	0.897	11.5	1.39	C_{12} acrylamide	0.00
3.2	C_{16}	AN	0.674	11.5	1.39	C_{16} acrylamide	0.00
3.3	C_{20}	AN	0.539	11.5	1.39	C_{20} acrylamide	0.00
3.4	C_{12}	DCM/ hexane	0.990	1.27	1.53	acrylamide isomers	0.032
3.5	C_{16}	DCM/ hexane	0.744	1.27	1.53	acrylamide isomers	0.049
3.6	C_{20}	DCM/ hexane	0.595	1.27	1.53	acrylamide isomers	0.076

The propensity for oligomer isomerization via carbocation rearrangement when the nitrile reactant is diluted by solvent, particularly when the polarity of the reaction medium is thereby also decreased, further validates our findings in Trials 1.1-1.5 (Table 3.1), in which *exo*-olefin PIB was used as the substrate. Although exact structures could not be assigned via ^{1}H NMR, loss of chain end fidelity was observed as indicated by the disappearance of the olefinic protons, which were replaced with new, unidentifiable peaks in the aliphatic region. Additionally, molecular weight analysis via GPC showed considerable degradation of the polymer backbone in the presence of moderately polar solvents, which was reflected in the formation of *tert*-butyl acrylamide when PIB oligomers were used as the substrate (e.g. Figure 3.5 and Figure 3.6.)

Proclivity of carbocation rearrangement in the Ritter reaction has been reported in the literature; however amidated products have still been isolated on small-molecule substrates.[172,173,174] Christol and coworkers published a large body of work on the application of the Ritter reaction, including a thorough investigation of the effect of solvent conditions and acid strength on the acid catalyzed carbocation rearrangement of a variety of substrates.[175,176,177,178,179,180] Generally, solvent polarity and acid choice were both found to directly affect amide yields; when acetonitrile or benzonitrile acted as the nitrile/solvent, carbocation rearrangement was considerably suppressed.[180] When the reaction was diluted with non-polar solvents such as CCl_4, hexanes, or moderately polar solvents like diethyl ether, Christol demonstrated that isomeric mixtures of products were formed.[181, 182] Unfortunately, the aliphatic backbone of PIB necessitates the use of non-polar solvents, and our results demonstrate that H_2SO_4 causes chain end degradation of the PIB substrate. According to the literature, using (non)halogenated organic acids as a

catalyst or diluent often resulted in ester formation which competed with amide formation.[166,167] In our hands, these acids did not cause protonation of the *exo*-olefin PIB chain end.

3.5 Conclusions

The Ritter reaction remains an attractive, although elusive, option for PIB chain end functionalization. Under living polymerization conditions, the use of acrylonitrile as a quenching reagent resulted in the formation of either *tert*-chloride terminated PIB or PIB that degraded via carbocation rearrangement of the chain end. Under more traditional Ritter conditions using *exo*-olefin PIB as the substrate, solvent polarity and the presence of oxygen moieties were found to determine the formation of *exo*-olefin PIB or severely degraded PIB, but an acrylamide functionalized product was not isolated. Modification of the acid catalyst or the nitrile substrate did not result in the formation of the acrylamide.

In the presence of e*xo*-olefin functionalized PIB oligoisobutylenes, the Ritter reaction has provided a route towards a new family of hydrophobic acrylamide monomers bearing isobutenyl moieties. Additionally, the reaction on oligoisobutylenes also provided insight towards the various mechanistic pathways of the failure of the Ritter reaction on *exo*-olefin functionalized PIB, namely, the competition between carbocation rearrangement and nitrilium ion formation. Under concentrated conditions, quantitative formation of the acrylamide product was observed for C_{12}, C_{16}, and C_{20}. Although isomerization was heavily suppressed under these conditions, the length of the isobutenyl tether directly correlated with the solubility of the oligoisobutylene in the AN solvent and the extent of isomerization. Under dilute conditions, significant carbocation

rearrangement and degradation of the oligomer backbone resulted in the formation of acrylamide functionalized isomers and *tert*-butyl acrylamide.

CHAPTER IV – END-QUENCHING OF TICL4-CATALYZED POLYISOBUTYLENE WITH SYMMETRIC RESORCINOL ETHERS FOR DIRECT CHAIN END FUNCTIONALIZATION

Co-authored by Robson Storey

4.1 Abstract

Symmetric resorcinol ethers were used to end-quench $TiCl_4$-catalyzed living isobutylene polymerizations initiated from 5-*tert*-butyl-1,3-di(1-chloro-1-methylethyl)benzene in 60/40 (v/v) methyl chloride/hexane at -70 °C. The total effective $TiCl_4$/chain end molar ratios were in the range of 0.868-1.85, and the quencher/chain end molar ratio was held constant at 2. Alkylation, exclusively at C4 of the aromatic ring, was generally very rapid for all resorcinol ethers and multiple alkylations were not observed; however, systems in which the effective$TiCl_4$/chain end molar ratio < 1.85 demonstrated less than quantitative end-capping. The latter materials possessed a mixture of *tertiary*-chloride and resorcinol ether end groups. Resorcinol quenching was also attempted in the presence of an HCl saturated solution, but alkylation was not observed.

4.2 Introduction

Polyisobutylene (PIB) is a fully saturated, synthetic polymer that exhibits excellent gas barrier and mechanical damping properties, high elasticity, and biocompatibility.[135] PIB homopolymers have found commercial use as the primary components in heat-resistant sealants, adhesives, and oil-miscible rheology modifiers and lubricants, as they exhibit excellent chemical resistivity due to the fully saturated aliphatic backbone of the polymer. Low molecular weight PIBs have also found

commercial use as an additive in synthetic oils,[181] but these materials require chemical modification of the polymer chain end.[80] To this end, telechelic PIBs have generated great technological interest due to their potential applications in the areas of thermoplastic elastomers,[182] "instant-set" sealants,[69,99,] and drug-delivery vehicles.[183]

Traditionally, telechelic PIBs were synthesized via a multistep process that involved transformation of tertiary chloride functionalized PIB (PIB-Cl, obtained from quenching a controlled PIB polymerization with chilled methanol) to *exo*-olefin (methyl vinylidene) functionalized PIB, via reflux with a sterically hindered base such as potassium tert-butoxide.[66,72] A variety of different telechelic PIB's have been reported via this intermediate, including primary hydroxyl,[184,185] ether,[66] thioether,[85,186,] epoxide,[57] aldehyde,[187] carboxylic acid,[188] and primary halides**Error! Bookmark not defined.**; however this method has proved cumbersome due to the long reaction times, multi-step processes, and the inevitable formation of a small amount of the *endo*-olefin.[55]

A less cumbersome method, which also has the additional benefit of yielding quantitative *exo*-olefin termini, has been reported by multiple groups and is known in the field as "end-quenching." In this method, a small molecule is added, *in situ*, to a living PIB polymerization that has reached full monomer conversion. Small molecules such as alkylsilanes,[74] hindered bases,[189] alkoxysilanes,[190] alkyl ethers,[191] and alkyl sulfides[192] have been shown to yield quantitative *exo*-olefin functionalized PIBs, reducing the formation of *endo*-olefin termini to less than detectable levels. The end-quenching approach can also be modified to yield PIBs bearing functionalities other than *exo*-olefin. By using small molecules containing either a suitable nucleophile or nonpolymerizable monomer, multiple groups have reported the synthesis of a wide range of telechelic

PIBs.[193197] To this end, recent work in our laboratory has involved investigation of the efficacy of alkoxybenzene,[96,98] heterocyclic aromatic,[93,94] and functionalized aliphatic olefin[198] substrates on the formation of telechelic PIB via end-quenching. Alkoxybenzene substrates represent an attractive option for *in situ* end-quenching reactions of $TiCl_4$-catalyzed living PIB for a variety of reasons. A diverse array of alkoxybenzenes containing important functionalities (primary halide, hydroxyl, and amine) are either commercially available or can be easily synthesized, and have been shown to yield quantitatively functionalized PIBs at moderate timeframes (4-6 h) under easily modified polymerization conditions.[96] Other functionalities, specifically (meth)acrylate moieties, can be synthesized from commercially available alkoxybenzenes and used without detriment to the quenching process.[98] Additionally, all alkoxybenzenes to date have been shown to yield exclusively monoalkylated products when used in stoichiometric excess (e.g. 2-fold excess) to chain ends. Moreover, alkylation has been shown to occur only at the *para* position, allowing for easy monitoring of reaction progress via ^{1}H NMR. Post-polymerization modification reactions of a variety of alkoxybenzene quenched products have also been reported, which can be easily monitored via the shift in ^{1}H resonances of the alkyl tether.[96]

The benefits of using alkoxybenzene substrates have been well demonstrated since their first reported use in 2010; however, current alkoxybenzene quenchers have displayed two notable limitations. Friedel-Crafts alkylation of an alkoxybenzene by the PIB carbenium ion is relatively slow, and to achieve reasonable quenching rates (reaction time < 3 h) requires relatively high concentrations of the $TiCl_4$ Lewis acid catalyst, typically in the range of $10^{-2} – 2 \times 10^{-1}$ M.[96] For alkoxybenzenes bearing basic moieties

(e.g. carbonyls, hydroxyls, amines, etc.), additional $TiCl_4$ is required. Less reactive Lewis acids, such as boron trichloride (BCl_3), are known to be ineffective towards alkylation while stronger Lewis acids like aluminum trichloride ($AlCl_3$) can result in a combination of functionalized chain ends and degraded chain-ends.[199] The second limitation is that current generations of alkoxybenzene quenchers possess only one reactive moiety. In the areas of lubricant additives,[200] photopolymerizable macromers,[69,99] and thermoplastic elastomers,[182] it may be desirable to impart multiple functionalities or reactive moieties to a single PIB chain end.

Herein, we report the successful alkylation of a library of resorcinol-based substrates in the $TiCl_4$-catalyzed living polymerization of isobutylene. Resorcinol, a cheap and commercially available alkoxybenzene containing two reactive sites, is a highly modular substrate that potentially allows for two functionalities per chain end. Moreover, resorcinol is primarily sourced from plant matter and represents a "greener" alternative to PIB functionalization compared to phenol-based alkoxybenzenes. Under a variety of quenching conditions, resorcinol ethers demonstrate remarkably faster quenching kinetics compared to traditional alkoxybenzene substrates, likely due to the synergistic effects of the electron donating character of the alkoxy moieties. As a result, we also demonstrate that resorcinol ethers require significantly lower Lewis acid demands than their phenol-based counterparts.

4.3 Experimental

4.3.1 Materials

Hexane (anhydrous, 95%), methanol (anhydrous, 99.8%), methylene chloride (anhydrous, 99.8%, DCM), dimethylformamide (anhydrous, 99%, DMF), titanium

tetrachloride ($TiCl_4$) (99.9%), 2,6-lutidine (99.5%), *N*,*N* diisopropylethylamine (99%), dichloromethane-d_2 (CD_2Cl_2), allyl bromide (97%), resorcinol (99%), 1,3-dimethoxybenzene (98%), 2-bromopropane (99%), and potassium carbonate (anhydrous, 99%, K_2CO_3) were purchased from Sigma-Aldrich and used as received. Sodium sulfate (Na_2SO_4), sodium chloride (anhydrous, NaCl), chloroform-*d* ($CDCl_3$), sulfuric acid (ACS reagent grade 95.0-98.0%, H_2SO_4), tetrahydrofuran (anhydrous, 99.9%, THF), and diethyl ether (anhydrous, 95%) were purchased and used as received from Fisher Scientific. Isobutylene (IB, BOC Gases) and methyl chloride (MeCl, Gas and Supply) were dried by passing the gases through columns of $CaSO_4$/molecular sieves/$CaCl_2$ and condensed within a N_2-atmosphere glovebox immediately prior to use. The monofunctional initiator, 2-chloro-2,4,4-trimethylpentane (TMPCl), was prepared by bubbling HCl gas through neat 2,4,4-trimethyl-1-pentene (Sigma-Aldrich) at 0 °C. The HCl-saturated TMPCl was stored at 0 °C, and immediately prior to use it was neutralized with $NaHCO_3$ (ACS reagent grade, Fisher Scientific), dried over anhydrous $MgSO_4$, and filtered. The difunctional initiator, 5-*tert*-butyl-1,3-di(2-chloro-2-propyl)benzene (bDCC), was synthesized as previously reported, stored at 0°C, and freshly recrystallized before use.[96]

4.3.2 Instrumentation

. Nuclear magnetic resonance (NMR) spectra were obtained using a 300 MHz Bruker AVANCE III NMR (TopSpin 3.1) spectrometer. All ^1H chemical shifts were referenced to TMS (0 ppm). Samples were prepared by dissolving the material in chloroform-*d* (5%, w/v) and charging this solution to a 5 mm NMR tube. For quantitative integration, 32 transients were acquired using a pulse delay of 27.3 s. For the

PIB polymers prepared via living polymerization, the signal due to the phenyl protons of the initiator (7.17 ppm, 3H, singlet) was chosen as an internal reference for functionality analysis. For the PIB distillates, the terminal methylene (~1.80 ppm, 2H, singlet) was used.

Real-time (RT)-ATR-FTIR monitoring of isobutylene polymerizations was performed using a ReactIR 45m (Mettler-Toledo) integrated with a N_2-atmosphere glovebox (MBraun Labmaster 130).[117] Isobutylene conversion during polymerization was determined by monitoring the area above a two-point baseline of the absorbance at 887 cm^{-1}, associated with the = CH_2 wag of isobutylene.

Number-average molecular weights ($\overline{M}_n$) and polydispersities (PDI = $\overline{M}_w/\overline{M}_n$) were determined using a gel-permeation chromatography (GPC) system consisting of a Waters Alliance 2695 separations module, a UV-Vis spectrophotometer (996 PDA, Waters Inc.) operating between 210-400 nm with a sampling rate of 1 scan/s, an online multi-angle laser light scattering (MALLS) detector fitted with a gallium arsenide laser (power: 20 mW) operating at 658 nm (miniDAWN TREOS, Wyatt Technology Inc.), an interferometric refractometer (Optilab t-rEX, Wyatt Technology Inc.) operating at 35°C and 685 nm, and two PLgel (Polymer Laboratories Inc.) mixed E columns (pore size range 50-10^3 Å, 3 μm bead size). Freshly distilled THF served as the mobile phase and was delivered at a flow rate of 1.0 mL/min. Sample concentrations were ca. 6-8 mg of polymer/mL of THF, and the injection volume was 100μL. The detector signals were simultaneously recorded using ASTRA software (Wyatt Technology Inc.), and absolute molecular weights were determined by MALLS using a *dn*/*dc* calculated from the refractive index detector response and assuming 100% mass recovery from the columns.

4.3.3 Synthesis of symmetric resorcinol ethers

Symmetric resorcinol ethers were synthesized using the Williamson reaction. The following procedure for synthesis of 1,3-diisopropoxybenzene is representative: To a 500 mL round bottom flask equipped with a magnetic stirrer and condenser were charged resorcinol (30.10 g, 0.272 mol), K_2CO_3 (56.80 g, 0. 411 mol), 2-bromopropane (64.8 mL, 0.700 mol), and 350 mL of DMF. The mixture was purged continuously with N_2 and stirred at 50 ºC overnight. Upon reaching quantitative conversion as indicated by ^1H NMR, the reactor was removed from heat. After cooling to room temperature, the mixture was quantitatively transferred to a separatory funnel, and 50 mL of DI H_2O was added. This mixture was extracted with two 125 mL portions of diethyl ether. The ethereal layers were combined and washed with three 100 mL portions of a 0.1 M solution of HCl. The ethereal layer was then washed with a sodium bicarbonate solution until neutral to pH paper, and then triple rinsed with a 30% (w/w) brine solution. The ethereal layer was finally dried over Na_2SO_4 and filtered, and the solvent was removed via vacuum stripping. The product, 1-3 diisopropoxybenzene, was isolated as a light orange oil. Further purification via vacuum distillation (98 °C @ < 0.0 mmHg) resulted in a colorless oil. Yield: 40.44 g (76.4%).

1,3-Diallyloxybenzene was synthesized using an identical procedure, starting with 17.0 g (0.154 mol) of resorcinol. The resulting orange oil was purified via vacuum distillation (125 °C @ <0.0 mmHg) resulting in a colorless oil. Yield: 23.94 g (81.5%).

4.3.4 *In situ* quenching reactions

In situ quenching reactions were carried out using the following procedure, which is representative. The polymerization of IB was performed within a N_2-atmosphere

glovebox equipped with a cryostated heptane bath. To a dry 250 mL 3 neck round-bottom flask, equipped with an overhead stirrer, thermocouple, and ReactIR probe, and immersed in the heptane bath at -70°C, were charged 72.7 mL chilled hexane, 109.7 mL chilled methyl chloride, 2,6-lutidine (0.073 mL, 0.63 mmol, neat and at room temperature), bDCC (1.44 g, 5.01 mmol), and chilled IB (25.1 mL, 0.312 mol). The mixture was equilibrated to -70 ºC with stirring, and polymerization was initiated by sequential additions of $TiCl_4$ (2 x 0.14 mL, 2.5 mmol, neat and at room temperature) spaced 15 minutes apart. Monomer conversion was monitored using RT-FTIR data, and upon full conversion, 1,3-dimethoxybenzene (2.62 mL, 0.020 mmol, room temperature) was added, immediately followed by a quenching increment of $TiCl_4$ (1.90 mL, 0.0173 mol). Aliquots were taken over the course of the quenching reaction to monitor conversion, and after 270 min the mixture was quenched with 25 mL of chilled methanol. The mixture was then transferred to a fume hood, where it was slowly warmed to room temperature and concentrated under an N_2 stream to allow for the evaporation of volatiles. The resulting mixture was then precipitated into methanol under vigorous stirring, after which the methanol layer was decanted. The precipitate was collected by re-dissolution in a minimal volume of fresh *n*-hexane, and the resulting solution was re-precipitated into excess methanol. After decanting the methanol, the precipitate was collected by re-dissolution in fresh hexane, and the resulting solution was washed twice with deionized water, dried over Na_2SO_4, and then vacuum stripped to yield the isolated polymer. The aliquots taken during the course of the quenching reaction and the final product were then characterized via ^1H NMR and compared. Chain end composition was

estimated by comparing the appropriate resonance signals to the resonance signal of the initiator residue (7.18 ppm).

4.3.5 End-quenching in HCl-saturated conditions

Monofunctional PIB bearing tertiary-chloride end-groups was synthesized using a slight modification to the procedure described above: To a dry 500 mL 3 neck round-bottom flask, equipped with an overhead stirrer, thermocouple, and ReactIR probe, and immersed in the heptane bath at -70°C, were charged 192.6 mL chilled hexane, 128.4 mL chilled methyl chloride, *N*,*N*-diisopropylethylamine (0.14 g, 3.0 mmol, neat and at room temperature), TMPCl (0.396 g, 2.70 mmol), and chilled IB (19.7 g, 0.313 mol). The mixture was equilibrated to -70 ºC with stirring, and polymerization was initiated by addition of $TiCl_4$ (2.14 g, 32.1 mmol, neat and at room temperature). Monomer conversion was monitored using RT-FTIR data, and upon full conversion, 30 mL of chilled methanol was added to the reactor to terminate the reaction. The polymer was purified using the procedure described above and analyzed via ^{1}H NMR and GPC-MALLS.

An end-quenching reaction was performed in the presence of excess HCl via the following procedure: To a dry 250 mL round-bottom flask equipped with a magnetic stirrer were charged tertiary chloride functionalized monofunctional PIB (6.01 g, 1.11 mmol), DCM (90.0 mL), and *n*-hexane (60.0 mL). In a separate reactor, anhydrous HCl gas was generated (via the dropwise addition of H_2SO_4 to NaCl) and bubbled through a Teflon tube containing finely ground $CaCl_2$, which was further bubbled into the PIB solution over an 8 h period. Afterwards, 1,3-dimethoxybenzene (0.320 g, 2.32 mmol) was added to the solution, and the reactor was tightly capped with a rubber septum. The

reactor was then chilled to -70 °C while maintaining stirring. After equilibration for 30 min, $TiCl_4$ (0.98 mL, 8.92 mmol, 8.03 x[CE]) was added to the reaction mixture via syringe, and the mixture was stirred for 240 min, after which reaction was terminated with 50 mL of chilled methanol. The polymer was precipitated into methanol and purified via the procedure described above.

4.4 Results and Discussion

4.4.1 Symmetric resorcinol ethers.

Diisopropyl and diallyl ethers of resorcinol were synthesized via the route depicted in Scheme 4.1, and 1,3-dimethoxybenzene was purchased from Sigma Aldrich. The ^{1}H NMR spectra of the dimethyl, diisopropyl, and diallyl resorcinol ethers are shown in Figures 4.1-4.3, respectively.

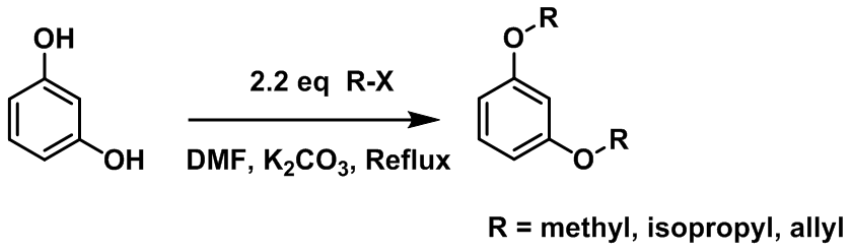

Scheme 4.1 Williamson reaction used to synthesize symmetric resorcinol ethers.

The ^{1}H NMR spectrum of the commercially available 1,3-dimethoxybenzene is shown in Figure 4.1. The resonance at 3.74 ppm (s, -OC*H*$_3$) was used as an internal standard for integration purposes. The resonance at 7.15 ppm was determined to correspond to the aromatic proton "a" as the splitting pattern (triplet) indicated that the proton was adjacent to two neighboring C-H groups, and integration of the resonance determined it was a single proton. Integration of the overlapping peaks at 6.44 and 6.55 showed that these peaks correlated to peaks "b" and "c" of the phenyl ring. The

resonance signal at 3.74 would prove especially useful as an internal reference during subsequent quenching experiments due to its isolation both from the PIB backbone resonances in the aliphatic region and the aromatic resonances associated with the initiator and quencher residue.

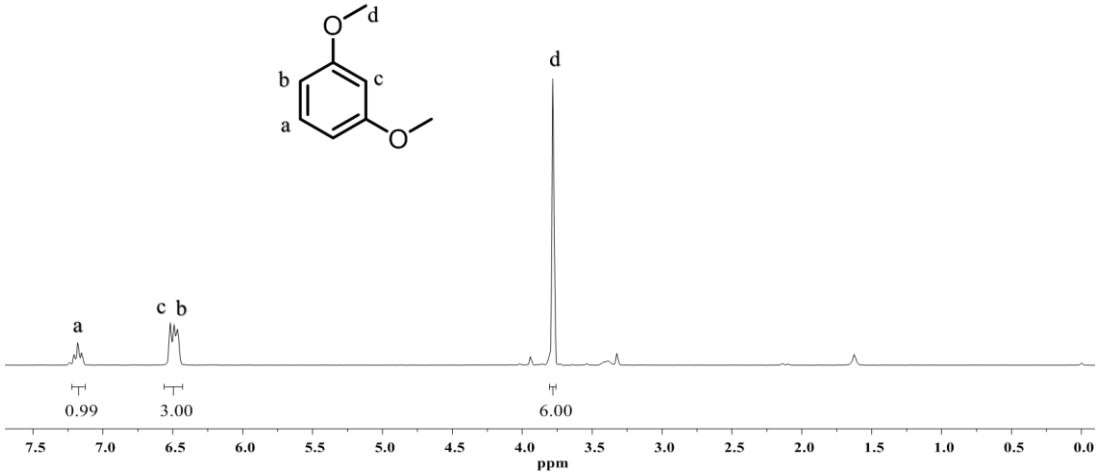

Figure 4.1 ^{1}H NMR (300 MHz, $CDCl_3$, 25 °C) spectrum of 1,3-dimethoxybenzene (DMB).

The ^{1}H NMR spectrum of 1,3-dimethoxybenzene also served as a reference for the structural characterization of the diisopropoxy and diallyloxy derivatives, which are prone to Claisen rearrangement or dealkylation when exposed to high temperatures (i.e. distillation). Accordingly, the splitting patterns in the aromatic region of the diisopropoxy and diallyloxy- derivatives were compared to the splitting patterns of the heat stable 1,3 dimethoxybenzene after vacuum distillation, to check for the formation of the rearranged products. Moreover, 1,3-dimethoxybenzene (DMB) has a well reported boiling point (85-87 °C at ≤ 7 mmHg) under vacuum distillation, which would serve as a boiling point reference during the purification of the diisopropyl and diallyl derivatives.

The synthesis of the diisopropoxy derivative proceeded via the reaction of resorcinol with excess 2-bromopropane. The extent of the etherification reaction was monitored via ^{1}H NMR by integration of the resonance signals at 1.32-1.34 ppm (d, -OCH(C*H*$_3$)$_2$) using the aromatic protons of the phenyl ring as the internal reference. The resonance signal at 4.52 ppm (m, -OC*H*(CH$_3$)$_2$), can also be used to determine the extent of etherification. Separation of the diisopropoxy product proceeded smoothly via an ether/water extraction, but vacuum distillation was required to obtain sufficiently pure diisopropoxybenzene (DIPB).

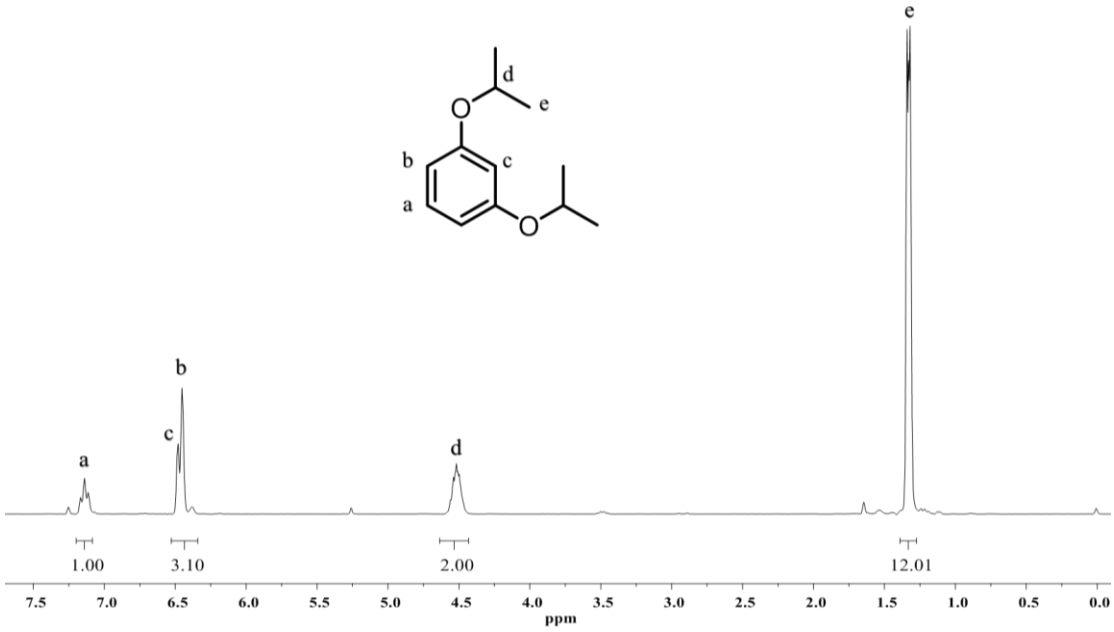

Figure 4.2 ^{1}H NMR (300 MHz, $CDCl_3$, 25 °C) spectrum of 1,3-diisopropoxybenzene (DIPB).

The synthesis of the diallyl derivative was performed similarly using allyl chloride, and the extent of the etherification reaction was monitored via ^{1}H NMR. Reaction progress was monitored via ^{1}H NMR by comparing the resonance at 4.52 ppm (s, -OC*H*$_2$-) to the aromatic protons of the phenyl ring. The resonance signals centered

around 4.37 and 4.72 (showing a doublet of doubtlets) and the multiplet at 6.00 ppm are characteristic of terminal allyl ethers. Separation and purification of the diallyloxybenzene (DAB) derivative were performed similarly to DIPB.

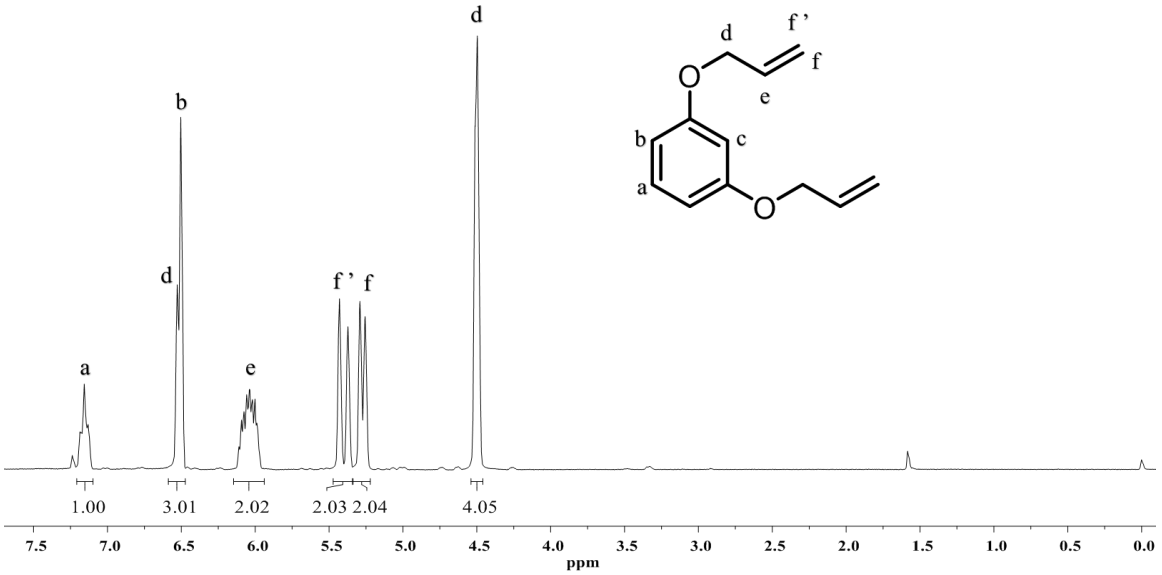

Figure 4.3 ^{1}H NMR (300 MHz, $CDCl_3$, 25 °C) spectrum of 1,3-diallyloxybenzene (DAB).

4.4.2 Quenching of living polyisobutylene polymerizations

A series of isobutylene polymerizations was performed, and upon quantitative isobutylene conversion (as indicated by RT-FTIR), end-quenching reactions were conducted using the previously described symmetric resorcinol ethers. The quenching conditions, time, and conversion of the isolated products are listed in Table 4.1. Initially, quenching reactions were carried out with the ratio of the total effective $TiCl_4$ concentration ($[TiCl_4]_{eff}$) and PIB chain-end concentration ([CE]) held constant at 1.85 (entries 1-3 in Table 4.1).

Table 4.1 The quenching conditions, time, and conversion of the isolated products for resorcinol quenching reactions of $TiCl_4$ catalyzed end-quenching of living isobutylene polymerizations.[a]

Entry	Quencher	$[TiCl_4]_{eff}/[CE]$	Quench time[b]	Conversion[c] (%)	Mn[d] (PDI)
1	DIPB	1.85	120	100	3,730 (1.02)
2	DAB	1.85	120	100	3,790 (1.05)
3	DMB	1.85	5	94.9	-
	-		120	100	3,700 (1.03)
4	DMB	0.868	5	48.5	-
			10	48.5	-
			30	48.3	-
			45	48.8	-
			60	48.4	-
	-		270	50.0	-
5	DMB	1.36	2	63.2	-
			10	64.5	-
	-		270	66.8	-

[a]Polymerization: hexane = 72.7 mL; methyl chloride = 109 mL; IB: 17.5 g; bDCC = 1.44 g ([CE] = 0.047 M); 2,6-lutidine = 70 mg (0.003 M); TiCl4 = 0.48 g (0.0125 M, added via two 0.24 g injections spaced 10 min apart). Quench: [Quencher]/[CE] = 2 (entries 1-5); after addition of quencher, additional $TiCl_4$ = 3.31 g (entries 1-3), 1.40 g (entry 4), 2.35 g (entry 5). Polymerization, quenching, and termination (with excess methanol) temperature = -70 °C.
[b]min
[c]Conversion calculated from comparison of the resonance signals from the quencher to the residual initiator resonance signals (entries 1-4) or the terminal methylene adjacent to the initiator (entry 5).
[d] g/mol

Previously, our lab has demonstrated that isopropoxybenzene acts as a useful synthon towards commercially relevant materials; namely, PIBs bearing terminal phenol functionality. In the seminal publication on the use of alkoxybenzene quenchers, Morgan *et al.* demonstrated that the addition of isopropoxybenzene to an *in situ* PIB polymerization resulted in the quantitative end-capping of the PIB chain by selective alkylation at the *para* position of the isopropoxybenzene moiety.[96] Subsequently, the dealkylation of the isopropyl moiety was shown to proceed smoothly via the addition of a protic acid to the reactor and gentle warming of the reactor to room temperature.

With these criteria informing our approach, an isopropyl functionalized derivative of resorcinol (DIPB) was used as a quenching agent (entry 1). An aliquot was taken after 120 min and analyzed via ^{1}H NMR (Figure 4.4). Conversion of the quenching reaction was measured by comparing the integrated intensity of the resonance signals at 4.54 ppm (-OC*H*$(CH_3)_2$) to that of the resonance signal at 7.18 ppm (Ar-*H*), which corresponds to the aromatic protons of the initiator residue. At full conversion, the ratio of these intensities should be 4:3. However, we observed significant overlap between the C5 aromatic protons (i.e. the aromatic protons labelled "a") of the quencher and the initiator residue. Thus, the entire area between 7.07 and 7.20 ppm, which contains both the initiator residue protons and proton "a" of the quencher, was integrated. The ratio of this combined integral to the integral of the 4.54 ppm resonance should be 4:5 at full conversion, and this is the ratio observed in Figure 4.4. indicating that the reaction was fully quenched after 120 min. Further evidence of DIPB alkylation is given in the ^{1}H NMR spectrum by the resonance for the ultimate PIB methylene unit adjacent to DIPB at 1.99 ppm. The resonances for the aromatic protons of the resorcinol moiety indicate that

alkylation by the PIB chain end occurred exclusively at C4. Protons h and i are coupled to one another and appear as doublets, centered at 7.10 and 6.33 ppm, respectively. Proton j appears as a singlet at 6.35 ppm. Because alkylation at C2 is prevented for steric reasons, the only other possibility would be alkylation at C5. However, this structure would be expected to produce two additional singlets in the aromatic region of the spectrum, with an intensity ratio of 2:1, and such signals were not observed.

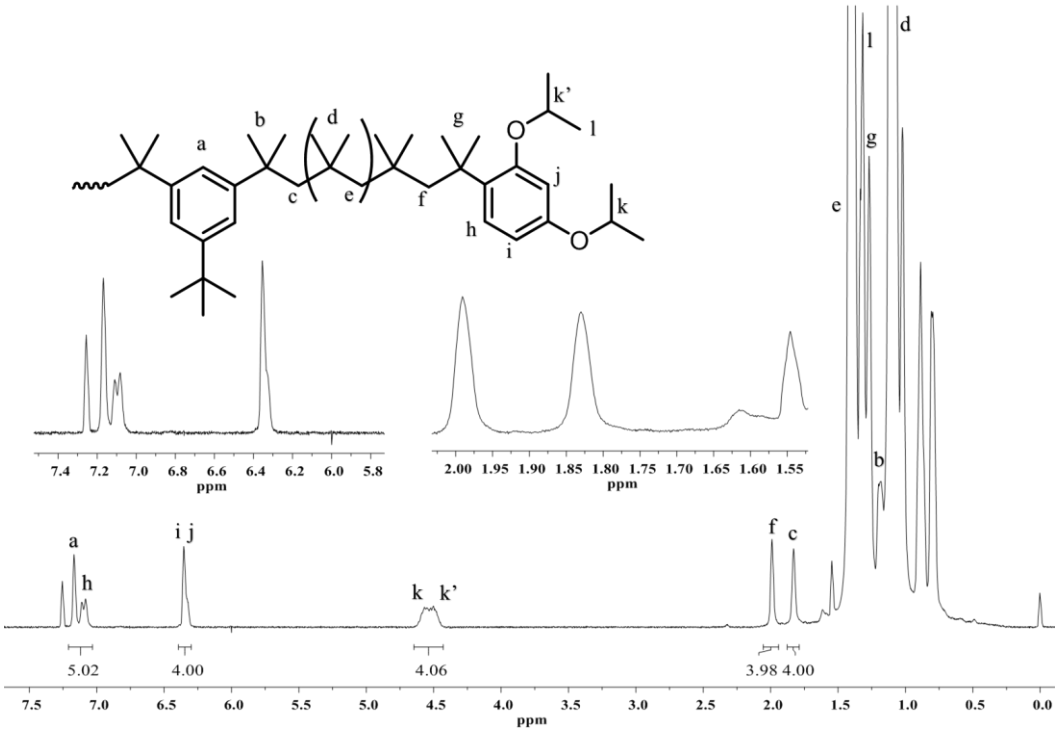

Figure 4.4 ^{1}H NMR (300 MHz, CDCl3, 25 °C) spectrum of 1,3-diisopropoxybenzene quenched PIB (Table 4.1, entry 1).

Although isopropoxybenzene (and isopropyl-functionalized resorcinols) provide a useful intermediate towards telechelic PIBs, other alkoxybenzenes offer a 1-pot approach towards telechelic PIBs (e.g. phenoxybutyl (meth)acrylates, 4-phenoxybutanol, and 6-phenoxyhexylamine). One attractive, yet hitherto elusive alkoxybenzene quencher is one that bears an α-olefin moiety. Morgan *et al.* reported that end-quenching by the simplest

alkoxybenzene bearing an α-olefin functionality, allyl phenyl ether, was plagued by Claisen rearrangement and ether cleavage.[96] They hypothesized that the high $TiCl_4$ concentration required for alkoxybenzene quenching (i.e. ≥ 4[CE]) caused a competing reaction between alkylation of the PIB chain-end and the Claisen rearrangement, resulting in a mixture of products. Initial quenching results with DIPB (Entry 1, Table 4.1) indicated that alkylated resorcinol quenchers require significantly less $TiCl_4$ and less time to reach quantitative conversion compared to alkoxybenzenes. In light of these results, we hypothesized that the diallyl ether of resorcinol might efficiently quench the living PIB chain end without competing Claisen rearrangement.

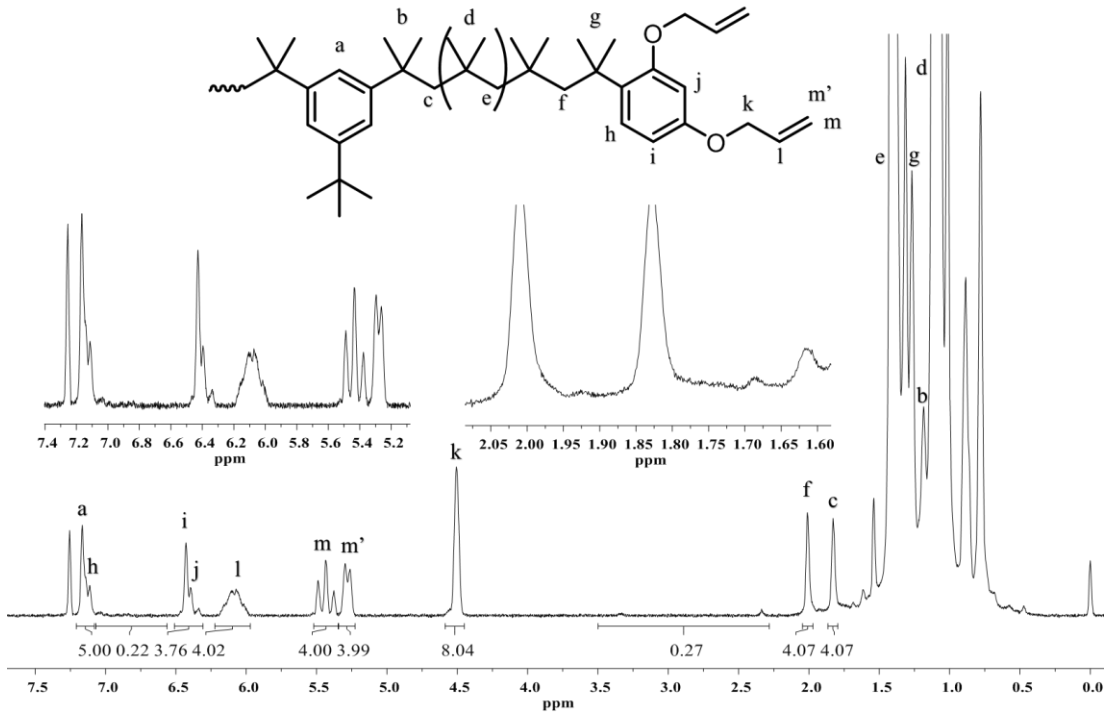

Figure 4.5 ^1H NMR (300 MHz, $CDCl_3$, 25 °C) spectrum of DAB quenched PIB (Table 4.1, entry 2).

Accordingly, end-quenching of living polyisobutylene was performed *in situ* using the diallyl-functionalized resorcinol (DAB, entry 2). The quenching reaction was

performed for 120 min at -70°C, at which time an aliquot was removed from the reaction and analyzed via ^{1}H NMR (Figure 4.5). The resonance at 4.50 ppm (-OC*H*$_2$-) was integrated and compared to the resonance for the aromatic protons of the initiator residue. For difunctional PIB fully quenched with DAB, the intensity ratio of these two resonances should be 8:3. As shown in Figure 4.5, we again observed significant overlap between the aromatic protons of the quencher and the initiator residue. Thus, the extent of quenching was determined using the same approach as described above. The ratio of this combined integral to the integral of the 4.50 ppm resonance should be 8:5 at full conversion, and this is the ratio observed in Figure 4.5.

The synthesis of 2-allyl phenol from allyl phenyl ether is a classic example of the Claisen rearrangement and is often part of the curriculum of undergraduate chemistry laboratory courses.[201] Consequently, there exists an abundance of literature on determining the extent of rearrangement.[202-205] In the present case, ^{1}H NMR provided sufficient evidence that the magnitude of Claisen rearrangement was very small, but not completely absent. In a study by Gozzo and coworkers, the 2-allyl and 4-allyl isomers of 1,3-dihydroxybenzene were synthesized via Claisen rearrangement, and the products were analyzed via ^{1}H NMR.[202] Most notably, a resonance at 3.34 ppm, belonging to the methylene of the allyl, was observed in the case of rearrangement. This resonance is observed in Figure 4.5 as well. Other notable resonances that suggest formation of rearranged isomers are at 6.36 and 6.96 ppm, which are in the aromatic region and are also reported by Gozzo *et.al.* Furthermore, integration of the resonances at 6.42-6.45 ppm display less than ideal values; loss of resonances in the aromatic region would be expected in the case of alkylation (i.e. via rearrangement).

In summary, the resorcinol derived quenchers used in entries 1 and 2 demonstrated quantitative capping of the PIB chain ends within 120 min, with minimal formation of side products. To further understand the quenching kinetics of resorcinol-based quenchers, a new quencher, dimethoxybenzene (DMB) was used. As a synthon, DMB is not particularly useful; the transformation of the methoxy groups to a more synthetically useful alternative often requires harsh conditions and excessive reaction times. However, DMB represents a convenient quencher in terms of commercial availability and ease of analysis via ^{1}H NMR. Thus, DMB was used in Trials 3-5 to investigate the kinetics of in situ quenching of living PIB.

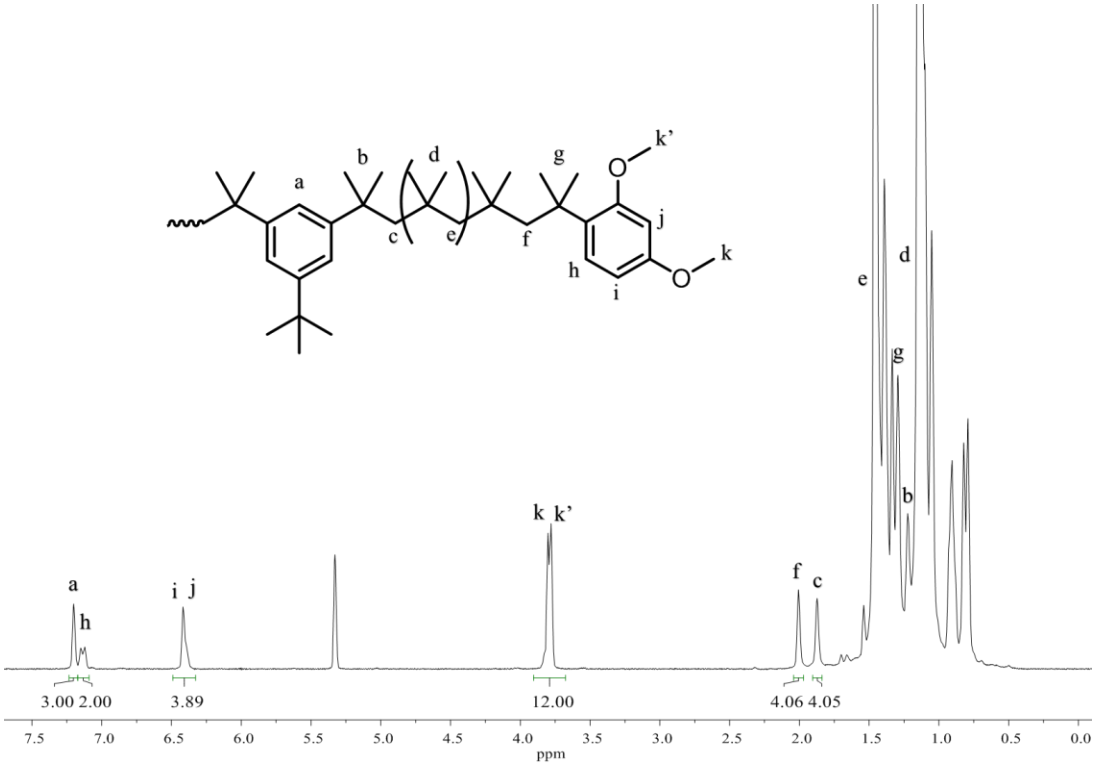

Figure 4.6 ^{1}H NMR (300 MHz, CD_2Cl_2, 25 °C) spectrum of 1,3-dimethoxybenzene quenched PIB (entry 3).

Figure 4.6 shows the ^{1}H NMR spectrum of the final product of entry 3, after quenching for 120 min. In the case of DMB, the resonance at 3.74 ppm (-OCH_3) was

integrated and compared to the resonance of the initiator residue. For difunctional PIB fully quenched with DMB, the intensity ratio of these two resonances should be 12:3, indicating a single addition of DMB to each chain end. This is observed in Figure 4.6. Moreover, the appearance of the resonances associated with the aromatic protons of the quencher (e.g. the overlapping peaks at 6.35-6.45 ppm and the doublet at 7.14 ppm) provides further evidence of alkylation. Integration of the resonance at 7.14 demonstrates quantitative end capping (showing an ideal ratio of 2:3), but integration of the resonances between 6.35-6.45 ppm show slightly less than ideal (3.89:3 rather than 4.0:3). Significantly, the spectrum shown in Figure 4.6 is similar to spectra of analogous structures in other studies, which provides further structural evidence of alkylation.[206]

During the quenching reaction in entry 3, an aliquot was taken 5 min after addition of the quencher in order to gain a more thorough understanding of the quenching process. This aliquot was analyzed via ^{1}H NMR, and the spectrum is shown in Figure 4.7 (bottom). Also included in Figure 4.7 is the ^{1}H NMR spectrum for the final product (top) for comparative purposes. Comparing the integrations of the resonance at 3.74 ppm for both spectra demonstrated that the sample taken 5 min after addition of the DMB quencher had already reached ~96 % conversion, which illustrates the high reactivity of resorcinol quenchers towards alkylation. A high expansion of the region between 1.5-2.05 ppm is also included in Figure 4.7; within this region, the resonances associated with terminal *gem*-dimethyl and methylene groups of the PIB chain end can be found.

When a living PIB polymerization is quenched with chilled methanol, the spontaneous collapse of the $Ti_2Cl_9^-$ gegenion results in the formation of *tert*-chloride terminated PIB (PIB-Cl). The resonances associated with the terminal *gem*-dimethyl and

methylene protons appear at 1.69 and 1.96 ppm, respectively. Tracking the disappearance of these peaks during an *in situ* PIB quenching reaction is often done to determine the extent of the quenching reaction,[98] and has been used to determine the quenching kinetics for a variety of alkoxybenzene quenchers. [96,98] In Figure 4.7 (bottom), the magnitude of the resonance at 1.69 ppm (associated with the gem-dimethyl protons of *tert*-chloride terminated PIB) supports the conclusion that the quenching reaction has not reached full conversion. Interestingly, the fully quenched product exhibits either a doublet centered at 1.67 ppm, or two singlets at 1.66 and 1.69 ppm; integration of these peaks show a nearly 1:1 ratio. An accurate assignment of these peaks is difficult due to the reduced resolution of this region (resulting from the multitude of peaks from aliphatic PIB backbone), but these peaks are also observed in the final products of DIPB and DMB quenched PIBs. In addition to these peaks, the resonance of the terminal methylene group does not shift significantly during the quenching process (i.e. 1.96 ppm for the tertiary chloride terminated PIB compared to 2.00 ppm for the resorcinol quenched PIBs), which limits its utility as an internal reference.

The final products from entries 1-3 were characterized via GPC-MALLS, and the chromatograms are shown in Figure 4.8. The molecular weights for each sample are included in Table 4.1. In all cases, the quenched products exhibited a slightly earlier elution time compared to the pre-quenched PIB due to their slightly higher molecular weight, which is expected. Moreover, the chromatograms display narrow molecular weights, indicating that coupling reactions were absent during the quenching process.

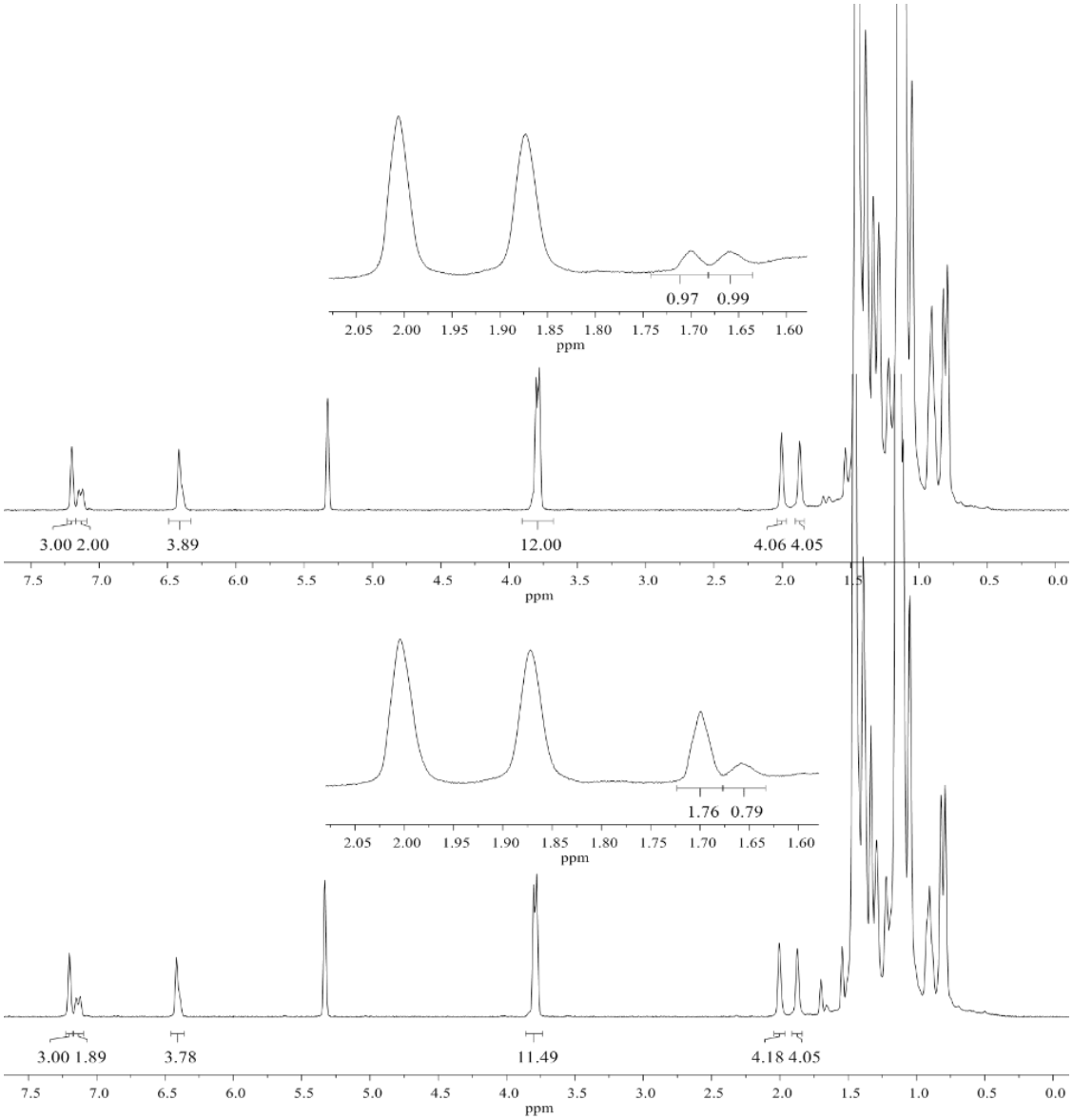

Figure 4.7 ^{1}H NMR (300 MHz, CD_2Cl_2, 25 °C) spectra of two PIB-DMB samples from entry 3. The bottom spectrum corresponds to the aliquot taken at 5 min, and the top spectrum corresponds to the final product obtained after 120 min.

Although coupling reactions have never been observed in alkoxybenzene quenching, we were originally concerned that resorcinol-based quenchers might result in a finite amount of coupling due to the multiple reactive sites on the phenyl ring. The absence of coupling, as evidenced by ^{1}H NMR and GPC analyses, indicates that resorcinol-based quenchers only undergo monoalkylation. Although the resorcinol

aromatic ring would be further activated by addition of a first PIB chain, the latter would cause steric crowding of the remaining potentially reactive sites. Additionally, the quenching reactions were performed using [Quencher] = 2.0[CE], which reduces the likelihood of multiple alkylations on the same quenching molecule.

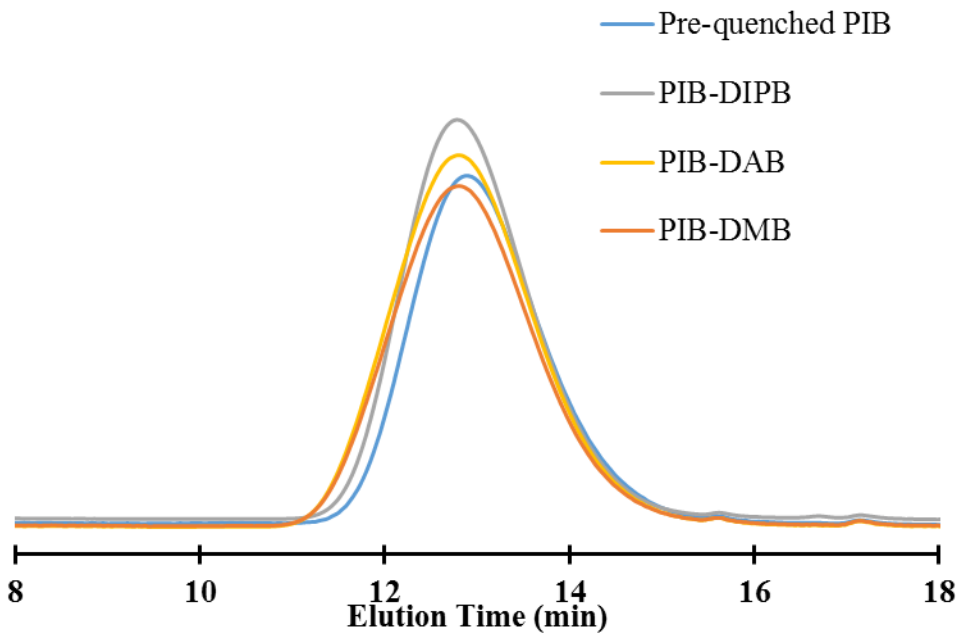

Figure 4.8 GPC chromatograms of the products from entries 1-3. Also included is an aliquot of PIB quenched with chilled methanol, to serve as a pre-quench comparison.

4.4.3 Lewis acid starvation

A significant barrier to the commercialization of phenoxy quenching is the high concentrations of Lewis acid that are required for quenching to occur on a convenient time scale. Upon realizing that resorcinol ethers quench at extremely fast rates (≤ 120 min) using $[TiCl_4]_{eff} \approx 1.85[CE]$, we elected to carry out a series of experiments in which the total $TiCl_4$ concentration was lowered. By simply lowering the quenching increment of $TiCl_4$ (added via syringe immediately after addition of the DMB quencher) we attempted to probe the quenching kinetics and achieve quantitative end capping of the

PIB chain, thereby demonstrating that resorcinol-based quenchers can approach commercial viability.

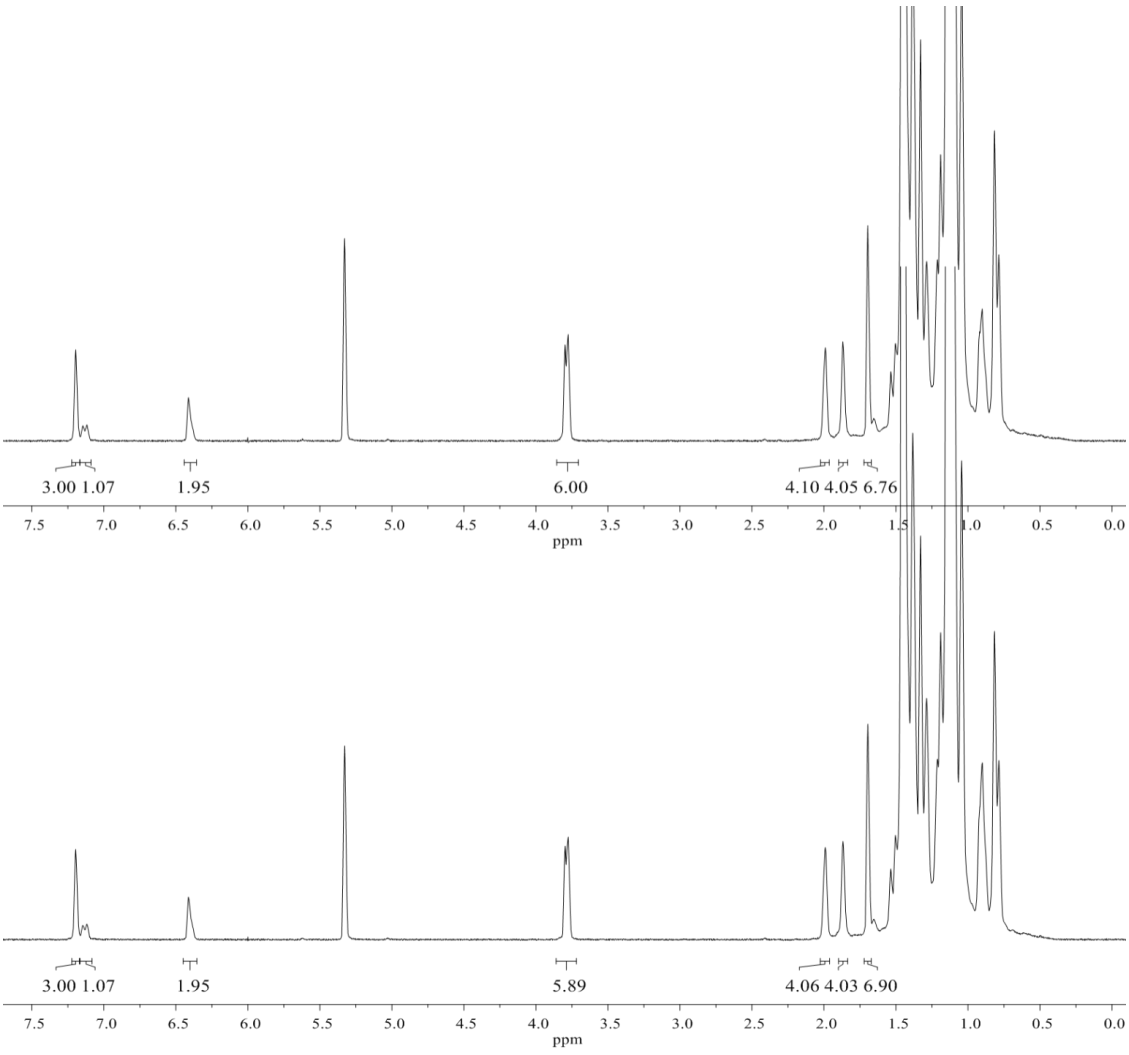

Figure 4.9 ^{1}H NMR (300 MHz, $CDCl_3$, 25 °C) spectra of two PIB-DMB samples from entry 4 ($[TiCl_4]_{eff}$ =0.868[CE]). The bottom spectrum corresponds to the aliquot taken after 5 min, while the top spectrum corresponds to the final product obtained after 270 min.

Two series of experiments were performed, and the quenching conditions are listed in entries 4 and 5 in Table 4.1. In entry 4, the quenching process was carried out at $[TiCl_4]_{eff} \approx 0.868[CE]$, and aliquots were taken at 5, 10, 30, 45, 60 min intervals and characterized via ^{1}H NMR. After 270 min, the reaction was terminated with chilled

methanol. Surprisingly, analysis of the ^{1}H NMR spectra for each aliquot demonstrated that the quenching reaction stalled after 5 min, with 49.3% of the PIB chain ends possessing a DMB moiety (as measured by integration of methoxy peak at 3.74 ppm). This is shown in Figure 4.9, where the bottom spectrum corresponds to the aliquot taken at 5 min. The top spectrum, representing the final product (270 min), shows that 50% of the PIB chain ends possess a DMB moiety. Further evidence of the reaction stalling is provided by the magnitude of the peak at 1.69 ppm, indicating that a significant amount of chain ends possessed a *tert*-chloride end group at both 5 and 270 min.

To further investigate this phenomenon, a second quenching reaction was performed at $[TiCl_4]_{eff} \approx 1.36[CE]$ (Table 4.1, entry 5). Aliquots were taken at 2 and 10 min, and the quenching reaction was terminated at 270 min. The samples were analyzed using ^{1}H NMR, and Figure 4.10 shows the spectra for the products obtained at 2 min (bottom) and 270 min (top). These samples were analyzed using chloroform-*d* as the NMR solvent, which caused slight changes in chemical shifts and splitting patterns of the samples. Unfortunately, this was most noticeable in the aromatic region, where significant overlapping of the aromatic quencher protons and the residual initiator protons occurred. Thus, the resonance at 1.83 ppm, which corresponds to the methylene protons adjacent to the initiator residue, was used as the internal standard. In the case of quantitative initiation, integration of this resonance should give a value of 4.00; this has been observed as demonstrated in Figures 4.4-4.7 and Figure 4.9. Integration of the resonance at 3.79 in both spectra indicated that 63.2% of the chain ends possessed DMB moieties after 2 min, which increased slightly to ~67% after 270 min. The resonance at 3.49 ppm is likely residual methanol, which was used during the purification process.

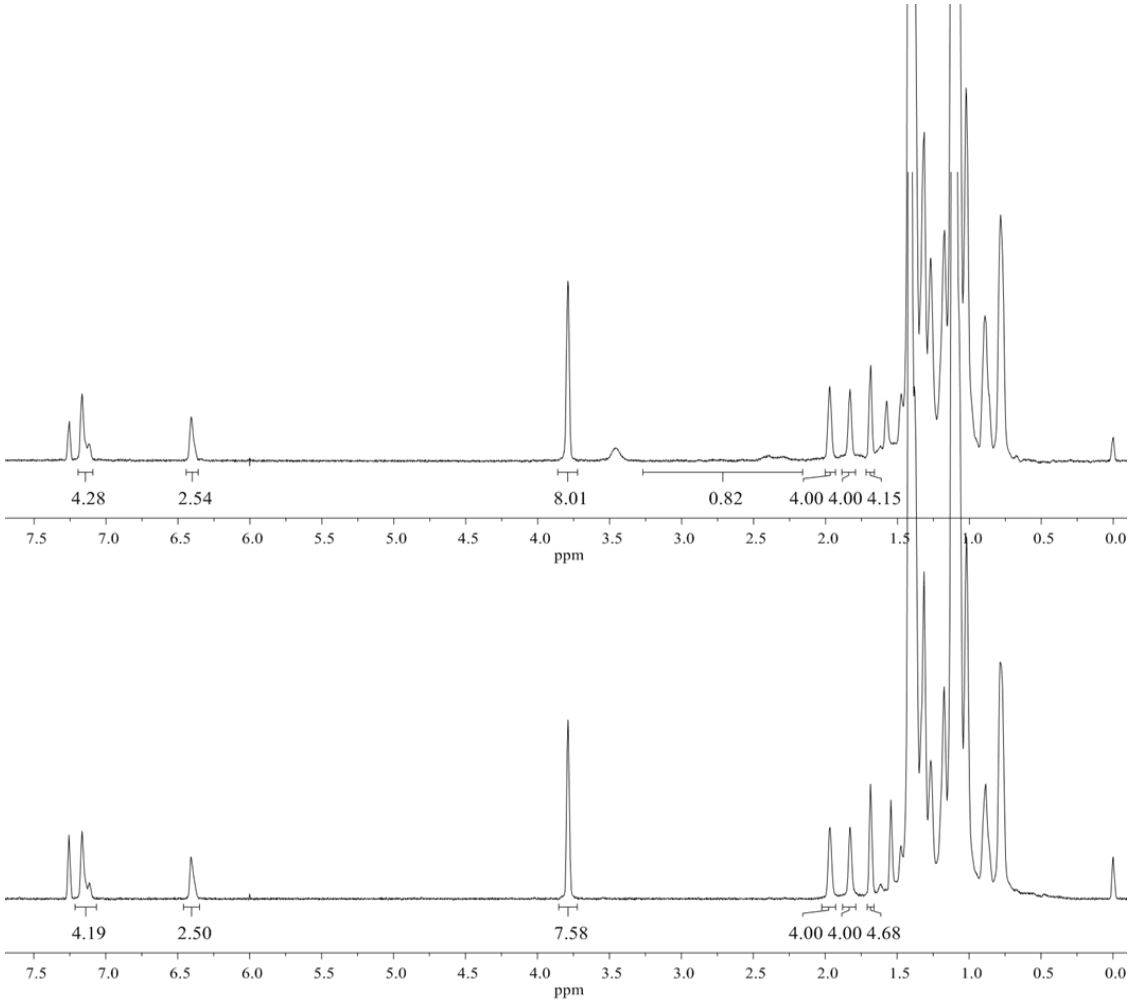

Figure 4.10 ^{1}H NMR (300 MHz, $CDCl_3$, 25 °C) spectra of two PIB-DMB samples from entry 5 ($[TiCl_4]_{eff}$ = 1.36[CE]). The bottom spectrum corresponds to the aliquot taken after 2 min, while the top spectrum corresponds to the final product obtained after 270 min.

In addition to the resonance at 1.69 ppm found in both spectra (indicating *tert*-chloride formation), the top spectrum also includes a series of resonances between 2.10-2.50 ppm. These peaks may indicate successive carbocationic rearrangement of the cationic chain-end, which is a known competing reaction during end-quenching.[118] This phenomenon is most often seen in the case of slow quenching, which can be caused by low reactivity of the quencher or complexation of the quencher with the Lewis acid.[98] Interestingly, these peaks were not observed in any previous trial, including entry 4 for

which the quencher concentration was lower. Moreover, neither of these possible explanations are satisfactory in the case of resorcinol ether quenchers; complexation of the Lewis acid with a methoxy moiety is unlikely (and was not observed in the case of anisole in a previous report)[96] and resorcinol quenchers have demonstrated extremely fast quenching kinetics. Thus, we suspect another failure mechanism may be the cause.

Comparison of the results from entries 3-5 showed an unexpected trend, which may provide clarification. In the case of entry 3, quantitative end-quenching was observed at ≤ 120 min at $[TiCl_4]_{eff} \approx 1.85[CE]$. When the $[TiCl_4]_{eff}$ was reduced by 50% (i.e. $[TiCl_4]_{eff} \approx 0.868[CE]$, entry 4), the final product was observed to reach ~50% conversion, even after significantly longer reaction times were employed. When $[TiCl_4]_{eff} \approx 1.36[CE]$, entry 5, the final product reached ~67% conversion at 270 min. Aliquots taken over the course of these reactions demonstrated that the bulk of the alkylation occurred extremely quickly, likely within 2 min. Significantly, $TiCl_4$ starvation during the quenching process did not appear to retard the rate of reaction; instead, the reaction stalled after reaching a particular percent conversion, which was found to vary approximately as $[TiCl_4]_{eff}/[CE]/2$.

These results suggest the existence of a hitherto unreported competing reaction during the quenching process; namely, the effect of HCl generation (as a byproduct of alkylation) on the Ti_2Cl_8 dimer when quenching at low $[TiCl_4]_{eff}$. Multiple research groups have contributed to a large body of research on the propagation and quenching kinetics of $TiCl_4$-catalyzed systems.[207-210] In all but two cases,[211,212] the kinetic order of propagation was found to be two with respect to $TiCl_4$, indicating that the dimeric Ti_2Cl_8 species is the active Lewis acid species, rather than monomeric $TiCl_4$. This was also found to be the case during end-quenching reactions with alkoxybenzenes.[96] This

phenomenon is thought to be caused by the apparent increased acidity of the Ti_2Cl_8 dimer compared to the monomeric $TiCl_4$.

In the case of alkoxybenzene quenching, Morgan *et al.* reported the effect of HCl generation and its subsequent interaction with electron donors present in the reaction mixture; however these experiments were performed using a high $[TiCl_4]_{eff}$.[96] Sterically hindered, tertiary amines (e.g. 2,6-lutidine) are often incorporated into cationic polymerizations at low concentrations (~3-5 mM) to act as protic scavengers. An auxiliary benefit of this process is the creation of onium salts, which through the common-ion effect, prevent dissociation of propagating chain end cations into free ions and thereby increase the livingness of the polymerization. For $TiCl_4$ co-initiated polymerizations, these onium salts possess dimeric $Ti_2Cl_9^-$ counterions.[213] This causes a reduction in available $TiCl_4$, which is why corrected $TiCl_4$ concentrations (i.e. $[TiCl_4]_{eff}$) are often reported. Because the [tertiary amine]/[CE] ratio is typically small, consumption of the tertiary amine (i.e. via onium salt formation) occurs relatively early in the quenching process, and as quenching continues, HCl begins to accumulate in the reaction solution. For alkoxybenzene quenching, a large concentration of $TiCl_4$ typically has been required to reach acceptable quenching times (4-6 h), and thus the amount of HCl generated was only a minor fraction of the total $TiCl_4$. Resorcinol quenchers, which have displayed significantly higher reactivity towards alkylation compared to alkoxybenzenes, have allowed the use of lower $TiCl_4$ concentrations. Under these conditions, the amount of HCl generated becomes a significant fraction of the total $TiCl_4$. To date, the effect of HCl generation on the activity of monomeric $TiCl_4$ and dimeric Ti_2Cl_8 in cationic polymerizations has not been studied, and only a cursory understanding

of their potential interaction is understood. The results from entries 3-5 suggest that the generation of HCl during the alkylation process may be a potential cause for the reaction stalling, but further experiments were required to better understand this phenomenon.

4.4.4 Quencher under HCl saturated conditions

To probe the effects of HCl generation on resorcinol quenching, an experiment was designed wherein the solution was saturated with gaseous HCl prior to quenching. The conditions are listed in Table 4.2, and the ^{1}H NMR spectra of the starting PIB-Cl and the final product are shown in Figure 4.11. A high expansion of the region ranging from 1.60-2.30 ppm is also provided. Analysis of the starting material (bottom) shows the standard resonances at 1.69 and 1.96 ppm corresponding to the *gem*-dimethyl and terminal methylene protons. The final product however, shows extensive degradation of the chain-end. Additionally, any resonances corresponding to DMB are conspicuously absent. This supports our findings in the previous section, where HCl generation caused eventual stalling of the quenching process (entries 4-5) and in some cases, resulted in loss of chain-end fidelity (entry 5).

Table 4.2 The quenching conditions, time, and conversion of PIB-Cl[a] in the presence of an HCl saturated solution.[b]

Entry	Quencher[c]	$[TiCl_4]_{eff}/[CE]$	Quench time[d]	Conversion (%)
1	DMB	8.0	240	-

[a]Mn: 5,500 g/mol; PDI: 1.09
[b]Quenching temperature = -70 °C
[c]min

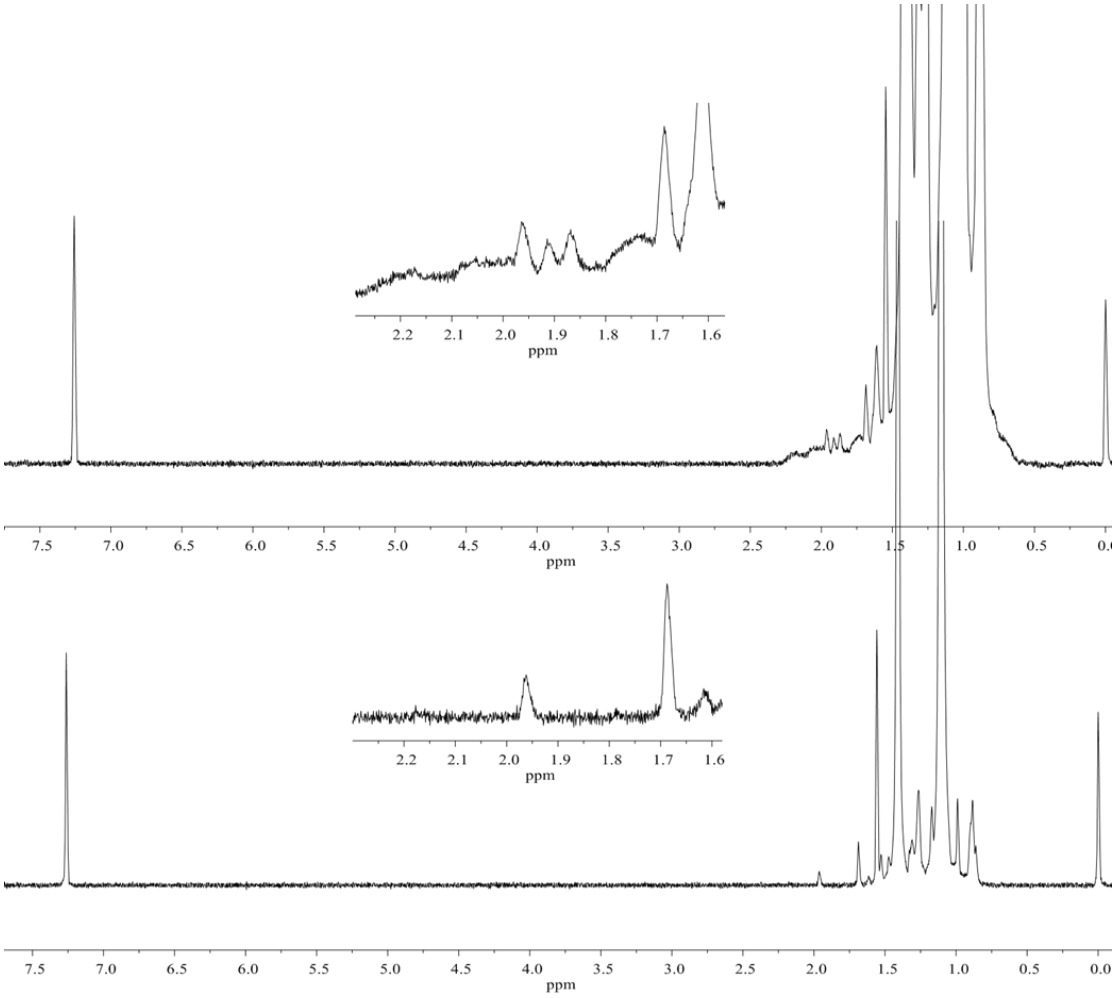

Figure 4.11 ^{1}H NMR (300 MHz, $CDCl_3$, 25 °C) spectra of the starting PIB-Cl (bottom) and the final product after quenching with DMB for 240 min in an HCl saturated solution.

4.5 Conclusion

We have demonstrated that addition of resorcinol ethers to $TiCl_4$-catalyzed living isobutylene polymerizations provides a versatile method for chain end functionalization. Similar to previously reported alkoxybenzenes, quenching proceeds via monoalkylation of the phenyl ring. Significantly, we have demonstrated that resorcinol ethers display extremely fast quenching kinetics, in some cases reaching up to 97% conversion in 5 min. Moreover, resorcinol quenching can reach quantitative conversion at $[TiCl_4]_{eff} \approx$

1.85[CE], which is less than half the required $TiCl_4$ used in the current generation of alkoxybenzene quenchers. In the case of DAB, quenching conditions were resistant towards Claisen rearrangement of the allyl group, which has been shown to plague other alkoxybenzene quenchers bearing an α-olefin moiety. Under conditions where $[TiCl_4]_{eff} \leq 1.85[CE]$, stalling of the quenching process was observed to occur, which upon further investigation was attributed to the formation of HCl during alkylation.

CHAPTER V – MULTIFUNCTIONAL POLYISOBUTYLENES CONTAINING COVALENTLY BOUND RADICAL INHIBITORS

This chapter was co-authored by Robson Storey

5.1 Abstract

A novel route towards multifunctional polyisobutylene (PIB) bearing covalently-bound antioxidants is reported. $TiCl_4$-catalyzed cleavage/alkylation reactions were conducted on poly(isobutylene-*co*-isoprene) (butyl rubber) at -70 °C in 60/40 hexane/methylene chloride cosolvents in the presence of 2,6-di-*tert*-butylphenol (DTP) at various concentrations and reaction times. The butyl rubber (EXXON® Butyl 068) possessed $\overline{M}_n$ = 3.37 x 10^5 g/mol, dispersity (Đ) = 1.29 (GPC/MALLS), and 1.08 mol% isoprene units. By modifying the quenching conditions during the cleavage/alkylation process, PIB molecular weights ranging from 33,000 to 62,000 g/mol were obtained in as little as 4 hr. For all trials, a minor reduction in molecular weight was observed beyond 4 hr, but negligible changes in molecular weight were observed for reactions longer than 9 hr. The number average functionalities (F_n) of these systems ranged from 4.86-10.2. Analysis via ^{1}H NMR demonstrated that between 25-40% of the DTP moieties underwent de-tertbutylation to form mono-tertbutyl phenol moieties. Thermal degradation profiles of a selection of the functionalized PIBs were measured and compared to PIBs synthesized via living polymerization and commercial PIB samples, using an inert atmosphere as well as an oxygen containing atmosphere. Generally, the samples tested in the oxygen containing atmosphere resulted in lower degradation temperatures and a much broader degradation profile; the temperature at 10% weight loss ranged from 312 – 343 °C, and 100% weight loss was achieved at temperatures ranging from 387-426 °C for the

non-DTP functionalized PIBs. The PIBs functionalized with DTP were measured to reach 100 % weight loss at around 547 °C, but this was thought to be due to charred byproducts of the DTP moiety. In the presence of an inert atmosphere, 10% weight loss ranged from 366 – 381 °C and 100 % weight loss was achieved between 431-468 °C for all PIB samples. Oxidation degradation profiles of the functionalized PIBs were measured and compared to the commercial and unfunctionalized PIBs to determine the efficacy of the covalently bound antioxidant moieties. Significantly, all unfunctionalized PIBs were observed to undergo catastrophic degradation within 2 min, but DTP functionalized PIBs were found to resist degradation even after 100 min.

5.2 Introduction

Commercially available polyisobutylenes (PIB) come in a variety of molecular weight grades, depending on their desired end-use. Medium molecular weight PIBs, possessing number average molecular weights (M_n) ranging from 35,000-75,000 g/mol, are marketed, for example, under the tradenames Oppanol® (BASF) and Vistanex® (ExxonMobil), and find use in sealants and adhesives, lubricants, coatings, and chewing gum.[214]

PIB-based sealants are thermoplastic materials typically applied as a preformed tape or extruded as a hot melt.[215] Upon cooling and solidification, they provide an excellent seal that exhibits low gas permeability, resistance to acid/base catalyzed degradation, and resistance to thermo-oxidative degradation throughout a broad temperature range. An application highly relevant to this work is their use as the primary seal in insulating glass units (IGUs), in which PIB plays a crucial role in maintaining the insulative integrity of the IGU. A typical IGU consists of an inner and outer glass lite

separated by a spacer element that extends around the perimeter of the unit. The PIB sealant is applied as a continuous film between the spacer and each glass lite. The principal function of the PIB sealant is to serve as a moisture barrier to prevent atmospheric moisture from entering the inter-pane space and causing fogging of the window.[215] A secondary function of the PIB sealant is to serve as a gas barrier to prevent outward migration of an insulating gas such as argon, which is often used to fill the inter-pane space during construction of IGUs.

Figure 5.1 Migration of a PIB sealant into the vision area of an IGU

Due to their hydrophobicity, superior gas barrier properties, and ease of application, thermoplastic PIB sealants are well suited for this application; however, they have been known to fail under adverse circumstances. The PIB can become plasticized, either from the migration of plasticizers from adjacent glazing materials (setting blocks, backer rods, secondary sealants, etc.) or via diffusion of cleaning solvent vapors. Plasticization of the PIB sealant results in a reduction in shear viscosity, which causes the PIB to creep down the glass (Figure 5.1), requiring replacement of the IGU.

Chemical degradation of the PIB backbone may also occur, presumably caused by thermal, ultraviolet (UV), or oxidative events facilitated by the harsh environment within the window envelope, i.e., cyclic and extreme temperature/humidity fluctuations and exposure to oxygen/ozone and UV radiation.[216,217] These mechanisms reduce the molecular weight of the PIB and lower the viscosity of the sealant. Whether viscosity reduction occurs by plasticization or molecular weight degradation, the constant force of gravity and the diurnal, expansion/contraction forces from the building cause the sealant to succumb to creeping and sagging.[218,219,220]

The processes of thermo- and photo-oxidative degradation, and the mechanism by which radical inhibitors suppress this process, are a complex combination of physicochemical phenomena.[221] Volumes of work have been dedicated to studying and understanding these processes on a wide body of base polymers and polymer formulations.[222,223,224] The sensitivity of saturated polyolefins, such as polyethylene and polypropylene, to oxidation has been widely recognized.[225,226,227] Polyisobutylene, however, exhibits more resistance to oxidation, but is still susceptible to molecular weight degradation over time. The oxidative process is a free radical chain reaction and is thought to occur via photolytic or oxidative scission of the C-H bonds within the polymer structure.[228,229,230]

Commercial polymers, especially those destined for outdoor use, are often formulated with antioxidants, antiozonants, and UV stabilizers that extend their lifetime and performance.[222,223] These additives are usually small molecules that contain hindered aromatic alcohol or aliphatic amine functional groups,[231] and they offer high inhibition efficiency and low cost. Larger molecules, such as BASF's Irganox product line, usually

contain multiple antioxidant moieties and are less volatile and more miscible within nonpolar polymer backbones.[232] Higher-order structures, such as carbon black, have complex chemical structures that include a number of these inhibitive groups, making them effective as radical inhibitors and UV stabilizers.[233] Due to the high surface area, low production cost, and high production volume of carbon black, the rubber industry has incorporated carbon black in their formulations for decades.[234]

Small molecule antioxidants, antiozonants, and UV stabilizers may be inappropriate or impractical in some cases. Due to potential toxicity, they should not be used in food contact applications such as chewing gum. In some cases, they may plasticize the polymer, causing an undesired reduction in hardness and/or glass transition temperature. Due to their small molecular size, they may migrate from the polymer via diffusion and may be prone to degradation and/or volatilization at elevated temperatures;[223,235,236,237] for these reasons, small-molecule additives are generally not used in IGU sealant formulations because of the risk of fogging. Migration, volatilization, and plasticization are especially problematic for liquid additives. Due to crystallization tendency, small molecule, solid additives may aggregate within the polymer or bloom to the surface. Regardless of whether it is a solid or liquid, homogenous dispersion of the additive is required to achieve peak performance, which in turn, requires good solubility/miscibility of the additive within the polymer matrix. Higher molecular weight inhibitors require high temperatures and extensive mixing to achieve uniform dispersion. Although carbon blacks are effective UV stabilizers, their homogenous dispersion is especially difficult,[238,239] and they can only be used when a black-colored sealant is acceptable.

A number of reports have appeared in which these shortcomings have been addressed through covalent attachment of stabilizing moieties directly into the polymer structure. A popular method is post polymerization modification; for example, transesterification reactions have been used to attach antioxidant groups into polyesters,[232] methacrylate copolymers,[240] and polythioethers,[241] and the modified polymers have been reported to display improved resistance to thermo-oxidative degradation compared to the unfunctionalized base polymers. An alternative approach is through copolymerization of an antioxidant-containing comonomer. This may be the only practical approach for polymers such as polyolefins that have no reactive functionality along the backbone. The comonomer method has been reported in the context of ring opening metathesis polymerizations,[242] acyclic diene metathesis polymerizations,[243] thiol-ene addition polymerizations,[241] and radical polymerizations.[244] Incorporation of antioxidants via reactive processing of polymers has also been reported using (meth)acrylates[245] and maleimides.[246]

The incorporation of antioxidants into polymers, and the process through which this is achieved, may be synthetically complex, cost-prohibitive, and/or can deleteriously alter the chemical composition of the polymer. For example, in a study on improving the oxidation resistance of oil lubricants, Atkinson *et al*. reported the modification of hydroxyl containing methacrylate copolymers using 3,5-di-*tert*-butyl-4-hydroxybenzoyl chloride, an acid chloride-functionalized derivative of butylated hydroxytoluene (BHT).[240] Although Atkinson *et al.* showed that the polymer-bound antioxidants provided the longest resistance to oxidative degradation (compared to the base copolymer and a mixture of the base copolymer and antioxidant), they also reported that the

chemical composition of the antioxidant-modified copolymer differed from the base copolymer to such a degree that the antioxidant-modified copolymer was no longer soluble in the base mineral oil. Also, the use of acid chloride intermediates is generally cost-prohibitive in a commercial process.

Ideally, a synthetic route toward covalent incorporation of antioxidant moieties into polymers, including relatively non-reactive polyolefins, should be simple, high yielding, and avoid expensive intermediates. Additionally, the chemical composition of the modified polymer should be sufficiently similar to the unmodified polymer, such that the two can be used interchangeably in formulations. Recently, we reported a method for producing multifunctional PIBs via acid-catalyzed cleavage/alkylation reactions of PIB-based copolymers in the presence of an alkoxybenzene.[247] The resulting PIB-based copolymers were of linear morphology and possessed multiple alkoxyphenyl moieties pendant to the polymer backbone, as well as covalently bound to the polymer chain ends. This process was shown to be highly modular and tunable to yield new families of PIBs for advanced applications possessing a variety of molecular weights and number average functionalities.

In a previous chapter, cleavage/alkylation was performed on commercial butyl rubbers containing varying amounts of isoprene content to prepare multifunctional PIB macromers bearing photopolymerizable moieties. Upon curing, the resulting networks exhibited superior resistance to creep and to attack by solvents that would normally plasticize/dissolve medium-molecular weight PIB thermoplastics. Using this approach, we have developed a new family of PIB thermoplastics, containing covalently-bound 3,5-di-*tert*-butyl-4-hydroxyphenyl moieties, which display superior resistance to thermo-

oxidative degradation compared to unmodified, commercially available PIB homopolymers.

5.3 Experimental

5.3.1 Materials.

Hexane (anhydrous, 95%), methanol (anhydrous, 99.8%), methylene chloride (DCM) (anhydrous, 99.8%), titanium tetrachloride ($TiCl_4$) (99.9%), 2,6-lutidine (99.5%), and tetrahydrofuran (THF) (anhydrous, 99.9%) were purchased and used as received from Sigma-Aldrich. 2,6-di-*tert*-Butylphenol (DTP) (99%) was purchased from Sigma-Aldrich and recrystallized from *n*-hexane (m.p. 35-37 °C) before use. Magnesium sulfate ($MgSO_4$, anhydrous), sulfuric acid (98%), *n*-hexane (Optima, 95%) chloroform-*d* ($CDCl_3$) were purchased and used as received from Fisher Scientific. Isobutylene (IB, BOC Gases) and methyl chloride (MeCl, Gas and Supply) were dried by passing the gas through a column of $CaSO_4$/molecular sieves/$CaCl_2$ and condensing within a N_2-atmosphere glovebox immediately prior to use. The monofunctional initiator, 2-chloro-2,4,4-trimethyl-pentane (TMPCl), was prepared via a previously described procedure.[248] Butyl rubber (EXXON™ Butyl 068) was donated by ExxonMobil Corporation and used as received. Characterization via GPC/MALLS and ^{1}H NMR indicated that Butyl 068 had a number average molecular weight ($\overline{M}_n$) of 3.37 x 10^5 g/mol and a dispersity (Đ) of 1.29. The mole fraction of isoprene (IP) comonomer units in the copolymer, F_{IP}, was determined to be 0.0108 (IB units/IP units ≅ 91.6),[Error! Bookmark not defined.] and the isoprene equivalent weight, EW_{IP}, was calculated to be 5.21 x10^3 g/mol. Oppanol samples was donated by BASF; characterization via GPC/MALLS indicated that Oppanol B14 SFN

had an $\overline{M}_n$ = 64,500 g/mol and Đ = 1.60, while Oppanol B15 SFN possessed an $\overline{M}_n$ = 74,100 g/mol and Đ = 1.53.

5.3.2 Instrumentation.

Nuclear magnetic resonance (NMR) spectra were obtained using either a 300 MHz Varian Mercury^{plus} (VNMR 6.1C) or a 600 MHz Bruker 94 Avance (TopSpin 3.5) NMR spectrometer. All ^{1}H chemical shifts were referenced to TMS (0 ppm). Samples were prepared by dissolving the polymer in chloroform-*d* (5%, w/v) and charging this solution to a 5 mm NMR tube. For quantitative integration, 64 transients were acquired using a pulse delay of 27.3 s.

Real time (RT)-FTIR monitoring of isobutylene polymerizations was performed using a ReactIR 45m (Mettler-Toledo) reaction monitoring system integrated with a N_2-atmosphere glovebox (MBraun Labmaster 130).[118,249,] Isobutylene conversion during polymerization was determined by monitoring the area above a two-point baseline of the absorbance at 887 cm^{-1}, associated with the = CH_2 wag of isobutylene.

Number-average molecular weights ($\overline{M}_n$) and dispersity (Đ = $\overline{M}_w/\overline{M}_n$) were determined using a gel-permeation chromatography (GPC) system consisting of a Waters Alliance 2695 separations module, an online multi-angle laser light scattering (MALLS) detector fitted with a gallium arsenide laser (power: 20 mW) operating at 658 nm (miniDAWN TREOS, Wyatt Technology Inc.), an interferometric refractometer (Optilab t-rEX, Wyatt Technology Inc.) operating at 35°C and 685 nm, and two PLgel (Polymer Laboratories Inc.) mixed D columns (pore size range 50-10^3 Å, 5 μm bead size). Freshly distilled THF served as the mobile phase and was delivered at a flow rate of 1.0 mL/min.

Sample concentrations were ca. 6-7 mg of polymer/mL of THF, and the injection volume was 100μL. The detector signals were simultaneously recorded using ASTRA software (Wyatt Technology Inc.), and absolute molecular weights were determined by MALLS using a *dn*/*dc* calculated from the refractive index detector response and assuming 100% mass recovery from the columns.

Thermogravimetric analysis (TGA) was performed using a Q50 (TA Instruments) thermogravimetric analyzer. The furnace atmosphere was defined by either N_2 or dry air flowing at a rate of 60 mL/min. Samples were prepared by loading a platinum sample pan with 10−20 mg of material. The samples were subjected to a temperature ramp of 10 °C/min from 30 to 600 °C. The data were analyzed using TA Universal software, and three temperatures were recorded: T_{10}, T_{50}, and T_{100}, which represent the temperatures at which 10 wt%, 50 wt%, and 100% wt% cumulative mass losses were reached, respectively.

Oxygen induction time (OIT) measurements were performed according to ASTM D3895-14, using a Q200 Differential Scanning Calorimeter (TA Instruments). Samples were prepared by adding ca. 10-13 mg of the subject polymer to an aluminum pan. Individual samples were tested using the following specifications. The uncovered sample was equilibrated at 25 °C and then heated to 200 °C using a heating rate of 20 °C min^{-1} under nitrogen (N_2). After holding isothermally at 200 °C for 5 min under N_2, the furnace gas was switched to dry air. For data analysis, the switch from N_2 to air was designated T_0 and used as the starting time for the OIT test. The sample was held isothermally at 200 °C in air for 100 min, or until the onset of oxidative degradation,

which was indicated by a sharp increase in the exothermic heat flow. Time to oxidation calculations were performed using TA Universal Analysis software.

Fourier-transform infrared (FTIR) spectroscopy was conducted using a Nicolet 8700 spectrometer with a KBr beam splitter and a DTSG detector under transmission mode. Each sample was blotted onto a NaCl plate and degassed under vacuum for 18 h. An average of 64 scans was recorded with a resolution of 6 cm^{-1}.

5.3.3 Acid Catalyzed Cleavage/Alkylation of Butyl Rubber.

The following is a representative procedure adapted from Campbell *et al.*[108] Butyl 068 (6.01 g, 1.15 mmol IP units) and dissolved in a mixture of 90 mL of *n*-hexane and 60 mL dichloromethane, within a 250 mL round bottom flask equipped with a magnetic stir-bar. The mixture was chilled to -70 °C, and 2,6-di-*tert*-butylphenol (15.5 g, 0.0751 mol), conc. H_2SO_4 (0.75 mL), and $TiCl_4$ (1.65 mL , 0.015 mol) were added in quick succession under stirring. The reaction was stirred at -70 °C for 24 h and aliquots were taken to monitor reaction progress. After 24 h the reaction was quenched with chilled methanol. The resulting solution was warmed to room temperature and concentrated under an N_2 stream. The concentrated mixture was then slowly precipitated into methanol under vigorous stirring, after which the methanol layer was decanted. The precipitate was collected by re-dissolution in fresh *n*-hexane, and the resulting solution was re-precipitated into excess methanol. The precipitate was collected by re-dissolution in fresh hexane, and the resulting solution was washed twice with deionized water, dried over Na_2SO_4, and then vacuum stripped to yield the isolated polymer. The product was then characterized via GPC-MALLS and ^1H NMR.

5.4 Results and Discussion

5.4.1 Cleavage/alkylation Reactions on Butyl Rubber

Cleavage/alkylation reactions on butyl rubber substrates represent a cost effective, highly modular approach towards multifunctional PIBs. A wide range of functional equivalent weights (EW_Q) and average functionalities (F_n) can be obtained by varying temperature, reaction time, F_{IP} of the butyl rubber starting material, identity/concentration of the Lewis acid, quencher concentration, and butyl rubber concentration. Recently, our lab reported the cleavage/alkylation reaction of butyl rubber (F_{IP} = 0.0230) using (3-bromopropoxy)benzene.**Error! Bookmark not defined.** The latter is a versatile quencher that yields primary-bromide functional groups along the PIB backbone for easy synthetic modification.[96,182] The authors overviewed some general mechanistic considerations of the cleavage/alkylation process; however their focus on achieving low molecular weight, difunctional PIB (~2,000 < $\overline{M}_n$ < 5,000 g/mol) deviated significantly from the goals of the present study. Herein, we were interested in conditions whereby the cleavage/alkylation process would yield PIBs with moderate-to-high $\overline{M}_n$'s, possessing moderately high F_n's. In this work we have also employed hindered phenolic quenchers as opposed to alkoxybenzenes, and the effect of quencher and Lewis acid concentration has not been studied for this class of quenchers. Finally, we have conducted a systematic study to explore conditions necessary to reach a targeted $\overline{M}_n$ range from a butyl rubber possessing a relatively low F_{IP}.

To gain an understanding of the cleavage/alkylation kinetics for Butyl 068 (F_{IP} = 0.108) in the presence of the hindered phenolic quencher, DTP, reactions were conducted under differing conditions, and aliquots were removed from the reactor at various times and analyzed with regard to molecular weight (GPC) and average functionality (^{1}H NMR). The results are listed in Table 5.1. GPC chromatograms for the Trial 1 aliquots, which are representative, along with that of the starting butyl rubber are shown in Figure 5.2. The corresponding GPC chromatograms for aliquots taken during Trials 2 and 3 are shown in Figures 5.3 and 5.4, respectively.

Table 5.1 Cleavage/alkylation Reactions on Butyl Rubber (Butyl 068) in the Presence of DTP

Trial	[Butyl][a]	[DTP] (M)	[$TiCl_4$] (mM)	Time (h)	$\overline{M}_n$ [b] (Đ)	EW_Q[b]	$\frac{IB}{Q}$	F_n
1	0.101	0.426	0.0854	4	62,270 (1.58)	6,080	103.3	10.2
				7	58,940 (1.60)	6,401	109.0	9.20
				9	57,670 (1.58)	6,259	142.0	9.27
				24	54,640 (1.51)	5,256	89.00	10.4
2	0.107	0.224	0.0898	4	33,110 (1.56)	6,411	109.2	5.16
				7	32,400 (1.51)	5,955	101.2	5.44
				9	30,210 (1.58)	7,007	119.7	4.31
				24	29,990 (1.51)	5,470	92.7	5.48
3	0.107	0.224	0.0449	2	85,270 (1.57)	195.5	11,330	7.57
				4	53,730 (1.62)	183.3	10,630	5.06
				6	49,520 (1.57)	158.5	9,215	5.37
				8	42,920 (1.67)	148.7	8,657	4.86

[a] mmol/IP repeat units/L
[b] g/mol

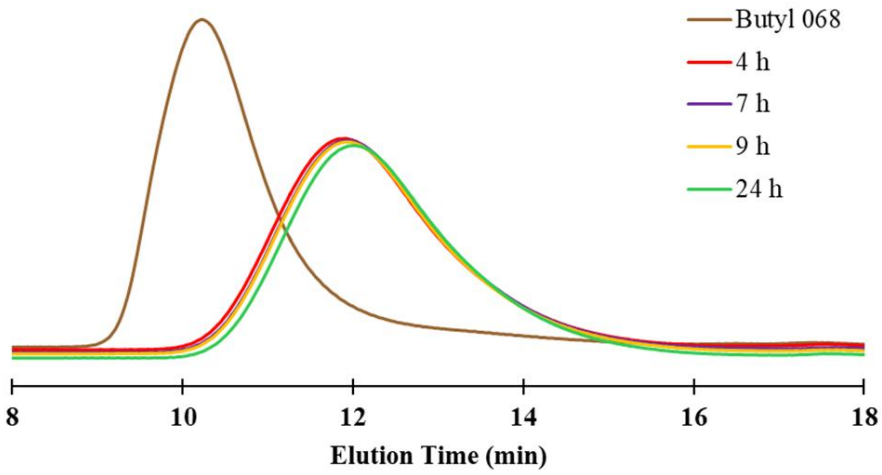

Figure 5.2 GPC chromatogram of the aliquots obtained from Trial 1 compared to Butyl 068.

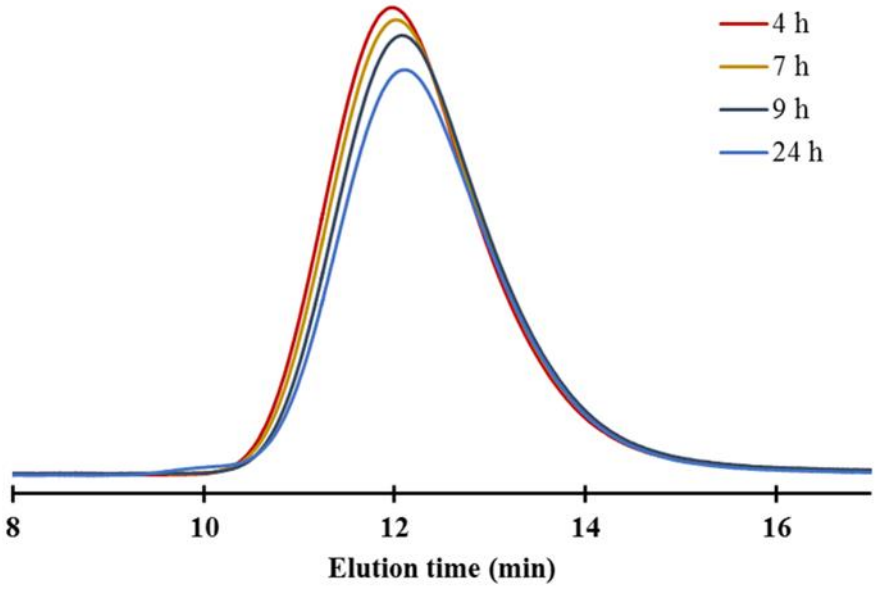

Figure 5.3 GPC chromatogram of the aliquots obtained from Trial 2.

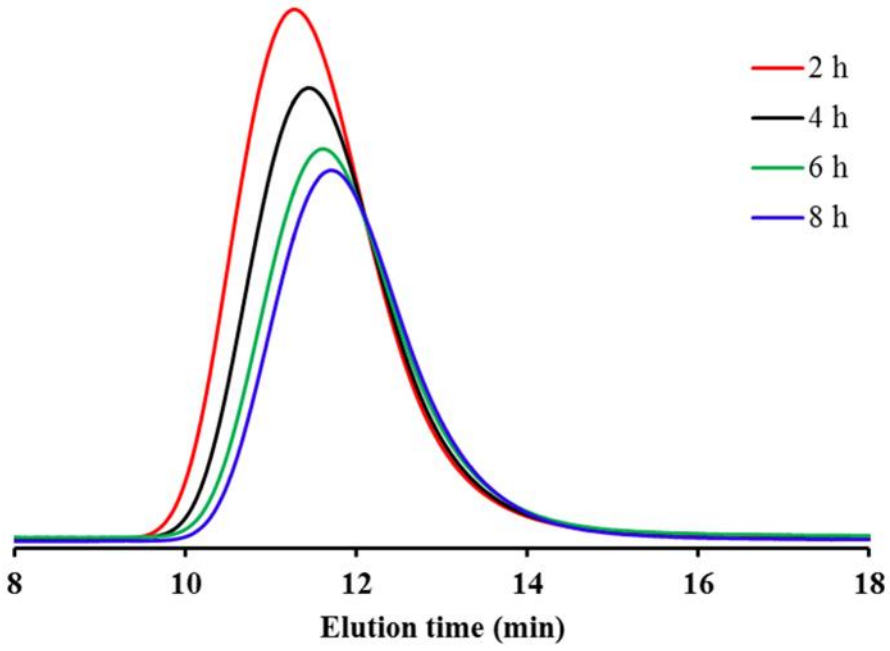

Figure 5.4 GPC chromatogram of the aliquots obtained from Trial 3.

The starting Butyl 068 was found to possess a characteristically high $\overline{M}_n$ and moderately narrow dispersity (337,000 g/mol and 1.27 respectively). As shown by the data in Table 5.1 and Figure 5.2, generally the $\overline{M}_n$ decreased as the reaction time increased, which is consistent with previous reports for cleavage/alkylation reactions.[34] However, the extent of cleavage/alkylation during the later stages of the reaction differed significantly from previously reported systems, and we attribute this mainly to the difference in quencher structure, i.e., alkoxybenzene vs. hindered phenol, as will be discussed below. In the systems studied by Campbell *et al.*, longer reaction times were used to yield PIBs possessing low molecular weights, and this was thought to be

facilitated by reversibility of the Friedel-Crafts alkylation in the case of an alkoxybenzene-type quencher.[108]

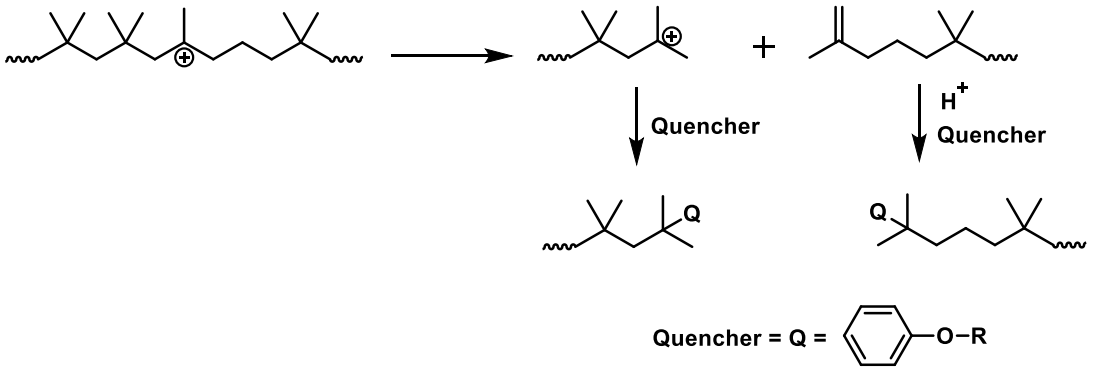

Scheme 5.1 Cleavage/alkylation process of butyl rubber in the presence of Bronsted and Lewis acids.

Scheme 5.1 shows the mechanism that is believed to occur during cleavage/alkylation.[108] The two reactions, cleavage and alkylation, are competitive. Both proceed from the same carbocation, which forms from the protonation of the residual isoprene double bond by H_2SO_4. In the presence of a Lewis acid, the carbocation can then react in one of two ways. It can react directly with the phenoxy quencher via a Friedel Crafts alkylation, resulting in the alkylation of the polymer backbone. This has been termed backbone quenching. The other reaction, which represents the primary chain degradation mechanism and is driven by relief of steric strain, is β-cleavage of the carbocation to form two chain ends, which then both undergo Friedel-Crafts alkylation with the phenoxy quencher. Cleavage is most prevalent during the beginning stages of the reaction and results in significant molecular weight degradation.

Interestingly, the nature of the phenoxy quencher apparently influences the likelihood of β-cleavage vs. backbone quenching. When using (3-

bromopropoxy)benzene as the quenching substrate, Campbell *et al.* reported that sites that had undergone backbone quenching during the early stages of the reaction were susceptible to retro Friedel-Crafts alkylation, leading to a second-stage cleavage/alkylation sequence.[108] This process was reported to be much slower, and relatively long reaction times (~24 h) were required to reach very low $\overline{M}_n$ PIBs. Notably, this second-stage chain breaking mechanism, and its progenitor, retro Friedel-Crafts alkylation, does not appear to occur in the case of hindered phenolic quenchers. The progression of $\overline{M}_n$ values in Table 5.1, Trials 1-3, showed that when using DTP as a quenching substrate, the cleavage/alkylation reactions proceeded quickly at early time frames (as evidenced by an immediate reduction in the polymer $\overline{M}_n$), and were generally stable after 4 h. The $\overline{M}_n$'s of the 4 aliquots taken during Trial 1 showed a continual, slow decrease in $\overline{M}_n$, but the later decreases were minor compared to the very large drop in molecular weight that occurred during the first 4 h of the reaction. This same pattern was especially pronounced in Trial 2, where the total drop in $\overline{M}_n$ between the 4 h and the 24 h aliquot was only 3,000 g/mol.

Generally, the $\overline{M}_n$'s for each aliquot taken in Trial 2 were significantly lower than those isolated in Trial 1. This was expected, as Trial 2 was formulated to contain half the concentration of DTP used in Trial 1. Although the concentration of DTP was decreased by a factor of 2, this didn't necessarily correlate to a decrease in $\overline{M}_n$ by a factor of 2. Interestingly, the 4 h aliquot for Trial 1 possessed an $\overline{M}_n$ that was 1.88 times

higher than the 4 h aliquot in Trial 2; as reaction time increased, this ratio fell to about 1.82.

Trial 3 was formulated with the same DTP concentration and half the $TiCl_4$ concentration as Trial 2, to provide insight into the effect of $TiCl_4$ concentration on the reaction kinetics. As expected, the PIB isolated at 4 h for Trial 3 possessed a higher $\overline{M}_n$ than the PIB taken at 4 h in Trial 2, but the PIB isolated at 8 h in Trial 3 began to approach the $\overline{M}_n$ for the PIB isolated at 4 h in Trial 2. Another significant finding in Trial 3 resulted from the decision to decrease the $TiCl_4$ concentration and take aliquots early in the reaction, which provided insight into the cleavage/alkylation behavior during the initial reaction phase. The PIB isolated at 2 h possessed a $\overline{M}_n$ of 85,270 g/mol, and the $\overline{M}_n$ continued to decrease until the 4 h mark (~53,730 g/mol) after which the degradation rate began to slow dramatically. This supports the findings of Campbell *et al.*, which showed that the main chain breaking process occurred early in the reaction but slowed considerably at longer reaction times.[34]

Table 5.2 Cleavage/alkylation Reaction of Butyl Rubber in the Presence of DTP

Trial	[Butyl][a]	[DTP] (mM)	[TiCl] (mM)	Time (h)	$\overline{M}_n$ [b] (Đ)	EW_Q[b]	$\frac{IB}{Q}$	F_n
4	0.101	0.426	0.0854	1	71,050 (1.67)	8,886	152.8	7.99
				2	72,630 (1.62)	6,982	119.3	10.4
				3	68,160 (1.73)	5,882	100.0	11.6
				4	67,370 (1.60)	6,349	108.2	10.6
				5	65,430 (1.62)	5,835	99.17	11.2
				6	65,470 (1.60)	5,446	92.33	12.0

[a] mmol/IP repeat units/L
[b] g/mol

To further understand the chain degradation process at short reaction times, an experiment was carried out under identical conditions to Trial 1, but aliquots were taken at 1 h intervals for 6 h, after which the reaction mixture was quenched. The $\overline{M}_n$ and F_n for each aliquot are listed in Table 5.2, and the GPC chromatograms are shown in Figure 5.5. As expected, extensive cleavage of the butyl rubber was observed within the first hour of the reaction. Interestingly, the cleavage reaction slowed considerably after 1 h, but the F_n showed a significant increase between the 1 h and 2 h aliquots. This suggests that residual isoprene unsaturations were present after 1 h, which were subsequently protonated and functionalized.

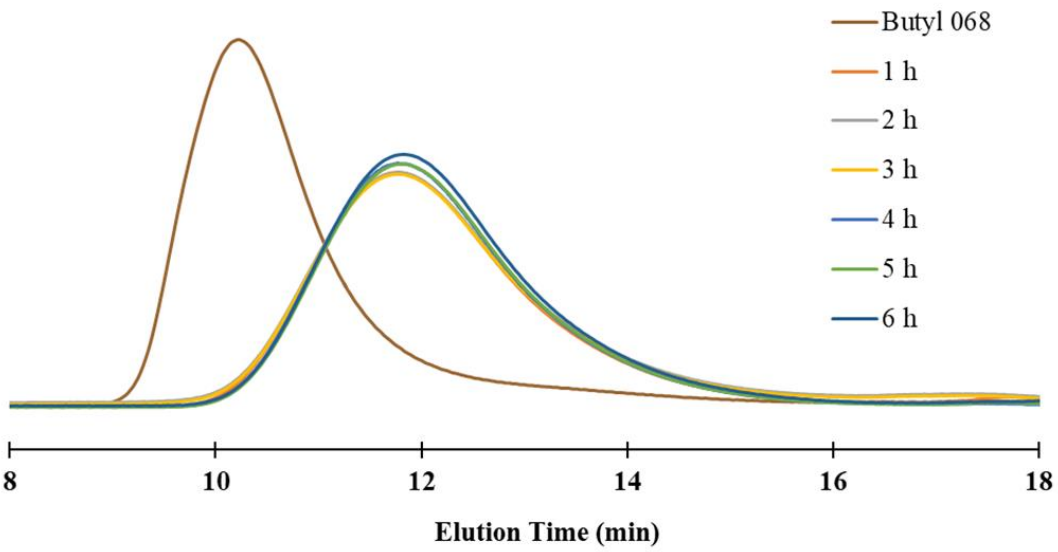

Figure 5.5 GPC chromatograms of the aliquots obtained from Trial 4 compared to Butyl 068.

5.4.2 Proton NMR Assignments and Determination of Number Average Functionality (F_n) and Functional Equivalent Weight (EW_Q).

F_n and EW_Q were calculated using a modification of a method previously reported by Campbell *et al.*[108] The latter report involved the use of (3-bromopropoxy)benzene as quencher. The $-CH_2Br$ protons of the resulting quencher residues within the product gave well resolved peaks in ^1H NMR, allowing for easy integration and quantification of functionality.[108] Additionally, (3-bromopropoxy)benzene has been reported to alkylate solely at the *para*-position relative to the alkoxy moiety, and there are no other substituents on the ring. This results in clearly defined doublets in the aromatic region.[96] The use of DTP, however, results in a plurality of structures and a more complex ^1H NMR spectrum.

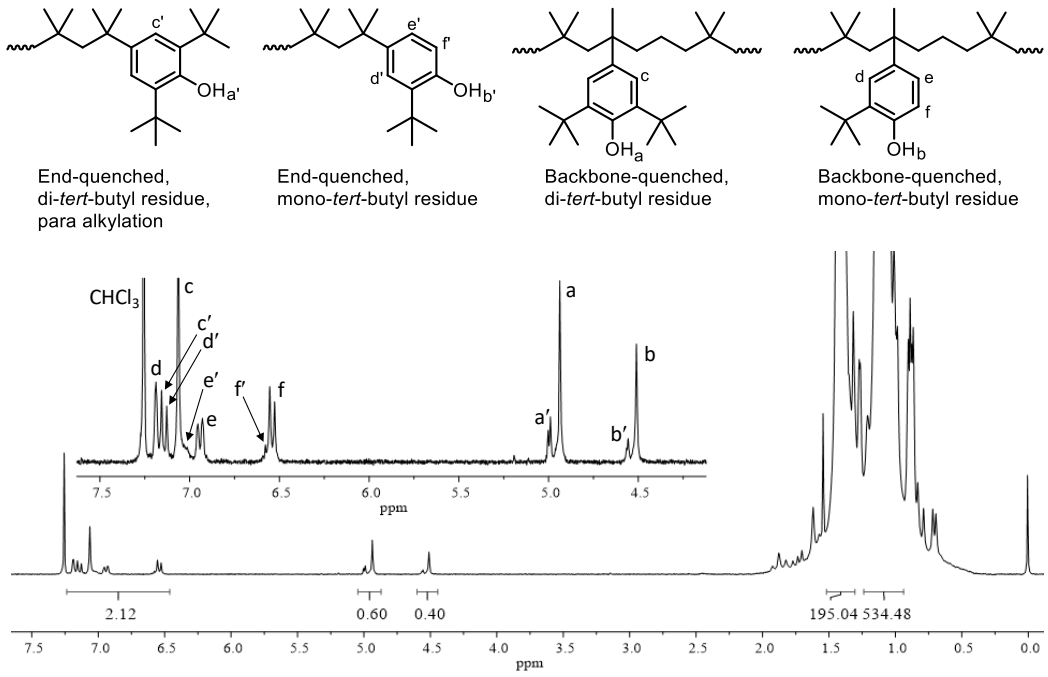

Figure 5.6 ^{1}H NMR spectrum (300 MHz, $CDCl_3$, 23 °C) of the reaction product of Trial 1, Table 5.1 after cleavage/alkylation in the presence of DTP for 24 h.

As described in the seminal publication on phenoxy quenching by Morgan *et al.*, the use of DTP to quench living PIBs results in a combination of di-*tert*-butylated and mono-*tert*-butylated structures; the latter result from de-*tert*-butylation, which proceeds via a retro Friedel-Crafts mechanism. This combination of products results in multiple peaks in the aromatic region, ranging from 6.50-7.20 ppm and multiple peaks in the 4.5-5.1 region due to the resonance signals of the phenolic hydroxyl proton of various mono- and di-alkylated phenolic species. The aliphatic protons from the *tert*-butyl groups of the mono- and di-*tert*-butylated products are not useful for characterizing the various quenched structures because they possess chemical shifts between 1.36-1.40 ppm, which overlap directly with the resonance signals of the methylene groups of the PIB backbone.

Figure 5.6 shows the ^{1}H NMR spectrum of Butyl 068 after cleavage/alkylation in the presence of DTP (Trial 1, Table 5.1). A high expansion of the aromatic region is

shown in Figure 5.7, which was measured on a 600 MHz NMR to provide better resolution. The phenolic proton resonances of the di-*tert*-butyl phenol and mono-*tert*-butyl phenol residues each appear as a set of two peaks: an intense singlet representing the more numerous backbone-quenched residues and a doublet of lesser intensity representing the less numerous chain end-quenched residues. These peak sets appear in the range 4.93-5.01 ppm for the di-*tert*-butyl species (peaks a and a′) and 4.53-4.68 ppm for the mono-*tert*-butyl species (peaks b and b′). With regard to the aromatic region, the normal quenched structures, i.e., those that retain both *tert*-butyl groups, are symmetrical and possess two equivalent protons that appear as a sharp singlet at 7.06 ppm (peak c) for the more numerous backbone-quenched residues and another sharp singlet at 7.15 ppm (peak c′) for the less numerous end-quenched residues. The de-*tert*-butylated structures are asymmetrical, and each possesses three non-equivalent aromatic protons. For the backbone-quenched residues, the new proton that replaces the *tert*-butyl group appears as an upfield doublet (peak f) at 6.53 ppm. It is coupled to neighboring proton, e, which appears as a downfield doublet at 6.94 ppm. The proton adjacent to the remaining *tert*-butyl group, d, appears as a broad singlet at 7.18 ppm. For the end-quenched residues, the d′ proton resonance appears as a sharp singlet at 7.15 ppm. The f′ and e′ proton residues overlap with other peaks and are difficult to see at 300 MHz, but their approximate locations are indicated in Figure 5.6. These proton resonances, however, are easily resolved at 600 MHz as shown in Figure 5.7. The higher resolution spectrum also reveals three-bond coupling between protons d and e.

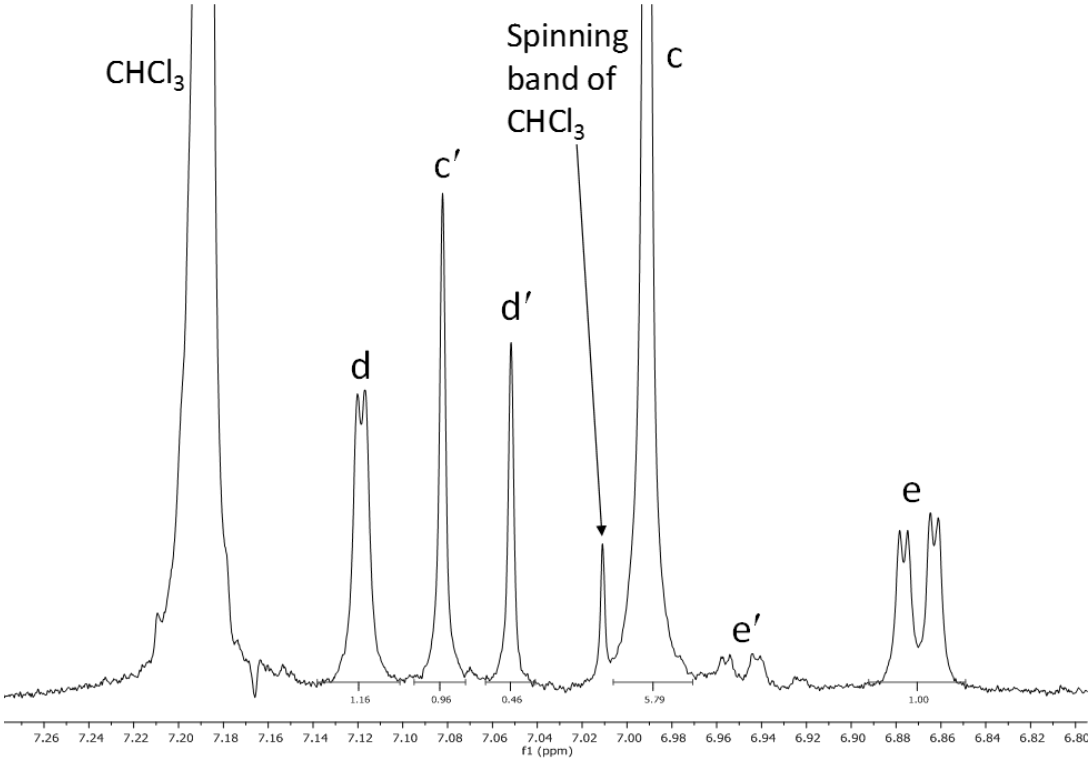

Figure 5.7 ^{1}H NMR spectrum (600 MHz, CDCl3, 23°C, expansion of aromatic region) of the cleavage/alkylation reaction product of Butyl 068 with DTP

The functional equivalent weight, EW_Q, of the product after cleavage/alkylation was calculated using eq 1, which is similar to eq 3 from Campbell *et al.*[108]:

$$EW_Q = \frac{IB}{Q}\left[M_{IB} + \frac{M_{IP}}{n_{IB}}\right] + f_{DTP}M_{DTP} + f_{MTP}M_{MTP} \quad (1)$$

M_{IB} and M_{IP} are, respectively, the molecular weights of the IB repeat unit (56.1 g/mol) and the IP repeat unit (68.1 g/mol). M_{DTP} and M_{MTP} are the molecular weights of the di-*tert*-butyl phenol quencher (206.33 g/mol) and the effective mono-*tert*-butyl phenol quencher (150.22 g/mol). As discussed above, the resonance signals of the phenolic hydroxyl protons display two chemical shifts: for the di-*tert*-butyl species, the shift is between 4.92-5.02 ppm, and for the mono-*tert*-butyl species, between 4.46-4.60. The integrated areas of these peaks were determined and designated A_{DTP} and A_{MTP},

respectively. The fraction of di-*tert*-butyl species, f_{DTP}, was calculated as $A_{DTP}/(A_{DTP} + A_{MDT})$, and the fraction of mono-*tert*-butyl species, f_{MTP}, was calculated as $1-f_{DTP}$. IB/Q is the mole ratio of IB units to Q units in the product and was calculated using eq 2,

$$\frac{IB}{Q} = \frac{A_{1.11}/6}{A_{DTP} + A_{MTP}} \quad (2)$$

where $A_{1.11}$ is the area of the peak from 0.95 to 1.22 ppm, representative of the *gem*-dimethyl protons of the PIB backbone. Number average functionality, F_n, of the cleaved/alkylated polymers was calculated via the method reported previously.[108]

Figure 5.8 shows the ^{1}H NMR spectrum of Butyl 068 after cleavage/alkylation in the presence of a lesser concentration of DTP (Trial 2, Table 5.1). As discussed earlier, decreasing quencher concentration depresses backbone quenching relative to cleavage. This leads to a lower molecular weight product and a greater fraction of chain end-quenched structures. This can be readily observed in Figure 5.8 as an increase in the intensity of peaks a′ and b′ relative to peaks a and b. The greater fraction of chain-end quenched structures can also be observed in the aromatic region. Peaks c′, d′, e′, and f′ are all of higher intensity relative to peaks c, d, e, and f.

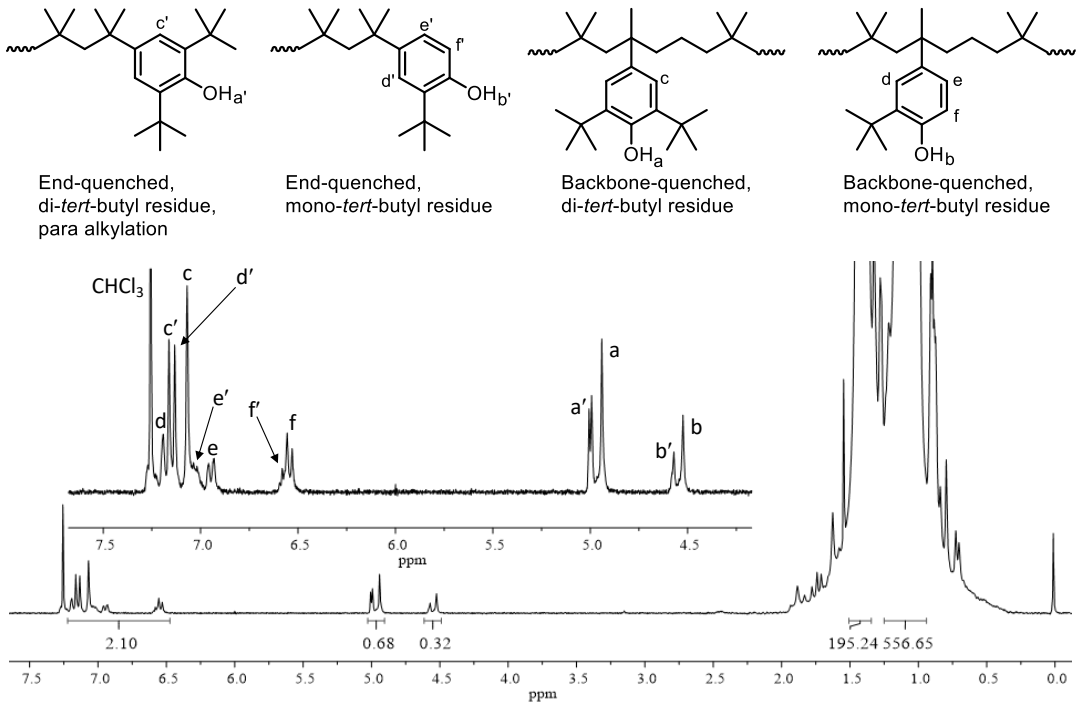

Figure 5.8 ^{1}H NMR spectrum (300 MHz, $CDCl_3$, 23 °C) of the reaction product of Trial 2, Table 5.1, after cleavage/alkylation in the presence of DTP for 24 h.

Figure 5.8 shows the ^{1}H NMR spectrum of Butyl 068 after cleavage/alkylation in the presence of a lesser concentration of DTP (Trial 2, Table 5.1). As discussed earlier, decreasing quencher concentration depresses backbone quenching relative to cleavage. This leads to a lower molecular weight product and a greater fraction of chain end-quenched structures. This can be readily observed in Figure 5.8 as an increase in the intensity of peaks a′ and b′ relative to peaks a and b. The greater fraction of chain-end quenched structures can also be observed in the aromatic region. Peaks c′, d′, e′, and f′ are all of higher intensity relative to peaks c, d, e, and f.

5.4.3 Characterization via FTIR Spectroscopy.

The products from Trials 1 and 2, both of which were isolated after reacting for 24 h, were characterized via FTIR spectroscopy. A sample of monofunctional PIB that

was synthesized via living polymerization and terminated with methanol (resulting in tertiary chloride end groups) was also characterized and used as a reference. The latter sample will be referred to as 56K-PIB-Cl. Figure 5.9 shows an overlay of the FTIR spectra of 56K-PIB-Cl and the product obtained from Trial 1 (hereinafter referred to as 55K-PIB-DTP). The presence of the *tert*-butylphenol quencher moieties within 55K-PIB-DTP is indicated by the two peaks in the region between 3600-3700 cm^{-1}, which are characteristic of the free hydroxyl of alkylated phenols.[250] The spectrum of the reference sample does not display these two peaks. Figure 5.10 shows similar data for the product obtained from Trial 2 (30K-PIB-DTP).

5.4.4 Thermal Decomposition Behavior.

Sufficiently convinced of the utility of DTP as a quenching substrate for cleavage/alkylation reactions on butyl rubber, we next set out to determine the thermal decomposition behavior of these systems. Although polyolefins possess excellent resistance to chemical degradation (due to the saturated C-C bonds within the polyolefin backbone), thermo-oxidative degradation has been shown to occur via radical chain scission mechanisms.[220] For this reason, commercial polyolefins are often formulated to include UV stabilizers and radical inhibitors to extend the polymer lifetime.

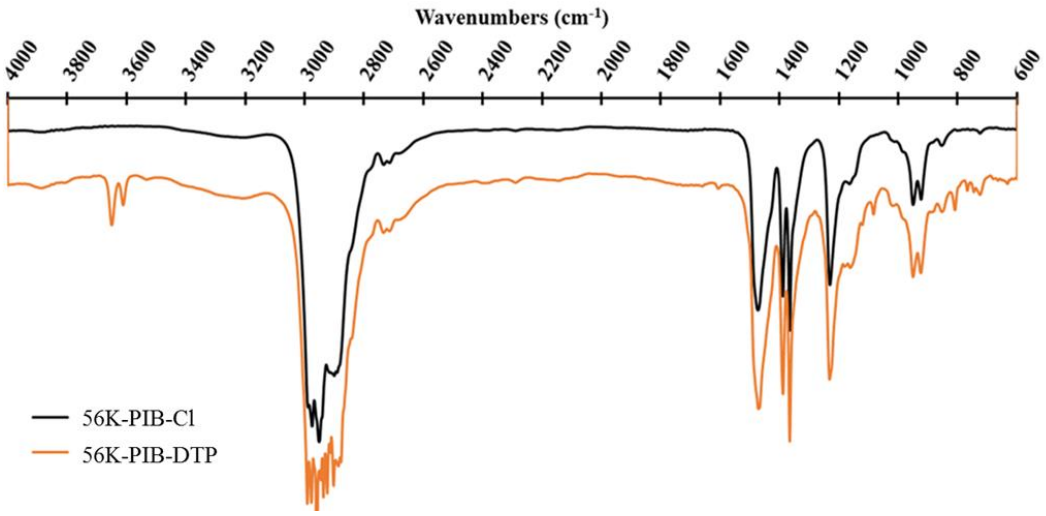

Figure 5.9 FTIR spectra of the product of Trial 1 after 24 h (55K-PIB-DTP) and a PIB sample containing *tert*-chloride end-groups (56K-PIB-Cl).

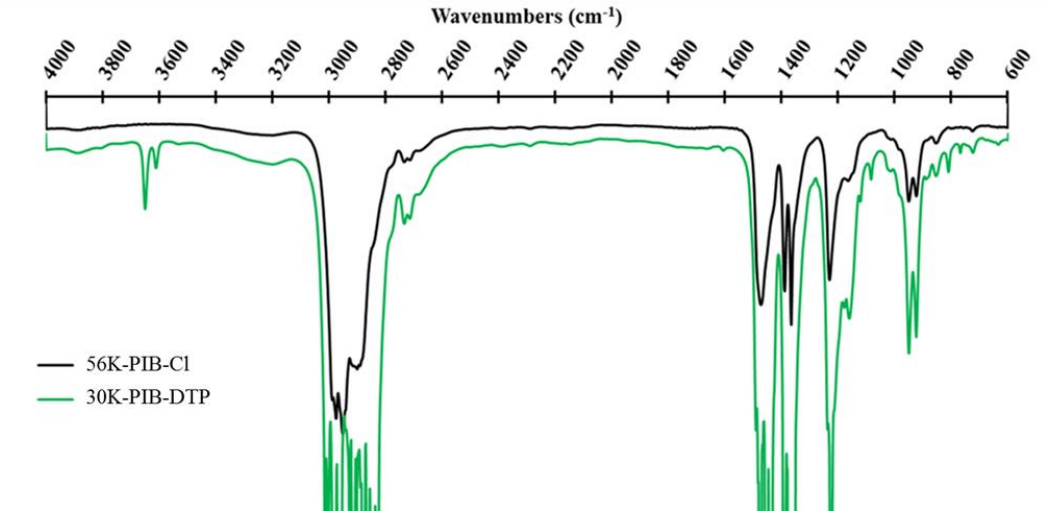

Figure 5.10 FTIR spectra of the product of Trial 2 after 24 h (30K-PIB-DTP) and a 56K-PIB-Cl.

To test the thermal resistance of DTP-modified PIBs, TGA analysis was performed under N_2 atmosphere (Figure 5.11) and in air (Figure 5.12). For comparison, two unfunctionalized PIBs prepared via living polymerization of IB and quenched with methanol (resulting in *tert*-chloride chain ends) and two commercial polyisobutylenes

(Oppanol B14 SFN and Oppanol B15 SFN) were also tested. Mass-loss data from Figures 5.11 and 5.12 are listed in Table 5.3.

An overlay of the TGA curves from the experiments performed in N_2 (Figure 5.11) show that, as expected, (T_{10}) between 360-370 °C, which has consistently been shown to be the onset of the degradation temperature of PIB.[69,220] Interestingly, both commercial PIBs displayed a slightly higher (380 °C) T_{10}. As the degradation profiles approached the 50% mass loss threshold (T_{50}) the unfunctionalized PIBs began to separate from the commercial and DTP-functionalized PIBs but were still within a narrow temperature range (397-411 °C). The unfunctionalized samples reached 100% mass loss in the 430-440°C range; whereas the commercial and DTP-functionalized samples reached 100% mass loss in the 445-470°C range.

Polyolefins generally display high resistance to thermal degradation while in inert atmospheres,[220] but are especially susceptible to thermo-oxidative degradation in the presence of pure oxygen or air.[251,252,253] Figure 5.12 shows an overlay of the TGA curves from the experiments performed in an air atmosphere, and the change in the degradation profiles of the PIB samples is readily apparent. For the unfunctionalized PIBs synthesized via living polymerizations, the T_{10} and T_{50} values are significantly lower than the corresponding values calculated from the test performed in N_2.

Table 5.3 Thermal Degradation Behavior of DTP Functionalized PIBs and Unfunctionalized PIBs

Sample	$\overline{M}_n$ [a] **(Đ)**	**N_2**			**Air**		
		T_{10}	**T_{50}**	**T_{100}**	**T_{10}**	**T_{50}**	**T_{100}**
56K-PIB-Cl	55,650 (1.07)	366.03	397.74	431.74	311.69	356.58	387.24
111K-PIB-Cl	110,800 (1.09)	370.17	398.65	437.01	316.79	352.94	385.50
Oppanol B14 SFN	64,500 (1.60)	380.50	408.46	445.14	326.21	378.15	419.39
Oppanol B15 SFN	74,100 (1.53)	381.36	410.91	447.3	343.00	388.05	426.78
30K-PIB-DTP	29,990 (1.51)	366.28	406.53	448.57	327.38	383.58	546.34
55K- PIB-DTP	54,640 (1.51)	366.89	407.48	468.37	339.17	387.87	547.52

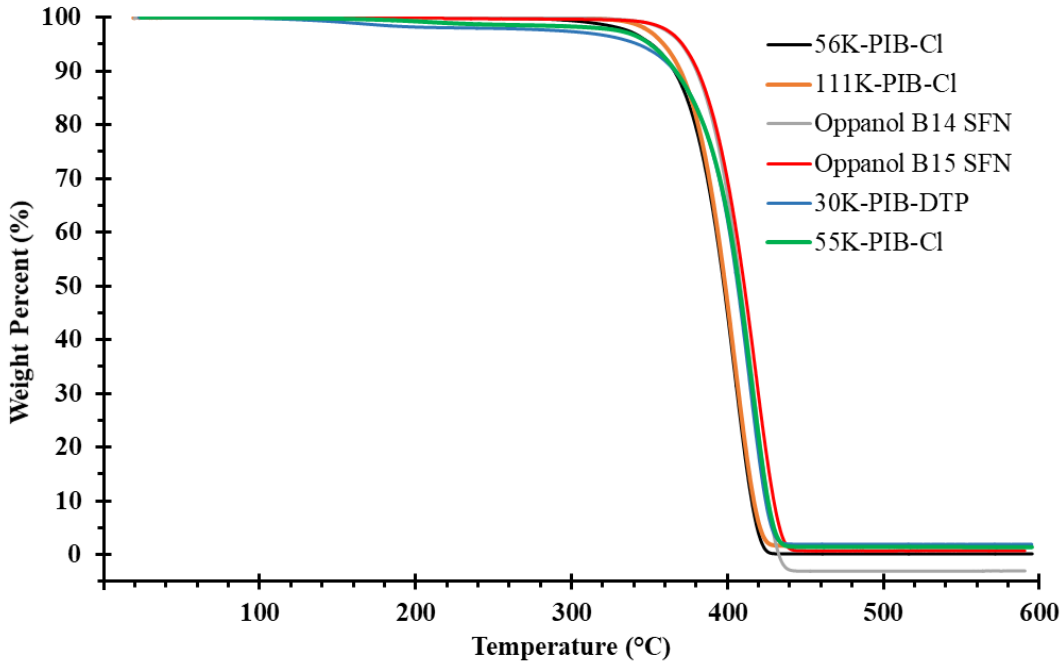

Figure 5.11 TGA overlay of various PIB samples degraded in an N_2 atmosphere.

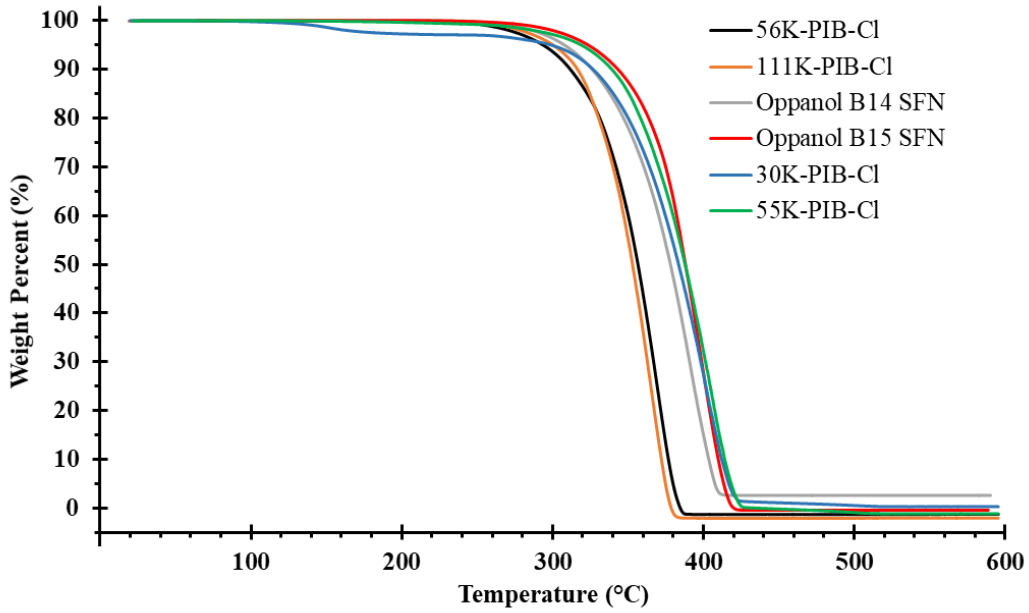

Figure 5.12 TGA overlay of various PIB samples degraded in an air atmosphere.

The most significant result from this series of TGA experiments is the degradation profiles of the DTP-functionalized PIBs. Compared to the living PIBs, these modified

PIBs displayed significantly higher T_{10} and T_{50} values. Comparison of the degradation profiles of the commercial PIBs and the DTP-functionalized PIBs is not as straightforward. The higher Mn DTP-functionalized PIB (56K-PIB-DTP) displayed a significantly higher T_{10} compared to the 30K-PIB-DTP and Oppanol B14 SFN materials but displayed a slightly lower T_{10} than Oppanol B15 SFN. As these systems approached T_{50}, the degradation profiles began to overlap; beyond T_{50}, the DTP-functionalized PIBs began to outperform the commercial PIBs. These results suggest that Mn and F_n of the DTP-functionalized PIBs may influence the onset of degradation, but the overall degradation profile of the PIB-DTP samples seems to be unaffected. These trends also suggest that the DTP functionalized PIBs possess a greater resistance to thermo-oxidative degradation, presumably due to radical suppression and sequestration.

Whereas TGA experiments can give a fundamental understanding of the degradation behavior of polymers, other tests are more suitable to measure the oxidative stability of polyolefins. One such test, Oxidative Induction Time (OIT), is often performed in the polyolefin industry as an accelerated aging test to provide an estimate of the performance lifetime of a specific polymer or formulation. OIT tests are usually performed on a differential scanning calorimeter (DSC) using a known sample weight in an uncovered copper or aluminum sample pan.[223] The sample is quickly heated in an N_2 environment, then held isothermally at an elevated temperature for a short duration, after which the environment transitions to pure oxygen or dry air. The time until the onset of oxidation, which is an exothermic phenomenon, is monitored by tracking the heat flow within the sample. Longer induction times are indicative of higher resistance against oxidative degradation, and consequently, a longer service lifetime. OIT measurements

were performed at 200 °C in dry air according to ASTM D3895-14 on the 5 samples listed in Table 5.3, and the results are plotted in Figure 5.13. Table 5.4 lists the OIT, which was measured using TA Universal Analysis software.

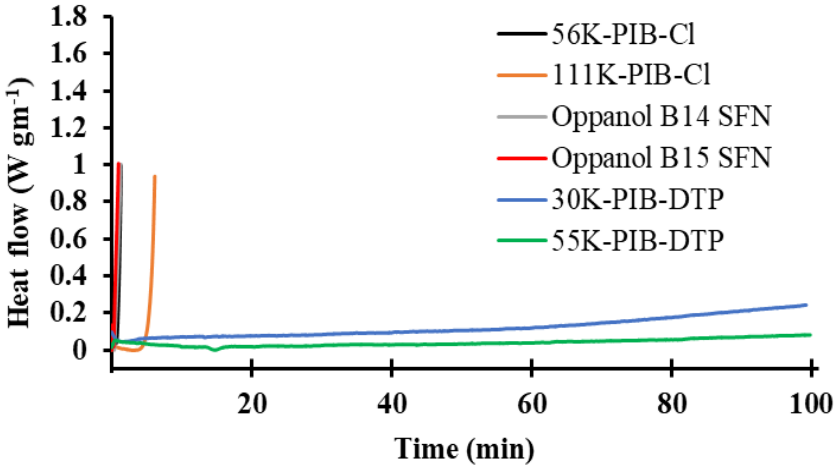

Figure 5.13 OIT measurements of unfunctionalized PIBs, commercially available PIBs (Oppanol B14 SFN and B15 SFN), and DTP-functionalized PIBs synthesized via the cleavage/alkylation reaction of Butyl 068.

Table 5.4 Oxidation Induction Time Measurements for Various PIB Samples

Sample	OIT
56K-PIB-Cl	0.69
111K-PIB-Cl	5.40
Oppanol B14 SFN	0.59
Oppanol B15 SFN	0.26
30K-PIB-DTP	-
55K-PIB-DTP	-

Figure 5.13 shows the results of OIT testing. For the two unfunctionalized PIBs produced by living polymerization, the lower molecular weight sample showed oxidative degradation almost immediately after switching from N_2 to air, but the higher molecular weight sample showed a delayed oxidation onset by about 4 min. Both Oppanol samples also showed immediate oxidative degradation. This suggests a direct correlation between the onset of oxidation and the molecular weight of the sample. The most significant

observation, however, is the stark difference between the DTP-functionalized and the unfunctionalized and commercial PIB samples. The DTP-functionalized PIBs exhibited excellent resistance to oxidative degradation due to the incorporation of DTP to the polymer backbone. Notably, the lower molecular PIB-DTP sample does begin to show signs of oxidative degradation towards the end of the test, but the exotherm is significantly broader than the unfunctionalized and commercial PIB samples. Comparatively, the higher molecular weight PIB-DTP shows very little exotherm throughout the test, probably due to the higher $\overline{M}_n$ and higher amount of DTP incorporated into the polymer backbone.

5.5 Conclusion

We have developed a novel synthetic route towards moderate molecular weight multifunctional polyisobutylenes bearing covalently-bound hindered phenols. By modifying the quenching conditions during the cleavage/alkylation process, a wide range of PIB molecular weights and functionalities can be isolated, and a general understanding of the quenching kinetics has been described.
been described.

The thermal degradation behavior of a selection of the functionalized PIBs was compared to unfunctionalized PIBs synthesized via living polymerization and to a commercial PIB, using an inert atmosphere as well as an oxygen containing atmosphere. The functionalized PIBs displayed characteristic degradation behaviors in the inert atmosphere but exhibited higher degradation temperatures in the oxygen atmosphere compared to the unfunctionalized and commercial PIBs.

Finally, we have demonstrated that the DTP-functionalized PIBs exhibit superior resistance towards oxidative degradation compared to the commercial and unfunctionalized PIBs. We showed that OIT measurements indicate a direct correlation between oxidation resistance and increasing PIB molecular weight. However, OIT measurements indicate that even the lowest molecular weight PIB-DTP, which begins to show oxidative degradation towards the latter portion of the OIT test, exhibits superior resistance to oxidative degradation compared to unfunctionalized and commercial PIBs.

The incorporation of covalently-bound antioxidants onto PIB represents a new paradigm in oxidation-resistance polyolefins. These functional polymers, and the process through which they are synthesized, have potential applications as lubricating oil additives, PIB adhesives and sealants, and new families of highly resistant PIB thermoplastics.

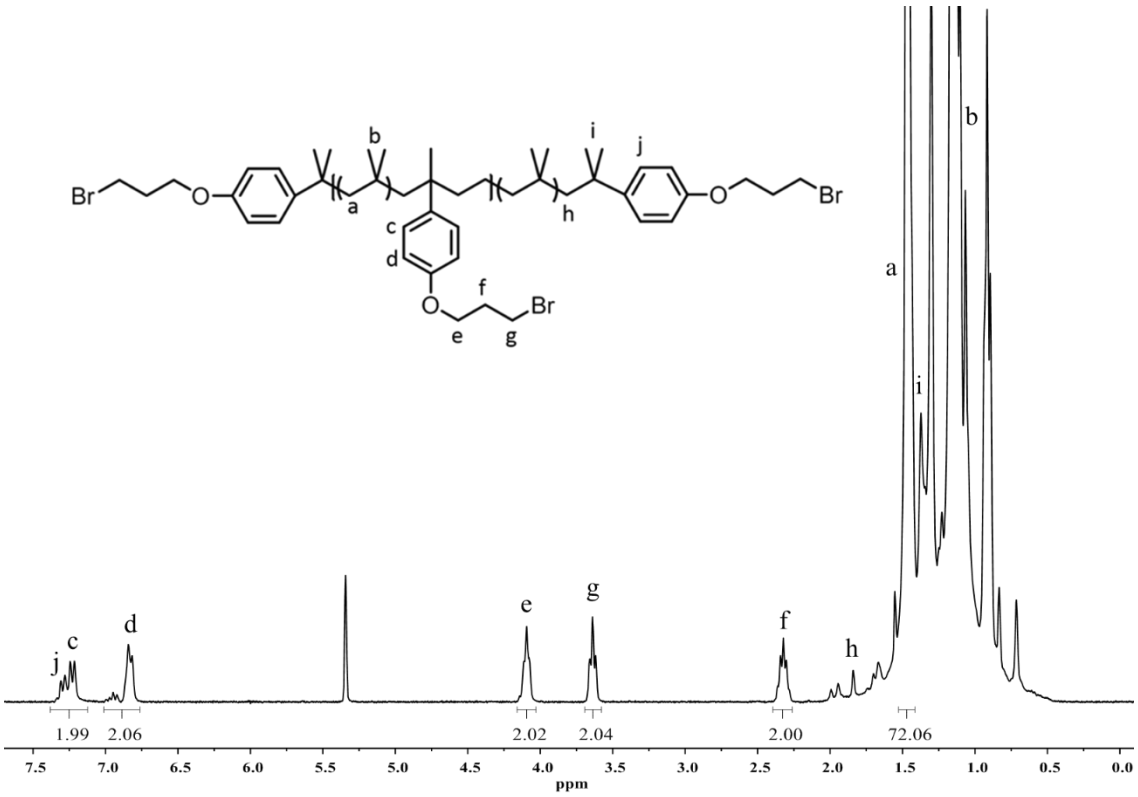

Figure A.1 ^{1}H NMR (300 MHz, DCM-d_2, 25 °C) spectrum of the (3-bromopropoxy)benzene- functionalized PIB macromer obtained from the cleavage/alkylation reaction of ExxonMobil Butyl 365, using the conditions listed in Table 2.1, Trial 1.

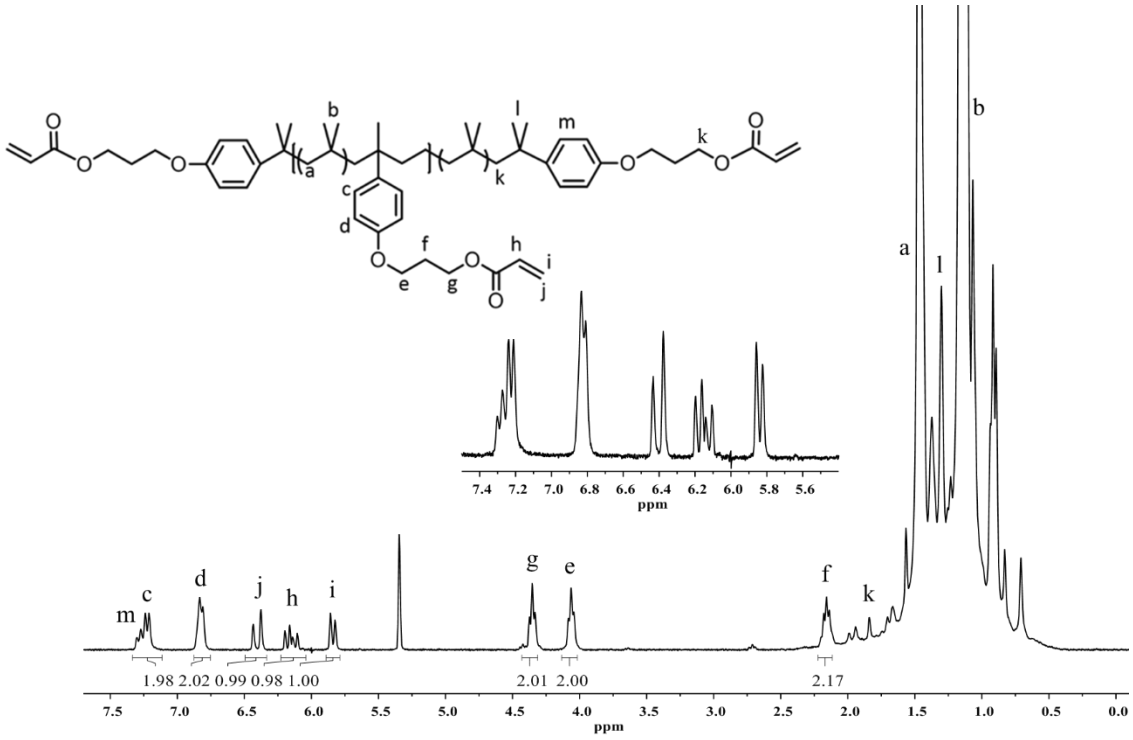

Figure A.2 ^{1}H NMR (300 MHz, DCM-d_2, 25 °C) spectrum of the acrylate-functionalized PIB macromer (17,400 Acrylate) derived from Butyl 365. This macromer was synthesized via a nucleophilic substitution reaction using potassium acrylate and the product from Table 2.1, Trial 1.

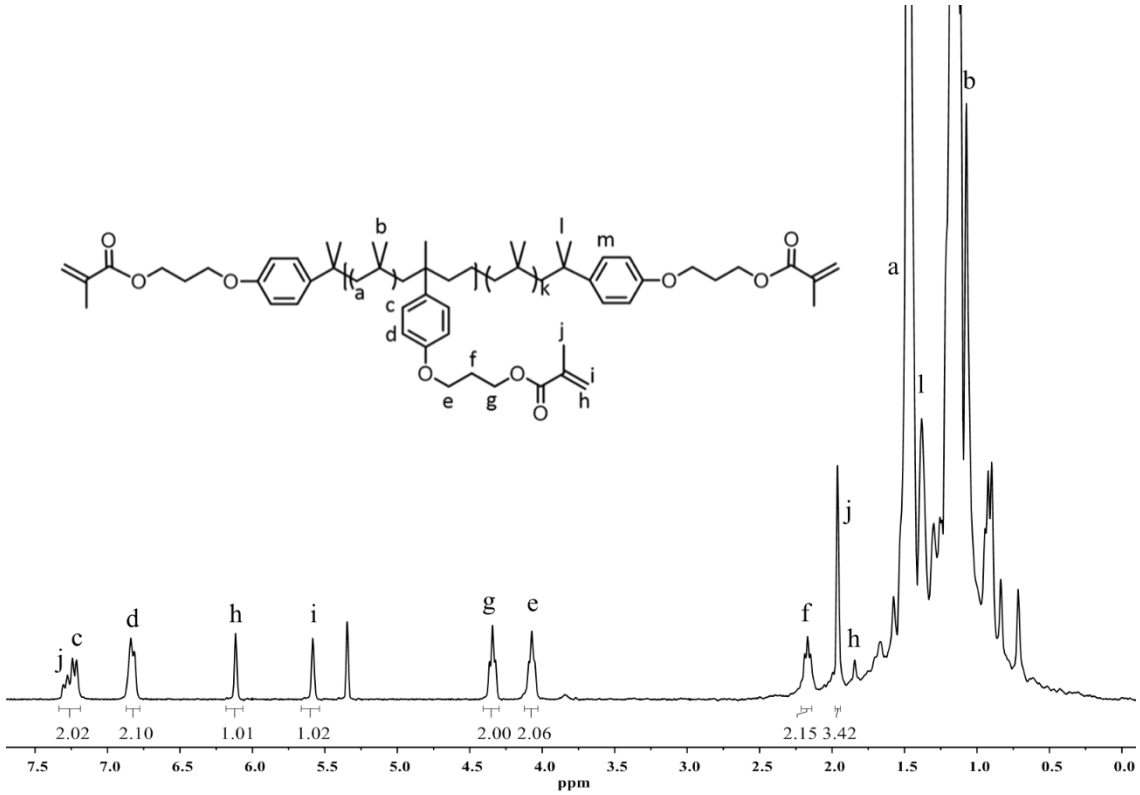

Figure A.3 ^{1}H NMR (300 MHz, DCM-d_2, 25 °C) spectrum of the methacrylate-functionalized PIB macromer (17,450 Methacrylate) derived from Butyl 365. This macromer was synthesized via a nucleophilic substitution reaction using potassium methacrylate and the product from Table 2.1, Trial 1.

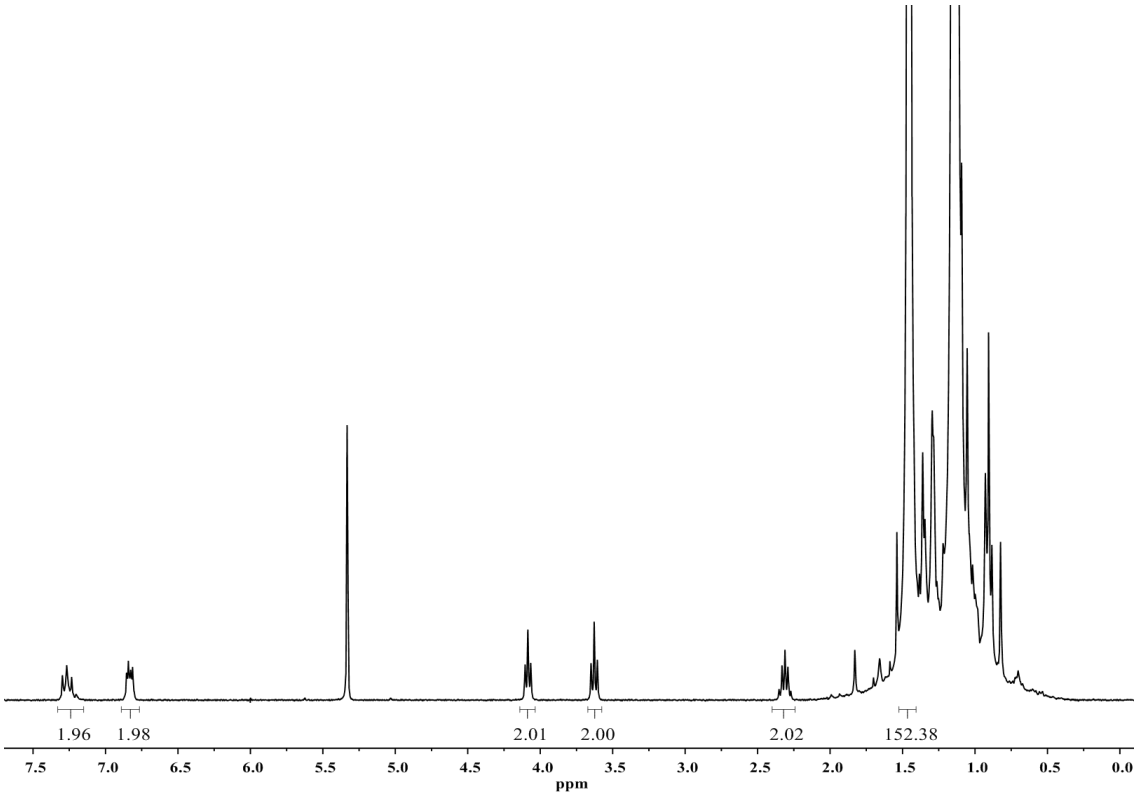

Figure A.4 ^{1}H NMR (300 MHz, DCM-d_2, 25 °C) spectrum of a (3-bromopropoxy)benzene-functionalized PIB macromer obtained from the cleavage/alkylation reaction of ExxonMobil Butyl 068, using the conditions listed in Table 2.1, Trial 2.

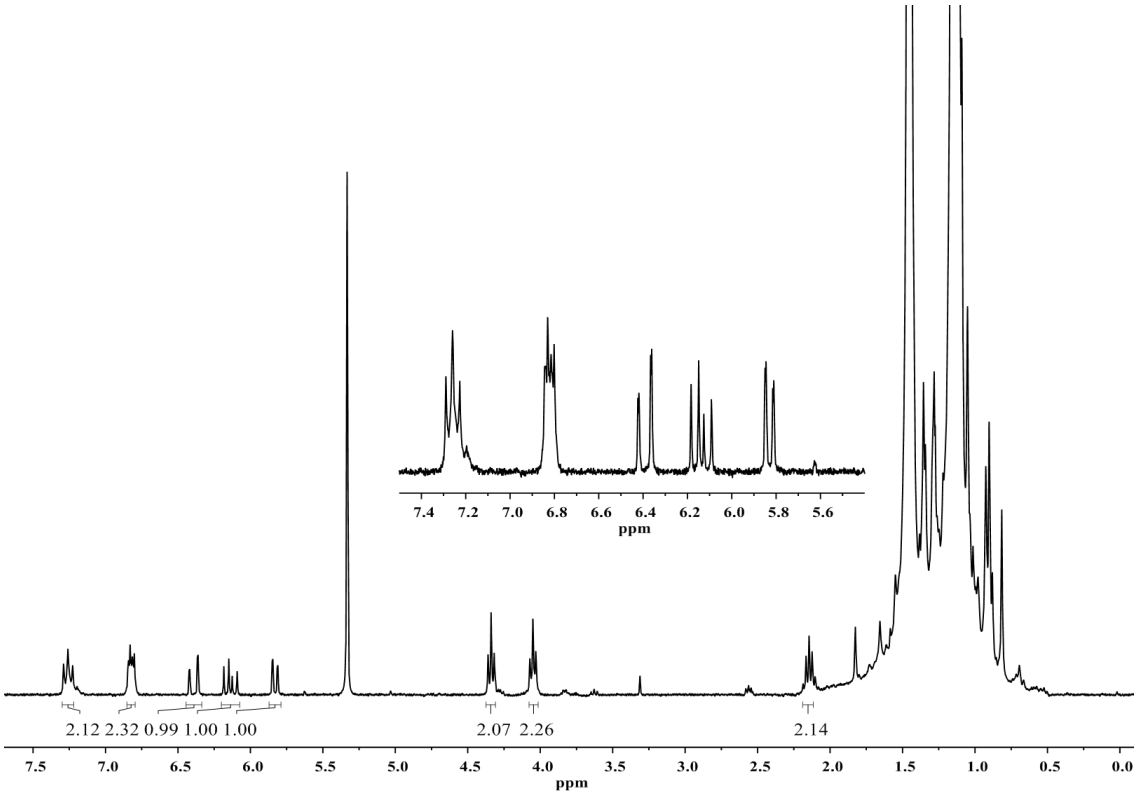

Figure A.5 ^{1}H NMR (300 MHz, DCM-d_2, 25 °C) spectrum of an acrylate-functionalized PIB macromer (12,900 Acrylate) derived from Butyl 068. This macromer was synthesized via a nucleophilic substitution reaction using potassium acrylate and the product from Table 2.1, Trial 2.

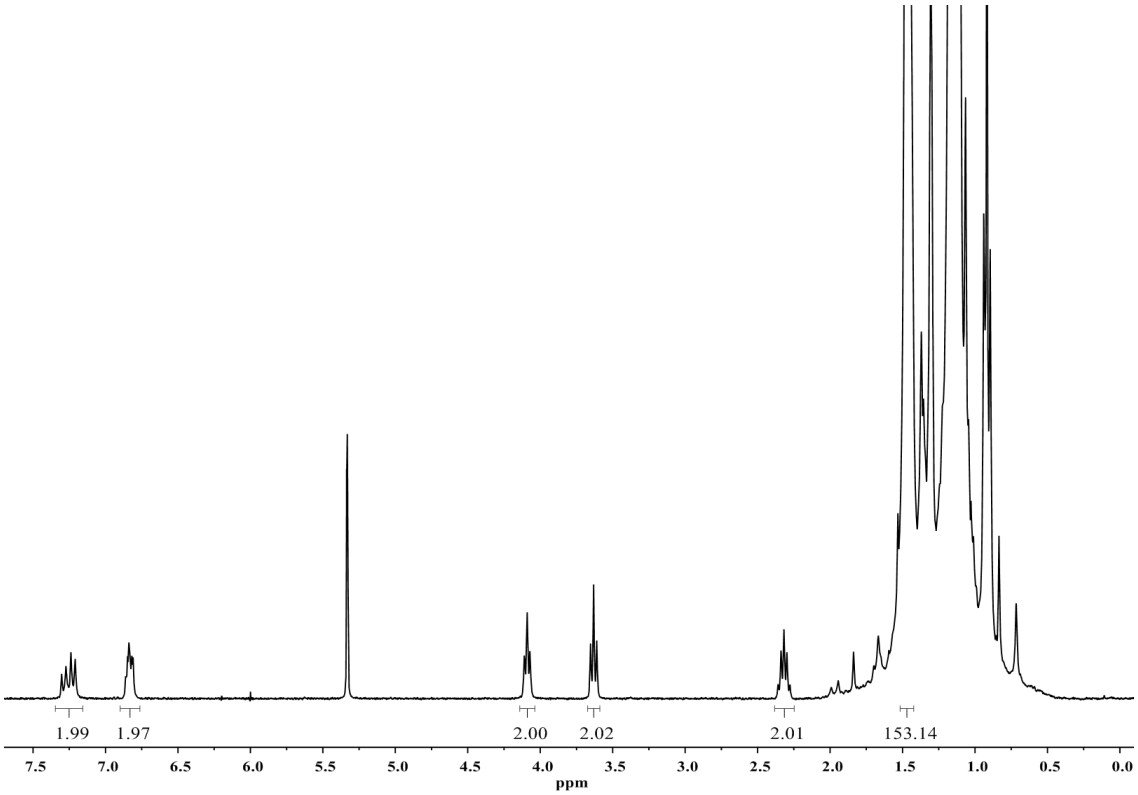

Figure A.6 ^{1}H NMR (300 MHz, DCM-d_2, 25 °C) spectrum of a (3-bromopropoxy)benzene-functionalized PIB macromer obtained from the cleavage/alkylation reaction of ExxonMobil Butyl 068, using the conditions listed in Table 2.1, Trial 3.

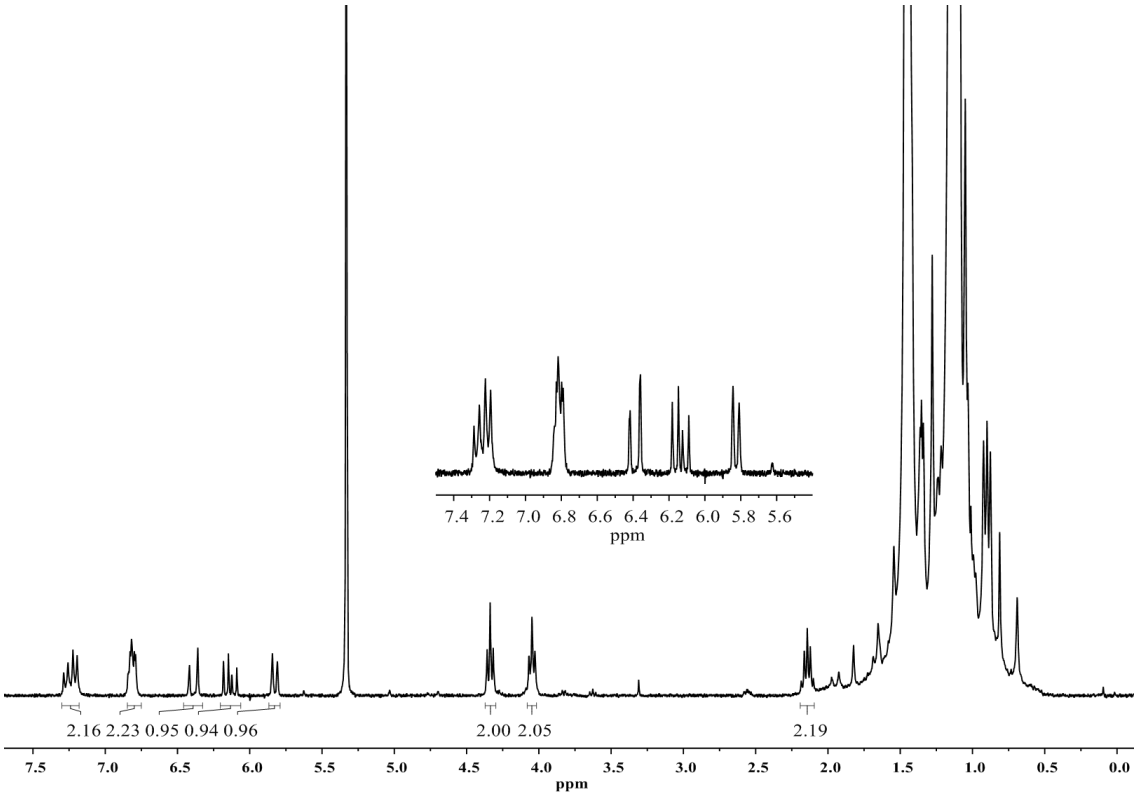

Figure A.7 ^{1}H NMR (300 MHz, DCM-d_2, 25 °C) spectrum of an acrylate functionalized-PIB macromer (28,000 Acrylate) derived from Butyl 068. This macromer was synthesized via a nucleophilic substitution reaction using potassium acrylate and the product from Table 2.1, Trial 3.

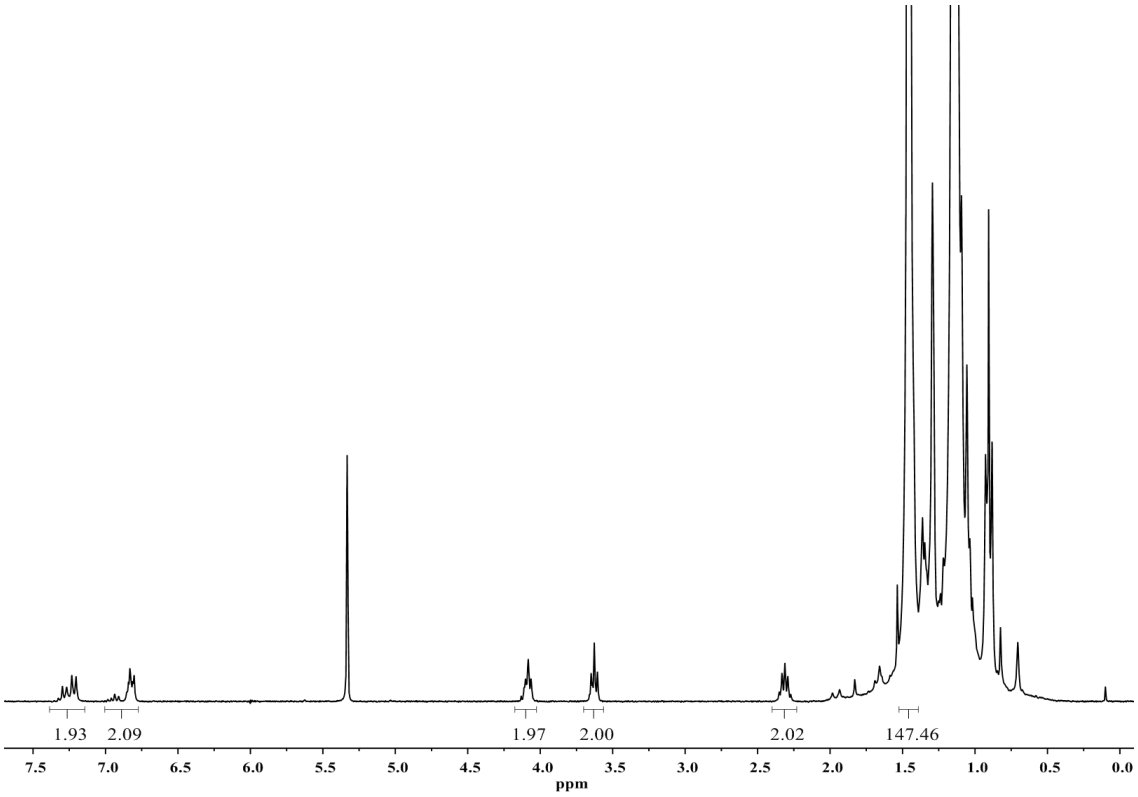

Figure A.8 ^{1}H NMR (300 MHz, DCM-d_2, 25 °C) spectrum of a (3-bromopropoxy)benzene-functionalized PIB macromer obtained from the cleavage/alkylation reaction of ExxonMobil Butyl 068, using the conditions listed in Table 2.1, Trial 4.

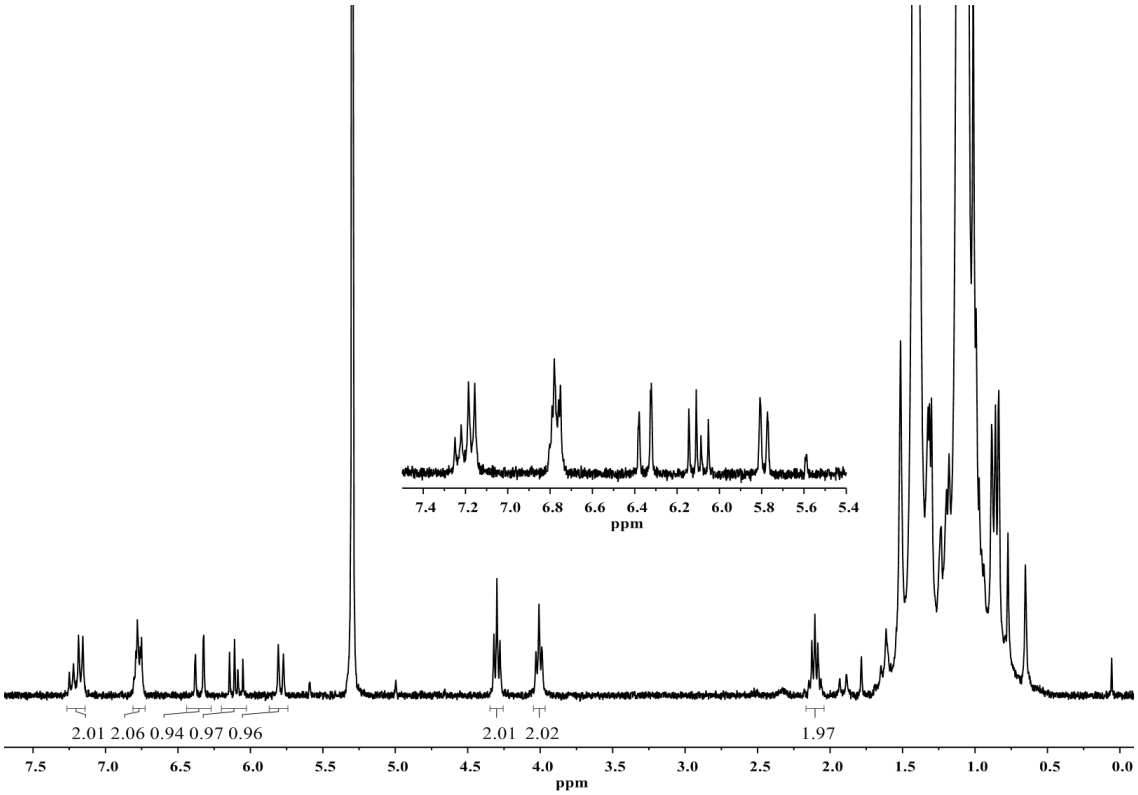

Figure A.9 ^{1}H NMR (300 MHz, DCM-d_2, 25 °C) spectrum of an acrylate-functionalized PIB macromer (39,400 Acrylate) derived from Butyl 068. This macromer was synthesized via a nucleophilic substitution reaction using potassium acrylate and the product from Table 2.1, Trial 4.

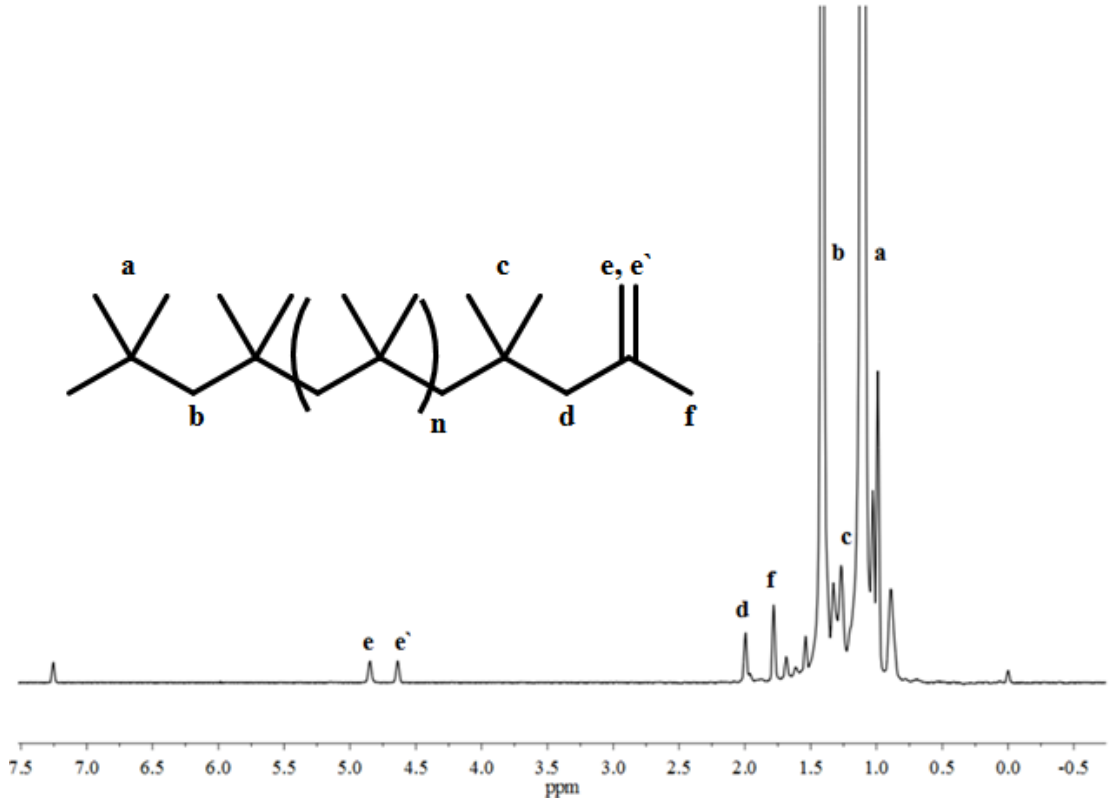

Figure A.10 ^{1}H NMR (300 MHz, $CDCl_3$, 25 °C) spectrum of monofunctional *exo*-olefin-terminated PIB (83% *exo* olefin, 17% *tert*-chloride).

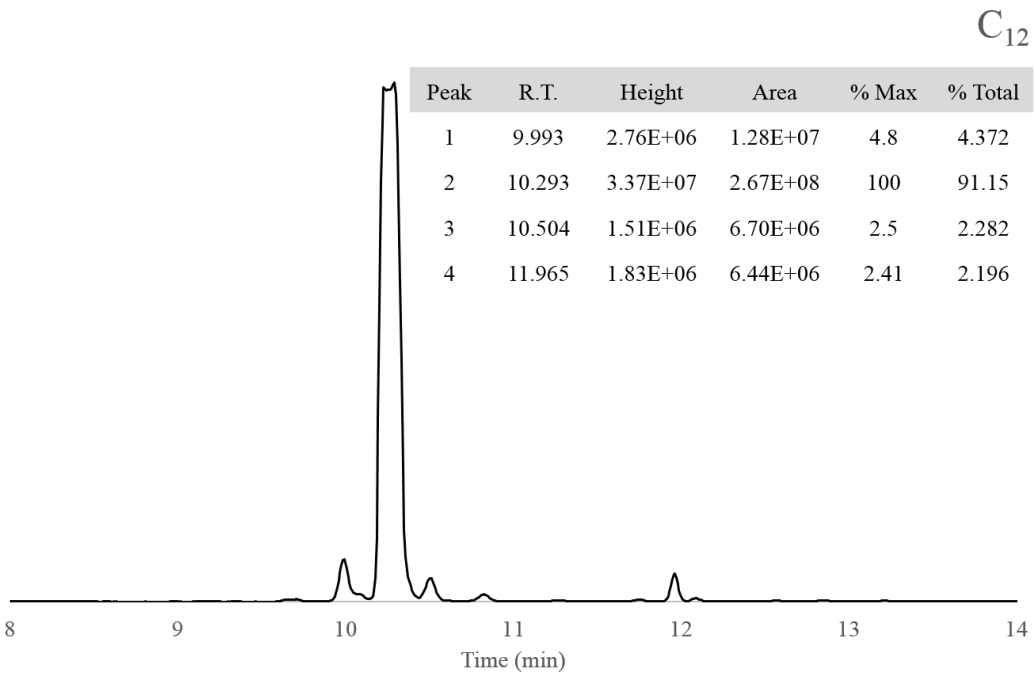

Figure A.11 High expansion of the gas chromatogram of C_{12} oligoisobutylene, injected at 180 ºC with a flow rate of 1.3 mL/min. The chromatogram is characterized by relative signal intensity (arbitrary units).

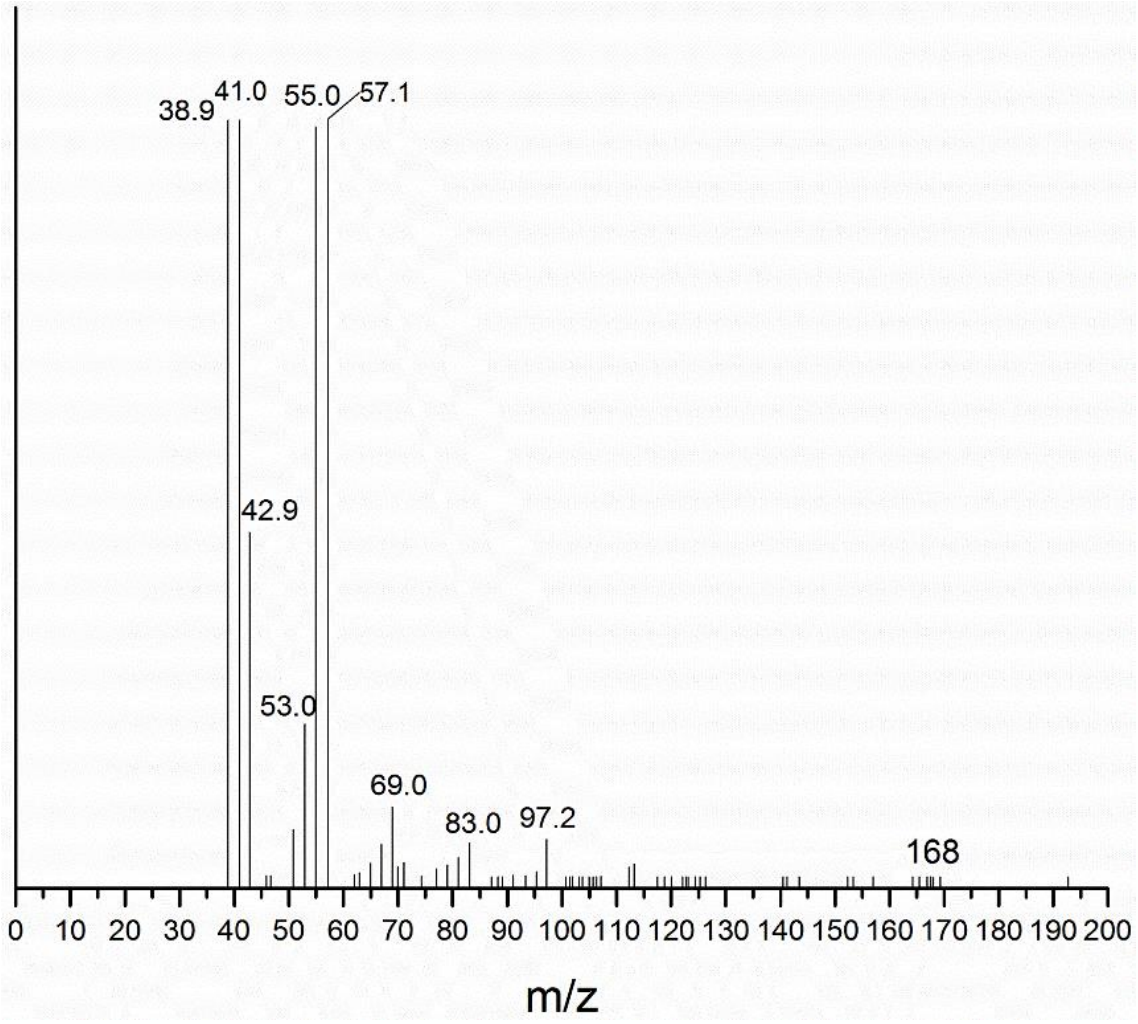

Figure A.12 Electron-impact mass chromatogram (m/z 0-200) of C_{12} oligoisobutylene, with electron ionization energy of 35.3 eV, trap current of 250 μA, and source temperature of 162 °C.

C_{16}

Peak	R.T.	Height	Area	% Max	% Total
1	13.161	1.07E+06	9.86E+06	3.06	2.387
2	13.445	1.15E+07	8.12E+07	25.21	19.66
3	13.932	3.35E+07	3.22E+08	100	77.96

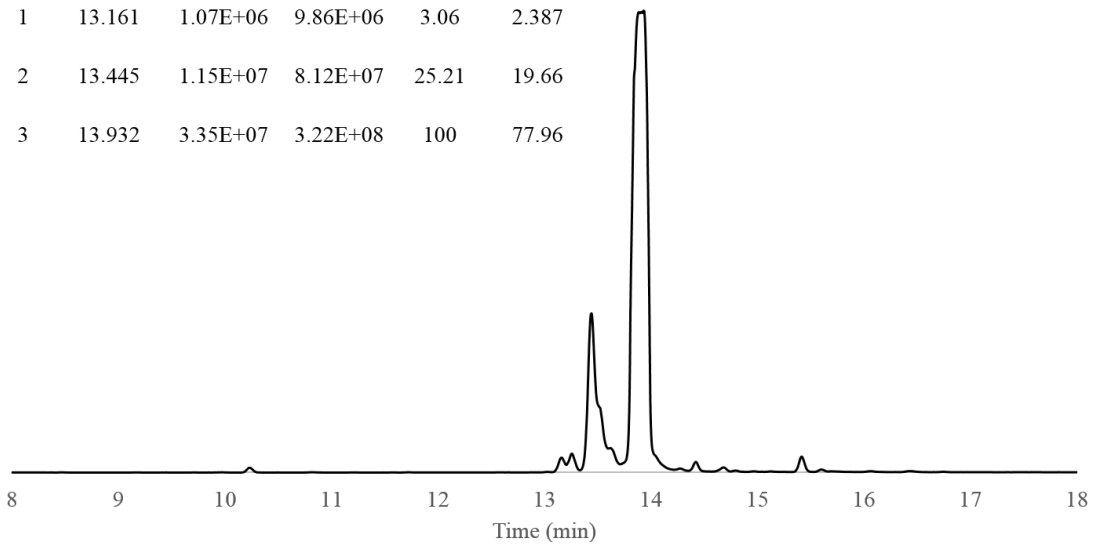

Figure A.13 High expansion of the gas chromatogram of C_{16} oligoisobutylene, injected at 180 ºC with a flow rate of 1.3 mL/min. The chromatogram is characterized by relative signal intensity (arbitrary units).

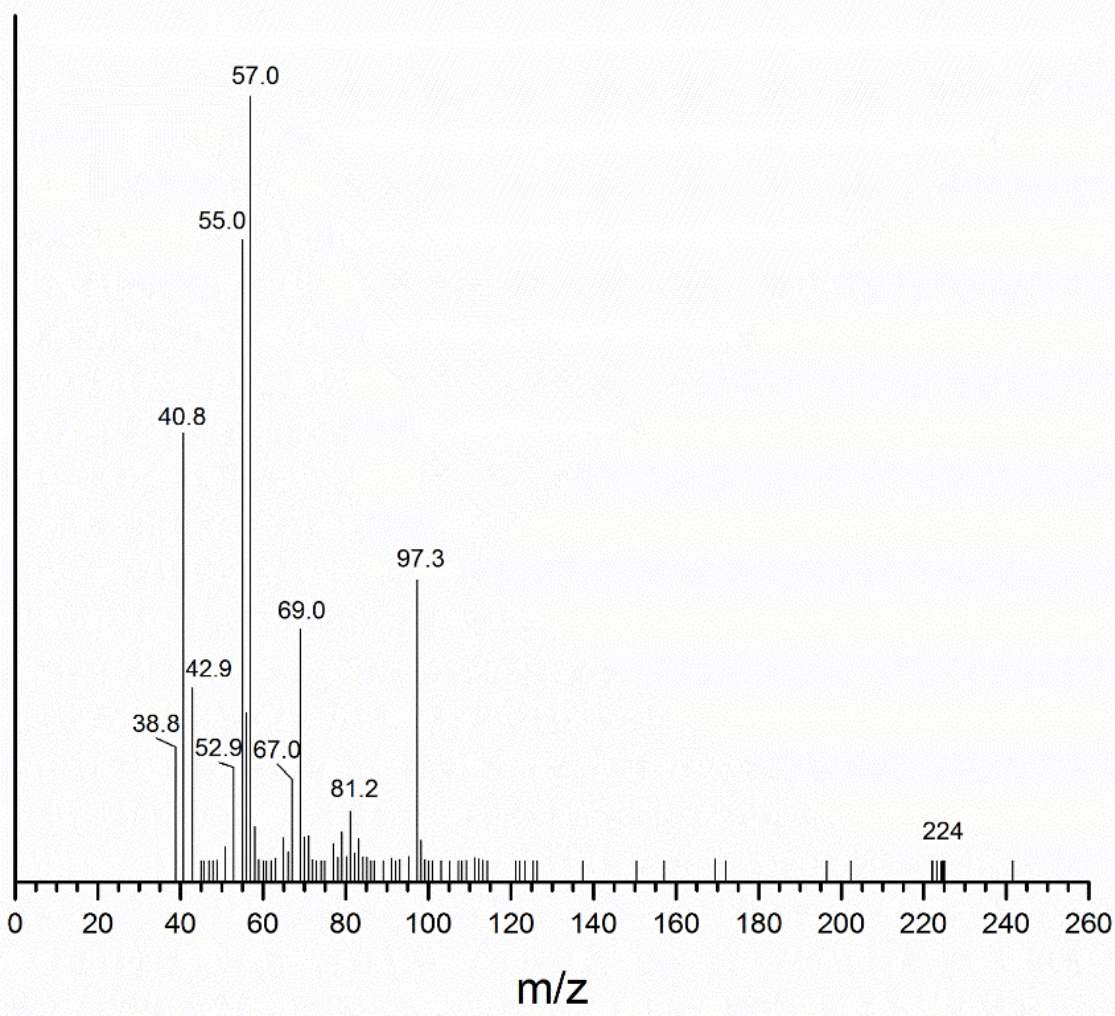

Figure A.14 Electron-impact mass chromatogram (m/z 0-260) of C_{16} oligoisobutylene, with electron ionization energy of 35.3 eV, trap current of 250 µA, and source temperature of 162 °C.

C_{20}

Peak	R.T.	Height	Area	% Max	% Total
1	10.258	3.50E+06	1.35E+07	3.43	3.209
2	16.953	2.22E+06	1.39E+07	3.54	3.306
3	17.545	3.26E+07	3.92E+08	100	93.49

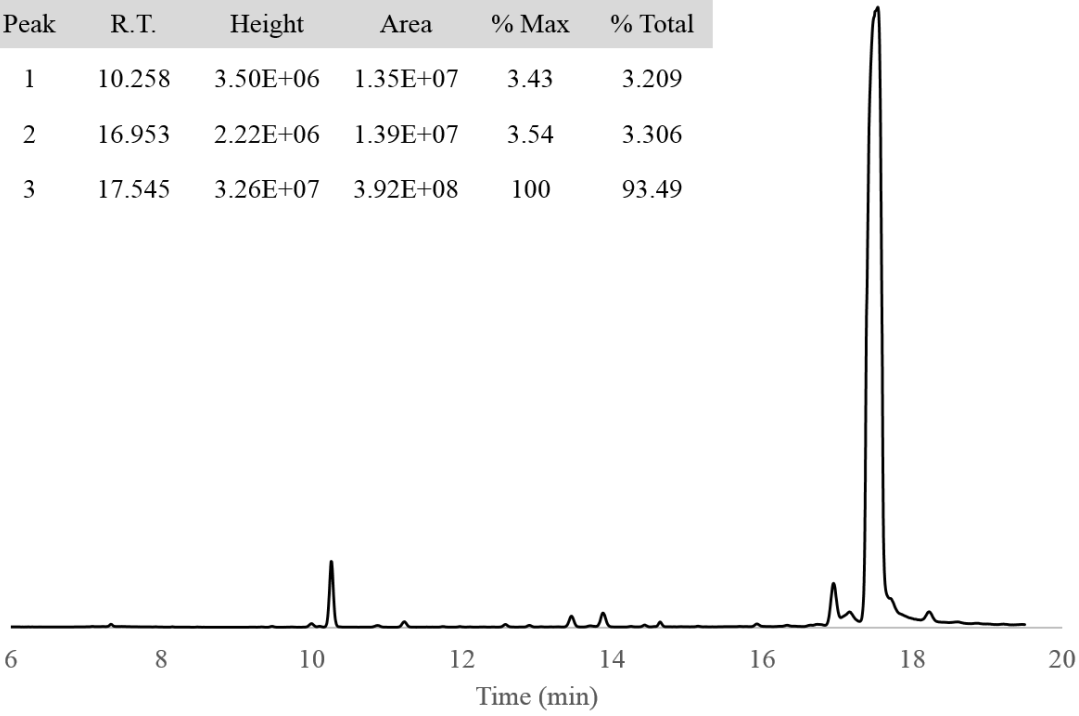

Figure A.15 High expansion of the gas chromatogram of C_{20} oligoisobutylene, injected at 180 ºC with a flow rate of 1.3 mL/min. The chromatogram is characterized by relative signal intensity (arbitrary units).

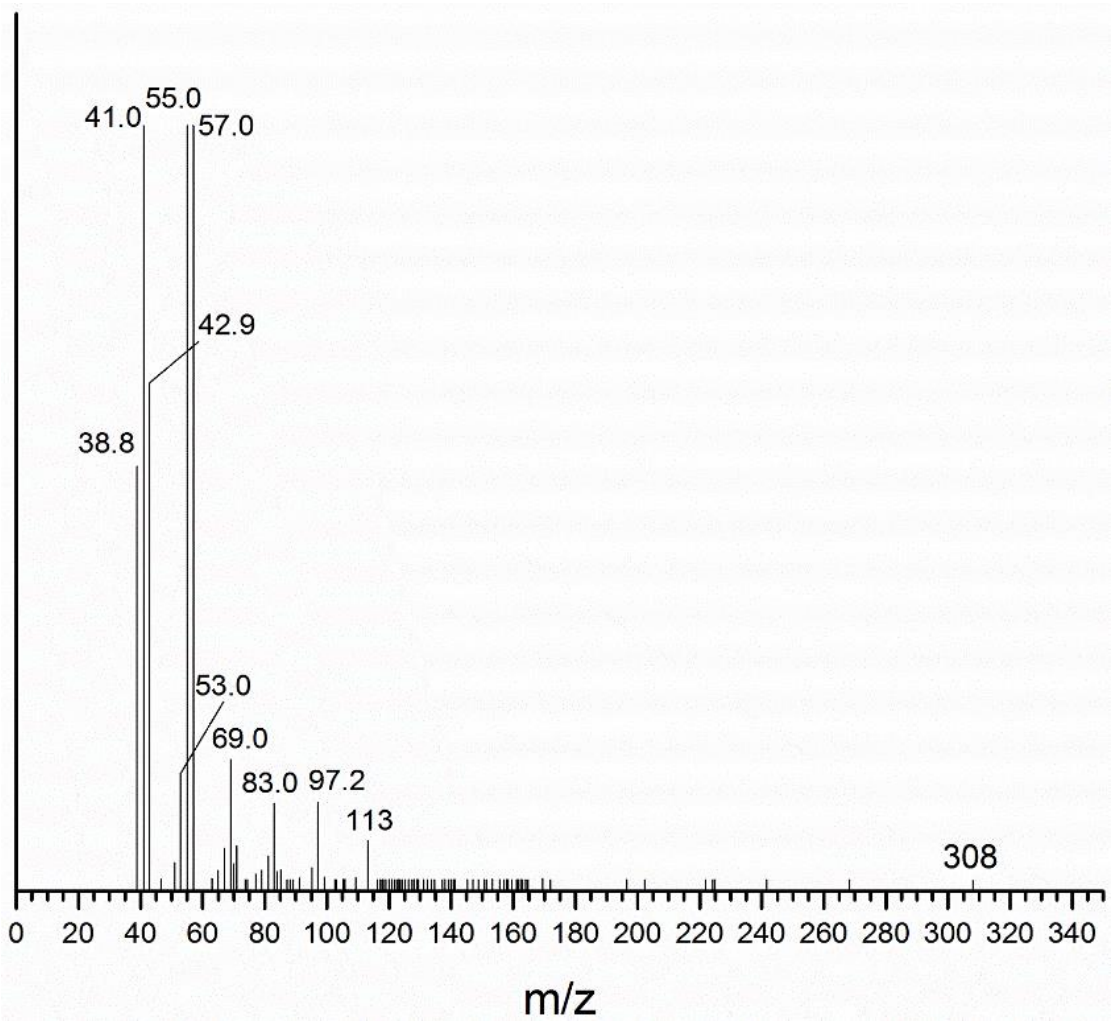

Figure A.16 Electron-impact mass chromatogram (m/z 0-260) of C_{20} oligoisobutylene, with electron ionization energy of 35.3 eV, trap current of 250 µA, and source temperature of 162 °C.

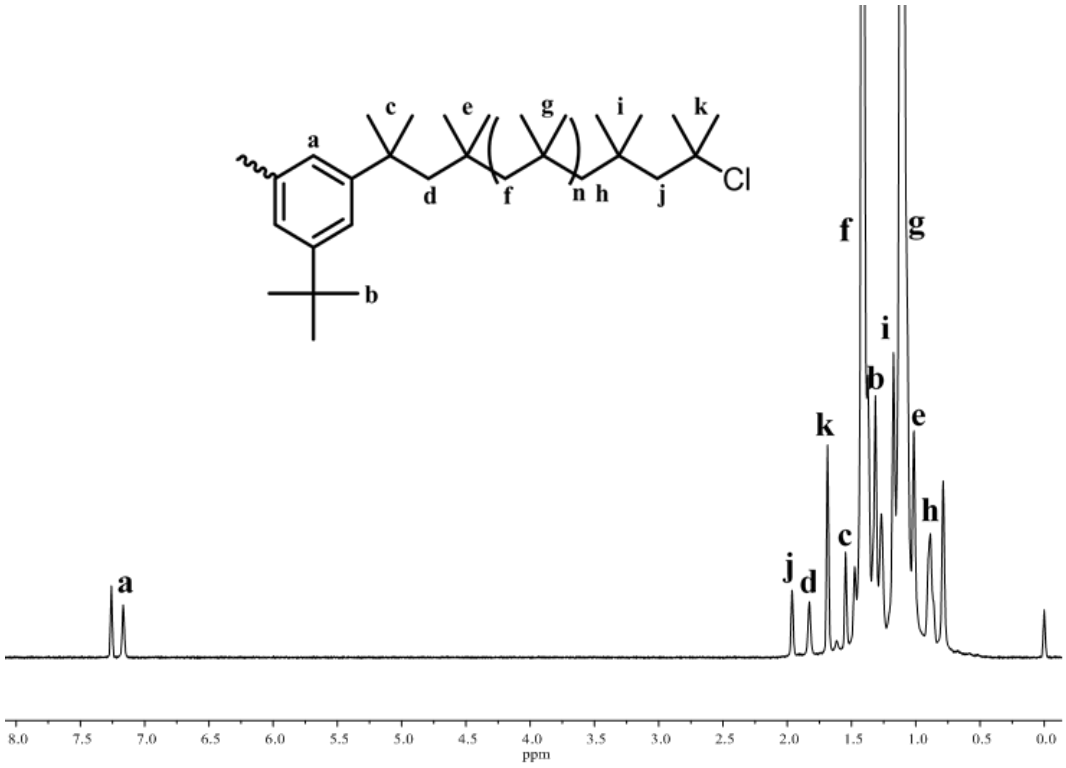

Figure A.17 ^{1}H NMR (300 MHz, $CDCl_3$, 25 °C) spectrum of *tert*-chloride PIB obtained by termination of living PIB with excess methanol (pre-quench aliquot). -70 ºC; 60/40 methyl chloride/hexane; [bDCC] = 0.020 M; [IB] = 2.0 M; [2,6 lutidine] = 0.003 M; $[TiCl_4]$ = 0.020 mol L^{-1}. (Expansion of Figure 3.1A).

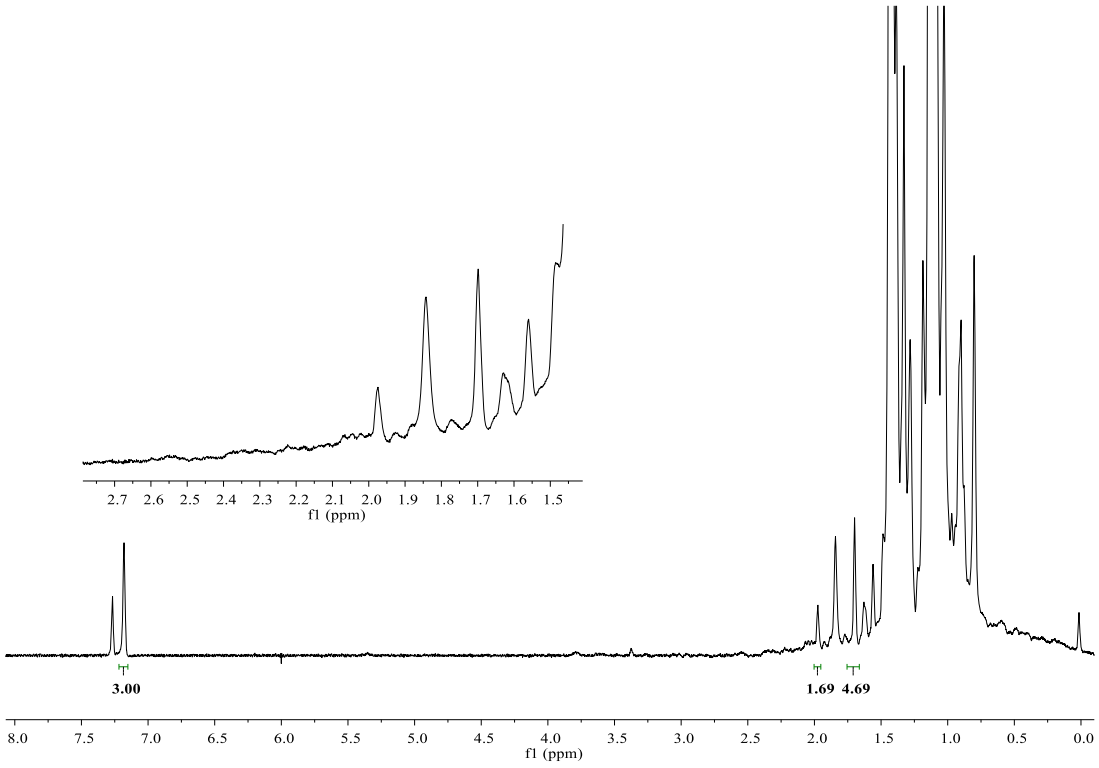

Figure A.18 ^{1}H NMR (300 MHz, $CDCl_3$, 25 °C) spectrum of PIB quenched with AN. -70 °C; 60/40 methyl chloride/hexane; [AN]/[CE] = 2.0; $[TiCl_4]_{eff}$ = 4[CE]; quenching time = 4 h. About 40% *tert*-chloride chain ends remain. (Expansion of Figure 3.1B).

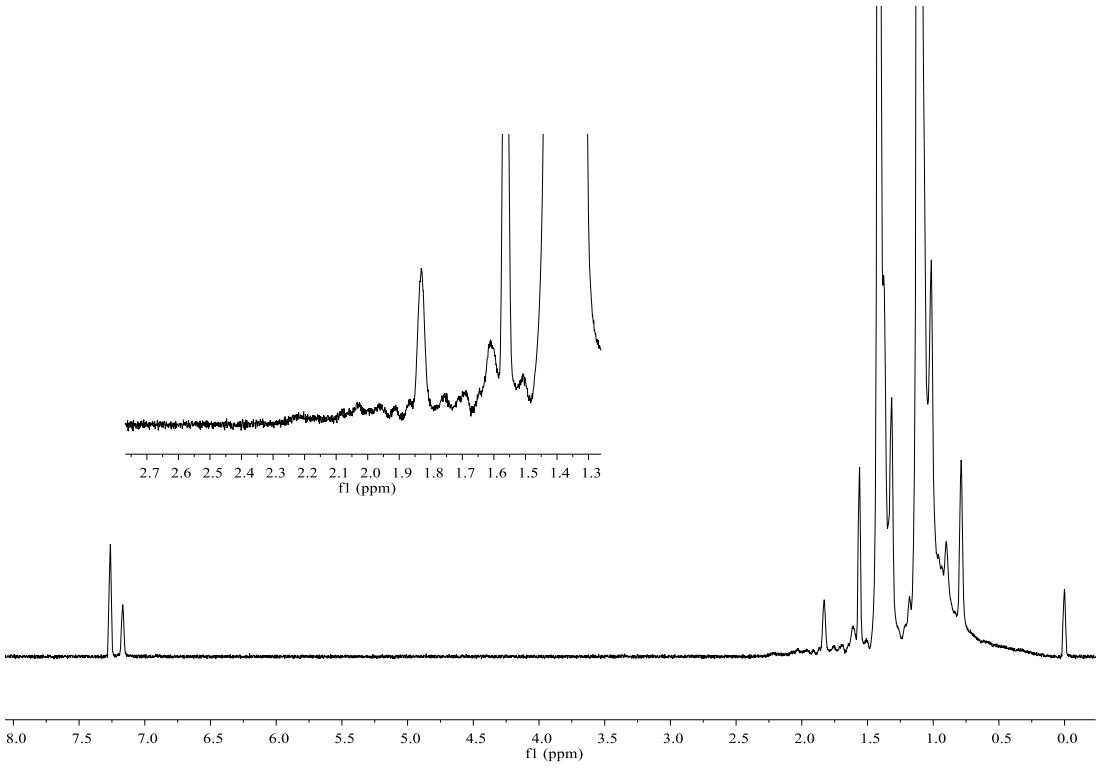

Figure A.19 ^{1}H NMR (300 MHz, $CDCl_3$, 25 °C) spectrum of PIB quenched with AN. -70 °C; 60/40 methyl chloride/hexane; [AN]/[CE] = 2.0; $[TiCl_4]_{eff}$ = 4.5[CE]; quenching time = 4 h. Chain ends have suffered extensive rearrangement. (Expansion of Figure 3.1C).

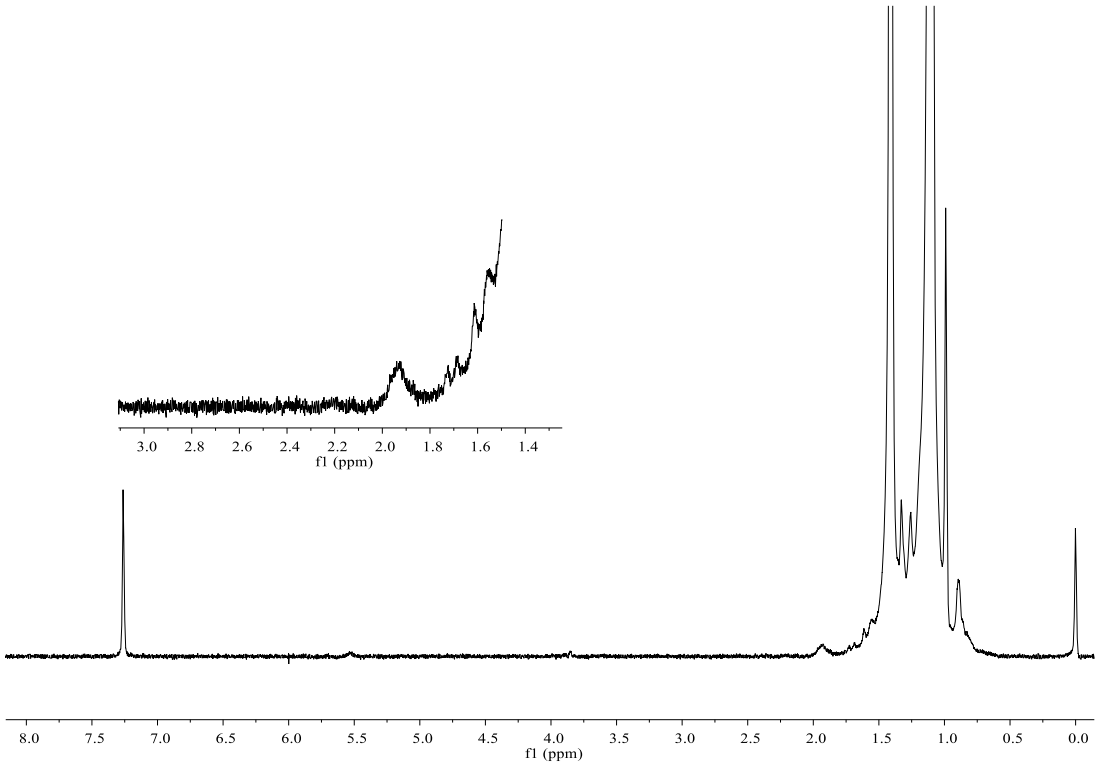

Figure A.20 MHz, $CDCl_3$, 25 °C) spectrum of the isolated product from the Ritter reaction of monofunctional *exo*-olefin PIB with AN in hexane. 25 °C; [CE] = 0.0322 M; [AN] = 0.694 M; [H] = 0.836 M; reaction time = 12 h.

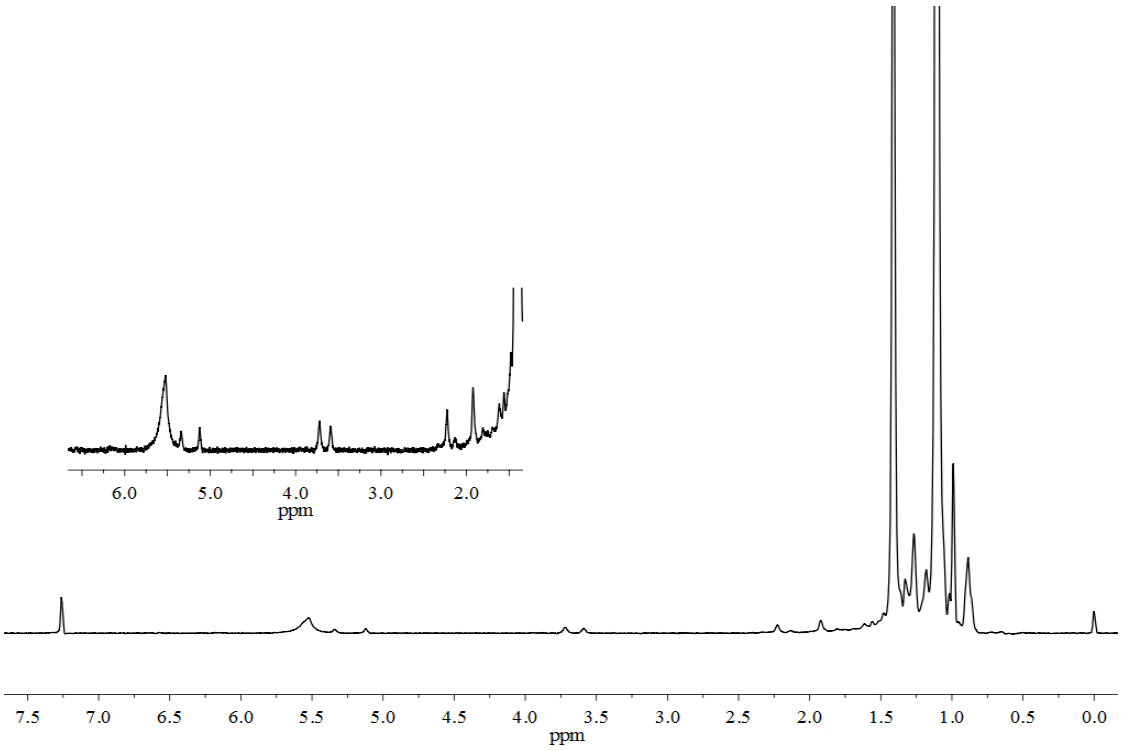

Figure A.21 ^{1}H NMR (300 MHz, $CDCl_3$, 25 °C) spectrum of the isolated product from the Ritter reaction of monofunctional *exo*-olefin PIB with AN in toluene. 25 °C; [CE] = 0.0322 M; [AN] = 0.694 M; [H] = 0.836 M; reaction time = 12 h.

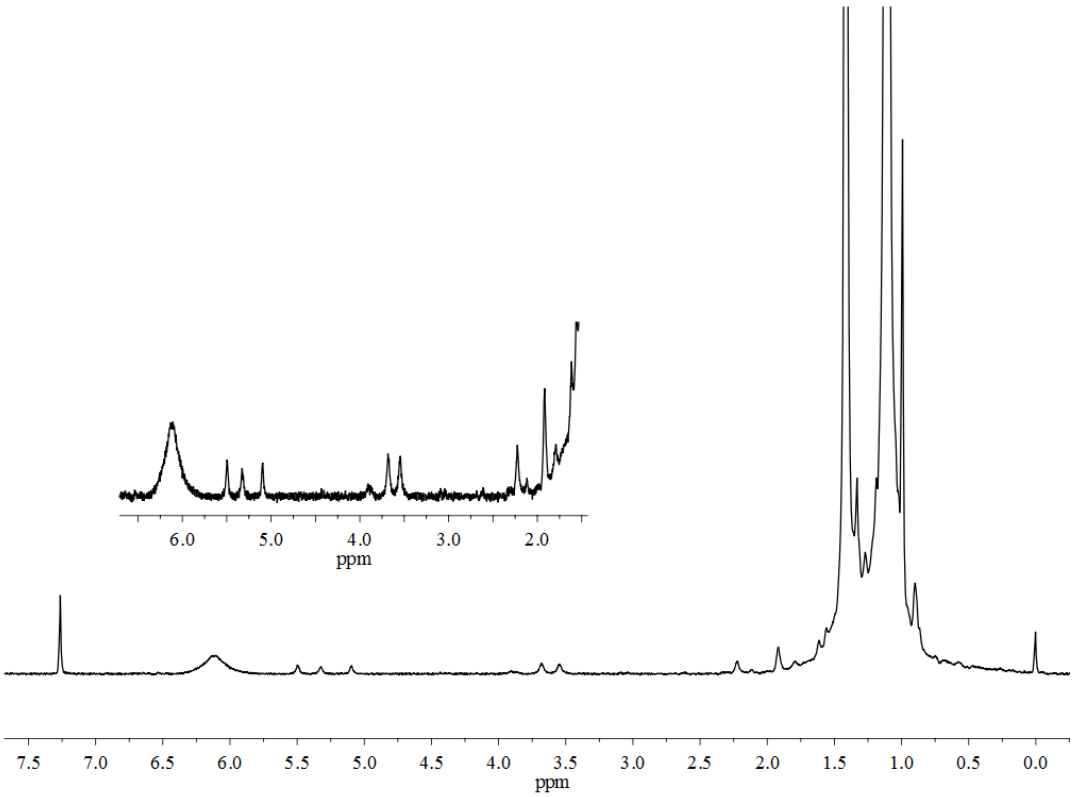

Figure A.22 ^{1}H NMR (300 MHz, $CDCl_3$, 25 °C) spectrum of the isolated product from the Ritter reaction of monofunctional *exo*-olefin PIB with AN in chloroform. 25 °C; [CE] = 0.0322 M; [AN] = 0.694 M; [H] = 0.836 M; reaction time = 12 h.

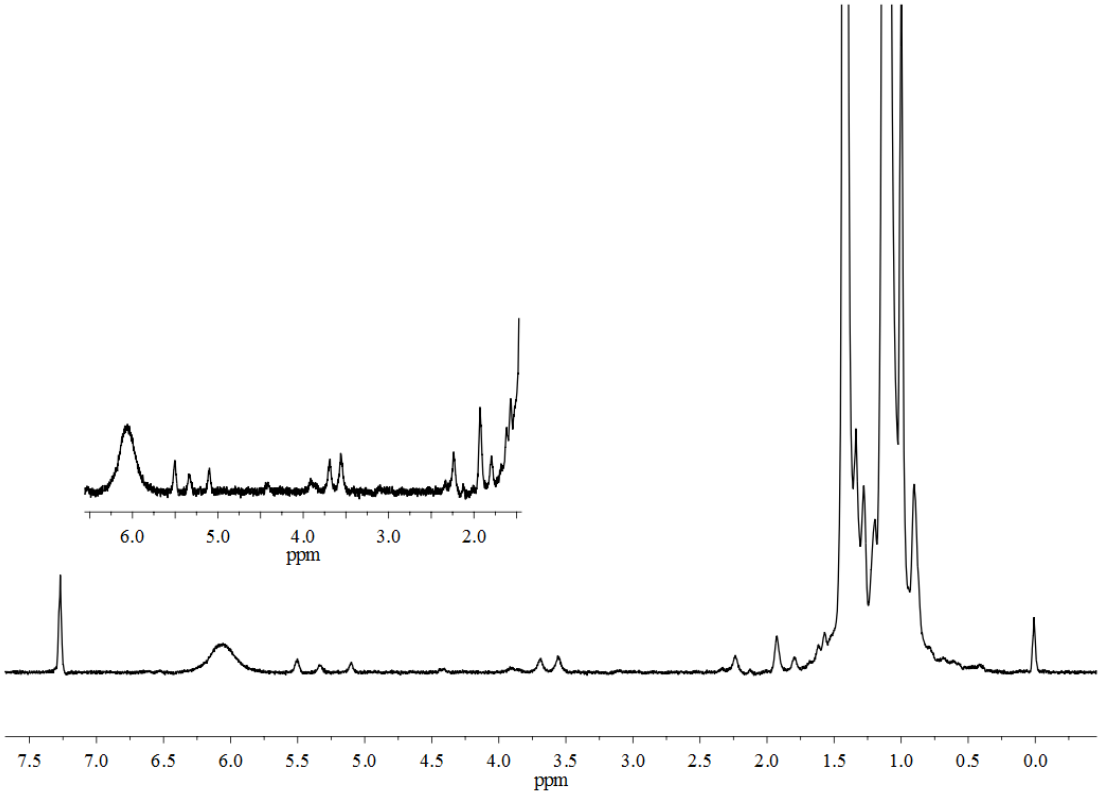

Figure A.23 ^{1}H NMR (300 MHz, $CDCl_3$, 25 °C) spectrum of the isolated product from the Ritter reaction of monofunctional *exo*-olefin PIB with AN in DCM. 25 °C; [CE] = 0.0322 M; [AN] = 0.694 M; [H] = 0.836 M; reaction time = 12 h.

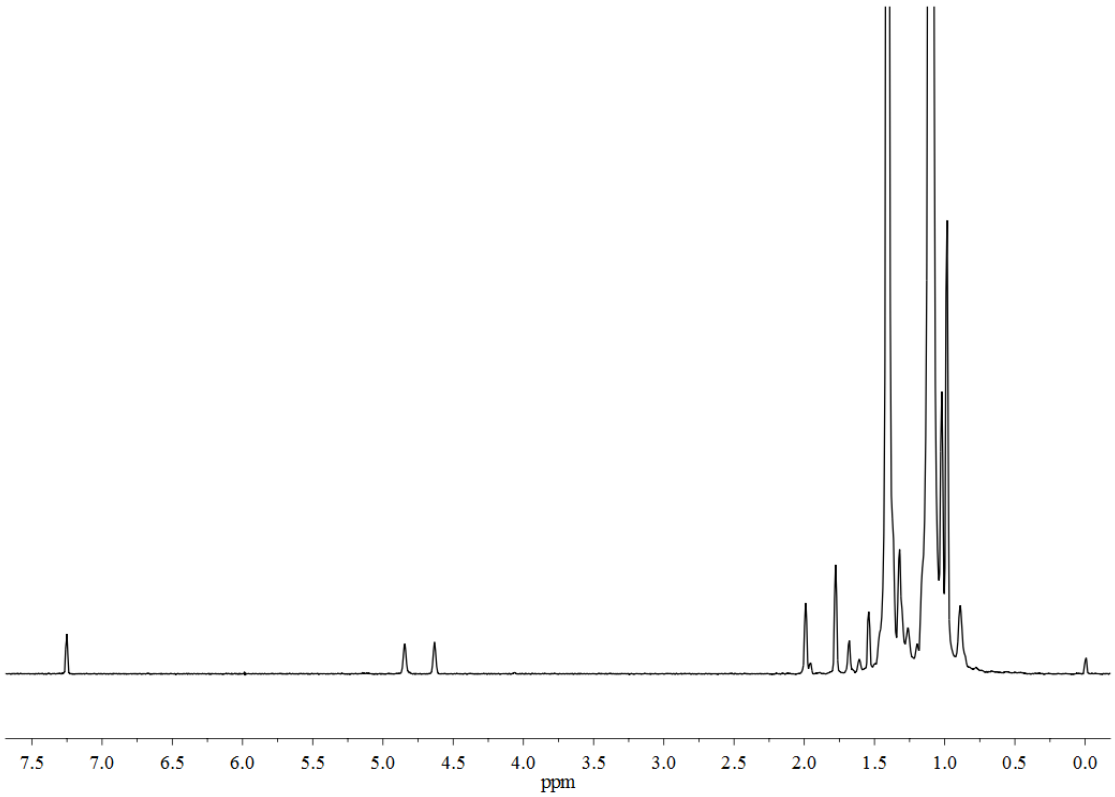

Figure A.24 ^{1}H NMR (300 MHz, $CDCl_3$, 25 °C) spectrum of the isolated product from the Ritter reaction of monofunctional *exo*-olefin PIB with AN in THF. 25 °C; [CE] = 0.0322 M; [AN] = 0.694 M; [H] = 0.836 M; reaction time = 12 h.

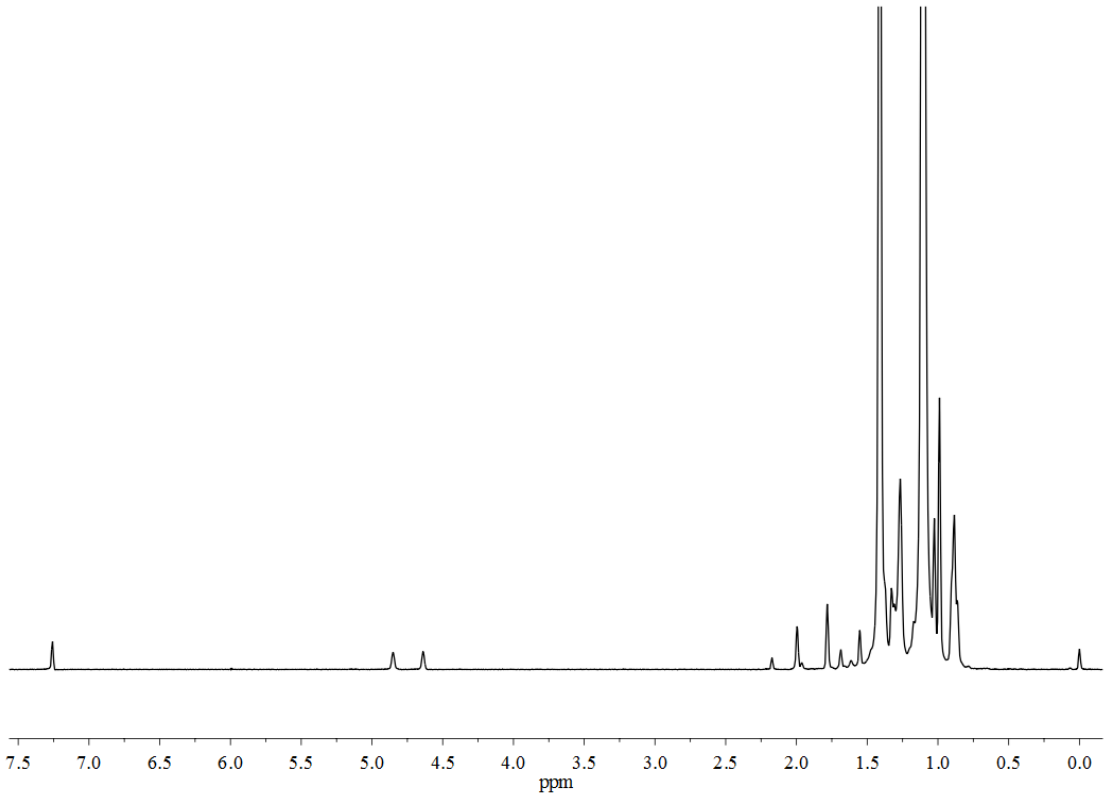

Figure A.25 ^{1}H NMR (300 MHz, $CDCl_3$, 25 °C) spectrum of the isolated product from the Ritter reaction of monofunctional *exo*-olefin PIB with AN in glyme. 25 °C; [CE] = 0.0322 M; [AN] = 0.694 M; [H] = 0.836 M; reaction time = 12 h.

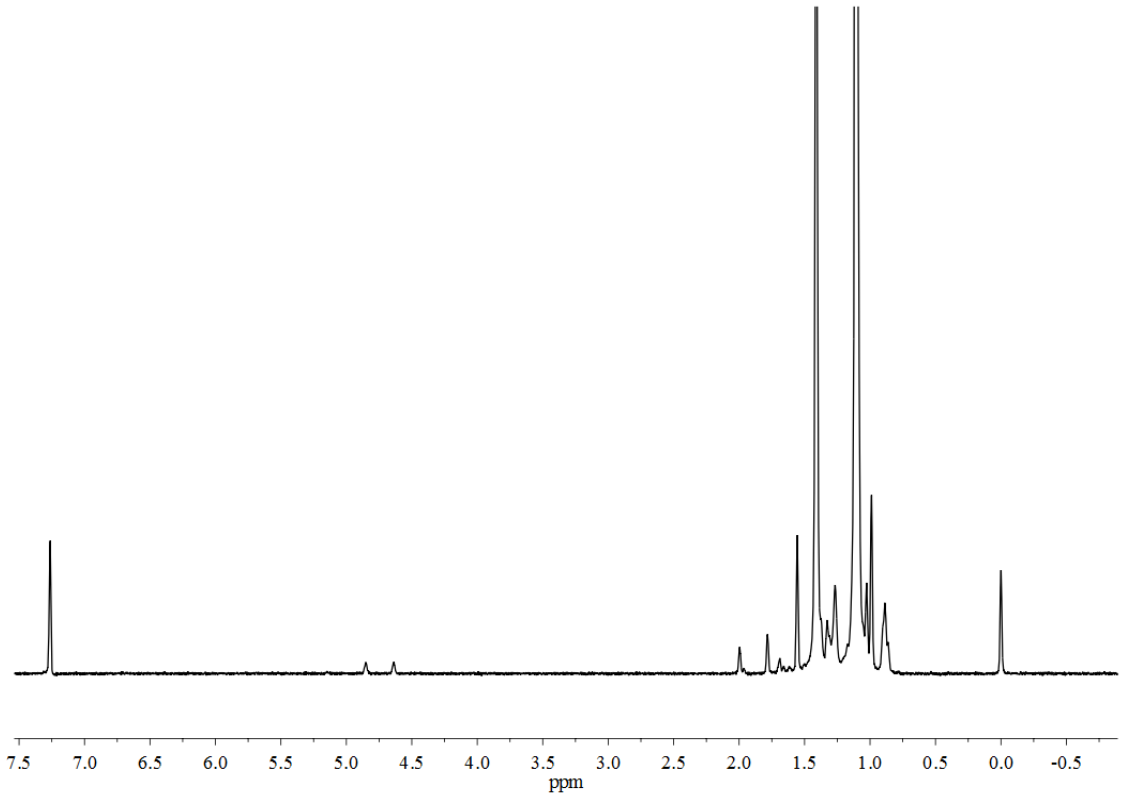

Figure A.26 ^{1}H NMR (300 MHz, $CDCl_3$, 25 °C) spectrum of the isolated product from the Ritter reaction of monofunctional *exo*-olefin PIB with AN in MIBK. 25 °C; [CE] = 0.0322 M; [AN] = 0.694 M; [H] = 0.836 M; reaction time = 12 h.

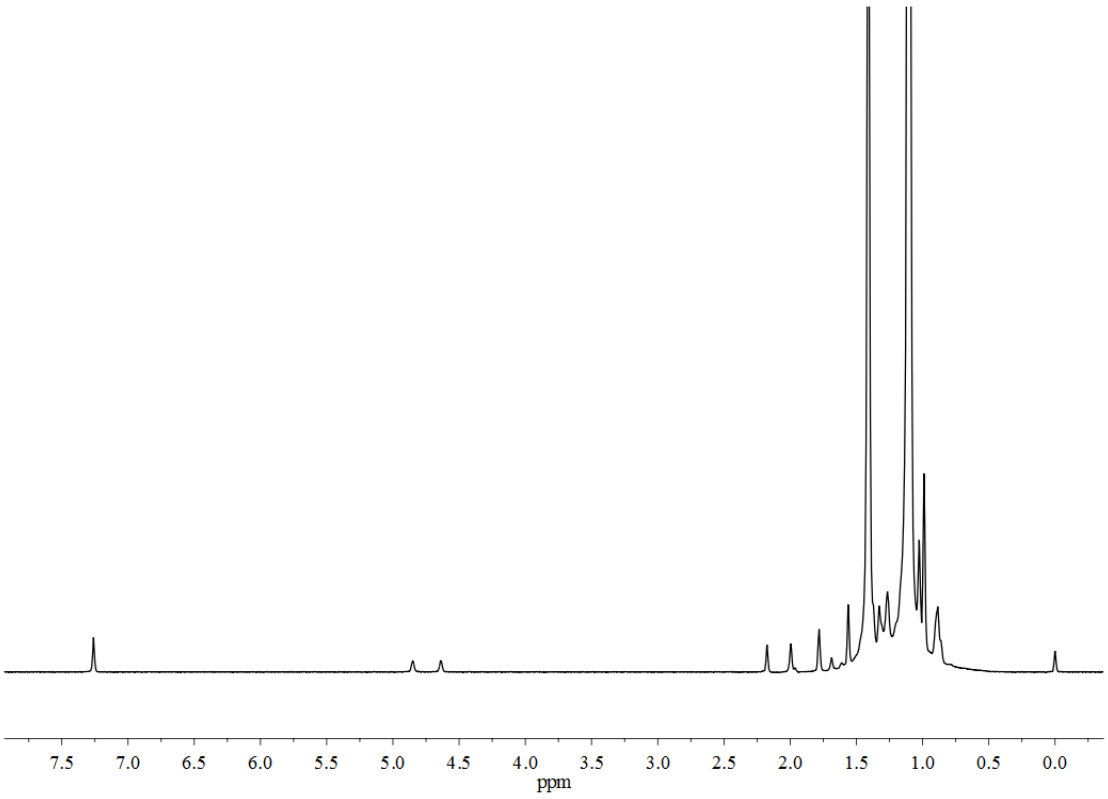

Figure A.27 ^{1}H NMR (300 MHz, $CDCl_3$, 25 °C) spectrum of the isolated product from the Ritter reaction of monofunctional *exo*-olefin PIB with AN in cyclohexanone. 25 °C; [CE] = 0.0322 M; [AN] = 0.694 M; [H] = 0.836 M; reaction time = 12 h.

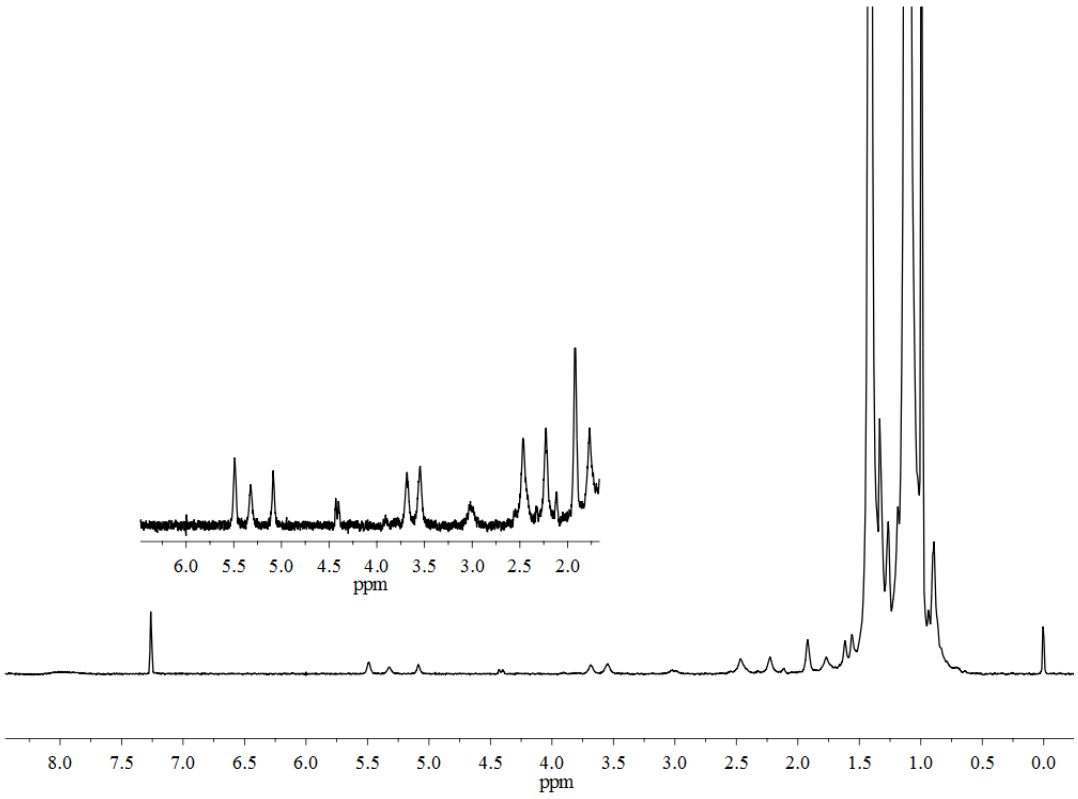

Figure A.28 ^{1}H NMR (300 MHz, $CDCl_3$, 25 °C) spectrum of the isolated product from the Ritter reaction of monofunctional *exo*-olefin PIB with acetonitrile in DCM. 25 °C; [CE] = 0.0325 M; [AceN] = 0.703 M; [H] = 0.844 M; reaction time = 12 h.

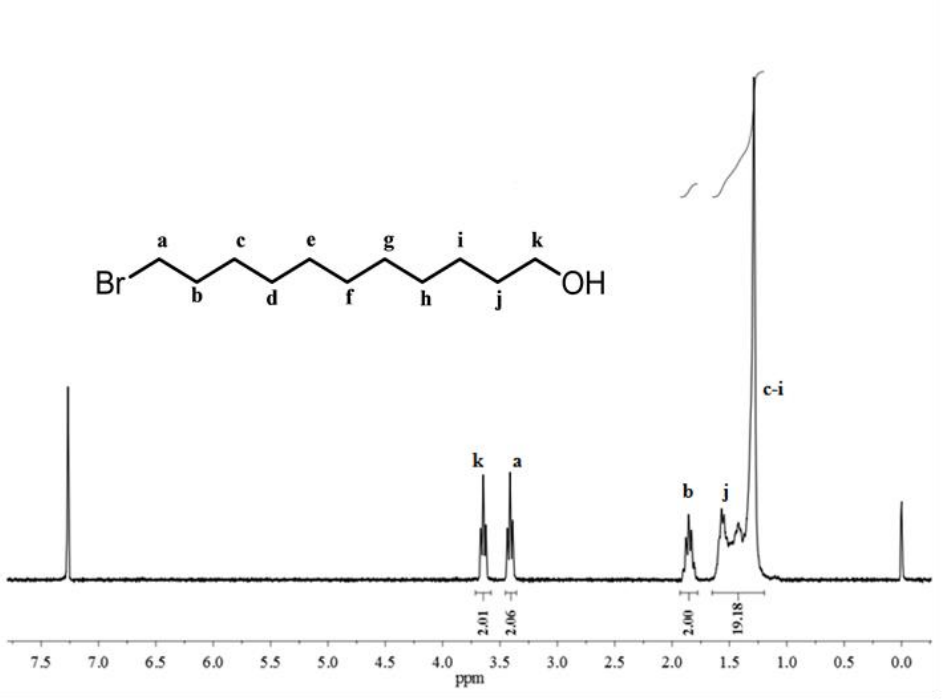

Figure A.29 ^{1}H NMR (300 MHz, $CDCl_3$, 25 °C) spectrum of 11-bromoundecan-1-ol.

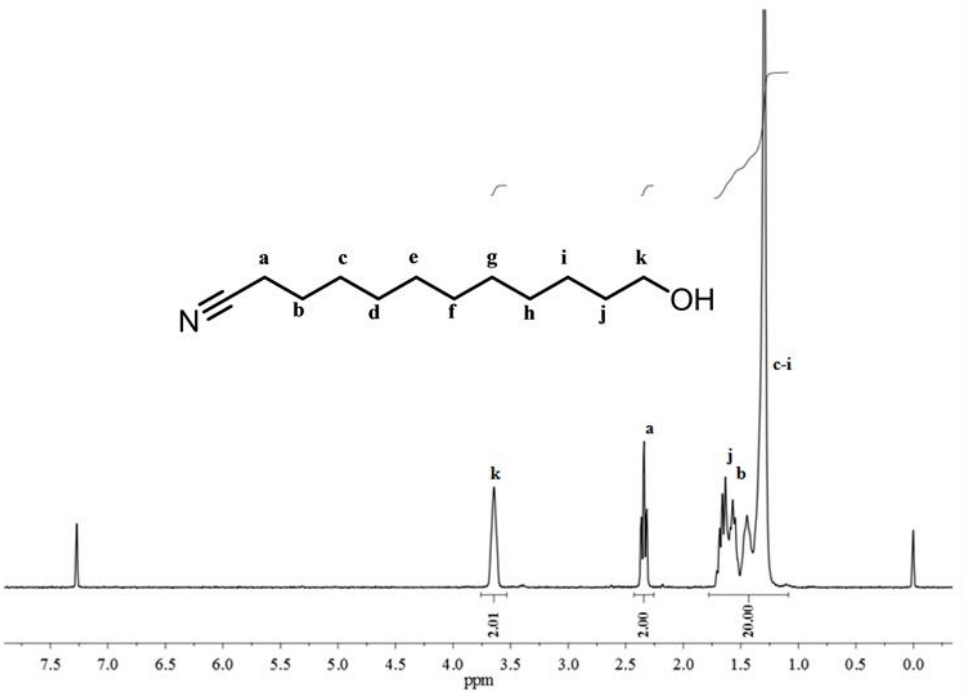

Figure A.30 ^{1}H NMR (300 MHz, $CDCl_3$, 25 °C) spectrum of 11-cyanoundecan-1-ol.

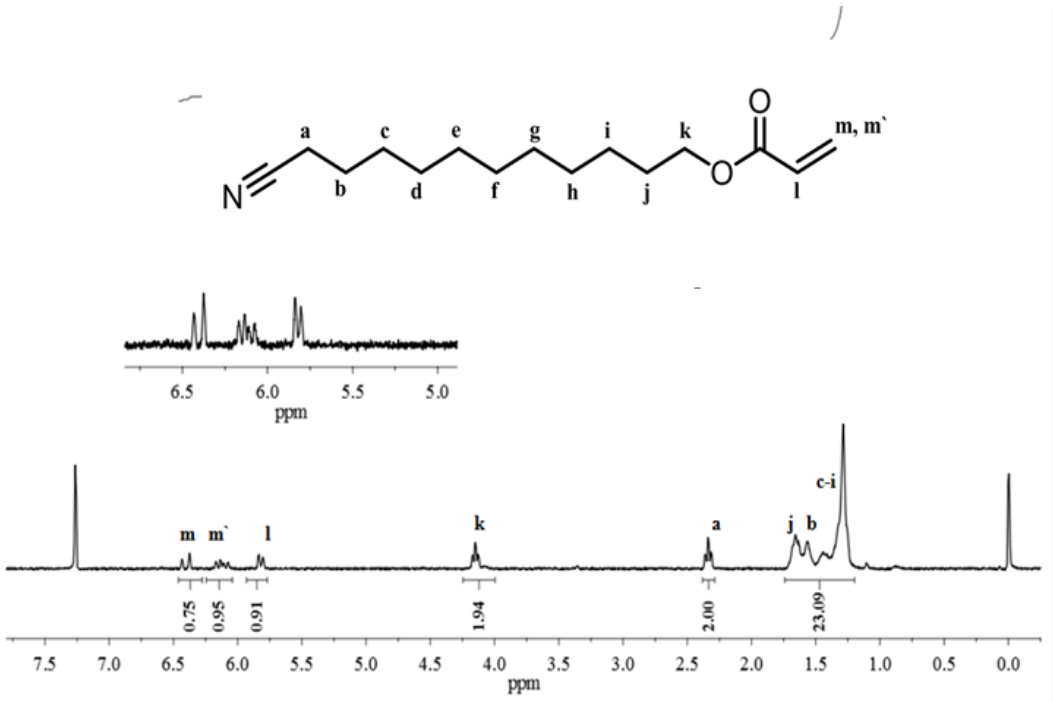

Figure A.31 ^{1}H NMR (300 MHz, $CDCl_3$, 25 °C) spectrum of 11-cyanoundecane acrylate (CUA).

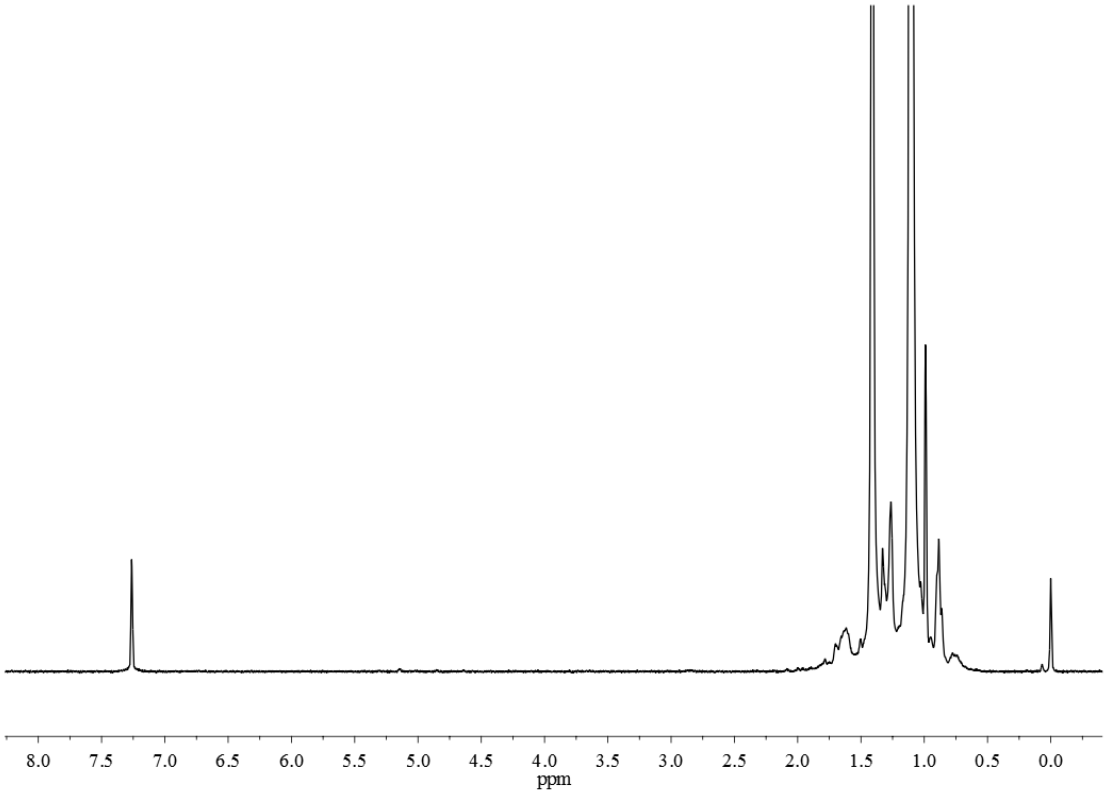

Figure A.32 ^{1}H NMR (300 MHz, $CDCl_3$, 25 °C) spectrum of the isolated product from the Ritter reaction of monofunctional *exo*-olefin PIB with CUA, using H_2SO_4 in DCM. 25 °C; [CE] = 0.0322 M; [CUA] = 0.154 M; reaction time = 12 h.

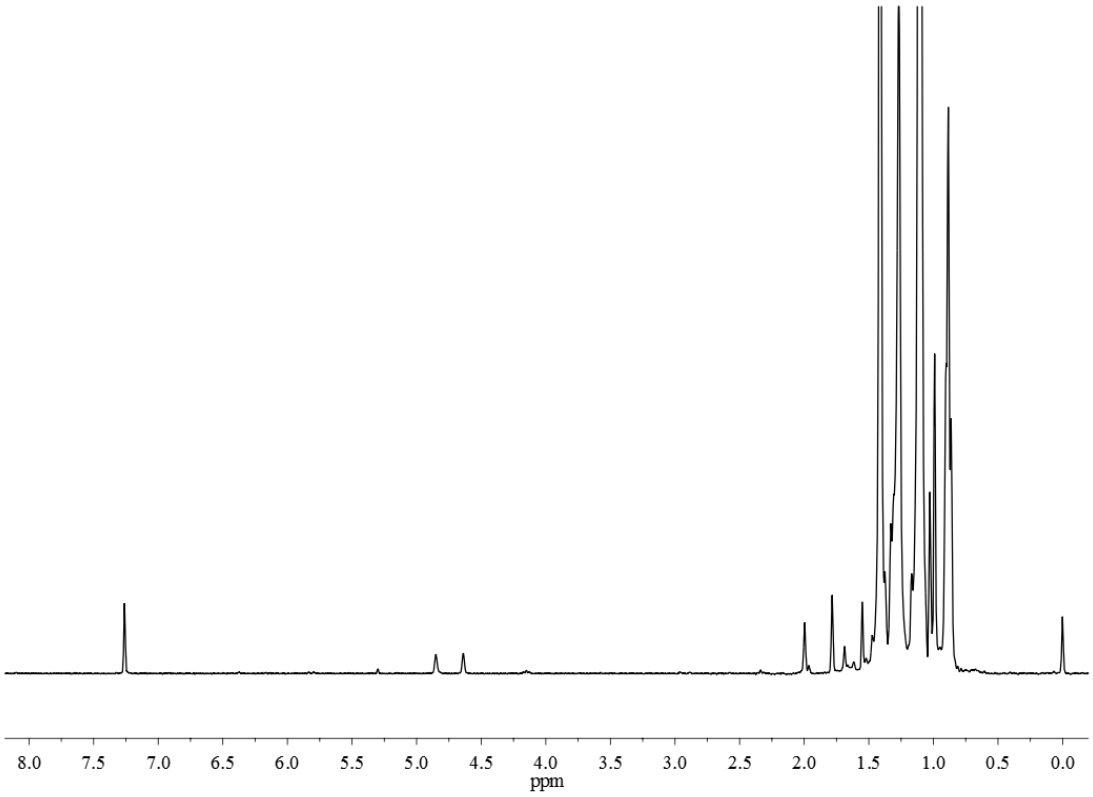

Figure A.33 ^{1}H NMR (300 MHz, $CDCl_3$, 25 °C) spectrum of the isolated product from the Ritter reaction of monofunctional *exo*-olefin PIB with CUA, using AcOH in DCM. 25 °C; [CE] = 0.0322 M; [CUA] = 0.154 M; reaction time = 12 h.

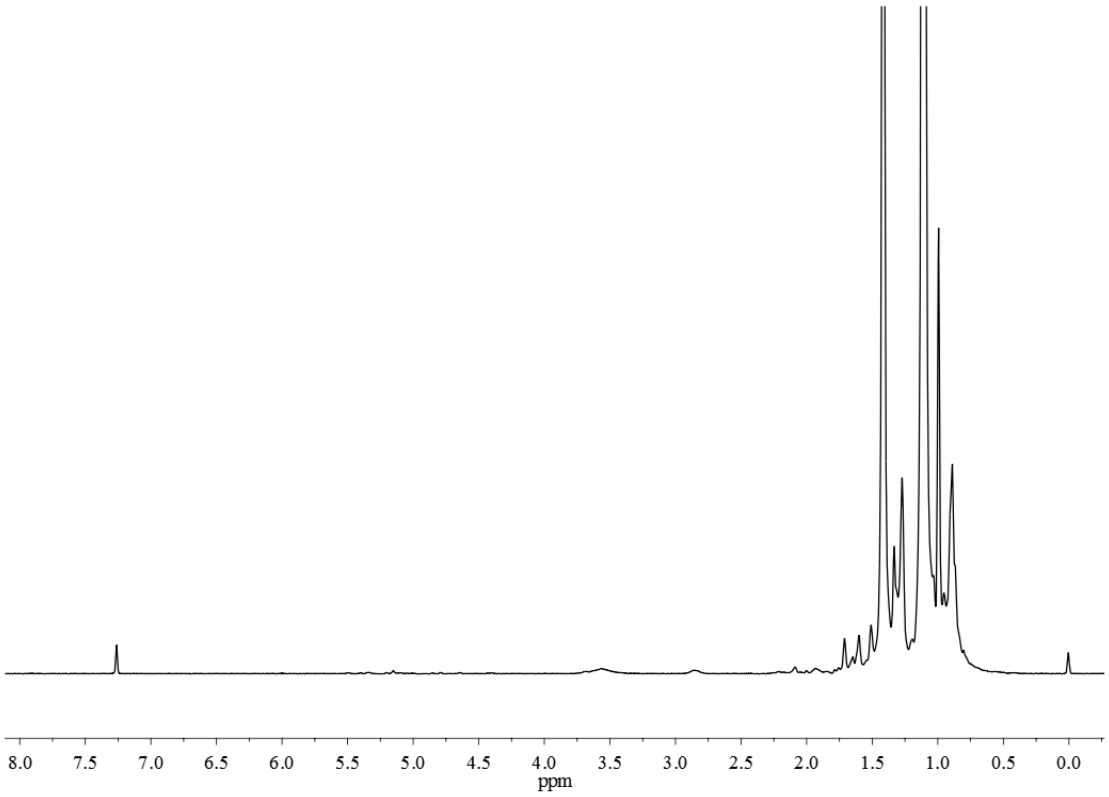

Figure A.34 ^{1}H NMR (300 MHz, $CDCl_3$, 25 °C) spectrum of the isolated product from the Ritter reaction of monofunctional *exo*-olefin PIB with CUA, using a 75:25 (v/v) mixture of AcOH:H_2SO_4 in DCM. 25 °C; [CE] = 0.0322 M; [CUA] = 0.154 M; reaction time = 12 h.

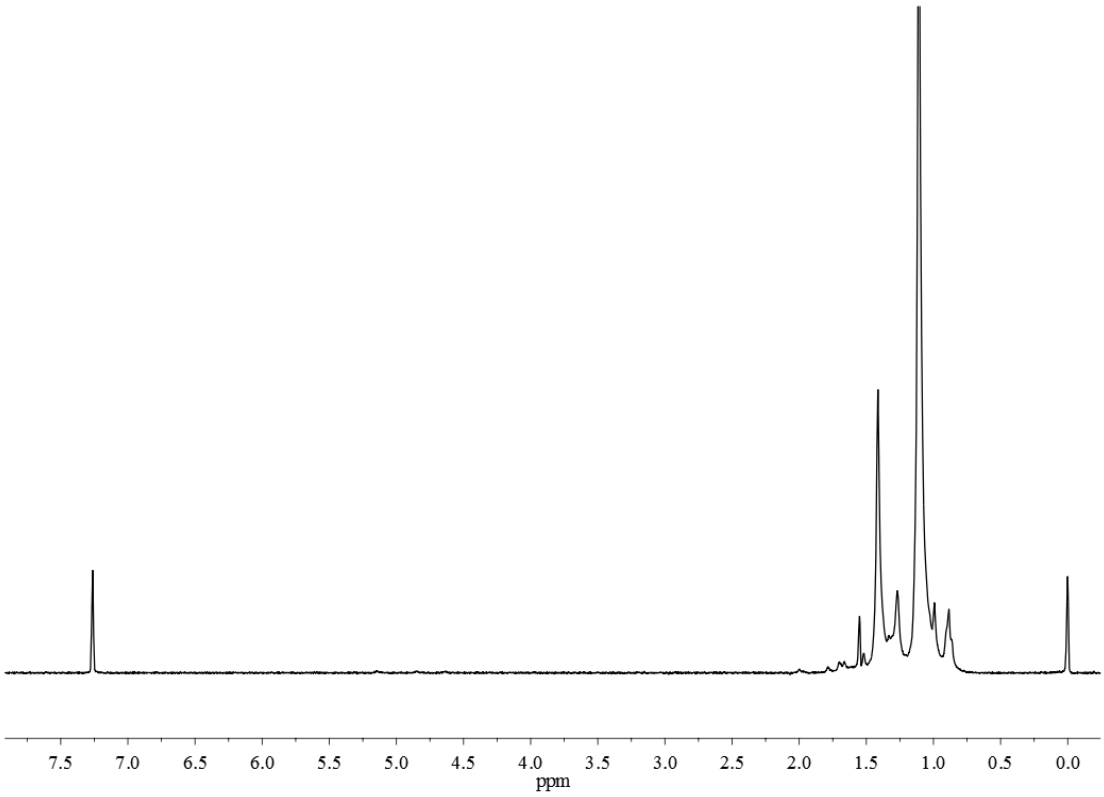

Figure A.35 ^{1}H NMR (300 MHz, $CDCl_3$, 25 °C) spectrum of the isolated product from the Ritter reaction of monofunctional *exo*-olefin PIB with CUA, using a 90:10 (v/v) ratio of AcOH:H_2SO_4 in DCM. 25 °C; [CE] = 0.0322 M; [CUA] = 0.154 M; reaction time = 12 h.

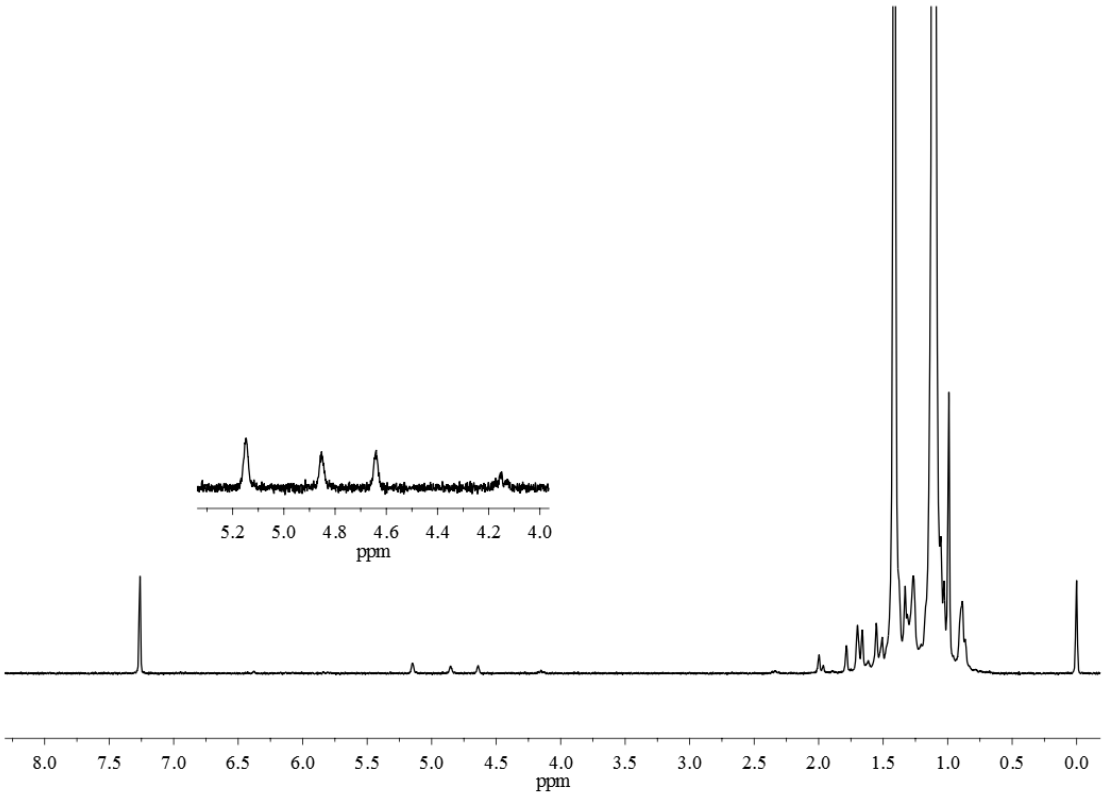

Figure A.36 ^{1}H NMR (300 MHz, $CDCl_3$, 25 °C) spectrum of the isolated product from the Ritter reaction of monofunctional *exo*-olefin PIB with AN, using a 90:10 (v/v) ratio of AcOH:H_2SO_4 in DCM. 25 °C; [CE] = 0.0322 M; [CUA] = 0.154 M; reaction time = 12 h.

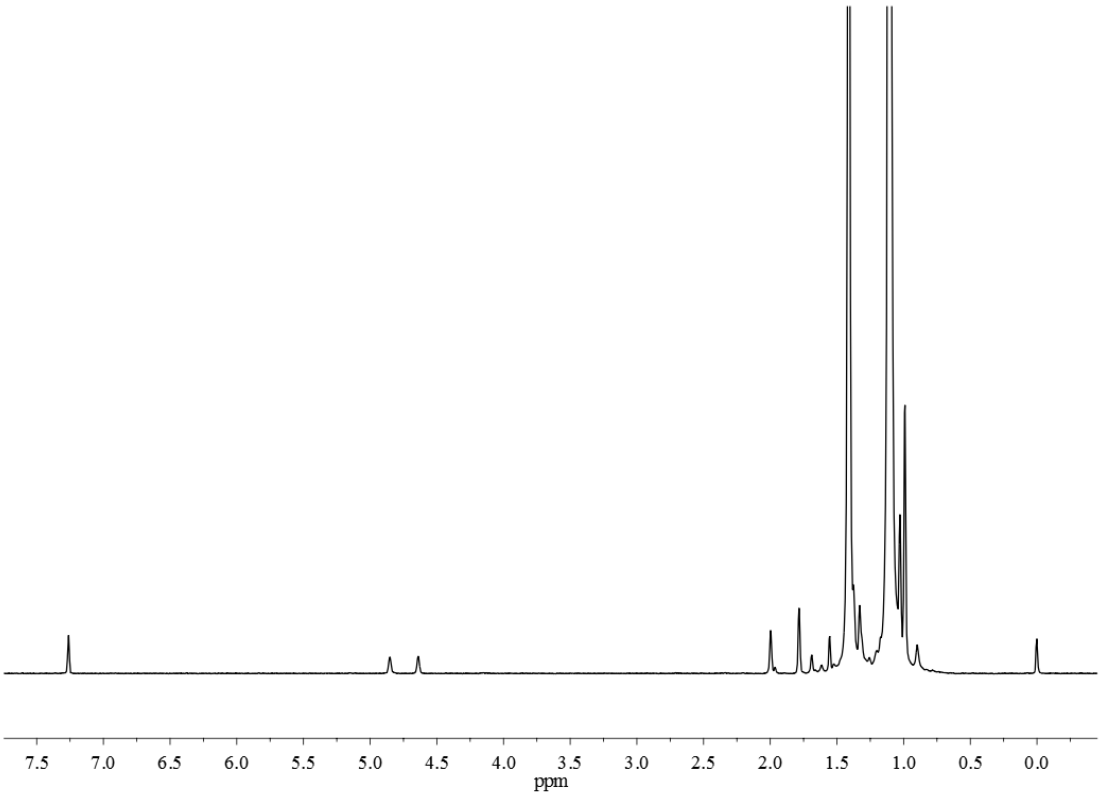

Figure A.37 ^{1}H NMR (300 MHz, $CDCl_3$, 25 °C) spectrum of the isolated product from the Ritter reaction of monofunctional *exo*-olefin PIB with CUA, using a 90:10 (v/v) ratio of AcOH:H_3PO_4 in $CHCl_3$. 25 °C; [CE] = 0.0322 M; [CUA] = 0.154 M; reaction time = 12 h.

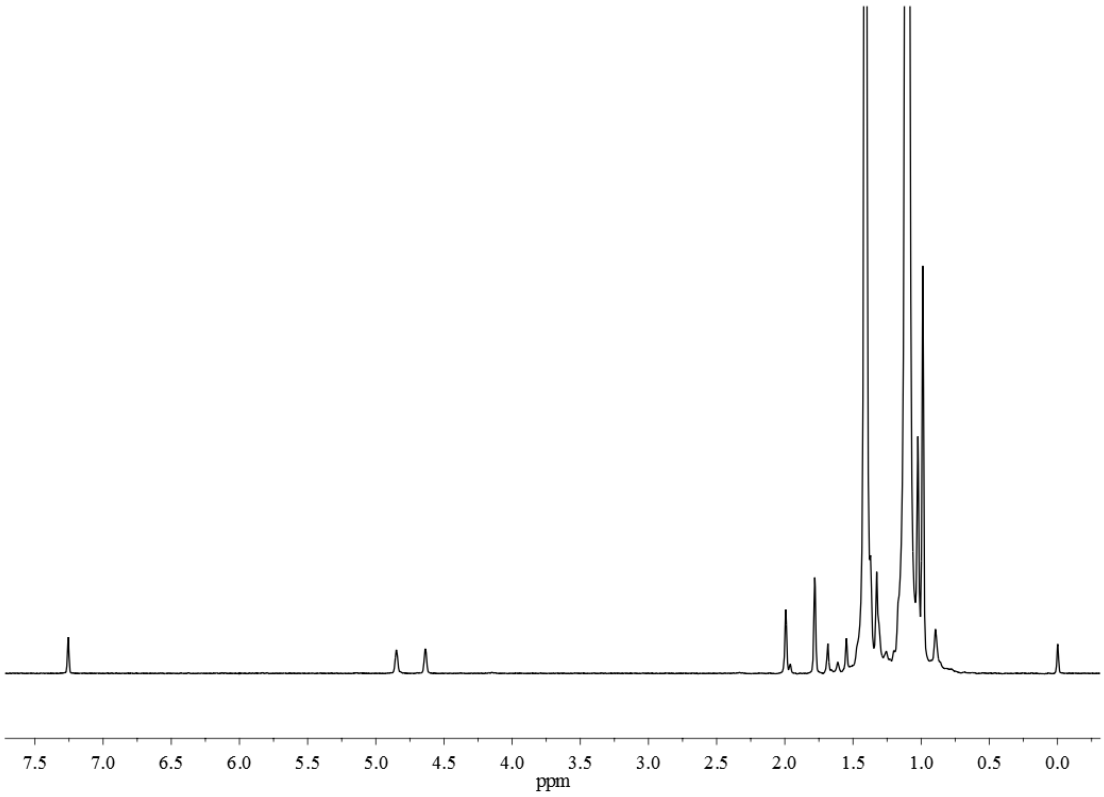

Figure A.38 ^{1}H NMR (300 MHz, $CDCl_3$, 25 °C) spectrum of the isolated product from the Ritter reaction of monofunctional *exo*-olefin PIB with CUA, using H_3PO_4 in $CHCl_3$. 25 °C; [CE] = 0.0322 M; [CUA] = 0.154 M; reaction time = 12 h.

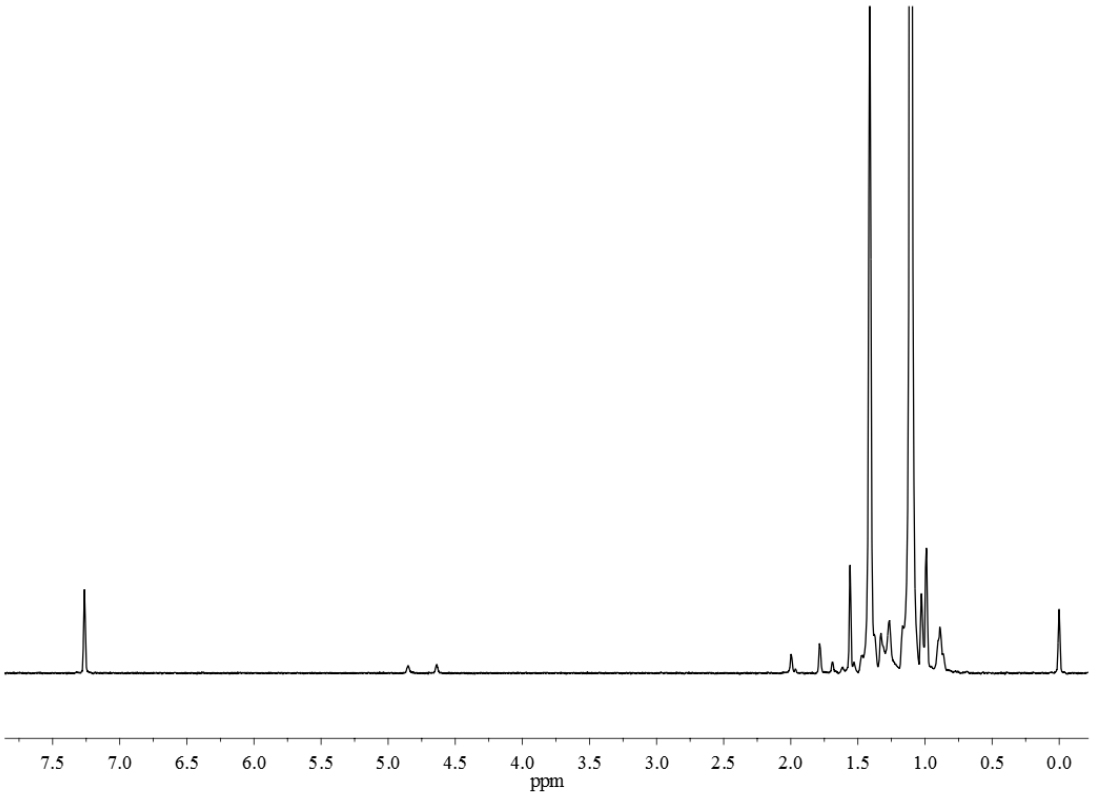

Figure A.39 ^{1}H NMR (300 MHz, $CDCl_3$, 25 °C) spectrum of the isolated product from the Ritter reaction of monofunctional *exo*-olefin PIB with CUA, using HCl (aq) in $CHCl_3$. 25 °C; [CE] = 0.0322 M; [CUA] = 0.154 M; reaction time = 12 h.

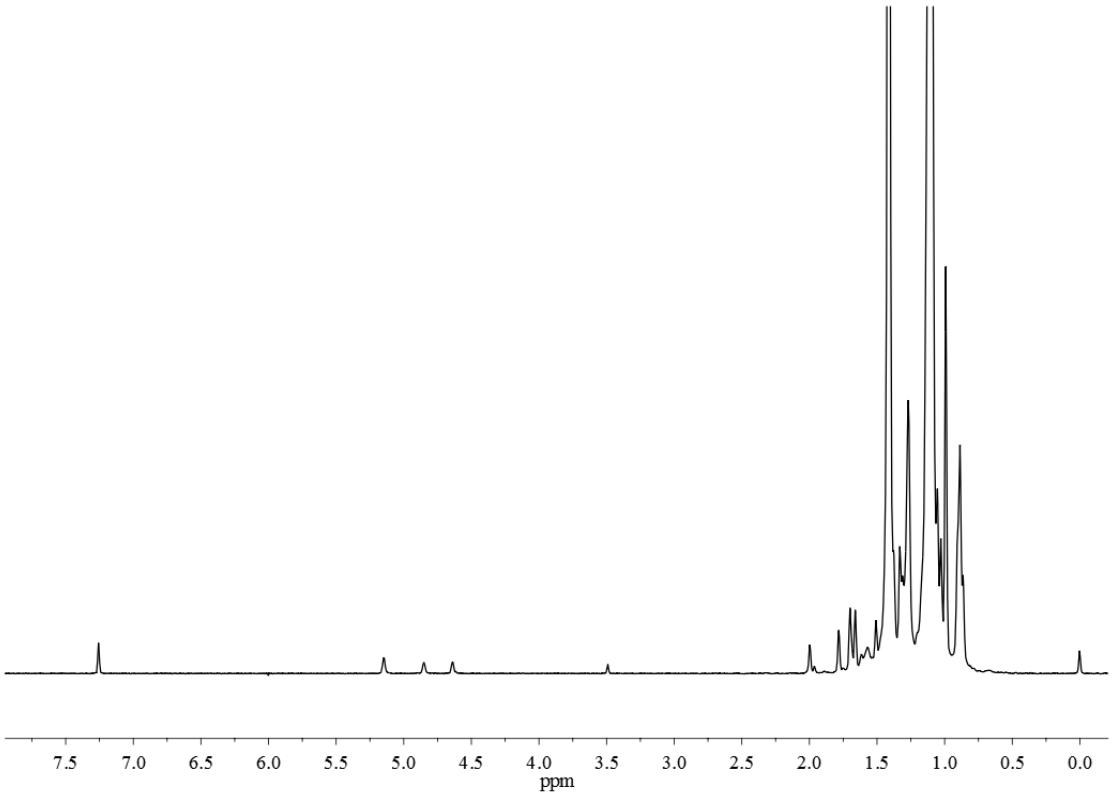

Figure A.40 ^{1}H NMR (300 MHz, $CDCl_3$, 25 °C) spectrum of the isolated product from the Ritter reaction of monofunctional *exo*-olefin PIB with CUA, using HI(aq) in $CHCl_3$. 25 °C; [CE] = 0.0322 M; [CUA] = 0.154 M; reaction time = 12 h.

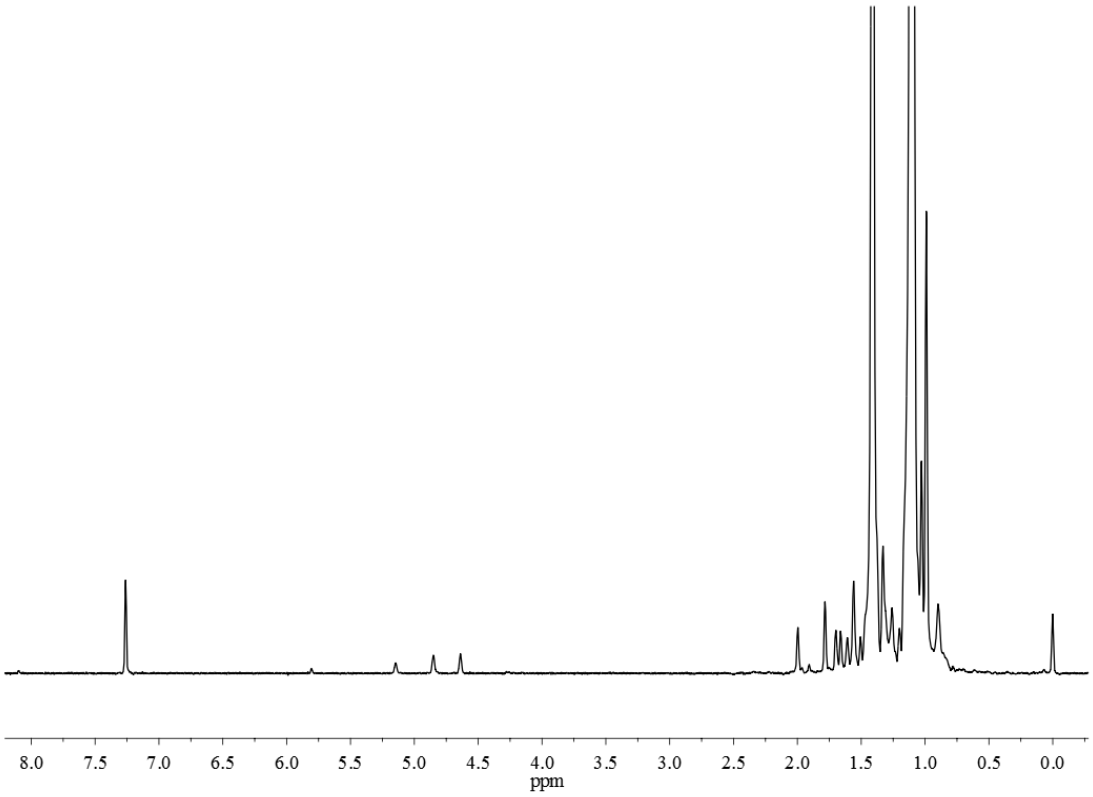

Figure A.41 ^{1}H NMR (300 MHz, $CDCl_3$, 25 °C) spectrum of the isolated product from the Ritter reaction of monofunctional *exo*-olefin PIB with CUA, using DCAc in $CHCl_3$. 25 °C; [CE] = 0.0322 M; [CUA] = 0.154 M; reaction time = 12 h.

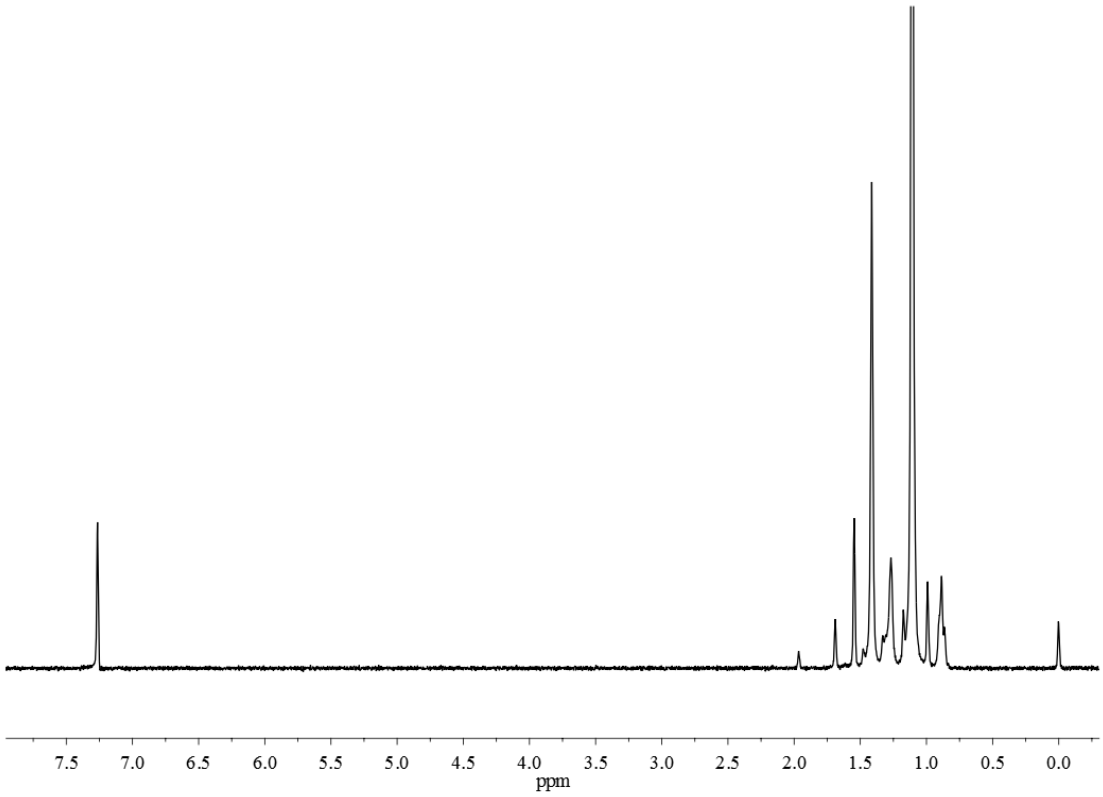

Figure A.42 ^{1}H NMR (300 MHz, $CDCl_3$, 25 °C) spectrum of the isolated product from the Ritter reaction of monofunctional *exo*-olefin PIB with CUA, using HCl(g) in $CHCl_3$. 25 °C; [CE] = 0.0322 M; [CUA] = 0.154 M; reaction time = 12 h.

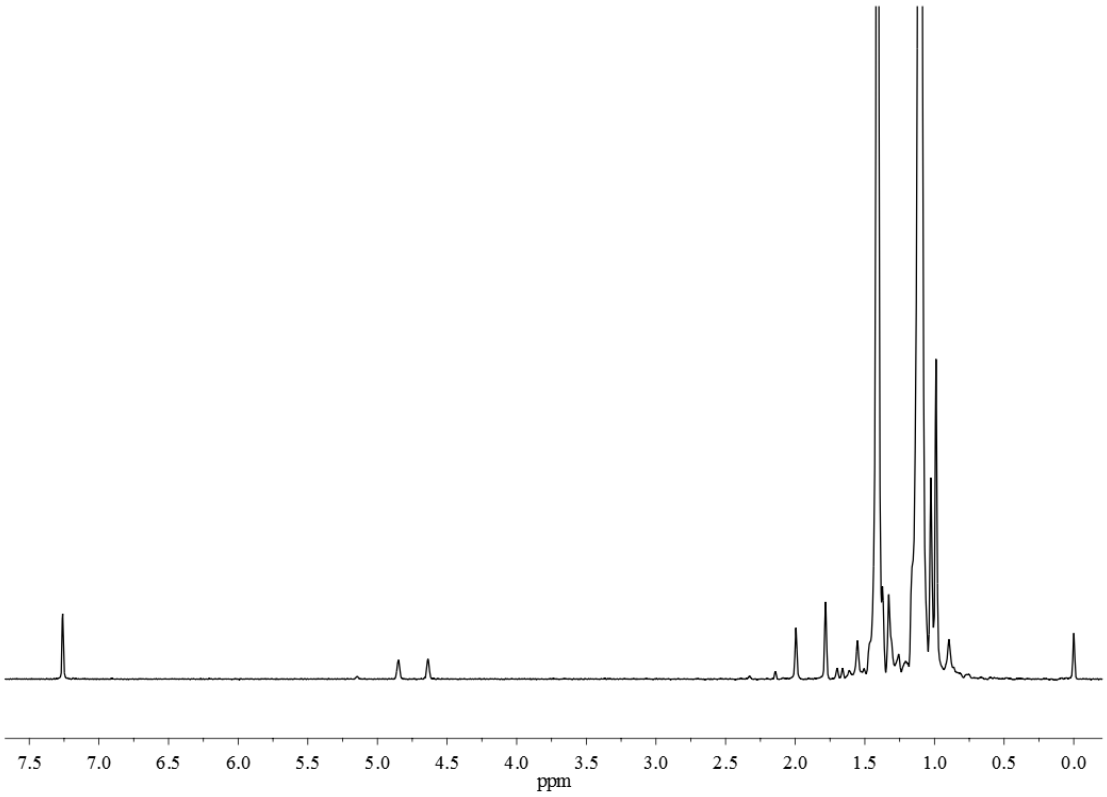

Figure A.43 ^{1}H NMR (300 MHz, $CDCl_3$, 25 °C) spectrum of the isolated product from the Ritter reaction of monofunctional *exo*-olefin PIB with CUA, using HI(g) in $CHCl_3$. 25 °C; [CE] = 0.0322 M; [CUA] = 0.154 M; reaction time = 12 h.

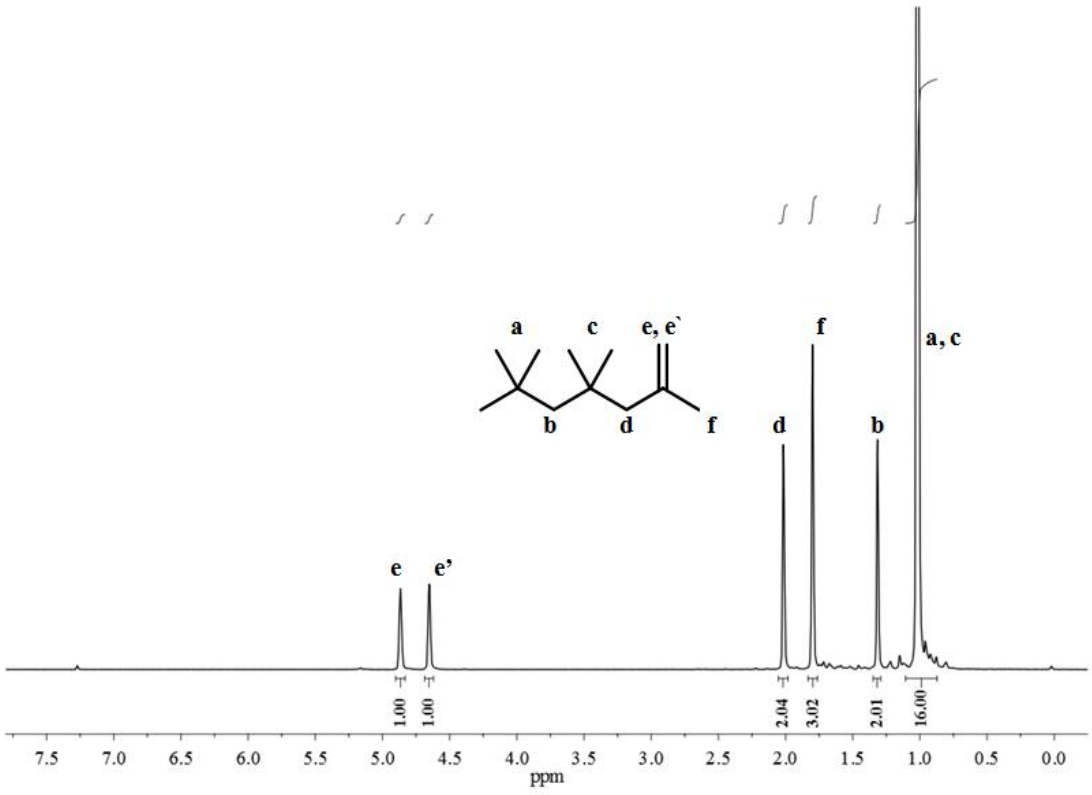

Figure A.44 ^{1}H NMR (300 MHz, $CDCl_3$, 25 °C) spectrum of C_{12} oligoisobutylene.

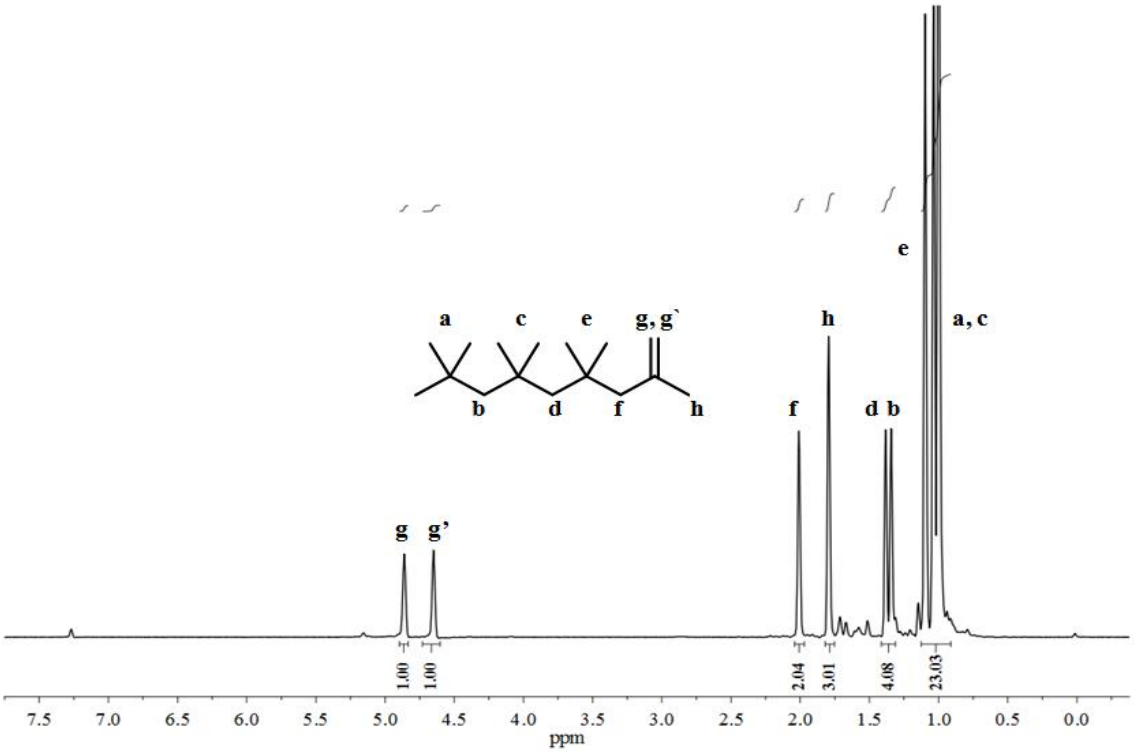

Figure A.45 ^{1}H NMR (300 MHz, $CDCl_3$, 25 °C) spectrum of C_{16} oligoisobutylene.

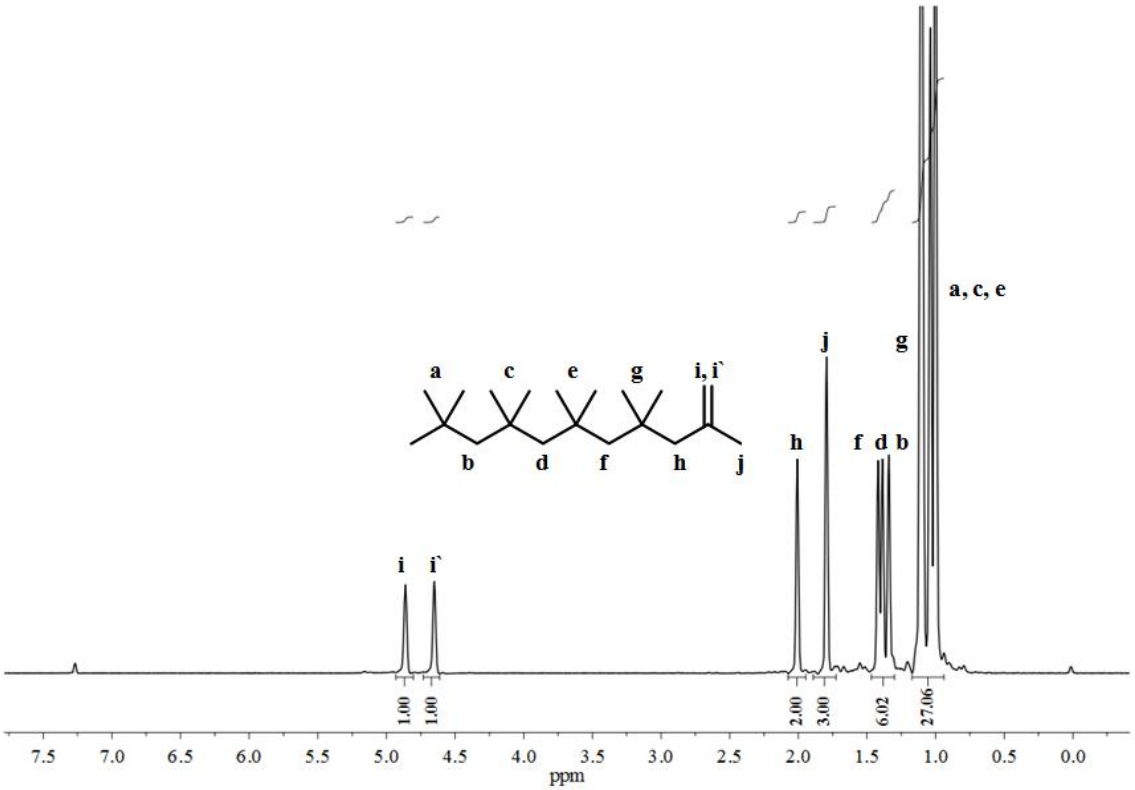

Figure A.46 ^{1}H NMR (300 MHz, $CDCl_3$, 25 °C) spectrum of C_{20} oligoisobutylene.

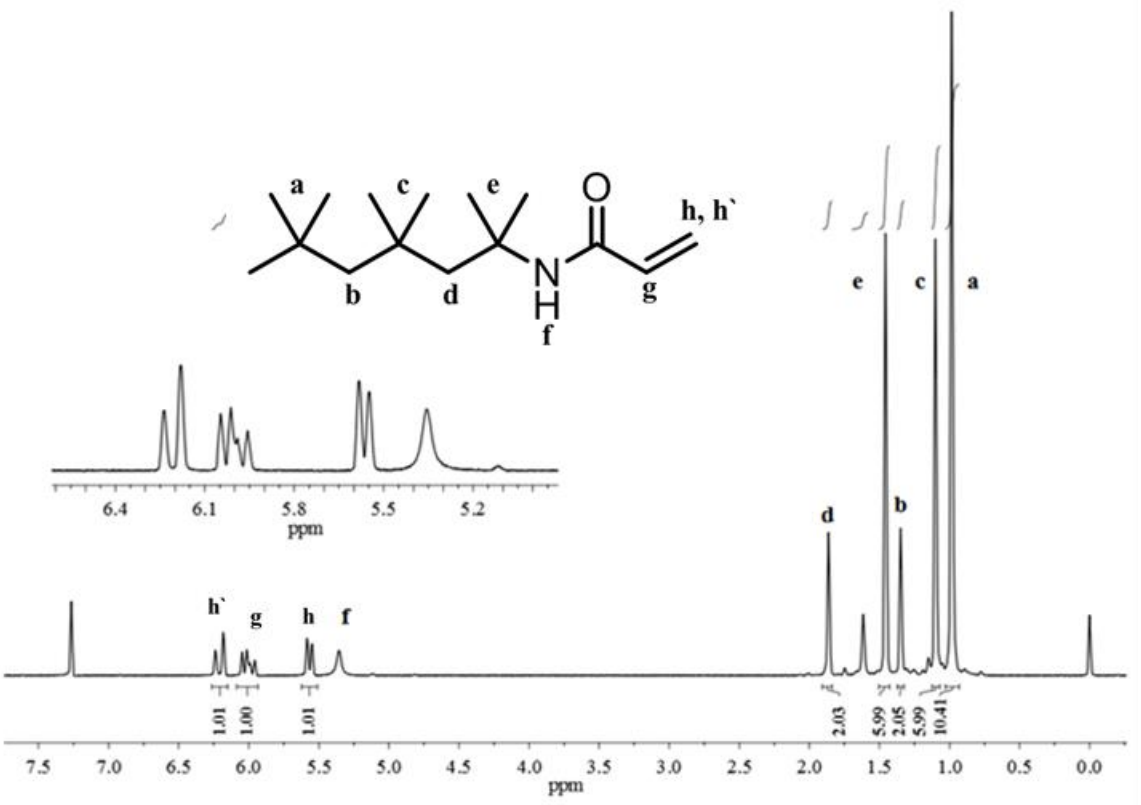

Figure A.47 ^{1}H NMR (300 MHz, $CDCl_3$, 25 °C) spectrum of the acrylamide product isolated from Trial 3.1.

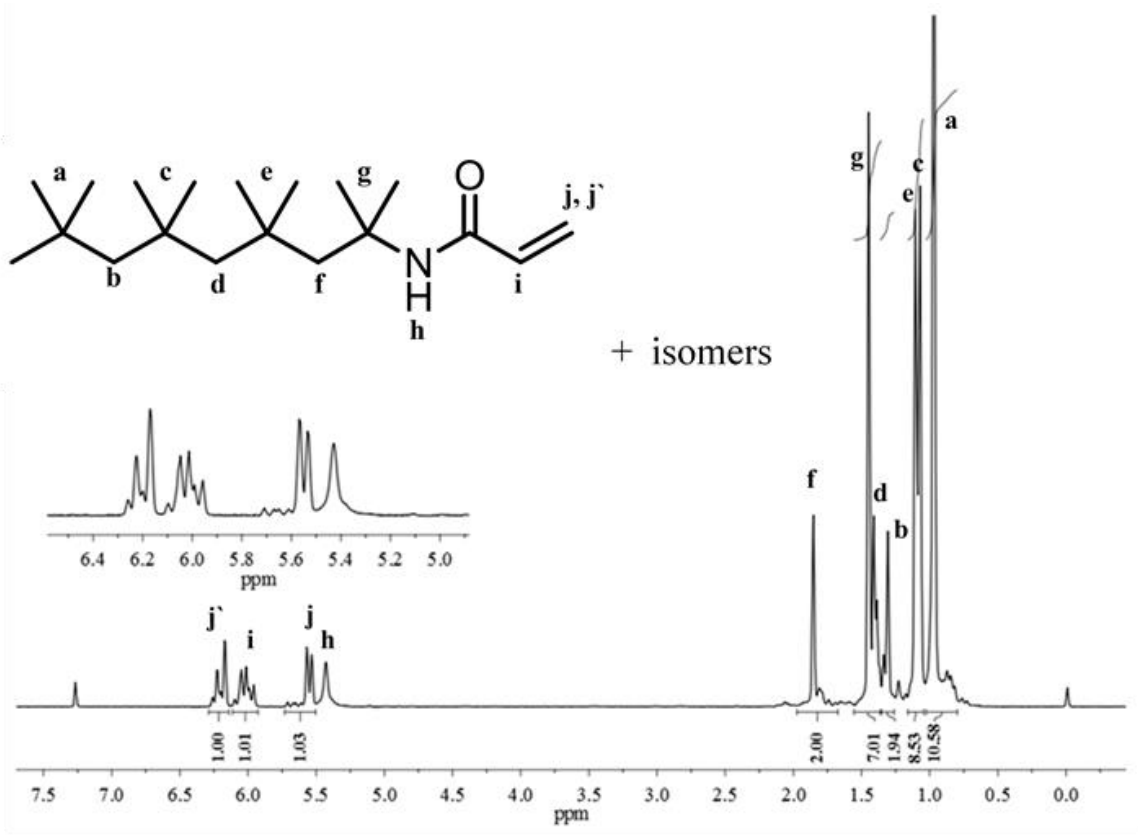

Figure A.48 ^{1}H NMR (300 MHz, $CDCl_3$, 25 °C) spectrum of the acrylamide product isolated from Trial 3.2.

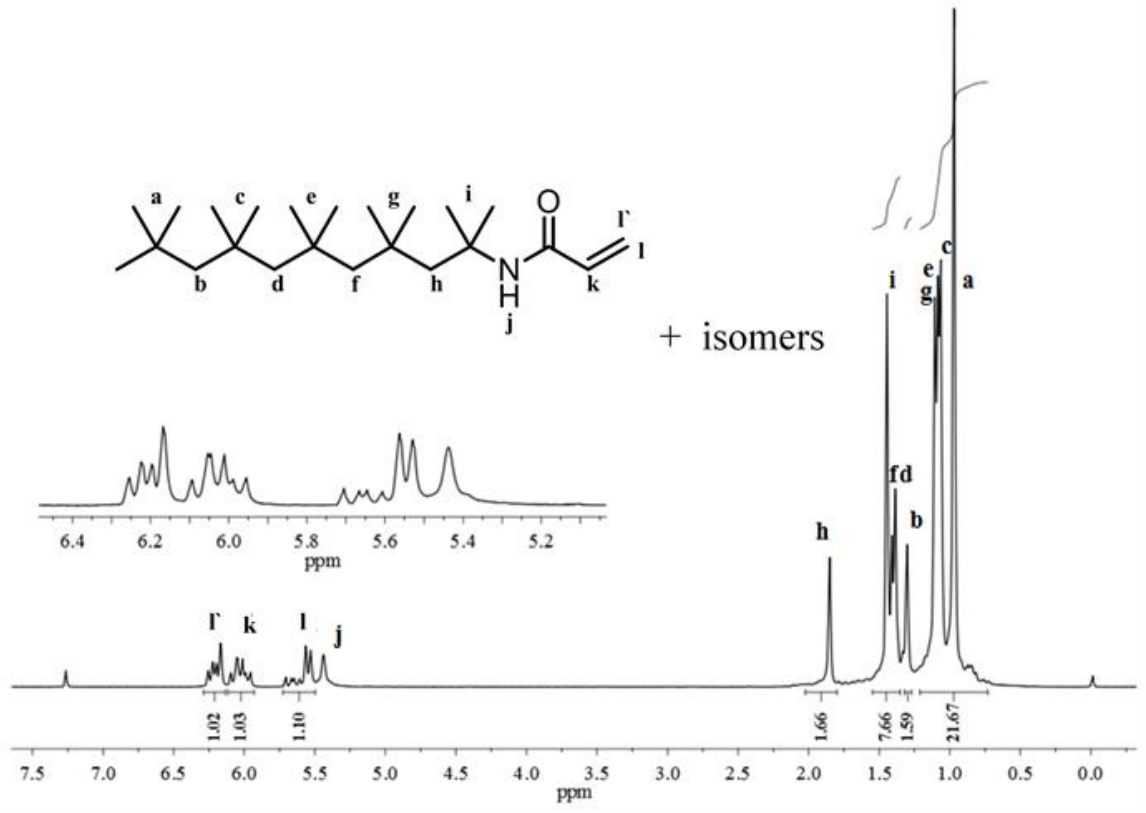

Figure A.49 ^{1}H NMR (300 MHz, $CDCl_3$, 25 °C) spectrum of the acrylamide product isolated from Trial 3.3.

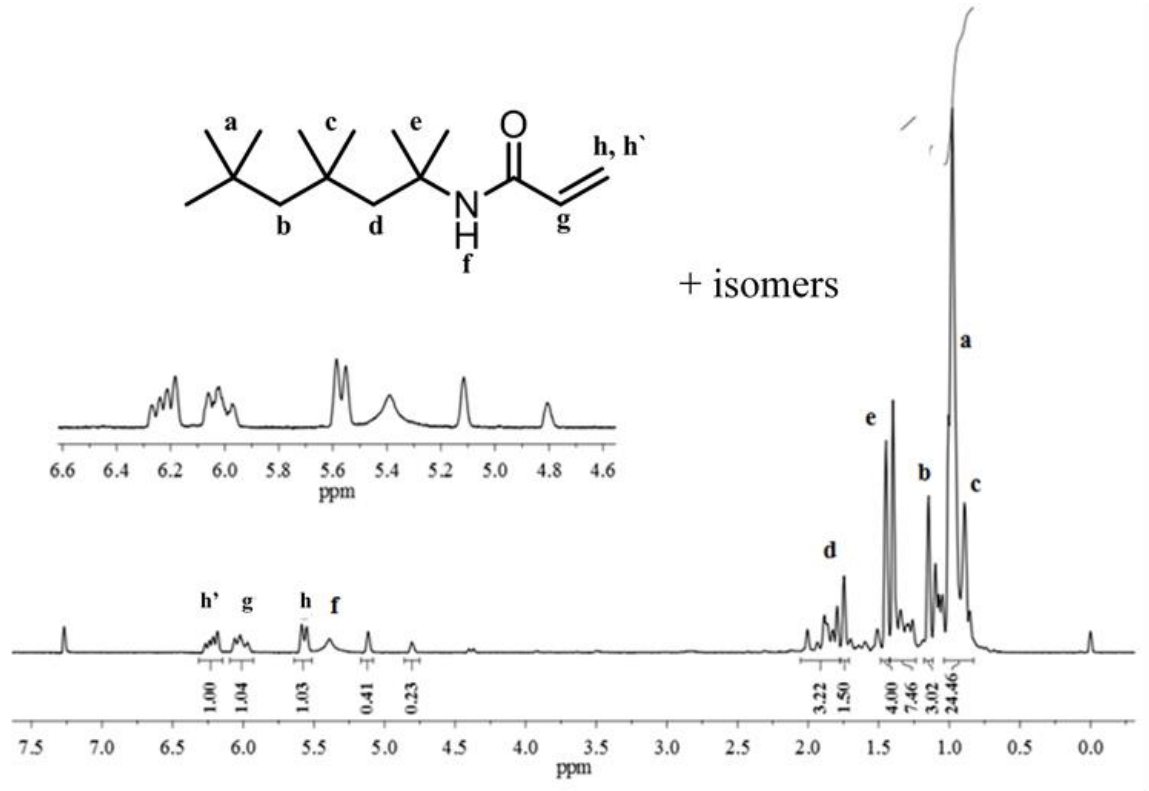

Figure A.50 ^{1}H NMR (300 MHz, $CDCl_3$, 25 °C) spectrum of the acrylamide product isolated from Trial 3.4.

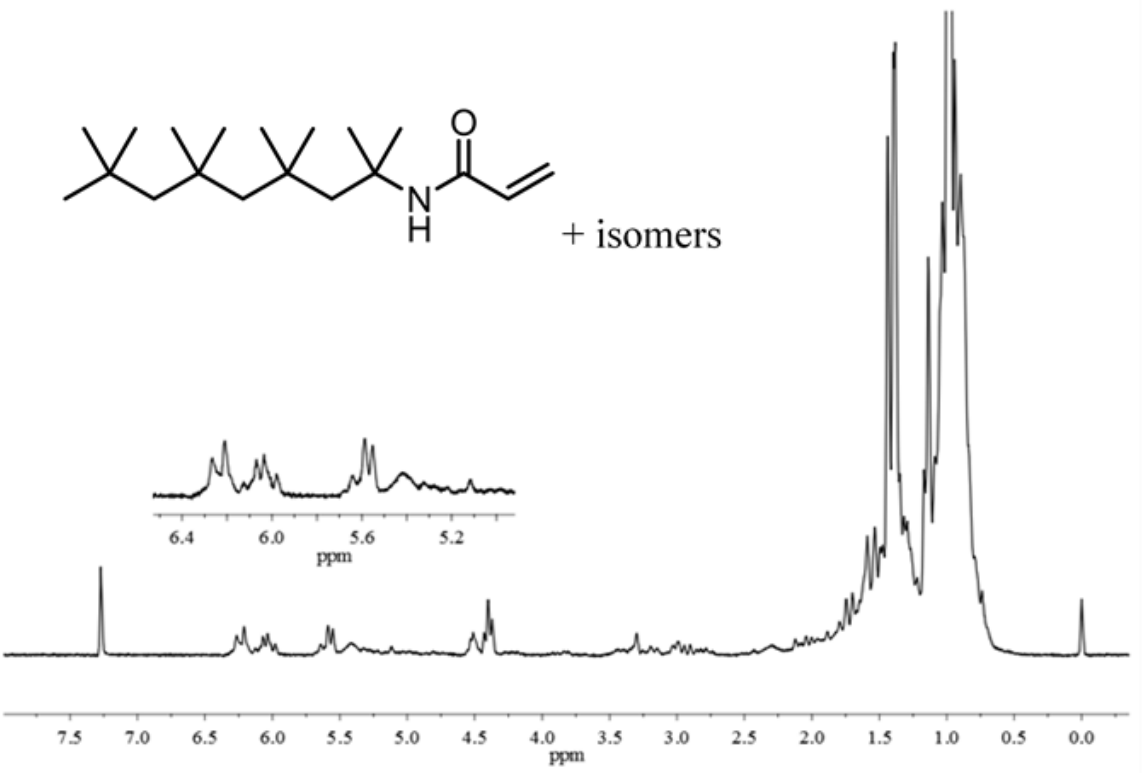

Figure A.51 ^{1}H NMR (300 MHz, $CDCl_3$, 25 °C) spectrum of the acrylamide product isolated from Trial 3.5.

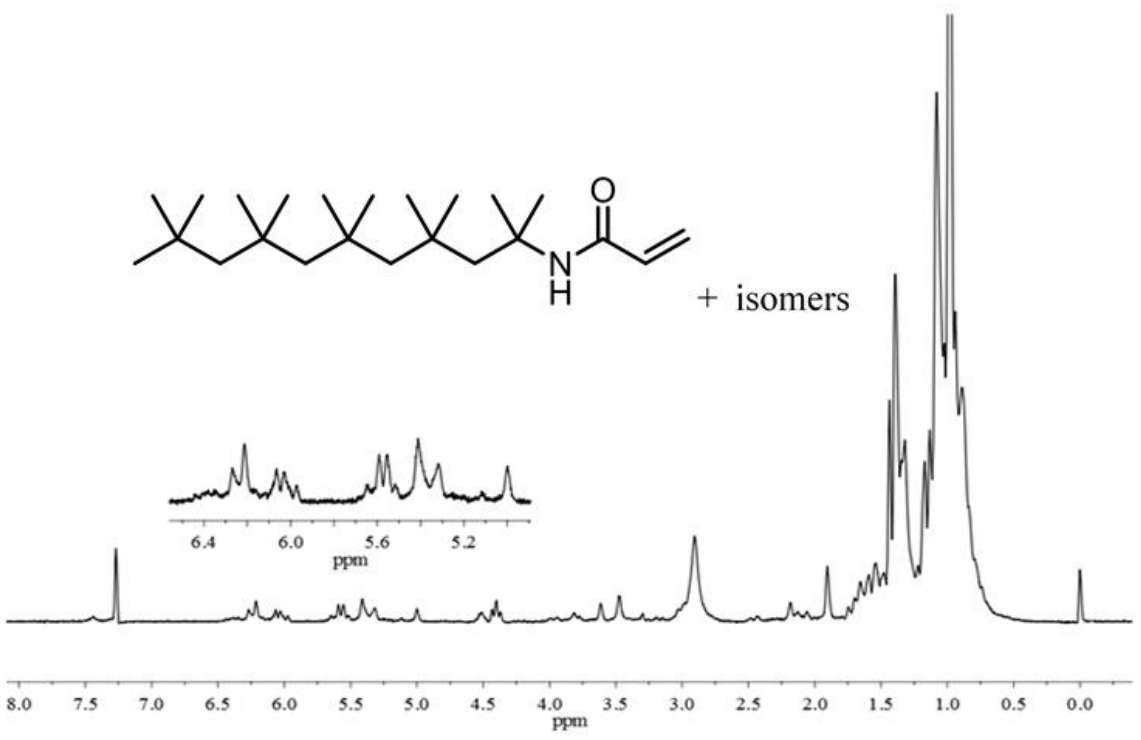

Figure A.52 ^{1}H NMR (300 MHz, $CDCl_3$, 25 °C) spectrum of the acrylamide product isolated from Trial 3.6.

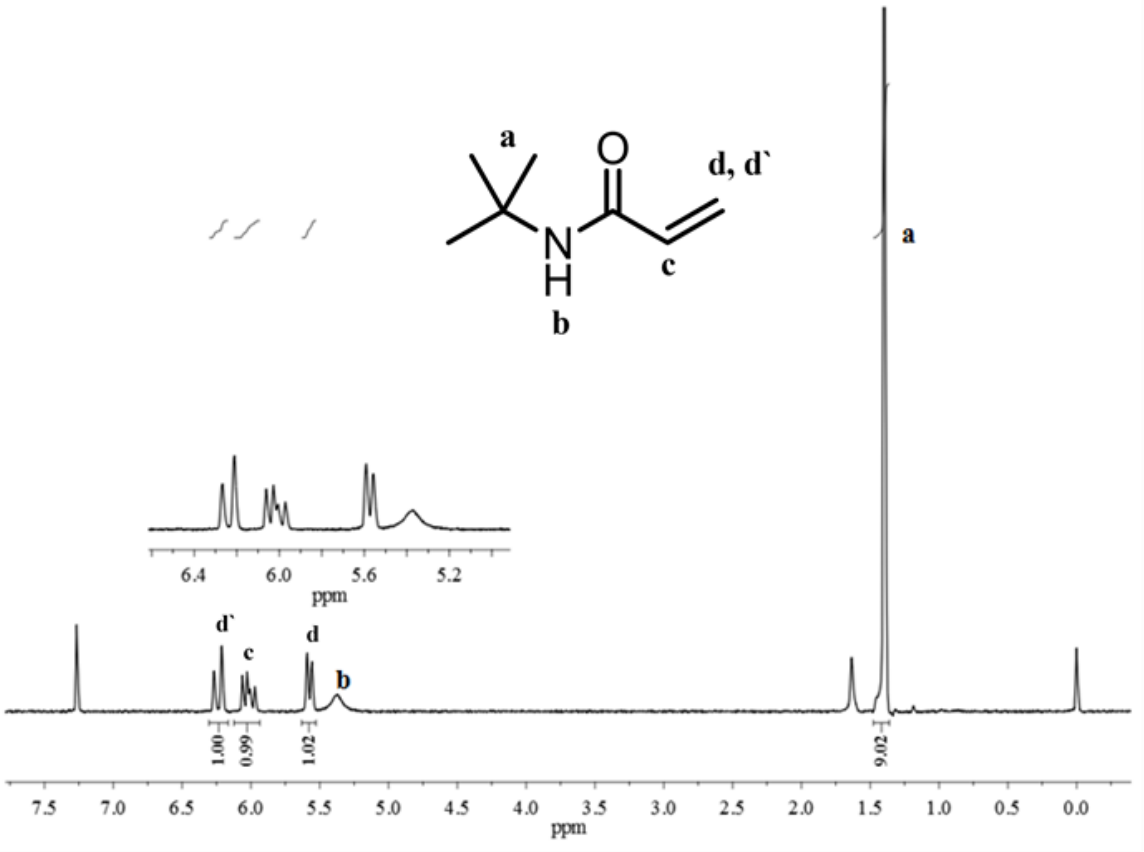

Figure A.53 ^{1}H NMR (300 MHz, $CDCl_3$, 25 °C) spectrum of *tert*-butyl acrylamide, isolated from Trials 3.4-3.6.

REFERENCES

1. Pande, J. B. History of Natural Rubber. *Rubber India* **1950**, 2 (No. 3), 5–10.

2. Tully, J. The Devils Milk; NYU Press, 2011.

3. Morton, M. History of Synthetic Rubber. *J. Macromol. Sci. Part A - Chem.* **1981**, 15 (7), 1289–1302.

4. Morawetz, H. History of Rubber Research. *Rubber Chem. Technol*. **2000,** 73 (3), 405–426.

5. Hurley, P. E. History of Natural Rubber. *J. Macromol. Sci. Part A - Chem.* **1981**, 15 (7), 1279–1287.

6. Brydson, J. A. *Rubber Chemistry*; Applied Science Publishers: Essex, England, 1978. pp 1-10

7. Blackley, D. C. Synthetic Rubbers: Their Chemistry and Technology; 1983. pp 1-6

8. Koch, A. Specific Properties of Artificial [Buna] Rubber. *Rubber Chem. Technol.* **1937**, 10 (1), 17–28.

9. Sieron, J. K. High-Temperature Elastomers for Extreme Aerospace Environments. *Rubber Chem. Technol.* **1966**, 39 (4), 1141–1160.

10. Rivera, M. Elastomers in Space and in Other High Vacuum Environments. *Rubber Chem. Technol.* **1966,** 39 (4), 1127–1140.

11. Kerns, M.; Henning, S.; Rachita, M.; Butadiene Polymers. In *Encyclopedia of Polymer Science and Technology*. Mark, H.F. Ed.; Wiley US, 2003; pp 317-355.

12. Quirk, R.P.; Anionic Polymerization. In *Encyclopedia of Polymer Science and Technology*. Mark, H.F. Ed.; Wiley US, 2003; pp 111-160.

13. Puskas, J.; Kaszas, G. Carbocationic Polymerization. In *Encyclopedia of Polymer Science and Technology*. Mark, H.F. Ed.; Wiley US, 2003; pp 383-418.

14. Higashimura, T.; Sawamoto, M. Recent Progress in Living Cationic Polymerization. In *Progress in Pacific Polymer Science*; Anderson, B. C., Imanishi, Y., Eds.; Springer Berlin Heidelberg: Berlin, Heidelberg, **1991**; pp 93–103.

15. Webb, R.N.; Shaffer, T.D.; Tsou, A.H.; Butyl Rubber. In *Encyclopedia of Polymer Science and Technology*. Mark, H.F., Ed.; Wiley US, 2003; pp 356-377

16. Takeda, T.; Sawamoto, M.; Higashimura, T. Transfer Reaction of the Two Propagating Species in Cationic Polymerization of Styrene by Acetyl Perchlorate or Trifluoromethanesulfonic Acid. *Polym. J.* **1977**, 9, 377.

17. Staudinger, H. Über Polymerisation. *Berichte der Dtsch. Chem. Gesellschaft* (A B Ser. **1920**, 53 (6), 1073–1085.

18. Watson, R. Chemical Essays; Printed for T. Evans: London, **1787**.

19. Ziegler, K.; Bähr, K. Über Den Vermutlichen Mechanismus Der Polymerisationen Durch Alkalimetalle (Vorläufige Mitteilung). *Berichte der Dtsch. Chem. Gesellschaft* (A B Ser. **1928**, 61 (2), 253–263.

20. Whitemore, F.C.; The Mechanism of the Polymerization and Depolymerization of Olefins; *Science*; **1934**, 79 (2038), 45 LP-47.

21. Williams, G.; Kinetics of the Catalysed Polymerisation of Styrene. Part III. On the Mechanism of Metal Chloride Catalysis. *J. Chem. Soc.* **1940**, No. 0, 775–784.

22. Mueller-Cunradi, M.; Otto, M. Valuable Hydrocarbon Products. U.S. Patent 2,084,501, June 22, 1937.

23. Butlerov, A. M. Isodibutylene, One of the Forms of Octylene. *J. Russ. Chem. Soc.* **1877**, 9, 38.

24. Thomas, R. M.; Sparks, W. J.; Frolich, P. K.; Otto, M.; Mueller-Cunradi, M. Preparation and Structure of High Molecular Weight Polybutenes. *J. Am. Chem. Soc.* **1940**, 62 (2), 276–280.

25. Sparks, W. J.; Thomas, R. M. Mixed Olefinic Polymerization Process and Product. U.S. Patent 2,356,128, August 22, 1944.

26. Coran, A. Y.; Vulcanization. In *The Science and Technology of Rubber*; Mark, J.; Erman, B. Eds.; Academic Press, 2005; pp 321–366.

27. Szwarc, M.; 'Living' Polymers. *Nature* **1956**, 178, 1168.

28. Szwarc, M.; Levy, M.; Milkovich, R.; Polymerization Initiated by Electron Transfer to Monomer. A New Method of Formation of Block Polymers. *J. Am. Chem. Soc.* **1956**, 78 (11), 2656–2657.

29. Hadjichristidis, N.; Pitsikalis, M.; Latrou, H.; Sakellariou, G.; Macromolecular Architectures by Living and Controlled/Living Polymerizations. In *Controlled and Living Polymerizations;* Matyjaszewski, K.; Müller, A. H. E. Eds.; Wiley, 2009. pp 343-443.

30. Matyjaszewski, K.; Pugh, C.; Mechanistic Aspects of Cationic Polymerization of Alkenes. In *Cationic Polymerizations: Mechanisms, Synthesis & Applications*; Matyjaszewski, K. Ed.; CRC Press: New York, 1996. pp. 200-245

31. Pepper, D. C. Analogies and Discrepancies between Cationic and Anionic Polymerizations. *J. Polym. Sci. Polym. Symp.* **1975**, 50 (1), 51–69.

32. Winstein, S.; Clippinger, E.; Fainberg, A. H.; Heck, R.; Robinson, G. C. Salt Effects and Ion Pairs in Solvolysis and Related Reactions. III. Common Ion Rate Depression and Exchange of Anions during Acetolysis. *J. Am. Chem. Soc.* **1956,** 78 (328).

33. Kennedy, J. P.; Trivedi, P. D. Cationic Olefin Polymerization Using Alkyl Halide Alkylaluminum Initiator Systems. II. Molecular Weight Studies. *Adv. Polym. Sci.* **1978**, 28, 113–151.

34. Fodor, Z.; Bae, Y. C.; Faust, R. Temperature Effects on the Living Cationic Polymerization of Isobutylene: Determination of Spontaneous Chain-Transfer Constants in the Presence of Terminative Chain Transfer. *Macromolecules* **1998**, 31 (14), 4439–4446.

35. Matyjaszewski, K. Carbocationic Polymerization: Styrene and Substituted Styrenes. In *Comprehensive Polymer Science and Supplements Vol.3.*; Eastmond, G.C.; Ledwith, A.; Russo, S.; Sigwalt, P., Eds.; Pergamon Press, 1989; pp 639–671.

36. Bae, Y. C.; Faust, R. β-Proton Elimination by Free Bases in the Living Carbocationic Polymerization of Isobutylene. *Macromolecules* **1997**, 30 (23), 7341–7344.

37. Krzysztof, M.; Chih-Hwa, L. Exchange Reactions in the Living Cationic Polymerization of Alkenes. *Makromol. Chemie. Macromol. Symp.* **2018**, 47 (1), 221–237.

38. Mayr, H.; Roth, M.; Lang, G. Kinetics of Carbocationic Polymerizations: Initiation, Propagation, and Transfer Steps. In *Cationic Polymerization*; ACS Symposium Series Vol. 665; American Chemical Society, **1997**; Vol. 665, pp 25–40.

39. Aoshima, S.; Kanaoka, S. A Renaissance in Living Cationic Polymerization. *Chem. Rev.* **2009**, 109 (11), 5245–5287.

40. Winstein, S.; Clippinger, E.; Fainberg, A. H.; Robinson, G. C. Salt Effects and Ion-Pairs in Solvolysis I. *J. Am. Chem. Soc.* **1954**, 76 (9), 2597–2598.

41. Winstein, S.; Klinedinst, P. E.; Clippinger, E. Salt Effects and Ion Pairs in Solvolysis and Related Reactions. XXI.1 Acetolysis, Bromide Exchange and the Special Salt Effect. *J. Am. Chem. Soc.* **1961**, 83 (24), 4986–4989.

42. Higashimura, T.; Kishiro, O.; Matsuzaki, K.; Uryu, T. Cationic Polymerization of Styrene by Acetyl Perchlorate. II. Steric Structure of the Polymer and Nature of the Propagating Species. J. Polym. Sci. Polym. Chem. Ed. 1975, 13 (6), 1393–1399.

43. Higashimura, T.; Kishiro, O.; Takeda, T. Studies on Propagating Species in Cationic Polymerization of Styrene Derivatives by Acetyl Perchlorate or Iodine. I. Bimodal Molecular Weight Distribution of Polymers Produced by Acetyl Perchlorate or Iodine. *J. Polym. Sci. Polym. Chem. Ed.* **1976**, 14 (5), 1089–1095.

44. Yamamoto, K.; Higashimura, T. Studies on Propagating Species in Cationic Polymerization of Styrene Derivatives by Acetyl Perchlorate or Iodine. II. Salt Effect on the Relative Reactivity in the Cationic Copolymerization of Styrene Derivatives with 2-Chloroethyl Vinyl Ether Initiators *J. Polym. Sci. Polym. Chem. Ed.* **1976**, 14 (11), 2621–2629.

45. Higashimura, T.; Yamamoto, K. Studies on Propagating Species in Cationic Polymerization of Styrene Derivatives by Acetyl Perchlorate or Iodine. III. Effect of Salt on Cationic Copolymerization of Styrene Derivatives with Vinyl Ethers by Acetyl Perchlorate. *J. Polym. Sci. Polym. Chem. Ed.* **1977**, 15 (2), 301–309.

46. Higashimura, T.; Kishiro, O. Possible Formation of Living Polymers of P-Methoxystyrene by Iodine. *Polym. J.* **1977**, 9, 87.

47. Kennedy, J. P.; Kelen, T.; Tüdös, F. Quasiliving Carbocationic Polymerization. I. Classification of Living Polymerizations in Carbocationic Systems. *J. Macromol. Sci. Part A - Chem.* **1982**, 18 (9), 1189–1207.

48. Puskas, J. E.; Kaszas, G.; Kennedy, J. P.; Kelen, T.; Tudos, F. Quasiliving Carbocationic Polymerization. IX. Forced Ideal Copolymerization of Styrene Derivatives. *J. Macromol. Sci. Chem.* **1982**, 18 (9), 1315–1338.

49. Sawamoto, M.; Kennedy, J. P. Quasi-Living Carbocationic Polymerization of Alkyl Vinyl Ethers and Block Copolymer Synthesis. *ACS Symp. Ser.* **1982**, 193, 213–227.

50. Held, D.; Iván, B.; Müller, A. H. E.; de Jong, F.; Graafland, T. Stability of Propagating Species in Living Cationic Polymerization of Isobutylene. In *Cationic Polymerization*; ACS Symposium Series; American Chemical Society, **1997**; 665, pp. 6–63.

51. Sawamoto, M.; Masuda, T.; Higashimura, T. Cationic Polymerization of Styrenes by Protonic Acids and Their Derivatives, 2. Two Propagating Species in the Polymerization by Trifluoromethanesulfonic Acid. *Makromol. Chemie* **1976**, 177 (10), 2995–3007.

52. Higashimura, T. The Nature of Propagating Species in Cationic Polymerization of Vinyl Compounds. Int. Symp. Cationic. Polym., 4th, *J. Polym. Sci. Polym. Symp.* **1976**, 56, 71–78.

53. Puskas, J.; Kaszas, G.; Kennedy, J. P.; Kelen, T.; Tudos, F. Quasi-Living Carbocationic Polymerization. III. Quasi-Living Polymerization of Isobutylene. *J. Macromol. Sci. Chem*. **1982**, 18 (9), 1229–1244.

54. Wondraczek, R. H.; Kennedy, J. P.; Storey, R. F. New Telechelic Polymers and Sequential Copolymers by Polyfunctional Initiator-Transfer Agents (Inifers). XIII. Influence of Lewis Acid Strength and Counteranion Stability on the Synthesis of Telechelic Polyisobutylenes. *J. Polym. Sci. Polym. Chem. Ed.* **1982**, 20 (1), 43–51.

55. Kennedy, J. P.; Chang, V. S. C.; Smith, R. A.; Iván, B. New Telechelic Polymers and Sequential Copolymers by Polyfunctional Initiator-Transfer Agents (Inifers) V. Synthesis of α-Tert-Butyl-ω-Isopropenylpolyisobutylene and α, ω-Di(Isopropenyl)Polyisobutylene. *Polym. Bull.* **1979**, 1 (8), 575–580.

56. Fehérvári, A.; Kennedy, J. P.; Tüdös, F. New Telechelic Polymers and Sequential Copolymers by Polyfunctional Initiator-Transfer Agents (Inifers). VI. Chain Transfer, Molecular Weight Distribution, and NMR Study of Telechelic α,ω-Di(Tert-Chloro)-Polyisobutylene. *J. Macromol. Sci. Part A - Chem*. **1981**, 15 (2), 215–230.

57. Kennedy, J. P.; Chang, V. S. C.; Francik, W. P. New Telechelic Polymers and Sequential Copolymers by Polyfunctional Initiator-Transfer Agents (Inifers). XVIII. Epoxy and Aldehyde Telechelic Polyisobutylenes. *J. Polym. Sci. Polym. Chem. Ed.* **1982**, 20 (10), 2809–2817.

58. Ivan, B.; Kennedy, J. P. Living Carbocationic Polymerization. 31. A Comprehensive View of the Inifer and Living Mechanisms in Isobutylene Polymerization. *Macromolecules* **1990**, 23 (11), 2880–2885.

59. Miyamoto, M.; Sawamoto, M.; Higashimura, T. Living Polymerization of Isobutyl Vinyl Ether with Hydrogen Iodide/Iodine Initiating System. *Macromolecules* **1984**, 17 (3), 265–268.

60. Miyamoto, M.; Sawamoto, M.; Higashimura, T. Synthesis of Monodisperse Living Poly(Vinyl Ethers) and Block Copolymers by the Hydrogen Iodide/Iodine Initiating System. *Macromolecules* **1984**, 17 (11), 2228–2230.

61. Mishra, M. K.; Wang, B.; Kennedy, J. P. Living Carbocationic Polymerization: Three-Arm Star Telechelic Polyisobutylenes by C6H3(C(CH3)2OCH3)3/BCl3 Complexes. *Polym. Bull.* **1987**, 17 (4), 307–314.

62. Hashimoto, T.; Ibuki, H.; Sawamoto, M.; Higashimura, T. Living Cationic Polymerization of 2-Vinyloxyethylphthalimide: Synthesis of Poly(Vinyl Ether) with Pendant Primary Amino Functions. *J. Polym. Sci. Part A Polym. Chem.* **1988**, 26 (12), 3361–3374.

63. Ishihama, Y.; Sawamoto, M.; Higashimura, T. Living Cationic Polymerization of Styrene by the Methanesulfonic Acid/Tin Tetrachloride Initiating System in the Presence of Tetra-n-Butylammonium Chloride; *Polym. Bull.* **1990**, 23, (4), 361-366

64. Higashimura, T.; Kojima, K.; Sawamoto, M. Living Cationic Polymerization of P-Methoxystyrene by Hydrogen Iodide/Zinc Iodide at Room Temperature. *Polym. Bull. (Berl).* **1988**, 19 (1), 7–11.

65. Shohi, H.; Sawamoto, M.; Higashimura, T. End-Functionalized Polymers of p-Alkoxystyrenes by Living Cationic Polymerization. 1. p-Methoxystyrene. *Macromolecules* **1992**, 25 (1), 53–57.

66. Kennedy, J. P. New Polymers and Polymer Derivatives by Cationic Techniques. Combination of Controlled Elementary Steps. *Die Makromol. Chemie* **1984**, 7 (S19841), 171–199.

67. Faust, R.; Kennedy, J. P. Living Carbocationic Polymerization. IV. Living Polymerization of Isobutylene. *J. Polym. Sci. Part A Polym. Chem.* **1996**, 34 (17), 1847–1869.

68. Kemp, L. K.; Donnalley, A. B.; Storey, R. F. Synthesis and Characterization of Carboxylic Acid-Terminated Polyisobutylenes. *J. Polym. Sci. Part A Polym. Chem.* **2008**, 46 (10), 3229–3240.

69. Yang, B.; Parada, C. M.; Storey, R. F. Synthesis, Characterization, and Photopolymerization of Polyisobutylene Phenol (Meth)Acrylate Macromers. *Macromolecules* **2016**, 49 (17), 6173–6185.

70. Higgins, J. J.; Jagisch, F. C.; Stucker, N. E. Butyl Rubber and Polyisobutylene. In *Handbook of Adhesives*; Skeist, I., Ed.; Springer US: Boston, MA, 1990; pp 185–205.

71. Kennedy, J. P.; Smith, R. A. New Telechelic Polymers and Sequential Copolymers by Polyfunctional Initiator-Transfer Agents (Inifers). III. Synthesis and Characterization of Poly(α-Methylstyrene-b-Isobutylene-b-α-Methylstyrene). *J. Polym. Sci. Polym. Chem. Ed.* **1980**, 18 (5), 1539–1546.

72. Mishra, M. K.; Sar-Mishra, B.; Kennedy, J. P. New Telechelic Polymers and Sequential Copolymers by Polyfunctional Initiator-Transfer Agents (Inifers). *Polym. Bull.* **1985**, 13 (5), 435–439.

73. Feldthusen, J.; Iván, B.; Müller, A. H. E. Synthesis of Linear and Star-Shaped Block Copolymers of Isobutylene and Methacrylates by Combination of Living Cationic and Anionic Polymerizations. *Macromolecules* **1998**, 31 (3), 578–585.

74. Nielsen, L. V; Nielsen, R. R.; Gao, B.; Kops, J.; Iván, B. Synthesis of Isobutenyl-Telechelic Polyisobutylene by Functionalization with Isobutenyltrimethylsilane. *Polymer*. **1997**, 38 (10), 2529–2534.

75. Wilczek, L.; Kennedy, J. P. Electrophilic Substitution of Organosilicon Compounds. II. Synthesis of Allyl-terminated Polyisobutylenes by Quantitative Allylation of Tert-chloro-polyisobutylenes with Allyltrimethylsilane. *J. Polym. Sci. Part A Polym. Chem.* **1986**, 25 (12), 3255–3265.

76. Simison, K. L.; Stokes, C. D.; Harrison, J. J.; Storey, R. F. End-Quenching of Quasiliving Carbocationic Isobutylene Polymerization with Hindered Bases: Quantitative Formation of Exo-Olefin-Terminated Polyisobutylene. *Macromolecules* **2006**, 39 (7), 2481–2487.

77. Storey, R. F.; Kemp, L. K. Preparation of Exo-Olefin Terminated Polyolefins via Quenching with Alkoxysilanes or Ethers. U.S. Patent 8,063,154 B2, November 11, 2011.

78. Ummadisetty, S.; Storey, R. F. Quantitative Synthesis of Exo-Olefin-Terminated Polyisobutylene: Ether Quenching and Evaluation of Various Quenching Methods. *Macromolecules* **2013**, 46 (6), 2049–2059.

79. Ummadisetty, S.; Morgan, D. L.; Stokes, C. D.; Storey, R. F. Synthesis of Exo -Olefin Terminated Polyisobutylene by Sulfide/Base Quenching of Living Polyisobutylene. *Macromolecules* **2011**, 44 (20), 7901–7910.

80. Pirouz, S.; Wang, Y.; Chong, J. M.; Duhamel, J. Chemical Modification of Polyisobutylene Succinimide Dispersants and Characterization of Their Associative Properties. *J. Phys. Chem. B* **2015**, 119 (37), 12202–12211.

81. Harrison, J. J.; Ruhe Jr., W. R. Polyalkylene Polysuccinimides and Posttreated Derivatives Thereof. U.S. Patent 6,146,431A, January 18, 2000.

82 Liao, T. P.; Kennedy, J. P. New Telechelic Polymers and Sequential Copolymers by Polyfunctional Initiator-Transfer Agents (Inifers). 17. Synthesis and Characterization of Acryl and Methacryl Telechelic Polyisobutylenes (Polyisobutenyl Diacrylate and -Dimethacrylate). *Polym. Bull.* **1981**, 6 (3–4), 135–141.

83. Percec, V.; Guhaniyogi, S. C.; Kennedy, J. P.; Ivan, B. New Telechelic Polymers and Sequential Copolymers by Polyfunctional Initiator-Transfer Agents (Inifers). 22. Synthesis and Characterization of Linear and Three-Arm Star Block Copolymers of Isobutylene and N-Acetylethyleneimine. *Polym. Bull.* **1982**, 8 (1), 25–32.

84. Liao, T. P.; Kennedy, J. P. New Telechelic Polymers and Sequential Copolymers by Polyfunctional Initiator-Transfer Agents (Inifers). 15. Synthesis and Characterization of Telechelic Acid-Ester Polyisobutylenes. *Polym. Bull.* **1981**, 5 (1), 11–18.

85. Magenau, A. J. D.; Chan, J. W.; Hoyle, C. E.; Storey, R. F. Facile Polyisobutylene Functionalization via Thiol-Ene Click Chemistry. *Polym. Chem.* **2010**, 1 (6), 831–833.

86. Kennedy, J.; C. Guhaniyogi, S.; Percec, V. New Telechelic Polymers and Sequential Copolymers by Polyfunctional Initiator-Transfer Agents (Inifers); *Polym. Bull.* **1982**; 8 (11-12), 551-555

87. Béla, I.; Kennedy, J.P.; Chang, V.S. New Telechelic Polymers and Sequential Copolymers by Polyfunctional Initiator-transfer Agents (Inifers). VII. Synthesis and Characterization of α,Ω-di(Hydroxy)Polyisobutylene. *J. Polym. Sci. Polym. Chem. Ed.* **1980**, 18 (11-12), 3177–3191.

88. Kennedy, J.; C. Guhaniyogi, S.; Percec, V. New Telechelic Polymers and Sequential Copolymers by Polyfunctional Initiator-Transfer Agents (Inifers) - 27. Bisphenol- and Trisphenol-Polyisobutylenes; *Polym. Bull.* **1982**; 8 (11-12), 571-578

89. Heskett, M. D. Structure-Property Relationships of Polyisobutylene-Block-Polyamide Thermoplastic Elastomers, Masters Thesis, University of Southern Mississippi, August 2016.

90. Tripathy, R.; Ojha, U.; Faust, R. Syntheses and Characterization of Polyisobutylene Macromonomers with Methacrylate, Acrylate, Glycidyl Ether, or Vinyl Ether End-Functionality. *Macromolecules* **2009**, 42 (12), 3958–3964.

91. Feldthusen, J.; Ivan, B.; Mueller, A. H. E.; Kops, J. End-Functional Polymers by Functionalization of Living Cationic Chain Ends with 1,1-Diphenylethylene. *Macromol. Reports* **1995**, A32 (Suppl. 5&6), 639–647.

92. De, P.; Faust, R. Relative Reactivity of C4 Olefins toward the Polyisobutylene Cation. *Macromolecules* **2006**, 39 (20), 6861–6870.

93. Martinez-Castro, N.; Morgan, D. L.; Storey, R. F. Primary Halide-Terminated Polyisobutylene: End-Quenching of Quasiliving Carbocationic Polymerization with N-(ω-Haloalkyl)Pyrrole. *Macromolecules* **2009**, 42 (14), 4963–4971.

94. Morgan, D. L.; Storey, R. F. Primary Hydroxy-Terminated Polyisobutylene via End-Quenching with a Protected N-(ω-Hydroxyalkyl)Pyrrole. *Macromolecules* **2010**, 43 (3), 1329–1340.

95. Morgan, D. L.; Storey, R. F. End-Quenching of Quasi-Living Isobutylene Polymerizations with Alkoxybenzene Compounds. *Macromolecules* **2009**, 42 (18), 6844–6847.

96. Morgan, D. L.; Martinez-Castro, N.; Storey, R. F. End-Quenching of TiCl4-Catalyzed Quasiliving Polyisobutylene with Alkoxybenzenes for Direct Chain End Functionalization. *Macromolecules* **2010**, 43 (21), 8724–8740.

97. Kucera, L. R.; Brei, M. R.; Storey, R. F. Synthesis and Characterization of Polyisobutylene-b-Polyamide Multi-Block Copolymer Thermoplastic Elastomers. *Polymer*. **2013**, 54 (15), 3796–3805.

98. Roche, C. P.; Brei, M. R.; Yang, B.; Storey, R. F. Direct Chain End Functionalization of Living Polyisobutylene Using Phenoxyalkyl (Meth)Acrylates. *ACS Macro Lett.* **2014**, 3 (12), 1230–1234.

99. Tripathy, R.; Crivello, J. V; Faust, R. Photoinitiated Polymerization of Acrylate, Methacrylate, and Vinyl Ether End-Functional Polyisobutylene Macromonomers. *J. Polym. Sci. Part A Polym. Chem.* **2013**, 51 (2), 305–317.

100. Parada, C. M.; Storey, R. F. Functionalization of Polyisobutylene and Polyisobutylene Oligomers via the Ritter Reaction. *J. Polym. Sci. Part A Polym. Chem.* **2018**, 56 (8), 840–852.

101. Miller Jr., J. A. A Method of Forming Difunctional Polyisobutylene. U.S. Patent 3,634,383A, January 11, 1972.

102. Puskas, J. E.; Wilds, C. Kinetics of the Epoxidation of Butyl Rubber; Development of a High Precision Analytical Method for Unsaturation Measurement. *Rubber Chem. Technol.* **1994**, 67 (2), 329–341.

103. Ungar, I. S.; Lutz, G. A. Ozonation of Butyl Rubber to Estimate Unsaturation. *Rubber Chem. Technol.* **1961**, 34 (1), 205–210.

104. Ho, K. W.; Guthmann, J. E. The Ozonolysis of Butyl and Halobutyl Elastomers. *J. Polym. Sci. Part A Polym. Chem.* **1989**, 27 (7), 2435–2455.

105. Ebdon, J. R. Synthesis of New Telechelic Oligomers and Macro-monomers by "Constructive Degradation." *Macromol. Symp.* **1994**, 84 (1), 45–54.

106. Chasmawala, M.; Chung, T. C. Telechelic Polyisobutylene: A Facile Synthesis via the Cross-Metathesis Reaction and Trialkylborane-Containing Olefins. *Macromolecules* **1995**, 28 (5), 1333–1339.

107. Kennedy, J. p.; Phillips, R. R. The Influence of Aluminum-Containing Lewis Acids on Polyisobutylene, Isobutylene-Lsoprene Copolymers (Butyl Rubber), and Chlorinated Isobutylene-Lsoprene Copolymer (Chlorobutyl). *J. Macromol. Sci. Part A - Chem.* **1970**, 4 (8), 1759–1784.

108. Campbell, G. C.; Storey, R. F. Functional Polyisobutylenes via Electrophilic Cleavage/Alkylation. *J. Polym. Sci. Part A Polym. Chem.* **2017**, 55 (12), 1991–1997.

(109) Puskas, J. E.; Chen, Y. Biomedical Application of Commercial Polymers and Novel Polyisobutylene-Based Thermoplastic Elastomers for Soft Tissue Replacement. *Biomacromolecules* **2004**, *5* (4), 1141–1154.

(110) Shanks, R.A.; Kong, I. General Purpose Elastomers: Structure, Chemistry, Physics and Performance. In *Advances in Elastomers I: Blends and Interpenetrating Networks*, Visakh, P.M., Thomas, S., Chandra, A.K., Mathew, A.P., Eds.; Springer Berlin Heidelberg: Berlin, Heidelberg, 2013; pp 11-45.

(111) Kang, J., Erdodi, G. and Kennedy, J. P., Polyisobutylene-based Polyurethanes with Unprecedented Properties and How They Came About. *J. Polym. Sci. A Polym. Chem.* **2011**, 49: 3891-3904.

(112) Keszler, B.; Chang, V. S. C.; Kennedy, J. P., Styryl-Telechelic Polyisobutylenes. I. Synthesis of Linear and Tri-Arm Star Styryl-Telechelic Polyisobutylenes. *J. Macromol. Sci., Part A* **1984**, *21* (3), 307-318.

(113) Mishra, M. K.; Wang, B.; Kennedy, J. P., Living carbocationic polymerization: Three-arm star telechelic polyisobutylenes by C6H3(C(CH3)2OCH3)3/BCl3 complexes. *Polymer Bulletin* **1987**, *17* (4), 307-314.

(114) Maenz, K.; Stadermann, D., Macromonomers based on low-molecular-weight polyisobutenes. *Die Angewandte Makromolekulare Chemie* **1996**, *242* (1), 183-197.

(115) Magenau, A. J. D.; Chan, J. W.; Hoyle, C. E.; Storey, R. F., Facile polyisobutylene functionalization via thiol-ene click chemistry. *Polymer Chemistry* **2010**, *1* (6), 831-833.

(116) Storey, R.F.; Lee, Y. Living Carbocationic Polymerization of Isobutylene Using Blocked Dicumyl Chloride or Tricumyl Chloride/TiCl4/Pyridine Initiating System. *J. Macromol. Sci., Part A* **1992,** *29* (11), 1017-1030.

(117) Storey, R.F.; Donnalley, A.B.; Maggio, T.L. Real-Time Monitoring of Carbocationic Polymerization of Isobutylene Using in Situ FTIR-ATR Spectroscopy with Conduit and Diamond-Composite Sensor Technology. *Macromolecules* **1998**, *31* (5), 1523–1526.

(118) Storey, R.F.; Curry, C.L.; Brister, L.B. Carbocation Rearrangement in Controlled/Living Isobutylene Polymerization. *Macromolecules* **1998**, *31* (4), 1058–1063.

(119) Andrzejewska, E. Photopolymerization Kinetics of Multifunctional Monomers. *Prog. Polym. Sci.* **2001**, *26* (4), 605–665.

(120) Cook, W.D. Thermal Aspects of the Kinetics of Dimethacrylate Photopolymerization. *Polymer* **1992**, *33* (10), 2152–2161.

(121) Dickens, S.H.; Stansbury, J.W.; Choi, K.M.; Floyd, C.J.E. Photopolymerization Kinetics of Methacrylate Dental Resins. *Macromolecules* **2003**, *36* (16), 6043–6053.

(122) Esposito Corcione, C.; Frigione, M. Factors Influencing Photo Curing Kinetics of Novel UV-Cured Siloxane-Modified Acrylic Coatings: Oxygen Inhibition and Composition. *Thermochim. Acta* **2012**, *534*, 21–27.

(123) Khudyakov, I.V.; Legg, J.C.; Purvis, M.B.; Overton, B.J. Kinetics of Photopolymerization of Acrylates with Functionality of 1-6. *Ind. Eng. Chem. Res.* **1999**, *38* (9), 3353–3359.

(124) Kim, S.K.; Guymon, C.A. Effects of Polymerizable Organoclays on Oxygen Inhibition of Acrylate and Thiol-Acrylate Photopolymerization. *Polymer* **2012**, *53* (8), 1640–1650.

(125) Jung-Dae, C.; Hyoung-Tae, J.; Jin-Who, H. Photocuring Kinetics of UV-initiated Free-radical Photopolymerizations with and without Silica Nanoparticles. *J. Polym. Sci. Part A Polym. Chem.* **2004**, *43* (3), 658–670.

(126) Decker, C. Recent Developments in Photoinitiated Radical Polymerization. *Macromol. Symp.* **1999**, *143* (1), 45–63.

(127) Kaminsky, W. Polyolefin-Carbon Nanotube Composites by In-Situ Polymerization, In *Polymer-Carbon Nanotube Composites: Preparation, Properties and Applications*; McNally, T., Pötschke, P., Eds.; Woodhead Publishing Limited: Oxford, 2011; pp. 3-24.

(128) Ewa, A.; Maciej, A. Polymerization Kinetics of Photocurable Acrylic Resins. *J. Polym. Sci., Part A: Polym. Chem.* **2000**, *36* (4), 665–673.

(129) Falk, B.; Vallinas, S.M.; Crivello, J.V. Monitoring Photopolymerization Reactions with Optical Pyrometry. *J. Polym. Sci., Part A: Polym. Chem.* **2003**, *41* (4), 579–596.

(130) Porter, R.S.; Johnson, J.F. Shear Viscosities of Polyisobutene Systems—A Study of Polymer Entanglement. *Polymer* **1962**, *3*, 11–16.

(131) Menard, K. P. and Menard, N. R. Dynamic Mechanical Analysis in the Analysis of Polymers and Rubbers. In *Encyclopedia of Polymer Science and Technology*, Mark, H.F. Ed. Wiley, 2015. pp 8-16

(132) Ibarra, L. The Effect of Crosslinking Type on the Physical Properties of Carboxylated Acrylonitrile Butadiene Elastomers. *J. Appl. Polym. Sci.* **1999**, *73* (6), 927–933.

(133) Hamed, G.R.; Han, K.T. Mechanical Properties of Vulcanizates Containing Covalent, Ionic, and Mixed Crosslinks. *Rubber Chem. Technol.* **1990**, *63* (5), 806–824.

(134) Rizos, A.K.; Ngai, K.L.; Plazek, D.J. Local Segmental and Sub-Rouse Modes in Polyisobutylene by Photon Correlation Spectroscopy. *Polymer* **1997**, *38* (25), 6103–6107.

(135) Wypych, G. PIB Polyisobutylene. In *Handbook of Polymers*; Wypych, G. Ed. Elsevier: Oxford, 2012; pp. 422–424.

(136) Rivlin, R.S. The Elasticity of Rubber. *Rubber Chem. Technol.* **1992**, *65* (3), 51–66.

(137) Robertson, C.G.; Lin, C.J.; Rackaitis, M.; Roland, C.M. Influence of Particle Size and Polymer−Filler Coupling on Viscoelastic Glass Transition of Particle-Reinforced Polymers. *Macromolecules* **2008**, *41* (7), 2727–2731.

(138) Mullins, M.J.; Liu, D.; Sue, J. Mechanical Properties of Thermosets. In *Thermosets: Structure, Properties and Applications*; Gui, Q. Ed.; Woodhead Publishing, 2012. pp 35-49

(139) Reinitz, S.D.; Carlson, E.M.; Levine, R.A.C.; Franklin, K.J.; Van Citters, D.W. Dynamical Mechanical Analysis as an Assay of Cross-Link Density of Orthopaedic Ultra High Molecular Weight Polyethylene. *Polym. Testing* **2015**, *45*, 174-178.

(140) Wypych, G., IIR isobutylene-isoprene rubber. In *Handbook of Polymers*, Wypych, G. Ed.; Elsevier: Oxford, 2012; pp 164-167.

(141) Mittal, K. L.; Pizzi, A., *Handbook of Sealant Technology*. CRC Press: 2009; p 541.

(142) Mach, H.; Rath, P. Highly Reactive Polyisobutene as a Component of a New Generation of Lubricant and Fuel Additives. *Lubr. Sci.* **1999**, *11*, 175−185

(143) Mortier, R.M.; Fox, M.F.; Orszulik, S., *Chemistry and Technology of Lubricants*. 3rd ed.; Springer Netherlands: 2011; p 560.

(144) Vasilenko, I.V.; Shiman, D.I.; Kostjuk, S.V. Alkylaluminum Dichloride-Ether Complexes Which are Fully Soluble in Hydrocarbons as Catalysts for the Synthesis of *exo*-Olefin Terminated Polyisobutylene at Room Temperature. *Polym. Chem.* **2014**, *5*, 3855-3866

(145) Kumar, R.; Zheng, B.; Huang, K.-W.; Emert, J.; Faust, R. Synthesis of Highly Reactive Polyisobutylene Catalyzed by EtAlCl2/Bis(2-chloroethyl) Ether Soluble Complex in Hexanes. *Macromolecules* **2014**, *47*, 1959−1965.

(146) Liu, Q.; Wu, Y.; Yan, P.; Zhang, Y.; Xu, R. Polyisobutylene with High exo-Olefin Content via β-H Elimination in the Cationic Polymerization of Isobutylene with H2O/FeCl3/Dialkyl Ether Initiating System. *Macromolecules* **2011**, *44*, 1866−1875.

(147) Kennedy, J.P.; Iván, B. *Designed Polymers by Carbocationic Macromolecular Engineering: Theory and Practice*; Hanser: Munich, Germany, 1991; pp. 96-102.

(148) Feldthusen, J.; Iván, B.; Müller, A.H.E. The Effect of Reaction Conditions on the Chain End Structure and Functionality During Dehydrochlorination of *tert*-Chlorine-Telechelic Polyisobutylene by Potassium *tert*-Butoxide. *Macromol. Rapid Commun.* **1998**, *19*, 661-663.

(149) Simison, K.L.; Stokes, C.D.; Harrison, J.J.; Storey, R.F. End-Quenching of Quasiliving Carbocationic Isobutylene Polymerization with Hindered Bases: Quantitative Formation of *exo*-Olefin-Terminated Polyisobutylene. *Macromolecules* **2006,** *39* (7), 2481-2487.

(150) Storey, R.F.; Kemp, L.K. Preparation of Exo-Olefin Terminated Polyolefins via Quenching with Alkoxysilanes or Ethers. U.S. Patent No. 8,063,154, November 22, 2011.

(151) Ummadisetty, S.; Storey, R.F. Quantitative Synthesis of *exo*-Olefin-Terminated Polyisobutylene: Ether Quenching and Evaluation of Various Quenching Methods. *Macromolecules* **2013,** *46* (6), 2049-2059.

(152) Ummadisetty, S.; Morgan, D.L.; Stokes, C.D.; Storey, R.F. Synthesis of *exo*-Olefin Terminated Polyisobutylene by Sulfide/Base Quenching of Living Polyisobutylene. *Macromolecules* **2011,** *44* (20), 7901-7910.

(153) Iván, B.; Kennedy, J. P. Living Carbocationic Polymerization XXX. One-Pot Synthesis of Allyl-Terminated Linear and Tri-Arm Star Polyisobutylenes, and Epoxy- and Hydroxy-Telechelics Therefrom. *J. Polym. Sci., Part A: Polym. Chem.* **1990**, *28*, 89-104.

(154) Schlaad, H.; Erentova, K.; Faust, R.; Charleux, B.; Moreau, M.; Vairon, J.-P.; Mayr, H. Kinetic Study on the Capping Reaction of Living Polyisobutylene with 1,1-Diphenylethylene. I. Effect of Temperature and Comparison to the Model Compound 2-Chloro-2,4,4-trimethylpentane. *Macromolecules* **1998**, *31* (23), 8058–8062.

(155) De, P.; Faust, R. Carbocationic Polymerization of Isobutylene Using Methylaluminum Bromide Coinitiators: Synthesis of Bromoallyl Functional Polyisobutylene. *Macromolecules* **2006**, *39* (22), 7527–7533

(156) Hadjikyriacou, S.; Faust, R. Cationic Macromolecular Design and Synthesis Using Furan Derivatives. *Macromolecules* **1999**, *32* (20), 6393-6399.

(157) Martinez-Castro, N.; Lanzendorfer, M.G.; Muller, A.H.E.; Cho, J.C.; Acar, M.H.; Faust, R. Polyisobutylene Stars and Polyisobutylene-*block*-Poly(*tert*-Butyl Methacrylate) Block Copolymers by Site Transformation of Thiophene End-Capped Polyisobutylene Chain Ends. *Macromolecules* **2003**, *36* (19), 6985-6994.

(158) Dimitrov, P.; Emert, J.; Hua, J.; Keki, S.; Faust, R. Mechanism of Isomerization in Cationic Polymerization of Isobutylene. *Macromolecules* **2011**, *44* (7), 1831-1840.

(159) Kali, G.; Georgiou, T.K.; Iván, B.; Patrickios, C.S. Anionic Amphiphilic End-Linked Conetworks by the Combination of Quasiliving Carbocationic and Group Transfer Polymerizations. *J. Polym. Sci., Part A: Polym. Chem.* **2009**, *47*, 4289-4301.

(160) Malins, E.L.; Waterson, C.; Becer, C.R. Controlled Synthesis of Amphiphilic Block Copolymers Based on Poly(isobutylene) Macromonomers. *J. Polym. Sci., Part A: Polym. Chem.* **2016**, *54* (5), 634-643.

(161) Kali, G.; Iván, B. Poly(methacrylic acid)-*l*-Polyisobutylene Amphiphilic Conetworks by Using an Ethoxyethyl-Protected Comonomer: Synthesis, Protecting Group Removal in the Cross-Linked State, and Characterization. *Macromol. Chem. Phys.* **2015**, *216* (6), 605-613.

(162) Kali, G.; Vavra, S.; László, K.; Iván, B. Thermally Responsive Amphiphilic Conetworks and Gels Based on Poly(N-isopropylacrylamide) and Polyisobutylene. *Macromolecules* **2013**, *46*, 5337-5344.

(163) Ritter, J.J.; Minieri, P.P. A New Reaction of Nitriles. I. Amides from Alkenes and Mononitriles. *J. Am. Chem. Soc.* **1948,** *70* (12), 4045-4048.

(164) Plaut, H.; Ritter, J.J. A New Reaction of Nitriles. VI. Unsaturated Amides. *J. Am. Chem. Soc.* **1951,** *73* (9), 4076-4077.

(165) Guérinot, A.; Reymond, S.; Cossy, J. Ritter Reaction: Recent Catalytic Developments. *Eur. J. Org. Chem.* **2012,** *2012* (1), 19-28.

(166) Jiang, D.; He, T.; Ma, L.; Wang, Z. Recent Developments in Ritter Reaction. *RSC Advances* **2014,** *4* (110), 64936-64946.

(167) Anavi, M.; Zilkha, A. The "Ritter" Reaction on Polymers. *Eur. Polym. J.* **1969,** *5* (1), 21-28.

(168) Zil'berman, E.N. Reactions of Nitriles with Hydrogen Halides and Nucleophilic Reagents. *Russ. Chem. Rev.* **1962,** *31* (11), 615-633.

(169) Zil'berman, E.N. Some Reactions of Nitriles with the Formation of a New Nitrogen-Carbon Bond. *Russ. Chem. Rev.* **1960,** *29* (6), 331-344.

(170) Baum, J.C.; Milne, J.E.; Murry, J.A.; Thiel, O.R. An Efficient and Scalable Ritter Reaction for the Synthesis of *tert*-Butyl Amides. *J. Org. Chem.* **2009,** *74* (5), 2207-2209.

(171) Reichardt, C.; Welton, T. *Solvents and Solvent Effects in Organic Chemistry, 3rd Ed.*; Wiley: New York, **2003**; p 598.

(172) Colombo, M.I.; Bohn, M.L.; Rúveda, E.A. The Mechanism of the Ritter Reaction in Combination with Wagner-Meerwein Rearrangements. A Cooperative Learning Experience. *J. Chem. Ed.* **2002,** *79* (4), 484.

(173) Xu, S.-C.; Zhu, S.-J.; Chen, Y.-X.; Wang, J.; Bi, L.-W.; Lu, Y.-J.; Gu, Y.; Zhao, Z.-D. Skeletal Rearrangement in the Ritter Reaction of Turpentine: A Novel Synthesis of *p*-Menthane Diamides. *J. Chem. Res.* **2017,** *41* (2), 124-127.

(174) Vankar, Y.D.; Kumaravel, G.; Rao, C.T. Ritter Reaction with Cyclopropyl Ketones and Cyclopropyl Alcohols: Synthesis of N-Actyl- γ-Keto and N-Acyl Homoallyl Amines. *Synthetic Commun.* **1989,** *19* (11-12), 2181-2198.

(175) Mousseron, M.; Jacquier, R.; Christol, H. Molecular rearrangement reactions in the preparation of amines from alicyclic alcohols. *Compt. rend.* **1952,** *235*, 57-59.

(176) Mousseron, M.; Jacquier, R.; Christol, H. Acid-Catalyzed Rearrangements. II. A Study of the Ritter Reaction. 1. *Bull. Soc. Chim. Fr.* **1957**, 596-600.

(177) Mousseron, M.; Jacquier, R.; Christol, H. Acid-Catalyzed Rearrangements. III. A Study of the Ritter Reaction. 2. *Bull. Soc. Chim. Fr.* **1957**, 600-610.

(178) Christol, H.; Laurent, A.; Mousseron, M. Acid-Catalyzed Rearrangements. XI. The Ritter Reaction of Tertiary Benzyl Alcohols. *Bull. Soc. Chim. Fr.* **1961**, 2319-2324.

(179) Christol, H.; Laurent, A.; Solladie, G., Acid-Catalyzed Rearrangements. XIII. Ritter Reaction of Some Diphenylcarbinols and Diphenylpropanols. *Bull. Soc. Chim. Fr.* **1963,** (4), 877-881.

(180) Christol, H.; Solladie, G., Acid-Catalyzed Rearrangements. XIV. Effect of the Solvent in the Ritter Reaction on Spiro[4.5]decan-6-ol and the Decalols. *Bull. Soc. Chim. Fr.* **1966,** (4), 1299-1307.

181. Seddon, E.J.; Friend C.L.; Roski J.P.; *Chemistry and Technology of Lubricants*. 3rd ed.; Mortier, R. M.; Fox, M. F.; Orszulik, S., Eds.; Springer Science and Business Media: Netherlands, **2011**; p 213-236

182. Heskett, M. D. Structure-Property Relationships of Polyisobutylene-Block-Polyamide Thermoplastic Elastomers, Masters Thesis, University of Southern Mississippi, August 2016.

183. Iván, B.; Kennedy, J. P.; Mackey, P. W. Amphiphilic Networks. In *Polymeric Drugs and Drug Delivery Systems*; ACS Symposium Series; American Chemical Society, **1991**; Vol. 469, pp 18–194.

184. Li, J.; Sung, S.; Tian, J.; Bergbreiter, D. E., Polyisobutylene supports—a non-polar hydrocarbon analog of PEG supports. *Tetrahedron* **2005,** *61* (51), 12081-12092.

185. Ummadisetty, S.; Kennedy, J. P., Quantitative syntheses of novel polyisobutylenes fitted with terminal primary -Br, -OH, -NH2, and methacrylate termini. *Journal of Polymer Science Part A: Polymer Chemistry* **2008,** *46* (12), 4236-4242.

186. Boileau, S.; Mazeaud-Henri, B.; Blackborow, R., Reaction of functionalised thiols with oligoisobutenes via free-radical addition. *European Polymer Journal* **2003,** *39* (7), 1395-1404.

187. Lubnin, A. V.; Kennedy, J. P.; Goodall, B. L., Synthesis and characterization of aldehyde-capped polyisobutylenes. *Polymer Bulletin* **1993,** *30* (1), 19-24.

188. Kemp, L. K.; Donnalley, A. B.; Storey, R. F., Synthesis and characterization of carboxylic acid-terminated polyisobutylenes. *Journal of Polymer Science Part A: Polymer Chemistry* **2008,** *46* (10), 3229-3240.

189. Simison, K. L.; Stokes, C. D.; Harrison, J. J.; Storey, R. F., End-Quenching of Quasiliving Carbocationic Isobutylene Polymerization with Hindered Bases: Quantitative Formation of exo-Olefin-Terminated Polyisobutylene. *Macromolecules* **2006,** *39* (7), 2481-2487.

190. Storey, R. F.; Kemp, L. K., Preparation of exo-olefin terminated polyolefins via quenching with alkoxysilanes or ethers. U.S. Patent 8,063,154B2: November 22, 2011.

191. Ummadisetty, S.; Storey, R. F., Quantitative Synthesis of exo-Olefin-Terminated Polyisobutylene: Ether Quenching and Evaluation of Various Quenching Methods. *Macromolecules* **2013,** *46* (6), 2049-2059.

192. Ummadisetty, S.; Morgan, D. L.; Stokes, C. D.; Storey, R. F., Synthesis of exo-Olefin Terminated Polyisobutylene by Sulfide/Base Quenching of Living Polyisobutylene. *Macromolecules* **2011,** *44* (20), 7901-7910.

193. Hadjikyriacou, S.; Fodor, Z.; Faust, R., Synthetic Applications of Nonpolymerizable Monomers in Living Cationic Polymerization: Functional Polyisobutylenes by End-Quenching. *Journal of Macromolecular Science, Part A* **1995,** *32* (6), 1137-1153.

194. Iván, B.; Kennedy, J. P., Living carbocationic polymerization. XXX. One-pot synthesis of allyl-terminated linear and tri-arm star polyisobutylenes, and epoxy- and hydroxy-telechelics therefrom. *Journal of Polymer Science Part A: Polymer Chemistry* **1990,** *28* (1), 89-104.

195. Feldthusen, J.; Iván, B.; Müller, A. H. E., Synthesis of Linear and Star-Shaped Block Copolymers of Isobutylene and Methacrylates by Combination of Living Cationic and Anionic Polymerizations. *Macromolecules* **1998,** *31* (3), 578-585.

196. Schunack, M.; Gragert, M.; Döhler, D.; Michael, P.; Binder, W. H., Low-Temperature Cu(I)-Catalyzed "Click" Reactions for Self-Healing Polymers. *Macromolecular Chemistry and Physics* **2012,** *213* (2), 205-214.

197. Martinez-Castro, N.; Lanzendörfer, M. G.; Müller, A. H. E.; Cho, J. C.; Acar, M. H.; Faust, R., Polyisobutylene Stars and Polyisobutylene-block-Poly(tert-Butyl Methacrylate) Block Copolymers by Site Transformation of Thiophene End-Capped Polyisobutylene Chain Ends. *Macromolecules* **2003,** *36* (19), 6985-6994.

198. Yang, B.; Storey, R. F. Chain-End Functionalization of Living Polyisobutylene via an End-Quenching Comonomer That Terminates by Indanyl Ring Formation. *Macromolecules* **2018**.

199. Yang, B.; F. Storey, R. End-Quenching of Tert-Chloride-Terminated Polyisobutylene with Alkoxybenzenes: Comparison of AlCl3 and TiCl4 Catalysts; *Polymer Chemistry* **2015**, *6*, 3764-3774

200. P. Holbrook, T.; M. Masson, G.; F. Storey, R. Synthesis, Characterization, and Evaluation of Polyisobutylene-based Imido-amine-type Dispersants Containing Exclusively Non-nucleophilic Nitrogen; *J. Polym. Sci. Part A: Polym. Chem.* **2018**, *56*, 1657-1675.

201. Sanford, E. M.; Lis, C. C.; McPherson, N. R. The Preparation of Allyl Phenyl Ether and 2-Allylphenol Using the Williamson Ether Synthesis and Claisen Rearrangement. *J. Chem. Educ.* **2009**, *86* (12), 1422.

202. Gozzo, F. C.; Fernandes, S. A.; Rodrigues, D. C.; Eberlin, M. N.; Marsaioli, A. J. Regioselectivity in Aromatic Claisen Rearrangements. *J. Org. Chem.* **2003**, 68 (14), 5493–5499.

203. Kupczyk-Subotkowska, L.; Saunders, W. H.; Shine, H. J. Claisen Rearrangement of Allyl Phenyl Ether: Heavy-Atom Kinetic Isotope Effects and Bond Orders in the Transition Structure. *J. Am. Chem. Soc.* **1988**, *110* (21), 7153–7159.

204. Gómez, B.; Chattaraj, P. K.; Chamorro, E.; Contreras, R.; Fuentealba, P. A Density Functional Study of the Claisen Rearrangement of Allyl Aryl Ether, Allyl Arylamine, Allyl Aryl Thio Ether, and a Series of Meta-Substituted Molecules through Reactivity and Selectivity Profiles. *J. Phys. Chem. A* **2002**, *106* (46), 11227–11233.

205. Kupczyk-Subotkowska, L.; Subotkowski, W.; Saunders, W. H.; Shine, H. J. Claisen Rearrangement of Allyl Phenyl Ether. 1-Carbon-14 and .Beta.-Carbon-14 Kinetic Isotope Effects. A Clearer View of the Transition Structure. *J. Am. Chem. Soc.* **1992**, *114* (9), 3441–3445.

206. Dryzhakov, M.; Moran, J. Autocatalytic Friedel–Crafts Reactions of Tertiary Aliphatic Fluorides Initiated by B(C6F5)3·H2O. *ACS Catal.* **2016**, *6* (6), 3670–3673.

207. Storey, R. F.; Choate, K. R. Kinetic Investigation of the Living Cationic Polymerization of Isobutylene Using a T-Bu-m-DCC/TiCl4/2,4-DMP Initiating System. *Macromolecules* **1997**, *30* (17), 4799–4806.

208. Storey, R. F.; Maggio, T. L. Real-Time Monitoring of Carbocationic Polymerization of Isobutylene via ATR-FTIR Spectroscopy: The t-Bu-m-DCC/DMP/BCl3 System. M*acromolecules* **2000**, *33* (3), 681–688.

209. Storey, R. F.; Chisholm, B. J.; Brister, L. B. Kinetic Study of the Living Cationic Polymerization of Isobutylene Using a Dicumyl Chloride/TiCl4/Pyridine Initiating System. *Macromolecules* **1995**, *28* (12), 4055–4061.

210. Michel, A. J.; Puskas, J. E.; Brister, L. B. Real-Time Mid-IR Monitoring of the Initiation and Propagation in Epoxi-Initiated Living Isobutylene Polymerizations. *Macromolecules* **2000**, *33* (10), 3518–3524.

211. Kaszas, G.; Puskas, J. Kinetics of the Carbocationic Homopolymerization of Isobutylene with Reversible Chain Termination. *Polym. React. Eng.* **1994**, *2* (3), 251–273

212. Puskas, J. E.; Lanzendörfer, M. G. Investigation of the TiCl4 Reaction Order in Living Isobutylene Polymerizations. *Macromolecules* **1998**, *31* (25), 8684–8690.

213. Storey, R. F.; Curry, C. L.; Hendry, L. K. Mechanistic Role of Lewis Bases and Other Additives in Quasiliving Carbocationic Polymerization of Isobutylene. *Macromolecules* **2001**, *34* (16), 5416–5432.

(214) Willenbacher, N.; Lebedeva, O.V. Polyisobutylene-Based Pressure-Sensitive Adhesives. In *Technology of Pressure-Sensitive Adhesives and Products*, Benedek, I., Feldstein, M.M., Eds.; CRC Press, Taylor & Francis Group, LLC: Boca Raton, FL, 2009; pp. 41–45.

(215) Klosowski, J.M.; Wolf, A.T. The History of Sealants. In *Handbook of Sealant Technology*, Mittal, K.L., Pizzi, A. Eds.; CRC Press, Taylor & Francis Group, LLC: Boca Raton, FL, 2009; pp. 7–9.

(216) Tan, K.T.; White, C.C.; Benatti, D.J.; Stanley, D.; Hunston, D.L. Chemorheological Investigation on the Environmental Susceptibility of Sealants. In

Handbook of Sealant Technology, Mittal, K.L., Pizzi, A. Eds.; CRC Press, Taylor & Francis Group, LLC: Boca Raton, FL, 2009; p. 89.

(217) Kolawole, E.G.; Olugbemi, P.O. Natural Weathering, Photo and Thermal Degradation of the Two-Phase System Poly(Vinyl Chloride) and Poly(Isobutylene). *Eur. Polym. J.* **1985**, *21* (2), 187–193.

(218) Wolf, A. Sealant Durability and Service Life of Sealed Joints. In *Handbook of Sealant Technology*, Mittal, K.L., Pizzi, A. Eds.; CRC Press, Taylor & Francis Group, LLC: Boca Raton, FL, 2009; p. 158.

(219) Hung, J.-M. Hot Melt Sealants. In *Handbook of Sealant Technology*, Mittal, K.L., Pizzi, A. Eds.; CRC Press, Taylor & Francis Group, LLC: Boca Raton, FL, 2009; p. 242

(220) Kiran, E.; Gillham, J.K. Pyrolysis-Molecular Weight Chromatography: A New On-line System for Analysis of Polymers. II. Thermal Decomposition of Polyolefins: Polyethylene, Polypropylene, Polyisobutylene. *J. Appl. Polym. Sci.* **2003**, *20* (8), 2045–2068.

(221) Wypych, G. *Handbook of Material Weathering, 5th Ed.* Wypych, G. Ed.; Elsevier: Oxford, 2013; pp. 1–25.

(222) Andrady, L. Ultraviolet Radiation and Polymers. In *Physical Properties of Polymers Handbook, Second Edition*, Mark, J., Ed.; Springer Science and Business Media, LLC: New York, NY, 2007; pp. 857-866.

(223) Crompton, T.R., Ed. *Thermo-Oxidative Degradation of Polymers*; Crompton, T.R. Ed.; Smithers Rapra Technology Ltd., 2010. pp 21-46

(224) Shalaby, S.W. Thermoplastic Polymers. In *Thermal Characterization of Polymeric Materials, Second Edition,* Turi, E.A. Ed.; Elsevier, 2012. pp 281-316

(225) Peterson, J.D.; Vyazovkin, S.; Wight, C.A. Kinetics of the Thermal and Thermo-Oxidative Degradation of Polystyrene, Polyethylene and Poly(propylene). *Macromol. Chem. Phys.* **2001**, *202* (6), 775–784.

(226) Hawkins, W.L.; Matreyek, W.; Winslow, F.H. The Morphology of Semicrystalline Polymers. Part I. The Effect of Temperature on the Oxidation of Polyolefins. *J. Polym. Sci.* **1959**, *41* (138), 1–11.

(227) Iring, M.; László-Hedvig, S.; Kelen, T.; Tüdós, F.; Füzes, L; Samay, G.; Bodor, G. Study of Thermal Oxidation of Polyolefins. VI. Change of Molecular Weight Distribution in the Thermal Oxidation of Polyethylene and Polypropylene. *J. Polym. Sci., Polym. Symp.* **1976**, *57* (1), 55–63.

(228) Gonon, L.; Troquet, M.; Fanton, E.; Gardette, J.-L. Thermo and Photo-Oxidation of Polyisobutylene—II. Influence of the Temperature. *Polym. Degrad. Stab.* **1998**, *62* (3), 541–549.

(229) Sawaguchi, T.; Seno, M. Detailed Mechanism and Molecular Weight Dependence of Thermal Degradation of Polyisobutylene. *Polymer* **1996**, *37* (25), 5607–5617.

(230) Grimbley, M.R.; Lehrle, R.S. The Thermal Degradation Mechanism of Polyisobutylene. Part 1: Comparison of Results with Statistical Predictions Provides a General Interpretation of the Mechanisms of Decomposition. *Polym. Degrad. Stab.* **1995**, *49* (2), 223–229.

(231) Lánská, B. Stabilization of Polyamides—I. The Efficiency of Antioxidants in Polyamide 6. *Polym. Degrad. Stab.* **1996**, *53* (1), 89–98.

(232) Bergenudd, H.; Eriksson, P.; DeArmitt, C.; Stenberg, B.; Malmström Jonsson, E. Synthesis and Evaluation of Hyperbranched Phenolic Antioxidants of Three Different Generations. *Polym. Degrad. Stab.* **2002**, *76* (3), 503–509.

(233) Ayala, J.A.; Hess, W.M.; Dotson, A.O.; Joyce, G.A. New Studies on the Surface Properties of Carbon Blacks. *Rubber Chem. Technol.* **1990**, *63* (5), 747–778.

(234) Medalia, A.I. Effect of Carbon Black on Dynamic Properties of Rubber Vulcanizates. *Rubber Chem. Technol.* **1978**, *51* (3), 437–523.

(235) Hamama, A.A.; Nawar, W.W. Thermal Decomposition of Some Phenolic Antioxidants. *J. Agr. Food Chem.* **1991**, *39* (6), 1063–1069.

(236) Mahmoud Allam, S.S.; Aly Mohamed, H.M. Thermal Stability of Some Commercial Natural and Synthetic Antioxidants and Their Mixtures. *J. Food Lipids* **2002**, *9* (4), 277–293.

(237) Santos, N.A.; Cordeiro, A.M.T.M.; Damasceno, S.S.; Aguiar, R.T.; Rosenhaim, R.; Carvalho Filho, J.R.; Santos, I.M.G.; Maia, A.S.; Souza, A.G. Commercial Antioxidants and Thermal Stability Evaluations. *Fuel* **2012,** 97, 638–643..

(238) Hawkins, W.L.; Hansen, R.H.; Matreyek, W.; Winslow, F.H. *J. Appl. Polym. Sci.* **1959**, *1* (1), 37–42.

(239) Kovács, E.; Wolkober, Z. The Effect of the Chemical and Physical Properties of Carbon Black on the Thermal and Photooxidation of Polyethylene. *J. Polym. Sci., Polym. Symp.* **1976**, *57* (1), 171–180.

(240) Atkinson, D.; Lehrle, R. A Model Polymer-Bound Antioxidant System for Lubricants. *Eur. Polym. J.* **1992**, *28* (12), 1569–1575.

(241) Beer, S.; Teasdale, I.; Brueggemann, O. Macromolecular Antioxidants via Thiol-Ene Polyaddition and Their Synergistic Effects. *Polym. Degrad. Stab.* **2014**, *110*, 336–343.

(242) Xue, B.; Ogata, K.; Toyota, A. Synthesis and Radical Scavenging Ability of New Polymers from Sterically Hindered Phenol Functionalized Norbornene Monomers via ROMP. *Polymer* **2007**, *48* (17), 5005–5015.

(243) Beer, S.; Teasdale, I.; Brueggemann, O. Immobilization of Antioxidants via ADMET Polymerization for Enhanced Long-Term Stabilization of Polyolefins. *Eur. Polym. J.* **2013**, *49* (12), 4257–4264.

(244) Oh, D.R.; Kim, H.-K.; Lee, N.; Chae, K.H.; Kaang, S.; Lee, M.S.; Kim, T.H. Synthesis of New Polymeric Antioxidants. *Bull. Korean Chem. Soc.* **2001**, *22* (6), 629–632.

(245) Al-Malaika, S.; Suharty, N. Reactive Processing of Polymers: Mechanisms of Grafting Reactions of Functional Antioxidants on Polyolefins in the Presence of a Coagent. *Polym. Degrad. Stab.* **1995**, *49* (1), 77–89.

(246) Kim, T.H.; Oh, D.R. Melt Grafting of Maleimides Having Hindered Phenol Antioxidant onto Low Molecular Weight Polyethylene. *Polym. Degrad. Stab.* **2004**, *84* (3), 499–503.

(247) Campbell, G.C.; Storey, R.F. Functional Polyisobutylenes via Electrophilic Cleavage/Alkylation. *J. Polym. Sci., Part A: Polym. Chem.* **2017**, *55* (12), 1991–1997.

(248) Morgan, D.L.; Martinez-Castro, N.; Storey, R.F. End-Quenching of TiCl4-Catalyzed Quasiliving Polyisobutylene with Alkoxybenzenes for Direct Chain End Functionalization. *Macromolecules* **2010**, *43* (21), 8724–8740.

(249) Storey, R.F.; Donnalley, A.B.; Maggio, T.L. Real-Time Monitoring of Carbocationic Polymerization of Isobutylene Using in Situ FTIR-ATR Spectroscopy with Conduit and Diamond-Composite Sensor Technology. *Macromolecules* **1998**, *31* (5), 1523–1526.

(250) Ammawath, W.; Che Man, Y.B.; Abdul Rahman, R.B.; Baharin, B.S. A Fourier Transform Infrared Spectroscopic Method for Determining Butylated Hydroxytoluene in Palm Olein and Palm Oil. *J. Am Oil Chem. Soc.* **2006**, *83* (3), 187–191.

(251) Da Cruz, M.; Van Schoors, L.; Benzarti, K.; Colin, X. Thermo-Oxidative Degradation of Additive Free Polyethylene. Part I. Analysis of Chemical Modifications at Molecular and Macromolecular Scales. *J. Appl. Polym. Sci.* **2016**, *133* (18), 43287; pp. 1–16.

(252) Setnescu, R.; Jipa, S.; Osawa, Z. Chemiluminescence Study on the Oxidation of Several Polyolefins—I. Thermal-Induced Degradation of Additive-Free Polyolefins. *Polym. Degrad. Stab.* **1998**, *60* (2–3), 377–383.

(253) Holmström, A.; Sörvik, E.M. Thermooxidative Degradation of Polyethylene. I and II. Structural Changes Occurring in Low-density Polyethylene, High-density Polyethylene, and Tetratetracontane Heated in Air. *J. Polym. Sci.: Polym. Chem. Ed.* **1978**, *16* (10), 2555–2586.